Universitat de Girona

PHYSIOLOGICAL ROLE OF MITOCHONDRIAL AND PLASMA MEMBRANE CHANNELS IN SPERM

Ariadna Delgado Bermúdez

Universitat de Girona

DOCTORAL THESIS

Physiological role of mitochondrial and plasma membrane channels in sperm

Ariadna Delgado Bermúdez

2022

Universitat de Girona

DOCTORAL THESIS

Physiological role of mitochondrial and plasma membrane channels in sperm

Ariadna Delgado Bermúdez

2022

Doctoral programme in Technology

Supervised by:
Dr. Marc Yeste Oliveras

Thesis Dissertation submitted to obtain the degree of PhD at the University of Girona

Universitat de Girona

Dr **Marc Yeste Oliveras**, Associate Professor of Cell Biology at the Department of Biology, University of Girona,

DECLARES:

That the thesis entitled "*Physiological role of mitochondrial and plasma membrane channels in sperm*", submitted by Miss. Ariadna Delgado Bermúdez to obtain the doctoral degree, has been completed under my supervision and meets the requirements for the International Doctorate mention.

And for all intents and purposes, hereby signs the document.

Signature

Girona, 3 May 2022

This work has been mainly funded by the Ministry of Science and Innovation from the Spanish Government (Fellowship reference PRE2018-083488).

All figures in this work have been created with BioRender.

Tornar sempre és la millor part de l'aventura.
(Els amics de les arts)

Acknowledgements

Aquesta tesi és el resultat d'un llarg viatge i l'he fet acompanyada de persones molt boniques que han fet possible que en els moments complicats recordés per què vaig decidir embarcar-m'hi. Però encara més important: han estat al meu costat en els moments feliços, i m'han omplert d'experiències que no tindré mai prou paraules per agrair.

No puc començar per una altra persona que no sigui el Dr Marc Yeste. Poc em podia imaginar el 2016 que estava enviant el meu primer correu electrònic al meu futur tutor de tesi. Marc, gràcies per confiar en mi i per veure en mi la investigadora que jo mateixa no havia sabut veure. Mentiria si digués que la meva manera de veure't a nivell professional no ha canviat gens des que vaig entrar al grup, i més d'una vegada he pensat que he fet la mateixa evolució que fem tots quan pensem en els nostres pares: de nens pensem que son uns superherois que poden amb tot i ho saben tot; d'adolescents ens adonem que son persones igual que nosaltres; i d'adults admirem com, sent persones normals, son capaços de fer tot el que fan. I per això, més que el meu tutor, et considero el meu pare científic, a qui admiro profundament. Gràcies pel grup de persones que has ajuntat, per ensenyar-nos una filosofia de grup basada en el treball dur, el respecte i la cooperació, i per ser la persona que ha lluitat contra el món per nosaltres. I a nivell personal no tinc més que paraules de gratitud per totes les vegades que hem parlat de la vida més enllà de la ciència, pels teus consells i pel teu suport incondicional.

Al Dr Sergi Bonet, el director del grup, gràcies per fer possible TechnoSperm. La teva labor blinda la nostra feina del dia a dia, i és la base sobre la que es sustenta el grup. I a la Dra Elisabeth Pinart, col·laborar amb tu és sempre un plaer. Beth, gràcies per comptar amb mi en projectes científics i també per donar-me la oportunitat de participar en la organització de congressos. M'emporto l'experiència de treballar amb tu, que ha estat molt important per mi.

I la resta de l'equip de TechnoSperm. Marc, Yentel, Sandra, Estel, Jordi, Albert, Carolina, Lore, Isabel, Bea i Estela. Sou l'hòstia. Us valorava abans de marxar i us

valoro encara més ara que he vist que serà molt difícil que algun dia posi el peu en un laboratori on es visqui tan bé com amb vosaltres.

Us toca als *Becaris de l'apocalipsi*. Sou unes persones molt boniques amb les que la vida m'ha sorprès. Compartir la mateixa manera de veure i de viure la ciència amb algú que està en el mateix moment vital (Marc i Yentel, no accepto que em poseu en una altra generació, ho sento), ha estat molt important per tirar endavant. Marc, encara que hagis perdut una mica de la sort del principiant que tenies i tot i la teva impaciència, m'ho passo genial treballant amb tu. Segueix esperant sempre el millor dels altres, i no perdis mai el teu humor negre. Yentel, no deixis mai d'escandalitzar-te pel seu humor. Ets una dona forta que lluita pel que vol i defensa les seves idees, gràcies per ser una gran companya de lluites. Recuperem tots els vins que tenim pendents, que mai no seran prou. Sandra, gràcies per aportar el teu cor immens i el teu toc canalla als *Becaris*. Has anat davant meu en això de la tesi i no et podré agrair mai prou la teva ajuda. Continuaré inventant-me noms d'*animes*, perquè sé que sabràs quins son i ens en podrem riure sempre una estona. Als tres, gràcies, perquè sense vosaltres el meu creixement personal i professional d'aquests anys no hagués estat igual. Sou persones genuïnes i honestes, i hem fet un equip envejable. Ens ha tocat viure moments complicats i tenir-nos ha estat la clau per no deixar-ho córrer tot i enviar la resta del món a passeig. Estel, fa poquet que t'has sumat a l'equip de *predocs*, però t'has fet el teu lloc treballant fort i sempre amb un somriure. No deixis mai d'entrar per la porta al matí cantant. Ens devem més congressos i sopars, perquè ho peteu molt fort.

La primera vegada que vam sentir a parlar d'un tal Jordi que havia estat a Honolulu i que vindria a fer un postdoc a TechnoSperm, poc em podia imaginar el que m'esperava. Ets una de les persones més treballadores que he vist mai, i a sobre converteixes 5 μL de mostra en un article (això encara m'has d'ensenyar com t'ho fas, *boss*!). I ara de debò, l'Èlia i tu ens heu acollit i ens heu fet sentir com a casa a l'altra punta del món. Ens heu ensenyat llocs espectaculars, i és molt difícil trobar gent amb qui es visqui tan bé i tan fàcil. Sou uns companys de viatge increïbles i us mereixeu el millor. *Mahalo*. Albert, ens vam conèixer en plena pandèmia i a través d'una pantalla, però ens vas salvar de l'angoixa d'estar tancats i impotents

sense poder fer res. I en persona ens has demostrat que ets tot bon cor i bon rotllo. Tot i que tens mil projectes oberts, sempre estàs disposat a fer un cop de mà i t'apuntaries a un bombardeig (dins i fora del laboratori), i ens has ensenyat què vol dir ser un RTV (real). Carolina y Lore, os habéis sumado hace poco también al equipo y hacéis un combo brutal. Gracias por vuestro humor, tenéis una energía muy guay. Y de las nuevas incorporaciones murcianas me voy a la murciana que lleva más tiempo con nosotros. Isabel, eres toda corazón y una gran currante. Nos encanta que sigas con un pie en Girona, porque es súper fácil trabajar contigo. Y Bea, que te has vuelto a Madrid después de dar mil vueltas por el mundo, nos enseñaste que también se puede discutir sobre ciencia con una cerveza delante y entonces salen las buenas ideas. Estela, vas ser la meva persona de referència des del primer dia que vaig trepitjar el laboratori. TechnoSperm es va quedar una mica coix quan vas marxar, però esperem que no deixis de fer-nos visites i explicar-nos les teves aventures sempre amb un somriure dels teus.

I no em puc deixar la part del grup que veiem menys sovint, els companys de la UAB. Als Drs Jordi Miró i Joan Enric, que cada vegada que han vingut a Girona n'hem après alguna cosa, gràcies. I a tots els doctorands que han vingut a fer experiments, que amb els seus *backgrounds* ben diferents sempre és interessant que ens expliquin els seus projectes: Meritxell, Federico, Sebastián, Marion, Jaime, Iris i Tània.

During this last year I have had the chance to visit two different labs, which has been an amazing experience. I would like to thank Dr Andrew Gilmore for his unconditional support with the project, as well as Rob, Charlotte and Sara for their help. Thank you for making it so easy to adapt at the University of Manchester, I almost felt like at home (except for the weather and the early evenings). And to compensate the British weather I traveled to the other side of the world to the Institute of Biogenesis Research at the University of Hawaii. I must thank Dr Steve Ward for being so supportive and helping Jordi and I define the project, as well as Hieu and Winnie for their support in the lab.

Acknowledgements

Laia, Aida i Alba, sou el meu botó de desconnexió. Gràcies per ser-hi sempre, i que les nostres vides de dones adultes, que a vegades ens deixen menys temps del que voldríem, no canviïn mai el que tenim. Als *Malalts*, Gerard, Paula, Eva, Benji i Oscar. Tinc molta sort de tenir-vos des de fa tant de temps al meu costat i haver-nos vist créixer en tots els sentits, espero que continuem compartint estones, perquè sou una càrrega de piles molt guai. Oscar, espero visitar-te molts anys més i que xulegis d'exalumna, que això un cop l'any pels egos ens va molt bé. Natàlia i Martí, gràcies per estimar-me tant, i tan de pressa. Per escoltar sempre, tant quan pregunteu curiositats com quan ens desfoguem de les feines o de la vida, i per totes les partides de Munchkin. Per fer-me el regal de ser padrina de la Júlia, gràcies.

I no hagués pogut arribar mai on soc sense els meus pares. Sou el meu suport i sempre heu tingut clar, fins i tot més que jo mateixa, tot el que podia fer. Gràcies per no deixar que m'acomodés ni em quedés estancada en els moments complicats i per alegrar-vos de les meves petites victòries. Saber que sempre puc comptar amb vosaltres és el que m'ha permès tenir la confiança en mi mateixa per embarcar-me en un projecte com aquest. Marc, gràcies per ser casa. També crec que pots arribar més lluny del que tu mateix penses, i tot i que t'ha tocat viure la universitat a mig gas, pots fer el que et proposis. A les meves iaies, que tot i no entendre massa bé el que faig, no han tingut res més que amor per mi, gràcies.

Jordi, tinc poques més paraules per escriure't que les que ja saps. Gràcies per fer que la vida flueixi fàcil i per fer-me sortir fora de la meva zona de confort (i per les figures). Sense tu al meu costat potser no m'hauria tirat a la piscina del doctorat, ni a algunes altres piscines que han vingut (ni hauria fet aquestes figures). He tingut la sort de tenir al meu costat una persona que comparteix la meva manera d'intentar compaginar la ciència i la vida, i que a més em posa en perspectiva les pedres del camí per què hi pugui passar per sobre sense entrebancar-m'hi (i a més m'ajuda a fer figures). Sempre des d'aquí al Parc i tornar, pel camí més llarg.

Soc molt afortunada de tenir-vos a la meva vida.

Aloha nui loa.

List of publications

This Dissertation is presented as a compendium of five publications:

Paper I

Delgado-Bermúdez A, Recuero S, Llavanera M, Mateo-Otero Y, Sandu A, Barranco I, Ribas-Maynou J, Yeste M. (2021) **Aquaporins are essential to maintain motility and membrane lipid architecture during mammalian sperm capacitation.** *Front Cell Dev Biol*, 9:656438. doi: 10.3389/fcell.2021.656438.

- **Impact factor**: 6.684
- **JCR category**: Developmental biology
- **Category quartile**: Q1

Paper II

Delgado-Bermúdez A, Llavanera M, Fernández-Bastit L, Recuero S, Mateo-Otero Y, Bonet S, Barranco I, Fernández-Fuertes B, Yeste M. (2019) **Aquaglyceroporins but not orthodox aquaporins are involved in the cryotolerance of pig spermatozoa.** *J Anim Sci Biotechnol*, 10:77. doi: 10.1186/s40104-019-0388-8.

- **Impact factor**: 4.167
- **JCR category**: Agriculture, dairy and animal science
- **Category quartile**: Q1

Paper III

Delgado-Bermúdez A, Llavanera M, Recuero S, Mateo-Otero Y, Bonet S, Barranco I, Fernandez-Fuertes B, Yeste M. (2019) **Effect of AQP inhibition on boar sperm cryotolerance depends on the intrinsic freezability of the ejaculate**. *Int J Mol Sci* 20(24):6255. doi: 10.3390/ijms20246255.

- **Impact factor**: 4.556
- **JCR category**: Biochemistry and molecular biology
- **Category quartile**: Q1

Paper IV

Delgado-Bermúdez A, Noto F, Bonilla-Correal S, Garcia-Bonavila E, Catalán J, Papas M, Bonet S, Miró J, Yeste M. (2019) **Cryotolerance of stallion spermatozoa relies on aquaglyceroporins rather than orthodox aquaporins**. (2019) *Biology (Basel)*. 8(4):85. doi: 10.3390/biology8040085.

- **Impact factor**: 3.796
- **JCR category**: Biology
- **Category quartile**: Q1

Paper V

Delgado-Bermúdez A, Mateo-Otero Y, Llavanera M, Bonet S, Yeste M, Pinart E. (2021) **HVCN1 but not potassium channels are related to mammalian sperm cryotolerance**. *Int J Mol Sci*. 22(4):1646. doi: 10.3390/ijms22041646.

- **Impact factor**: 4.556
- **JCR category**: Biochemistry and molecular biology
- **Category quartile**: Q1

List of abbreviations

AQP	Aquaporin
AC	Acetazolamide
2-GBI	2-guanidino benzimidazole
4-AP	4-aminopyridine
AgSDZ	Silver sulfadiazine
AI	Artificial insemination
AR	Acrosome reaction
ar/R region	Aromatic/arginine region
ART	Assisted reproduction technology
CA	Carbonic anhydrase
cAMP	Cyclic adenosine monophosphate
CASP3	Caspase-3
CatSper	Cation current in sperm / channel responsible for catsper
CFTR	Cystic fibrosis transmembrane conductance regulator
CPA	Cryoprotective agent
DCF	2',7'-dichlorofluorescein
DNA	Deoxyribonucleic acid
E	Ethidium
Em	Membrane potential
ER	Endoplasmic reticulum
FC	Flow cytometry
FT	Frozen-thawed
Gal T1	β1,4-galactosyl transferase 1
GFE	Good-freezability ejaculate
GLP	Aquaglyceroporin
GPCR	G protein-coupled receptor

GRAC	Guide to receptors and channels
HPV	Human papillomavirus
ICC	Immunocytochemistry
IF	Immunofluorescence
IGEM	Immunogold and scanning and transmission electron microscopy
IHC	Immunohistochemistry
JC1	5,5',6,6'-tetrachloro-1,1',3,3'tetraethyl-benzimidazolylcarbocyanine iodide
K_{2P}	Two-pore domain potassium channel
K_{IR}	Inward rectifier potassium channel
KO	Knockout
KSper	Potassium current in sperm / channel responsible for Ksper
K_V	Voltage-gated potassium channel
M540	Merocyanine 540
MMP	Mitochondrial membrane potential
NCB	Na^+-dependent (Cl^-/HCO_3^-) exchanger
NPA motif	Asparagine, proline, alanine motif
ODF	Outer dense fibres
PAX	Paxilline
PD	Pore domain
PDO	1,3-propanediol
PFE	Poor-freezability ejaculate
PHL	Phloretin
PI	Propidium iodide
PKA	Protein kinase A
PKC	Protein kinase C
PMOT	Progressive motility
PNA	Peanut agglutinine

pY	Tyrosine phosphorylation
ROS	Reactive oxygen species
RT-PCR	Real time-PCR
RVD	Regulatory volume decrease
sAC	Soluble adenylyl cyclase
sc-RNAseq	Single cell RNA sequencing
SEM	Standard error of the mean
SFK	Src family of kinases
SLC	Solute carrier
sNHE	Sperm-specific NHE
superAQP	Superaquaporin
T1	Tetramerisation domain
TEA	Tetraethyl ammonium
TM	Transmembrane helix
TMOT	Total motility
trAC	Transmembrane adenylate cyclase
TRP	Transient receptor potential
VCL	Curvilinear velocity
VSD	Voltage-sensing domain
VSL	Straight line velocity
WB	Western blot
ZP	Zona pellucida

List of figures

Introduction

Paper I

Paper II

Paper III

Paper IV

Paper V

List of tables

Paper IV

General contents

Abstract/Resum/Resumen

Abstract

The spermatozoon is a highly specialised cell that travels along the female reproductive tract to deliver its genome into the oocyte, and encounters varying extracellular conditions during its journey. The physiological interaction with this varying environment is crucial for sperm to undergo capacitation, which is a process they must go through to acquire effective fertilising ability and trigger the acrosome reaction. Cryopreservation, which is the most efficient procedure for long-term storage of sperm, also challenges the male gamete because of the drastic changes in extracellular medium composition. The adaptation and physiological response to these variations in extracellular medium are related to the exchange of water and other molecules across the plasma membrane, but also across intracellular membranes. Considering their hydrophobicity, additional mechanisms to simple diffusion are needed to allow the flow of water and solutes through the aforementioned membranes. Water permeability is facilitated by aquaporins (AQPs), a family of transmembrane water channels. Different groups of AQPs present distinct structure and permeability: orthodox AQPs, aquaglyceroporins (GLPs) and superAQPs. While the presence and subcellular distribution of AQPs in sperm varies between different species, their main function is linked to osmoadaptation and is highly conserved between species. Voltage-gated proton channel (H_V1 or HVCN1) has also been identified in sperm from different species of mammals. Because it regulates proton flow through the plasma membrane, its permeability is linked to intracellular pH, which regulates capacitation-associated events. Finally, different types of potassium channels have been found in mammalian sperm. Although many different types of K^+ channels have been identified in mammalian cells, the SLO subfamily of channels seems to be highly relevant in sperm. Essentially, K^+ channels are crucial in sperm physiology through the regulation of plasma membrane potential, which activates different signalling pathways, including those driving capacitation-related events. Acknowledging the relevance of these three types of channels (AQPs, HVCN1 and K^+ channels) in sperm function, their involvement in mammalian sperm capacitation and cryopreservation was investigated in this Dissertation. For this

purpose, in the first study, the role of AQPs during *in vitro* capacitation of pig sperm was explored through the use of three different inhibitors. Cooper sulphate, a specific inhibitor of AQP3, caused a drastic increase in reactive oxygen species (ROS) levels, which could be related to the intracellular accumulation of these molecules, as they can permeate certain members of the AQPs family. The presence of mercury chloride, an unspecific inhibitor of all AQPs but AQP7, impaired membrane lipid disorder and sperm motility. Finally, the inhibition of all AQPs using silver sulfadiazine (AgSDZ) caused a drastic decrease in intracellular pH and tyrosine phosphorylation levels after the induction of acrosomal reaction. Three additional studies aimed to explore the role of AQPs during pig and horse sperm cryopreservation. For this purpose, three different inhibitors were added to cryopreservation media, and their effects were also evaluated separately in ejaculates with good (GFE) and poor cryotolerance (PFE). On the one hand, 1,3-propanediol (PDO), an efficient inhibitor of orthodox AQPs with a mild inhibitory effect on GLPs, maintained better post-thaw sperm quality compared to control samples, suggesting that this molecule has a cryoprotective role in both species. Acetazolamide (AC), an inhibitor of AQP1 and AQP4, had some detrimental effects that could occur as a collateral impact on other sperm proteins. Finally, phloretin (PHL), which inhibits AQP3 and AQP7, impaired post-thaw sperm quality drastically. In addition, when GFE and PFE samples were analysed separately, GFE were more sensitive to positive effects, whereas PFE were less resilient to detrimental effects on their post-thawing quality. The last study aimed to explore the relevance of HVCN1 and K^+ channels, with a special focus on SLO1, during pig sperm cryopreservation; to this end, three different inhibitors were added to the cryopreservation medium. Paxilline (PAX), a specific inhibitor of SLO1, did not alter sperm quality and function after thawing. Similarly, the unspecific inhibition of 6TM K^+ channels through tetraethyl ammonium (TEA) did not cause significant effects on sperm cryotolerance. Yet, when 2-guanidino benzimidazole (2-GBI) was used as a specific inhibitor of HVCN1, sperm experienced a dramatic impairment in their function and survival after cryopreservation, including alterations in membrane integrity, including

mitochondrial, plasma and acrosomal membranes; and ROS levels. In conclusion, the results of this Dissertation support that membrane channels have a crucial role during both capacitation and cryopreservation processes, which might be in relation to osmoadaptability and intracellular pH regulation. Alterations in the permeability of membrane channels have drastic consequences for sperm quality and function, the most relevant alterations being an impairment of membrane structure and an increase in ROS levels.

Resum

L'espermatozoide és una cèl·lula altament especialitzada que viatja a través del tracte reproductor femení per fer arribar el seu genoma a l'oòcit; al llarg d'aquest aquest recorregut troba condicions extracel·lulars variables. La interacció fisiològica amb aquest entorn variable és crucial per la capacitació de l'espermatozoide, que és un procés necessari per l'adquisició de la seva capacitat fecundant i que culmina amb la reacció acrosòmica. La criopreservació, que és el procediment més eficient per la conservació d'espermatozoides a llarg termini, també suposa un repte pel gàmeta masculí a causa dels canvis dràstics en la composició del medi extracel·lular que es produeixen al llarg del procés de congelació i descongelació. L'adaptació i la resposta fisiològica a aquests canvis en el medi extracel·lular estan estretament lligades a l'intercanvi d'aigua i altres molècules a través de la membrana plasmàtica, i també a través de les membranes intracel·lulars. Tenint en compte la seva hidrofobicitat, calen altres mecanismes a banda de la difusió simple per tal de permetre el flux d'aigua i de soluts a través d'aquestes membranes. El transport d'aigua és possible gràcies a les aquaporines (AQPs), una família de canals transmembrana d'aigua. Les AQPs es poden classificar en diferents grups, que presenten variacions estructurals i de permeabilitat a diferents soluts: les AQPs ortodoxes, les aquagliceroporines (GLPs) i les superAQPs. Tot i que la presència i la distribució subcel·lular dels diferents tipus d'AQPs a l'espermatozoide varien entre les diferents espècies, el seu paper està relacionat amb l'osmoadaptació i és altament conservat entre elles. També s'han identificat en espermatozoides de diverses espècies els canals de protons operats per voltatge (H_V1 o HVCN1). Aquests canals regulen el flux de protons a través de la membrana plasmàtica i, per tant, la seva funció està lligada a canvis en el pH intracel·lular, que regula els esdeveniments associats al procés de capacitació. Finalment, també s'han trobat diferents tipus de canals de potassi en espermatozoides de mamífer i, tot i que se n'han identificat de diferents tipus, la subfamília de canals SLO sembla ser especialment rellevant. Essencialment, els canals de K^+ tenen un paper clau en la fisiologia espermàtica a través de la regulació del potencial de membrana, que activa diferents vies de senyalització, entre els

quals aquelles que estan involucrades en la capacitació. Considerant la rellevància d'aquests tres tipus de canals (AQPs, HVCN1 i K^+) en la fisiologia espermàtica, en aquesta Tesi s'ha explorat la seva possible funció durant la capacitació i la criopreservació dels espermatozoides de mamífer. Amb aquest objectiu, en el primer estudi es va avaluar el paper de les AQPs durant la capacitació *in vitro* d'espermatozoides de porc utilitzant tres inhibidors diferents. El sulfat de coure, un inhibidor específic de l'AQP3, va causar un augment dràstic en els nivells d'espècies reactives d'oxigen (ROS), que podria estar estretament relacionat amb l'acumulació intracel·lular d'aquestes molècules, atès que certs membres de la família de les AQPs en poden permetre el flux. La presència del clorur de mercuri, un inhibidor de totes les AQPs excepte l'AQP7, va augmentar el desordre lipídic de membrana i va disminuir la motilitat espermàtica. Finalment, la inhibició de totes les AQPs amb sulfadiazina de plata (AgSDZ) va comportar una alteració significativa del pH intracel·lular i dels nivells de fosforilació de tirosines després d'induir la reacció acrosòmica. Els següents tres estudis tenien l'objectiu d'explorar el paper de les AQPs durant la criopreservació espermàtica porcina i equina. Amb aquest propòsit es van afegir tres inhibidors al medi de criopreservació, i els seus efectes es van avaluar també separadament en ejaculacions amb bona (GFE) i mala criotolerància (PFE). D'una banda, el 1,3-propanediol (PDO), que és un inhibidor que té més afinitat per les AQPs ortodoxes que per les GLPs, va permetre un millor manteniment de la qualitat espermàtica després de la congelació en comparació amb les mostres control, fet que va suggerir que aquesta molècula podria tenir un paper crioprotector en ambdues espècies. L'acetazolamida (AC), un inhibidor de l'AQP1 i l'AQP4, va provocar efectes perjudicials que podrien ser causats per un efecte col·lateral sobre altres proteïnes espermàtiques. Finalment, la floretina (PHL), que inhibeix l'AQP3 i l'AQP7, va induir una reducció dràstica de la qualitat espermàtica després de la descongelació. A més, quan es van analitzar per separat les mostres corresponents a GFE i PFE, les GFE eren més sensibles als efectes beneficiosos, mentre que les PFE van mostrar menys resistència als efectes perjudicials després de la descongelació. L'últim estudi tenia com a objectiu explorar la rellevància dels canals HVCN1 i els canals de K^+ durant la

criopreservació espermàtica de porc, fent èmfasi en el canal SLO1; amb aquest objectiu es van afegir tres inhibidors diferents al medi de criopreservació. La paxil·lina (PAX), un inhibidor específic del SLO1, no va causar alteracions sobre la qualitat ni la funció espermàtiques després de la descongelació. De manera similar, la inhibició no específica dels canals de K^+ 6TM amb tetraetilamoni (TEA) no va tenir efectes significatius sobre la criotolerància espermàtica. Tot i així, quan es va utilitzar 2-guanidinobenzimidazol (2-GBI) com a inhibidor específic del canal HVCN1, es va observar una alteració dràstica de la qualitat espermàtica després de la criopreservació, incloent una alteració de les membranes mitocondrials, plasmàtiques i acrosòmiques, així com dels nivells de ROS. En conclusió, els resultats d'aquesta Tesi indiquen que els canals de membrana tenen una funció important durant els processos de capacitació i de criopreservació espermàtiques, que podrien estar lligats a l'osmoadaptabilitat i a la regulació del pH intracel·lular. L'alteració de la permeabilitat dels canals de membrana té conseqüències dràstiques per la qualitat i funció espermàtiques, entre les quals cal destacar les alteracions estructurals de la membrana i l'increment del contingut de ROS a nivell intracel·lular.

Resumen

El espermatozoide es una célula altamente especializada que viaja a través del tracto reproductor femenino para hacer llegar su genoma al oocito; a lo largo de este recorrido encuentra condiciones extracelulares cambiantes. La interacción fisiológica con este entorno variable es crucial para la capacitación del espermatozoide, que es un proceso necesario para la adquisición del poder fecundante y culmina con la reacción acrosómica. La criopreservación, que es el procedimiento más eficiente para la conservación de espermatozoides a largo plazo, también supone un reto para el gameto masculino debido a los cambios drásticos en la composición del medio extracelular que se producen durante el proceso de congelación y descongelación. La adaptación y respuesta fisiológica a estos cambios en el medio extracelular están estrechamente ligadas al intercambio de agua y otras moléculas a través de la membrana plasmática, pero también a través de las membranas intracelulares. Dada su hidrofobicidad, el flujo de agua y de solutos a través de las membranas requiere de mecanismos alternativos a la difusión simple. El transporte de agua es posible gracias a las acuaporinas (AQPs), una familia de canales transmembrana de agua. Las AQPs pueden clasificarse en distintos grupos, que presentan variaciones estructurales y de permeabilidad a diferentes solutos: las AQPs ortodoxas, las aquagliceroporinas (GLPs) y las superAQPs. A pesar de que la presencia y distribución subcelular de los diferentes tipos de AQPs en el espermatozoide varía entre las diferentes especies, su papel está relacionado con la osmoadaptación y está altamente conservado entre ellas. También se han identificado en espermatozoides de diversas especies los canales de protones operados por voltaje (H_V1 o HVCN1). Estos canales regulan el flujo de protones a través de la membrana plasmática y, por lo tanto, su función está ligada con variaciones en el pH intracelular, que regula los cambios asociados al proceso de capacitación. Por último, también se han encontrado diferentes tipos de canales de potasio en espermatozoides de mamífero, siendo la subfamilia de canales SLO especialmente relevante en el espermatozoide. Esencialmente, los canales de K^+ desempeñan un papel clave en la fisiología espermática a través de la regulación del potencial de membrana, que activa diferentes vías de señalización, incluyendo

las que están involucradas en la capacitación. Considerando la relevancia de estos tres tipos de canales (AQPs, HVCN1 y K^+) en la fisiología espermática, en esta Tesis se ha explorado su posible función durante la capacitación y la criopreservación de los espermatozoides de mamífero. Con este objetivo, en el primer estudio se evaluó el papel de las AQPs durante la capacitación *in vitro* de espermatozoides de cerdo utilizando tres inhibidores distintos. El sulfato de cobre, un inhibidor específico de AQP3, causó un aumento drástico en los niveles de especies reactivas de oxígeno (ROS), que podría estar estrechamente relacionado con la acumulación intracelular de estas moléculas, ya que ciertos miembros de la familia de las AQPs pueden permitir su paso. La presencia del cloruro de mercurio, un inhibidor de todas las AQPs excepto el AQP7, produjo un aumento del desorden lipídico de la membrana y una disminución de la motilidad espermática. Por último, la inhibición de todas las AQPs con sulfadiazina de plata (AgSDZ) indujo una alteración significativa del pH intracelular y de los niveles de fosforilación de tirosinas después de la inducción de la reacción acrosómica. Los siguientes tres estudios tenían el objetivo de explorar el papel de las AQPs durante la criopreservación espermática porcina y equina. Con este propósito se añadieron tres inhibidores en el medio de criopreservación, y sus efectos se evaluaron también separadamente en eyaculaciones con buena (GFE) y mala criotolerancia (PFE). Por un lado, el 1,3-propandiol (PDO), que es un inhibidor con más afinidad por las AQPs ortodoxas que por las GLPs, permitió un mejor mantenimiento de la calidad espermática después de la congelación en comparación con las muestras control, lo que sugirió que esta molécula puede desempeñar un papel crioprotector en ambas especies. La acetazolamida (AC), un inhibidor de AQP1 y AQP4, desencadenó efectos perjudiciales que podrían ser causados por un efecto colateral sobre otras proteínas espermáticas. Finalmente, la floretina (PHL), que inhibe AQP3 y AQP7, causó una reducción drástica de la calidad espermática después de la descongelación. Además, cuando se analizaron por separado las muestras correspondientes a GFE y PFE, las muestras de GFE fueron más sensibles a los efectos beneficiosos, mientras que las muestras PFE mostraron menor resistencia a los efectos perjudiciales después de la descongelación. El último

estudio tenía como objetivo explorar la relevancia de los canales HVCN1 y los canales de K^+, especialmente SLO1, durante la criopreservación espermática de cerdo, y con este objetivo se añadieron tres inhibidores distintos al medio de criopreservación. La paxilina (PAX), un inhibidor específico del SLO1, no causó alteraciones sobre la calidad ni la función espermáticas después de la descongelación. De forma similar, la inhibición no específica de los canales de K^+ 6TM con tetraetilamonio (TEA) no tuvo efectos significativos sobre la criotolerancia espermática. Sin embargo, cuando se utilizó 2-guanidinobenzimidazol (2-GBI) como inhibidor específico del canal HVCN1, las muestras espermáticas experimentaron una reducción drástica de la calidad espermática después de la criopreservación, incluyendo una alteración de las membranas mitocondriales, plasmáticas y acrosómicas, así como de los niveles de ROS. En conclusión, los resultados de esta Tesis indican que los canales de membrana tienen una función importante durante los procesos de capacitación y criopreservación espermáticas, que podría estar ligada a la osmoadaptabilidad y a la regulación del pH intracelular. La alteración de la permeabilidad de los canales de membrana tiene consecuencias drásticas sobre la calidad y función espermáticas, entre las cuales cabe destacar las alteraciones estructurales de la membrana y el incremento de los niveles de ROS a nivel intracelular.

Introduction

Introduction

1 Mammalian sperm

The male gamete, i.e., the spermatozoon, is a highly differentiated cell type, which is optimised for its function: traveling along the female reproductive tract to reach the oocyte and propagate the paternal genes. This optimisation requires the sperm cell to be motile, streamlined for speed and efficient in fertilisation (Alberts et al., 2008). Furthermore, in contrast to the oocyte, which is usually among the biggest cells in an organism, sperm cells are often the smallest. In domestic mammalian species, the size ranges from 50 µm in pigs to 90 µm in cattle (reviewed by (Pesch and Bergmann, 2006)).

Sperm cells present a characteristic structure, which consists of two main parts: the head and the tail, that are connected through the neck. In terms of organelles, sperm do not contain endoplasmic reticulum or Golgi apparatus, because they are not needed for their main function: the delivery of their DNA to the oocyte (Alberts et al., 2008). In spite of that, sperm present a Golgi-derived organelle, the acrosome, which contains digestive enzymes that are released via exocytosis to pass through the outer layers of the oocyte (Khawar et al., 2019). Nevertheless, mitochondria are highly abundant in sperm cells, because sperm motility requires an efficient power source and these organelles also play a significant role during capacitation (Alberts et al., 2008). In addition, the plasma membrane surrounds the sperm cell and presents a distribution of its lipids and proteins in surface domains. These domains are relevant for specific features of sperm physiology, including the fusion with the oocyte plasma membrane (Bearer and Friend, 1990).

1.1 Head

The sperm head contains the haploid nucleus, which is highly condensed to minimise its volume. To achieve this high degree of compaction, sperm chromatin is almost completely packed in protamines instead of histones, the latter being

almost completely replaced by the former during spermatogenesis. Some regions of the sperm genome, nevertheless, remain attached to sperm-specific histones (reviewed by (Schagdarsurengin et al., 2012)), and appear to be crucial for the organization of chromatin. While the high level of compaction allows sperm to be more hydrodynamic, it also causes a loss of transcriptional activity (Grunewald et al., 2005).

In an apical position to the sperm nucleus, the acrosome, a cap-like structure that covers two thirds of the sperm head, is localised. The acrosome is a vesicle that consists of an outer membrane, that is below the plasma membrane, and an inner membrane, that is close to the nuclear membrane (reviewed by (Pesch and Bergmann, 2006)). It contains hydrolytic enzymes, such as acrosin and hyaluronidase among others, that are released to help the penetration of the layers of cumulus cells and the zona pellucida that surround the oocyte. The content of the acrosome is released during the acrosome reaction (AR), which is triggered following the fusion of the outer acrosomal membrane with the plasma membrane of the spermatozoon (Barros et al., 1967).

1.2 Neck

The neck is a short segment that links the sperm head with the flagellum and serves as a connecting piece that articulates the movement of the tail. It is formed by the segmented columns and the capitulum, a dense fibrous structure. The proximal centriole is next to the capitulum, whereas the distal one is absent in mature sperm since it develops into the basal body, which attaches the flagellum to the sperm nucleus during spermatogenesis (reviewed by (Pesch and Bergmann, 2006)). Briefly, two major and five minor columns differentiate around the distal centriole, and the major columns then divide into two. After that, nine columns are formed together with nine outer dense fibres (ODF), which originate at the junction between the neck and the tail (reviewed by (Lehti and Sironen, 2017).

1.3 Tail

From proximal to distal, the sperm tail is divided into three different regions: the midpiece, the principal piece and the end piece. Regarding its structure, the sperm tail is a modified flagellum with some characteristics that are added to the basic structure of 9×2+2 axonemal microtubules of most flagella. In mammalian sperm, the central pair surrounded by nine pairs of microtubules is enclosed by nine ODF (Lindemann and Lesich, 2016). In the midpiece, one also finds the mitochondrial sheath, which consists of a layer of mitochondria arranged in circles that encircles the ODF. Mid- and principal pieces are connected by the annulus, which is formed by closely packed filaments that prevent mitochondria displacement during tail movement (reviewed by (Pesch and Bergmann, 2006)). In the principal piece, the mitochondrial sheath is replaced by a fibrous one, which forms two thickenings named lateral columns of the sheath that stand in lieu of two ODFs. In the principal piece, therefore, there are two lateral columns and seven ODFs surrounding the nine pairs of microtubules (reviewed by (Lindemann and Lesich, 2016)). Near the tip of the tail, the fibrous sheath ends abruptly, the ODFs also disappear and the central pair of microtubules is sometimes absent. In this distal portion of the flagellum, which is known as the end piece, the 9×2+2 microtubule structure is replaced by 18 single microtubules (reviewed by (Pesch and Bergmann, 2006)).

2 Sperm physiology

When sperm complete spermatogenesis and they reach the lumina of the seminiferous tubules, they are structurally formed, but they must still undergo major changes to gain full fertilizing capacity. These changes are named sperm maturation, which occurs in the male reproductive tract, and capacitation and acrosome reaction, that take place in the female tract. Only a few from all the sperm that are produced during spermatogenesis undergo these changes successfully and complete the journey towards the oocyte (Johnson, 2007).

2.1 Sperm epididymal maturation

Upon completion of spermatogenesis, sperm are not motile, therefore their transport through the *rete testis* and the efferent ducts towards the epididymis is facilitated through the flow of the surrounding fluid; in contrast, the sperm transport in the epididymis is driven by epididymal musculature contraction (Johnson, 2007). Efferent ducts start absorbing the fluid carrying sperm, and so does the epididymis in a decreasing trend, which increases sperm concentration progressively (Hess et al., 1997). This fluid reabsorption is oestrogen-dependant and is carried out through the coordinated function of both electrolyte and water channels (reviewed in (Joseph et al., 2011)).

In addition to an increase in concentration, sperm interact with epididymal secretions during their passage through the epididymis and, as a consequence, they undergo a series of modifications on their surface. These changes include an increase in the total negative charge, because of an increase in sialic acids in the sperm glycocalyx (Ma et al., 2016); modifications of lectin-binding proteins; changes in membrane lipid composition; and remodelling of plasma membrane structures, which comprehend surface antigen relocalisation and modifications to surface glycoproteins, including coating with epididymal-secreted proteins (reviewed in (Sullivan and Mieusset, 2016)). In addition, sperm also undergo structural changes, including the migration of the cytoplasmic droplet along the sperm tail and its shedding, the reshaping of the acrosome and changes in sperm chromatin (Robaire and Hinton, 2015). Concerning motility, sperm are immotile when they reach the epididymis, and acquire the ability to swim progressively, thus making them able to move forward and vigorously after being released from the male tract (Cooper and Yeung, 2006). This is possible due to an increase in cyclic adenosine monophosphate (cAMP) content and in the number of disulphide linkages between proteins in ODFs from the tail, which, in turn, makes the tail more rigid and rises its beating (Johnson, 2007).

Furthermore, the cauda epididymis is the major site for storage of sperm. The time of storage in this region differs among species, and ranges from several

months to a few days only, which is the case of human sperm (Robaire and Hinton, 2015).

2.2 Ejaculation and transport through the female reproductive tract

After leaving the cauda epididymis, sperm enter the *vas deferens* until ejaculation takes place, when sperm and seminal plasma are mixed. Seminal plasma is derived from accessory sex glands, which includes seminal vesicles, the prostate gland, and bulbourethral glands, in addition to the secretions of the epididymis (Mesiano and Jones, 2016). The composition of seminal plasma varies between different species, but also between individuals from the same species and even between ejaculates from the same individual. Even though sperm retrieved from the *vas deferens* are able to fertilise oocytes *in vitro*, they require a fluid vehicle for their transport after ejaculation, a function that is supplied by the seminal plasma. The seminal plasma, nevertheless, is not just a transport medium, but also a buffer to alkalinise the acid pH of the female tract, and a source of nutritional factors such as fructose and other monosaccharides, and of reducing agents to protect against potential oxidation following the exposure of sperm to atmospheric oxygen (Johnson, 2007). In addition, the interaction between sperm and seminal plasma activates sperm motility, delays capacitation to avoid a premature acrosome reaction, protects sperm from phagocytosis and assists sperm-oocyte interaction. Moreover, seminal plasma has an immunoregulatory role towards the female reproductive tract, which is beneficial for sperm survival during their transit towards the oocyte (reviewed in (Juyena and Stelletta, 2012)).

2.3 Transport through the female reproductive tract

After deposition in the female tract, sperm must reach the site of fertilisation. During this journey, few sperm survive. Some species, such as pigs, deposit sperm directly into the uterus, but in species with vaginal deposition (such as human and cattle), a significant proportion of sperm do not even reach the cervix, which is the first major barrier for sperm (reviewed in (Kölle, 2022)).

Once in the cervix, sperm are nourished by mucous secretions in the crypts, and they progress towards the uterus when the cyclic consistence of the mucus allows it. Most sperm that present morphological or motility alterations, however, are prevented from moving forward at this point and struggle to get to the middle of the lumen (Johnson, 2007). In the lumen of the uterus, in addition to their own propulsion, sperm move into the ampulla helped by smooth muscle contraction of the myometrium and fluid currents that are set up by the action of uterine cilia (reviewed in (Kölle, 2022)). The uterotubal junction seems to act as an intermittent sphincter, which regulates the entry of sperm into the oviduct, and is the second major barrier that sperm encounter during their journal towards the oocyte (Johnson, 2007).

Once in the isthmus, sperm linger and become immotile, and bind temporarily to oviductal epithelial cells. This binding of sperm to the epithelium helps preserve their fertility while they are stored, and it also reduces the incidence of polyspermy, as sperm are released gradually. The mechanism through which sperm survival is maintained within the female is based on the prevention of capacitation, which is achieved by impeding the increase of intracellular levels of Ca^{2+} (reviewed in (Suarez, 2008)). The release of sperm from this reservoir relies on chemo-attraction signals that are produced by the cumulus-oocyte complex. In response to these chemical signals, the sperm surface undergoes some changes, including the shedding of decapacitation factors from the plasma membrane (reviewed in (Bailey, 2010)), and a cAMP-mediated increase of intracellular levels of Ca^{2+}. This is associated to a raise in sperm motility, with a switch to an hyperactive flagellar beating allowing sperm to swim away from the epithelial crypts towards the ampullary-isthmic junction, where fertilisation occurs (Johnson, 2007). Not only is hyperactivated motility important to escape from the reservoir, but also to penetrate the viscous mucus and to reorientate towards the chemical gradients that lead them to the oocyte. Moreover, this vigorous motility is needed to assist sperm to physically penetrate the cumulus matrix and the zona pellucida (reviewed in (Suarez, 2008)). In fact, this hyperactivation of sperm motility is linked to the removal of capacitation-preventing proteins that are

attached on the sperm surface (see section 2.4 Sperm capacitation and acrosome reaction).

2.4 Sperm capacitation and acrosome reaction

Sperm capacitation is the process that the male gamete must undergo to acquire the ability to fertilise an oocyte. This process occurs during the transport of sperm through the female reproductive tract, during which these cells meet constantly changing environments, from which sperm receive different chemical and thermic signals (Chang, 1951). Consequently, sperm undergo a series of morpho-functional modifications. It is important to highlight that, even though the main signal transduction events involved in this process are common to distinct species of mammals, there are some differences in the sequence of their activation during the capacitation process, as well as in the molecules involved in the signalling pathways.

First of all, during ejaculation sperm are exposed to atmospheric oxygen, inducing the formation of reactive oxygen species (ROS) including H_2O_2 (Johnson, 2007), which is a capacitating agent in small amounts but acts as an inhibitor at high concentrations (Rivlin et al., 2004). All these molecular and structural changes alter the sperm motility pattern to an hyperactivated motility, in which stronger, wider beats of the sperm tail allow a more vigorous and progressive movement. In addition, these changes render sperm responsive to signals encountered in the proximity of the oocyte, which themselves induce further changes in sperm and trigger the acrosome reaction (Johnson, 2007).

In terms of structural modifications, plasma membrane properties are changed, basically through the stripping of most of the glycoprotein coating from the sperm surface (Johnson, 2007). This loss results in changes to the surface charge as well as in the reorganisation and elimination of proteins and lipids from the sperm plasma membrane. This includes the loss of cholesterol, which increases membrane instability and fusibility (reviewed in (Suarez, 2007)). Albumin is the most used cholesterol acceptor in *in vitro* capacitation experiments, and it is present in high abundance in the oviduct. Albumin-mediated cholesterol efflux is

facilitated by phospholipid scrambling, which is one of the earliest capacitation events that is initiated through an increase in intracellular levels of bicarbonate. Specifically, bicarbonate activates the translocation of different phospholipids causing phospholipid asymmetry and phosphatidylserine exposure in the sperm head. While both human and mouse sperm require bicarbonate and albumin to undergo capacitation (reviewed in (Bailey, 2010)), pig sperm can elicit it in the absence of exogenous bicarbonate but not in the absence of albumin (Chaves et al., 2021). Therefore, even if bicarbonate and albumin seem to be the most relevant molecules to induce plasma membrane destabilisation, the 5% CO_2 atmosphere used to induce *in vitro* capacitation in pig sperm is enough to trigger capacitation-associated events. In fact, sperm present intracellular and extracellular carbonic anhydrases (CAs), which transform bicarbonate to CO_2 (and vice versa) at both sides of the membrane, since CO_2 it can diffuse across the plasma membrane ((Wandernoth et al., 2010, 2015); reviewed in (Puga Molina et al., 2018))

The increase in intracellular levels of bicarbonate also activates the cAMP/PKA pathway primarily through the activation of a soluble adenylyl cyclase (sAC), with calcium being a secondary activator of cAMP synthesis (Gadella and Harrison, 2000; Harrison and Miller, 2000; Flesch et al., 2001). Bicarbonate is found at high concentrations in both seminal plasma and the female reproductive tract, which supports that it plays a vital role during activation upon ejaculation and later during capacitation (reviewed in (Puga Molina et al., 2018)). Plasma membrane changes lead to an increase in calcium permeability. This influx is also facilitated by the loss of calmodulin from the sperm surface, which increases the responsiveness of the cell to calcium signalling (Johnson, 2007). The increase of PKA activity, a serine/threonine protein kinase that activates different tyrosine kinases via phosphorylation, causes a rise in tyrosine phosphorylation (pY) residues which, in turn, triggers motility hyperactivation (reviewed in (Puga Molina et al., 2018)). This hyperactivated motility is acquired through an increase in mitochondrial activity, which, in mice, has been demonstrated to be a downstream event of the PKA signalling pathway (Giaccagli et al., 2021).

Another extracellular factor that influences sperm capacitation is pH. During their transit through the female tract, sperm encounter an alkaline pH. Consequently, intracellular pH is also alkalinised (Parrish et al., 1989). While, because of its relevance during capacitation, the mechanisms of pH regulation have been explored, the exact mechanism is still to be unveiled. Different protein channels are involved in this regulation, such as voltage-gated proton channels (HVCN1), Na^+/H^+ exchangers (NHE), bicarbonate transporters (including the families of solute carriers SLC26 and SLC4) and the cystic fibrosis transmembrane conductance regulator (CFTR). The changes in the intracellular concentration of charged ions and pH underlie variations in plasma membrane potential (Em). In fact, plasma membrane is hyperpolarised during capacitation through an increase in the concentration of negative charges in the intracellular compartment in response to changes in the permeability of membrane to ions like K^+, Cl^- and Na^+ (reviewed in (Puga Molina et al., 2018)). In addition, membrane hyperpolarisation is involved in ion currents through voltage-gated channels, among which calcium influx to the cytoplasm is essential, because it plays a central role in capacitation via the regulation of sperm motility hyperactivation and acrosome reaction (reviewed in (Bailey, 2010)).

Another important event that occurs during capacitation and is triggered by the PKA signalling pathway is actin polymerisation. Actin polymerises between acrosomal and plasma membranes to prevent a premature acrosome reaction of highly destabilised membranes. In this state, the spermatozoon only lasts for a limited amount of time until the acrosome reaction occurs or, alternatively, until it dies. Actin depolymerisation is triggered by PKC signalling, which is activated by a drastic increase in intracellular levels of calcium and initiates the acrosome reaction (reviewed in (Breitbart et al., 2005)).

The acrosome reaction is triggered once the spermatozoon is in the oocyte vicinity and is a prerequisite for *in vivo* fertilisation. The acrosome reaction consists of acrosome swelling, fusion between the outer acrosome membrane and the overlying plasma membrane, and ends up with the release of the contents of the acrosome, and the exteriorisation of the inner acrosome membrane. These

morphological changes occur in conjunction with an increase in intracellular calcium, cAMP, and pH (Johnson, 2007). While the agent responsible for triggering the acrosome reaction *in vivo* has long been thought to be a molecule from the zona pellucida, IVF experiments suggest that this reaction occurs before the interaction of sperm with oocyte vestments. Related with this, the progesterone released by the cumulus cells appears to play a crucial function (Buffone et al., 2014a), as not only does it act as a chemoattractant for sperm but it also interacts with a plasma membrane receptor that activates the G protein-coupled transduction pathway leading to acrosome reaction (Harper et al., 2006). When sperm are in the vicinity of the cumulus-oocyte complex, they interact with its components, among which progesterone that is released by cumulus cells. Upon sperm undergoing the acrosome reaction nearby the cumulus cells, the acrosome content is released and the extracellular matrix that joins these cells is digested, thus allowing sperm penetration through them. After passing through the layers of cumulus cells, sperm bind the zona pellucida through specific receptors; this binding also appears to be important (Wu et al., 2006)(Florman and Fissore, 2015). Different glycoproteins, ZP1, ZP2, ZP3 and ZP4, constitute the zona pellucida in mammals. Three different classes of eutherian mammals can be defined based on the glycoproteins present in their zona pellucida: those that present four glycoproteins (human, chimpanzee, macaque, and rat); those that exclusively present ZP2, ZP3, and ZP4 (dog, cattle, and possibly pig, cat, and rabbit); and those containing ZP1, ZP2, and ZP3 (mouse) (Florman and Fissore, 2015). From these proteins, ZP2 is essential for the structural organisation of ZP3, whereas the latter binds a receptor of capacitated sperm. Previous evidence supports that binding of ZP2/ZP3 complexes to sperm is species-specific and is the major natural block to cross-species fertilisation. The sperm ligand for this complex seems to be β1,4-galactosyl transferase 1 (GalT 1), which is located in the anterior sperm membrane that overlies the acrosome. Because plasma membrane undergoes vesiculation during the acrosome reaction, the receptor for ZP3 is lost; consequently, this first binding is transient. Finally, it is also worth mentioning

that the penetration of cumulus cells layers and zona pellucida also requires sperm to exhibit hyperactivated motility (Johnson, 2007).

After the acrosome reaction, the inner acrosomal membrane is exposed, and when sperm finally reach the oocyte, membranes interact, bind and fuse. The inner acrosome membrane establishes the first interaction with oocyte vestments, but sperm equatorial and posterior head segments are the regions that establish a more stable interaction with the oocyte plasma membrane before gamete fusion (Florman and Fissore, 2015). Once the acrosome reaction has occurred, sperm have a very short lifespan. Hence, only those sperm that undergo the acrosome exocytosis close to the oocyte have a chance of fertilisation. For this reason, the sperm reservoir is crucial to slow down capacitation changes, and the gradual release of sperm extends the fertilisation window. The existence of a sperm reservoir, therefore, increases the probabilities of a capacitated spermatozoon to encounter a recently ovulated oocyte (Johnson, 2007).

3 Ion channels and sperm physiology

The composition of biological membranes is responsible for their intrinsic, but highly limited, permeability to different molecules; thus, the transport of water and metabolites through the plasma membrane is of high importance for the maintenance of cell function and survival (Watson, 2015), because the regulation of ion balance is essential for cell physiology. Since several cell functions rely on the passing of water and solutes through the plasma membrane, mechanisms other than simple diffusion are required. In effect, different systems of transport allow the exchange of ions across plasma membranes and membranes of intracellular organelles (Hille, 2001).

The Guide to Receptors and Channels (GRAC; (Alexander et al., 2011)) presents a compilation of membrane proteins that are involved in transmembrane exchange of molecules. These proteins are classified into seven different groups: G protein-coupled receptors (GPCR), ligand-gated ion channels, ion channels, catalytic receptors, nuclear receptors, transporters, and enzymes. Among these

groups of membrane proteins, this section focuses on ion channels and explores the characteristics of those that have been identified in mammalian cells, with a special emphasis on aquaporins, proton channels and potassium channels as well as other channels that have been found in sperm cells.

3.1 Ion channels in mammalian cells

Many channels (such as most Na^+, K^+, Ca^{2+} and some Cl^- channels) are voltage-gated, but others present a relative sensitivity to voltage and are mainly gated by second messengers or other mediators (such as certain K^+ and Cl^- channels, transient receptor potential (TRP) channels, ryanodine receptors and IP3 receptors). The differentiation between ion channels and ligand-gated channels or transporters is, therefore, slightly blurry (Alexander et al., 2011). There are, nevertheless, certain differences between these three groups: ligand-gated ion channels are exclusively opened by neurotransmitters, transporters are not simple pores in the membrane, and the transport of ions requires a conformational change to move them from one side of the membrane to the other.

The following table (**Table 1**) is a summary of the groups of ion channels that have been identified in mammalian cells, as well as the members of each group, the main gating stimulus for channel opening and the domain of expression in cells.

The following subsections explore the structural and physiological characteristics of three different groups of ion channels: aquaporins, voltage-gated ion channels and potassium channels.

Table 1. Classification of ion channels that are present in mammalian cells.

Group	Members	Molecules transported	Gated by	Site of expr.
Aquaporins (AQP)	Orthodox AQPs (AQP0/1/2/4/5/6/8)	H_2O (some ammonia, H_2O_2)	CO	PM, I
	Aquaglyceroporins (GLPs) (AQP3/7/9/10)	H_2O, glycerol (some ammonia, H_2O_2)	CO	PM
	SuperAQPs (AQP11/12)	H_2O, glycerol	CO	I
	Orthodox AQPs (AQP0/1/2/4/5/6/8)	H_2O (some ammonia, H_2O_2)	CO	PM, I
Voltage-gated proton channel	Hv1 (HVCN1)	H^+	Voltage	PM
Epithelial sodium channels	ENac	Na^+	CO	PM
Sodium leak channel, non-selective	$Na_Vi2.1$	Na^+	CO, downstream phosphorylation from SFKs	PM
Acid-sensing (proton-gated) ion channels (ASICs)	ASIC1-3	Na^+	Extracellular H^+	PM
Voltage-gated sodium channels	$Na_V1.1/1.9$	Na^+	Voltage	PM
Hyperpolarisation-activated, cyclic nucleotide-gated (HCN) channels	HCN1/4	K^+ and Na^+	Hyperpolarisation, cyclic nucleotides	PM

(Cont.)

Group	Members		Molecules transported	Gated by	Site of expr.
Potassium channels	2TM or inward-rectifier K channel family (K_{IR})	Classical K_{IR} channels ($K_{IR}2.1/2.4$)	K^+	Membrane potentials negative to K reversal potential	PM
		G protein-gated K_{IR} channels ($K_{IR}3.1/3.4$)		G protein-coupled receptor signalling	PM
		ATP-sensitive K^+ channels ($K_{IR}6.1/6.2$)		ATP	PM
		K^+ transport channels ($K_{IR}1.1$, $K_{IR}4.1/4.2$, $K_{IR}5.1$, $K_{IR}7.1$)		CO	PM
	4TM or two-pore domain K channels family (K_{2P}) ($K_{2P}1.1/7.1$, $K_{2P}9.1/10.1$, $K_{2P}12.1/13.1$, $K_{2P}15.1/18.1$)		K^+	CO	PM
	6TM family	Voltage-gated K_v subfamilies ($K_v1.1/1.8$, $K_v2.1/2.2$, $K_v3.1/3.4$, $K_v4.1/4.3$)	K^+	Voltage	PM
		KCNQ subfamily ($K_v7.1/7.5$)	K^+	Voltage, ligands	PM
		KCNH subfamily ($K_v10.1/10.2$, $K_v11.1/11.3$, $K_v12.1/12.3$)	K^+	Voltage	PM
		Ca^{2+}-activated Slo subfamily ($K_{Ca}1.1$, $K_{Ca}4.1/4.2$, $K_{Ca}5.1$)	K^+	$K_{Ca}1.1$ (Slo1): Ca^{2+}; $K_{Ca}4.1/4.2$ (Slack, Slick): Na^+; $K_{Ca}5.1$, Slo3: pH	PM
		Ca^{2+}-activated SK subfamily ($K_{Ca}2.1/2.3$, $K_{Ca}3.1$)	K^+	Ca^{2+}	PM
CatSper channels	CatSper1-4		Ca^{2+}	CO, Intracellular alkalinisation	PM

(Cont.)

Group	Members		Molecules transported	Gated by	Site of expr.
IP_3 receptor	$IP_3R1/3$		Ca^{2+}	$Ins(1,4,5)P_3$	I
Ryanodine receptor	RyR1/3		Ca^{2+}	Cytosolic Ca^{2+}, cytosolic ATP...	I
Voltage-gated calcium channels	$Ca_v1.1/1.4$, $Ca_v2.1/2.3$, $Ca_v3.1/3.3$		Ca^{2+}	Voltage	PM
Cyclic nucleotide-gated channels	CNGA1/3		Cations	Voltage, cyclic nucleotides	PM
Transient receptor potential (TRP) cation channels	TRPC (canonical)	TRPC1/C4/C5 subgroup	Cations	Downstream of $G_{q/11}$-coupled receptors, or receptor tyrosine kinases	PM, I
		TRPC3/C6/C7 subgroup			
	TRPM (melastatin)	TRPM1/M3 subgroup	Cations	Heat (TRPM3)	PM
		TRPM2 subgroup	Cations	Redox status, heat, Ca^{2+}	PM
		TRPM4/M5 subgroup	Cations, impermeable to Ca^{2+}	Heat	PM
		TRPM6/M7 subgroup	Cations	CA (TRPM6); cAMP (TRPM7)	PM
		TRPM8 subgroup	Cations	Cold	PM
	TRPA (ankyrin)	TRPA1	Cations	Environmental irritants	PM
	TRPV (vanilloid)	TRPV1/V4 subfamily	Cations	Heat (not TRPV2)	PM
		TRPV5/V6 subfamily	Ca^{2+}	CO	PM
	TRPML (mucolipin)	TRPML1/3	Cations	CO	I
	TRPP (polycystin)	TRPP2/3	Cations	CO	PM

(Cont.)

Group	Members		Molecules transported	Gated by	Site of expr.
Chloride channels	ClC family	ClC-1/2/Ka/Kb	Cl^-	CO, activable by Ca^{2+}, voltage, cell swelling...	PM
		ClC-3/4/5	Cl^-/H^+ (antiporter)		I
		ClC-6/7	Cl^-/H^+ (antiporter)		I
	CFTR		Cl^-	cAMP (PKA)	PM
	Ca^{2+}-activated Cl^- channel (CaCC)			Ca^{2+}	PM
	Maxi Cl^-			Voltage, cell swelling...	PM
	Volume regulated chloride channels (or volume regulated anion channel; VRAC)			Cell swelling	PM
Connexins (Cx) and pannexins (Px)	Cx23, Cx25, Cx26, Cx30, Cx30.2, Cx30.3, Cx31, Cx31.1, Cx31.9, Cx32, Cx36, Cx37, Cx40, Cx40.1, Cx43, Cx45, Cx46, Cx47, Cx50, Cx59, Cx62		Molecules of ≤1,000 Da	CO	PM
	Px1, Px2, Px3				

Abbreviations: CO, constitutively open; KCNQ, potassium channel family Q; KCNH, potassium channel family H; Vi, voltage insensitive; SFKs, Src family tyrosine kinases;

3.1.1 Aquaporins

Aquaporins (AQPs), a family of transmembrane proteins whose main function is to allow the transport of water across cell membranes, are present ubiquitously in all species and cell types (reviewed in (Törnroth-Horsefield et al., 2010)). Some AQPs also exhibit permeability to small molecules, such as glycerol (Abrami et al., 1995), urea (Ma et al., 1997), ammonia (Saparov et al., 2007), hydrogen peroxide (Bienert et al., 2007) and arsenite (Liu et al., 2002).

Among the members of the AQP family, gene sequence, structure and function are highly conserved. In terms of structure, AQPs present a central pore surrounded by six transmembrane α-helices (TM1-6; **Figure 1A**) that, when resolved through X-ray, presents an "hourglass" shape (**Figure 1B**) (Jung et al., 1994; Fu et al., 2000). Each transmembrane segment is connected to the adjacent ones by loops (A–E). Loops B and E are half-transmembrane helices and locate

towards the centre of the channel creating a broken seventh-transmembrane helix (**Figure 1A,B**; reviewed in (Törnroth-Horsefield et al., 2010)). Two highly preserved structural features that modulate channel permeability to different molecules are present in the pore region. On the one hand, loops B and E present a NPA motif (asparagine, proline, alanine) each, which is the typical AQP signature motif (reviewed in (Tani and Fujiyoshi, 2014)). Water crosses AQPs forming a single-molecule well along the channel, and interacts with the lateral chains of the amino acids that form the pore through hydrogen bonds. The NPA motif locks the central molecule of water in a conformation that avoids its reorientation, thus disrupting any potential proton conduction (Savage et al., 2003). On the other hand, another highly preserved feature is the selectivity filter, which is the narrowest point in the channel and provides it with size-dependant selectivity (Savage et al., 2003). The region near these residues is also known as aromatic/arginine (ar/R) constriction region (**Figure 1A**), because it presents an arginine residue that is highly conserved among all AQPs (Sui et al., 2001).

The functional, quaternary structure of AQPs consists of a tetramer, with each monomer presenting their own permeable pore (**Figure 1C**). Interactions between TM1 and TM2 from one monomer, and TM4 and TM5 from the adjacent one, are essential for tetramer stabilisation. This tetrameric structure leads to the formation of an additional central pore; however, to the best of the author's knowledge, its role remains largely unknown (reviewed in (Ozu et al., 2018)). From a functional point of view, tetramerisation appears to be crucial for AQP mechanosensitivity (**Figure 2**), as it has been described for AQP1 and AQP4 (Tong et al., 2012; Ozu et al., 2013). According to the model presented by (Hill and Shachar-Hill, 2015), increasing tension in the plasma membrane in response to cell swelling might cause slight distortions in the monomers in response to membrane stretching. As a consequence, formation of hydrogen bonds between AQP amino acids and water molecules inside the pore might be impaired, thus leading to a decrease in the water transport rate of AQPs (reviewed in (Ozu et al., 2018)).

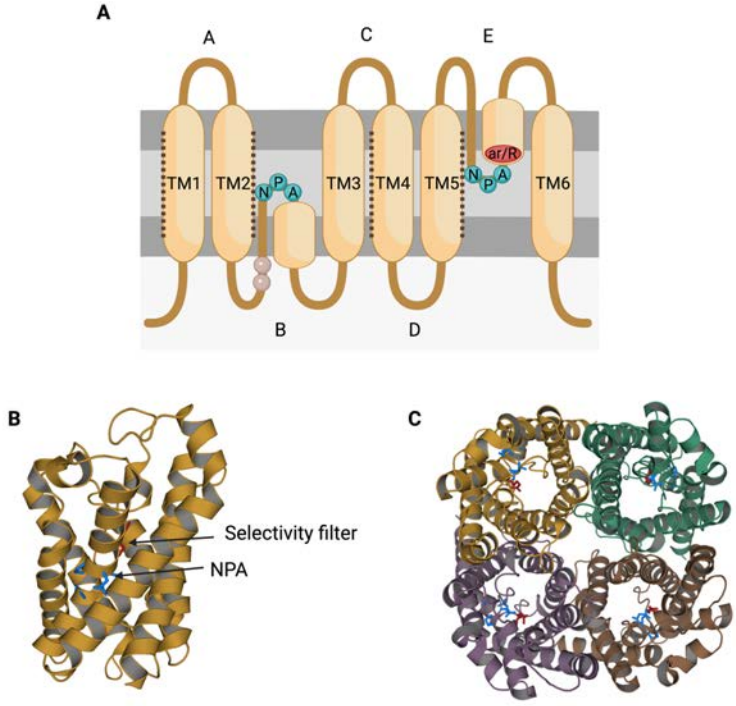

Figure 1. Structural characteristics of the family of aquaporins (AQPs). (A) Aquaporins present six transmembrane α-helices (TM1-6) connected through loops (A-E). Loops B and E are half-transmembrane helices oriented towards the centre of the pore that present a highly conserved NPA (asparagine, proline, alanine) motif. Some residues from loop B have been suggested to be involved in AQPs mechanosensitivity (light brown residues). In loop E, there is also a highly conserved arginine (R). The region near this R is formed by aromatic residues and is known as the aromatic/arginine (ar/R) region. Transmembrane helices TM1, TM2, TM4 and TM5 interact with TM of the adjacent monomers from an AQP tetramer (dark dot lines). (B) Each monomer folds in an hour-glass conformation. The ar/R region, which is also known as selectivity filter, forms the narrowest point of the AQP pore. After folding, the two NPA motifs are in the same region. (C) The quaternary structure of AQPs consists of the formation of tetramers, where each monomer has its own functional pore. This figure is based on PDB structure 6QZJ from AQP7. Modified from (Delgado-Bermúdez et al., 2022).

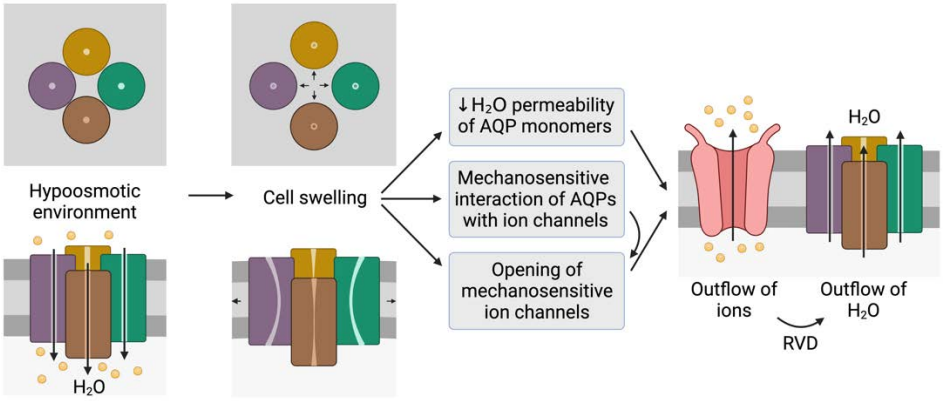

Figure 2. Representation of the mechanosensitive mechanism of aquaporins (AQPs). When cells encounter a hypotonic environment, they experience a water influx in response to solute concentration gradient. Consequently, cells may undergo swelling, which causes distortion in AQPs structure and decrease water permeability. Some AQPs present mechanosensitive interactions with ion channels that can trigger their opening and allow the outflow of ions. Moreover, some ion channels are mechanosensitive themselves, and open in response of cell swelling regardless of AQPs signalling. The outflow of ions generates a driving force that elicits the outflow of water; this process is also known as regulatory volume decrease (RVD). Modified from (Delgado-Bermúdez et al., 2022).

3.1.1.1 Aquaporin subfamilies

In spite of their highly preserved sequence and structure, the separate members of the AQP family present certain structural features that confer specific permeability to water and other molecules. Based on variations in their structure and selective permeability, AQPs can be classified into three different groups: orthodox AQPs, aquaglyceroporins (GLPs) and superAQPs (reviewed in (Ishibashi et al., 2009); (**Figure 3**).

The group of ***orthodox AQPs*** includes AQP0, AQP1, AQP2, AQP4, AQP5, AQP6 and AQP8. The channel diameter of orthodox AQPs is the smallest among the different groups of AQPs. This characteristic is highly related to the NPA motif, since in orthodox AQPs the side chains of the amino acids of this motif narrow the pore to a smaller diameter and are more hydrophilic than those of the other family members. Moreover, orthodox AQPs present a selectivity filter (Savage et al., 2003). These two structural properties confer to the members of this group of AQPs the exclusive permeability to water through a steric mechanism of selectivity (reviewed in (Huang et al., 2006)). The only exception in this group is AQP6,

which is also permeable to anions at low pH (Yasui et al., 1999a) and localises in intracellular organelles; remarkably, this differs from the plasma membrane localisation of the other orthodox AQPs (Yasui et al., 1999b).

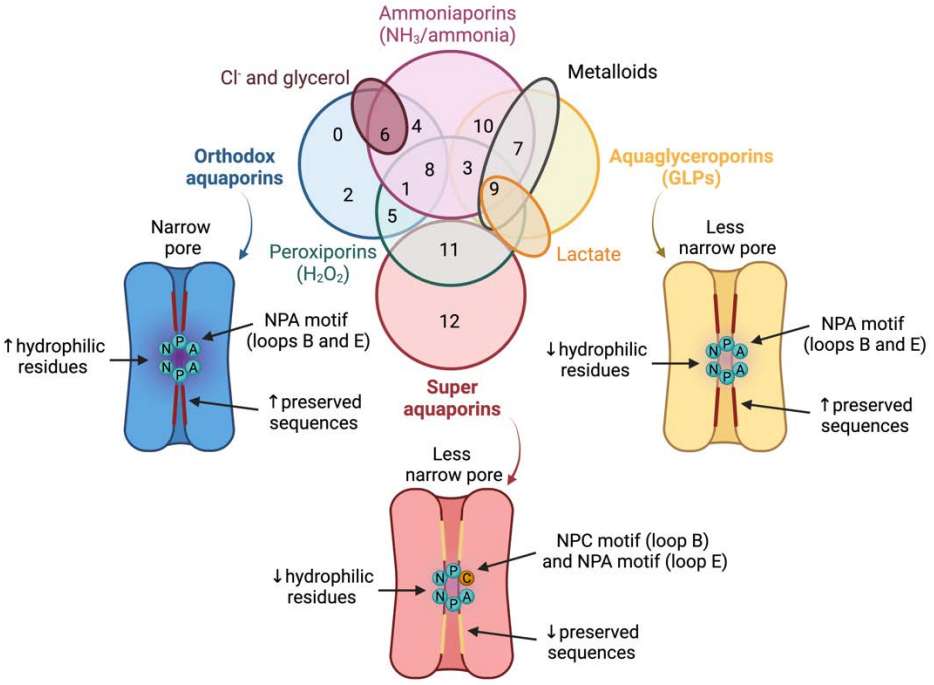

Figure 3. Classification of Aquaporins (AQPs). The three main groups into which AQPs are classified depending on their structure and permeability to different molecules are: orthodox AQPs (blue), aquaglyceroporins (GLPs; yellow) and superAQPs (red). Structural characteristics of these three groups are graphically represented and detailed in section 3.1.1.1. (*Groups of aquaporins*). In addition to the classical groups, some AQPs are classified as peroxiporins (green), as they present permeability to H_2O_2; others are considered ammoniaporins (pink), because they are permeable to ammonia and/or to NH_3. Other AQPs are permeable to other molecules, such as Cl^- (dark red), metalloids (grey) and lactate (orange). Modified from (Delgado-Bermúdez et al., 2022), with permission.

The group of ***GLPs*** includes AQP3, AQP7, AQP9 and AQP10. Water molecules also cross GLPs forming a single-molecule well as in orthodox AQPs. In GLPs, nevertheless, the pore is broader and less hydrophilic than in orthodox AQPs. These differences are due to variations in the NPA motif, whose orientation leads to a larger channel diameter. In addition, the region near the NPA motif is less hydrophilic than in orthodox AQPs and the selectivity filter has a hydrophobic patch of residues, which determines the lower hydrophilicity of this group of AQPs

(Savage et al., 2003). These two characteristics allow bigger molecules, together with water, to pass through GLPs.

It is worth noting that GLPs transport glycerol with preference to water. During fasting states, mammalian cells can obtain glycerol from the degradation of triglycerides in adipocytes; glycerol permeation is therefore highly important in these situations. In fact, AQP7 and AQP9 have been suggested as the entry and exit routes of glycerol in hepatocytes, where gluconeogenesis occurs (reviewed in (Agre et al., 2002)). Furthermore, the presence of GLPs in the plasma membrane, which facilitate glycerol transport, allows its use as a permeable cryoprotectant for cell preservation (Curry, 2007).

The GLPs AQP7 and AQP9 are also permeable to arsenite. Arsenite has been suggested as a treatment for promyelocytic leukaemia, because leukocytes express AQP9 (Liu et al., 2002). In fact, AQP9 is highly promiscuous in terms of permeability, since it transports a wide range of non-charged solutes, including polyols, purines (adenine), pyrimidines and urea, but is impermeable to amino acids, charged ions, cyclic sugars and nucleosides (Tsukaguchi et al., 1998).

The group of ***superAQPs*** includes AQP11 and AQP12. The members of this group present an endoplasmic reticulum (ER) retention signal at the carboxy-terminal region (reviewed in (Ishibashi, 2006)), and they are thus expressed intracellularly (Itoh et al., 2005; Morishita et al., 2005). Moreover, whereas orthodox AQPs and GLPs are highly homologous, superAQPs present a lower identity to the other groups of AQPs (reviewed in (Morishita et al., 2004)). On the one hand, the alanine of NPA in loop B is replaced by cysteine becoming an NPC motif; whereas the NPA motif in loop E is preserved (reviewed in (Ishibashi, 2006)). On the other hand, the sequences before and after the first and second NPA motifs are highly conserved in orthodox AQPs and GLPs, whereas they are different in superAQPs (reviewed in (Ishibashi, 2006)). As far as permeability is concerned, besides water, superAQPs have been identified as glycerol channels in human adipocytes (Madeira et al., 2014).

3.1.2 Voltage-gated proton channel HVCN1

The proton-selective channel HVCN1 is a voltage-gated ion channel. Voltage-gated ion channels regulate ion conductance in response to changes in voltage across the membrane. These channels share common structural and functional characteristics, such as a six transmembrane (TM) segment-structure, in which segments TM1-4 constitute the voltage-sensing domain (VSD) and segments TM5 and TM6 constitute the pore domain (PD). The VSD serves as a detector of voltage fluctuations and is formed by a series of positively charged aminoacidic residues distributed along the different TM segments. Changes in voltage cause a displacement of these residues, which is then transduced to the PD, leading to channel opening. Selectivity of the pore is determined by the presence of a selectivity filter in the PD (Gouaux and MacKinnon, 2005).

HVCN1 is a unique voltage-gated channel, because it only presents TM1-4 segments. Since it lacks the classical PD, proton permeation occurs through the VSD (**Figure 4**) (Takeshita et al., 2014). The TM4 segment presents multiple basic residues, which correspond to the functional voltage-sensing region. This segment moves upward relative to other helices during voltage-dependent gating (Gonzalez et al., 2010). Moreover, TM1 presents an acidic residue (Asp112 in human HVCN1), that is highly conserved among different species and is critical for proton selectivity (Musset et al., 2011). In addition to voltage, HVCN1 channel can be activated through phosphorylation of Thr29 by protein kinase C (PKC), which favours the open conformation of the channel (Musset et al., 2010).

The proton channel HVCN1 is expressed as a dimer in biological membranes, with every pore containing an independent proton pathway (Koch et al., 2008), each controlled by a different VSD (Tombola et al., 2008). Dimerization is possible through coiled-coil interactions at the C-terminus of the protein, but also through the interaction of the C-terminal region of TM1 with the loop between TM1 and TM2 (**Figure 4**) (Lee et al., 2008). In terms of proton permeation, cooperativity between different subunits of the dimer is essential, as TM4 segment in both subunits must move to activate the two proton pathways (Gonzalez et al., 2010).

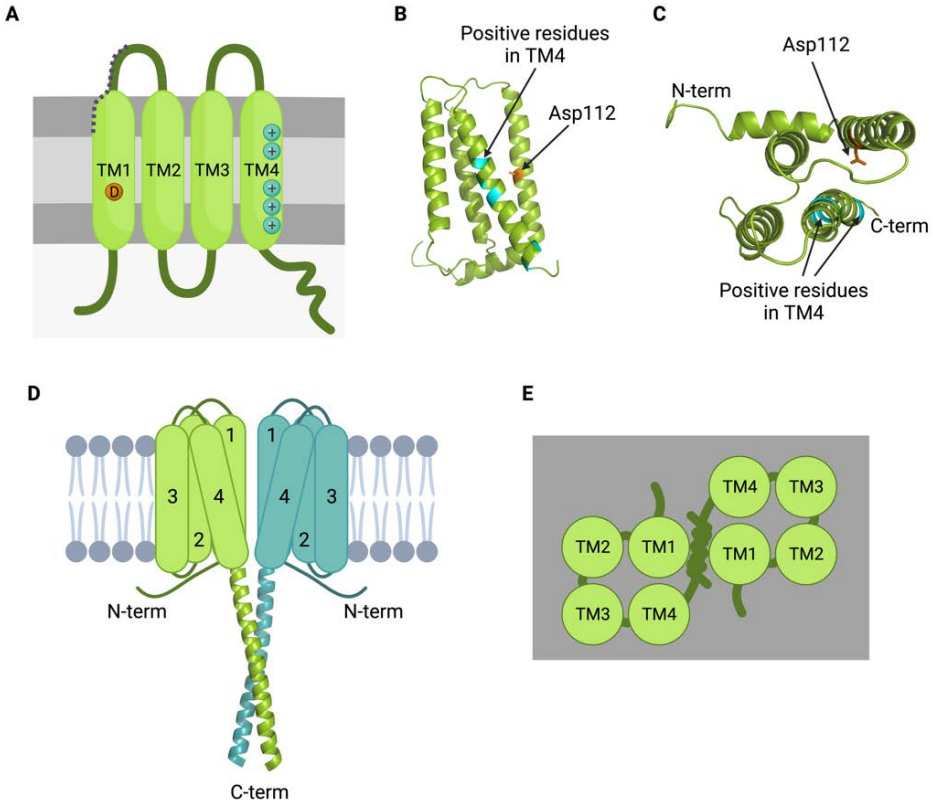

Figure 4 Structural characteristics of the voltage-gated proton channel (HVCN1). (A) The channel HVCN1 presents four transmembrane α-helices (TM1-4) connected through loops. In TM1, the residue Asp112 is highly conserved and is critical for proton selectivity (orange). TM4 segment presents multiple basic residues, which correspond to the functional voltage-sensing region (+). Both the loop between TM1 and TM2 (purple dot line) and the C-terminal coiled coil are essential for dimerization. (B,C) Each monomer folds to form a single ion permeation pathway that also contains the voltage sensing domain (VSD) (PDB reference 5OQK) (D) The quaternary structure of HVCN1 consists of a dimer; the two C-terminal coiled coils interact intracellularly (PDB reference 3VMX). (E) Dimers present two different permeation pathways.

3.1.3 Potassium channels

Potassium channels are a diverse family of transmembrane proteins that present K^+ permeability and are essential for the generation of electric currents across excitable membranes. The canonical structure of K^+ channels consists of two transmembrane helices and the connecting P loop (2TM/P), which presents the signature sequence (TXXTXGYG) and partially enters the pore (Heginbotham et al., 1994). The N-terminal domain is also known as tetramerisation domain (T1),

and the C-terminal domain is involved in protein-protein interaction. This basic structure of the ion conduction pore is preserved among the different subfamilies, which differ from one to another in terms of structure and physiological mechanisms of pore gating.

3.1.3.1 Groups of K^+ channels

Potassium channels are classified into three different families depending on their structure and permeability (**¡Error! No se encuentra el origen de la referencia.**).

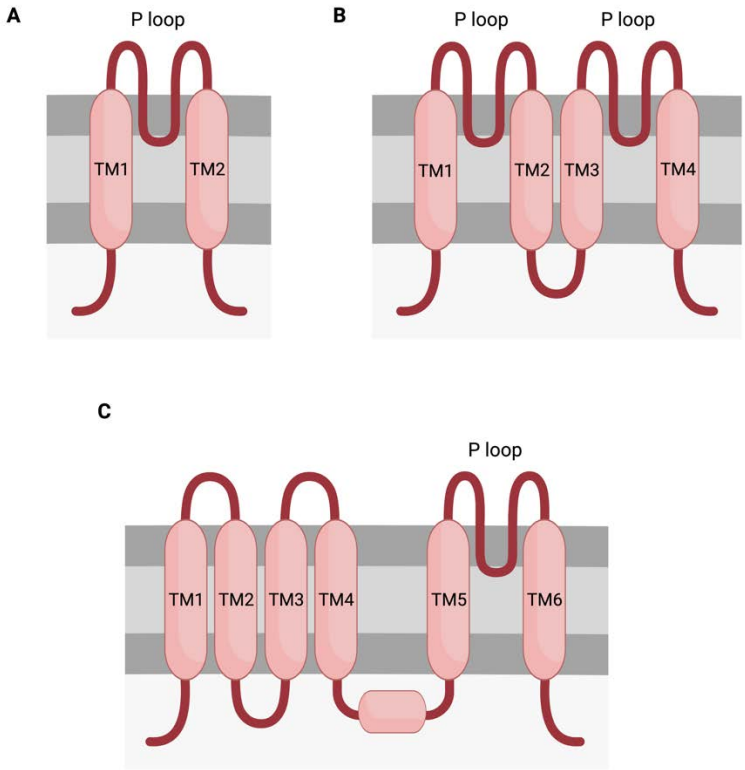

Figure 5. Classification of potassium channels. (A) The members of the 2TM/P family of K^+ channels present two transmembrane α-helices and a connecting P loop; this corresponds to the canonical structure of K^+ channels. (B) The members of the 4TM/2P family of K^+ channels contain two consecutive 2TM/P sequences. (C) The members of the 6TM/P family of K^+ channels have four transmembrane α-helices followed by a connecting loop and a 2TM/P sequence.

The ***2TM/P family*** of K^+ channels is mainly formed by inwardly rectifying (K_{IR}) channels, and their structure is strictly the 2TM/P. In contrast with other K^+ channels, the ion current in these channels flows inwardly. Different subfamilies of K_{IR} channels present different regulatory mechanisms: classical K_{IR} channels are constitutively active and present a strong inward rectification; G-protein gated K^+ channels show a low basal activity and are activated by membrane-bound G proteins; ATP-sensitive K^+ channels exhibit a strong basal activity and are inhibited by intracellular ATP; and K^+-transport channels, which participate in K^+ recycling and are frequently coupled to other mechanisms of K^+ transport across cell membranes (reviewed in (González et al., 2012).

The members of the ***4TM/2P family*** of K^+ channels consist of two repeats of the 2TM/P structure. While most of them are tandem pairs of two K_{IR}-like sequences, a few form ***8TM/2P*** channels through linking Kv-type and a K_{IR}-type in tandem. Instead of arranging in tetramers, the members of this subfamily presumably form dimers constituted by 4TM/2P or 8TM/2P monomers (reviewed in (Miller, 2000)). The members of this family are divided into six families depending on the regulatory mechanisms of ion transport: mechanogated, alkaline-activated, Ca^{2+}-activated, weak K_{IR}s, acid-inhibited and halothane-inhibited channels (reviewed in (González et al., 2012).

The members of the ***6TM/P family*** of K^+ channels consist of 4TM helices that precede the canonical 2TM/P permeation pore. To be fully functional, 6TM/P K^+ channels must form tetramers. This family includes different subfamilies: voltage-gated channels, including KCNA (K_V1 family), KCNB (K_V2), KCNC (K_V3), KCND (K_V4), KCNQ (K_V 7), KCNH (K_V 10, K_V11, and K_V12); SLO channels, that can be regulated by both Ca^{2+} and voltage; and small conductance (SK) channels, which are Ca^{2+}-activated K^+ channels (reviewed in (González et al., 2012).

3.1.3.2 Structure and regulatory mechanisms in K^+ channels

Most studies regarding the structure and physiology of K^+ channels have been focused on the study of voltage-gated K^+ channels; most information available, therefore, is based on their structure and dynamics (**Figure 6**).

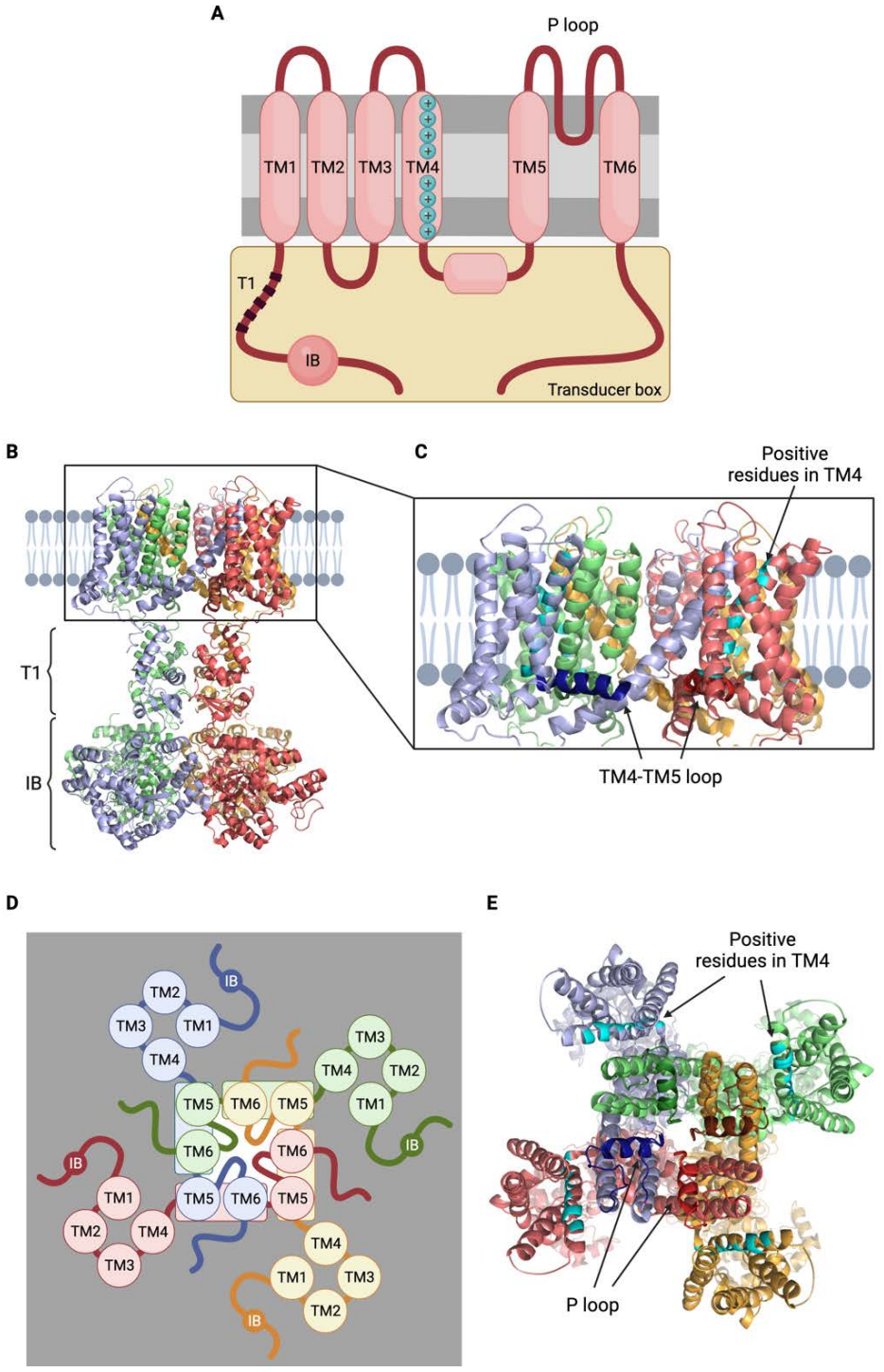

Figure 6. Structural characteristics of voltage-gated K^+ channels. (A) Voltage-gated K^+ channels present a large N-terminal domain, which includes the tetramerisation domain

(T1) and the inactivation ball (IB). The transmembrane segment TM4 presents a series of positively charged residues that participate in voltage sensing. The loop between TM4 and TM5 is the inactivation-ball-binding loop. (B) Voltage-gated K^+ channels arrange in tetramers and the regions corresponding to T1 and IB form a large intracellular domain. (C) Transmembrane domains from different monomers overlap. Darker residues highlight the TM4-5 connecting loop. (D) The tetrameric structure forms a central pore that involves TM5-6 and the connecting loop between TM4 and TM5 (squares) of each monomer, whereas TM1-4 are not directly involved in the structure of the central pore. (E) P loops (darker residues) are oriented towards the central pore, and the voltage-sensing domain (VSD) in TM4 (light blue) is found outside of the pore (PDB reference 7EJ1).

In ***voltage-gated K^+ channels***, TM1-4 form a module that controls pore gating, which is known as voltage-sensing domain (VSD). The first three segments are localised in the lipid-exposed periphery of the protein, whereas TM4 presents a characteristic sequence in which every third residue is positively charged, and the remaining ones are hydrophobic (reviewed in (Miller, 2000)). This sequence is known to be voltage-sensitive, and is also found in other channels that have reduced voltage sensitivity (reviewed in (Armstrong and Hille, 1998)). TM5-6 form the ion conduction pore, which is in contact with the connecting loop between TM4 and TM5 of an adjacent subunit (**Figure 6D**) (reviewed in (González et al., 2012).

The N-terminal sequences of K^+ channels are highly conserved across species, and different subunits from the same subfamily can co-assemble and form functional tetramers that arrange around the water-filled ion-conduction pathway (reviewed in (Miller, 2000)). This selective binding is determined by the tetramerisation domain (T1). The inactivation ball (IB) is a domain of approximately 30 amino acids at the N-terminal end of the protein that is capable of physically plugging the pore to inactivate ion conduction. It is present in some voltage-gated K^+ channels and is connected to T1 through a linker. Even though each tetramer presents four different inactivation balls, only one is needed to plug the ion permeation pathway (reviewed by (Choe, 2002)). When the inactivation ball is not blocking the permeation pathway, it is attached to the loop between TM4 and TM5, which is also known as inactivation-ball-binding loop (Isacoff et al., 1991). Concerning the C-terminal domain, it is involved in the protein-protein interactions that regulate channel opening and closing. There are different

examples of channel regulation by signalling pathways, such as the regulation of $K_{IR}3$ by G-protein-coupled receptors. Another example is the interaction of Kv1.5 with SRC and tyrosine kinase receptors, which indicates that this channel is phosphorylation-sensitive (reviewed by (Choe, 2002)).

Like other ion channels, pore selectivity occurs at the narrowest part of the ion-permeation pathway, which is known as the selectivity filter and is formed by certain residues of the P loop (Thr–Val–Gly–Tyr–Gly). The selectivity filter presents six K^+ binding sites. Because K^+ ions are surrounded by water molecules known as the hydration shell, the binding sites must recreate this shell to allow the dehydration of the ion, so oxygen atoms of carbonyl groups present in the pore chain form six oxygen squares that fit the K^+ ions. The transition from the non-conducting conformation to the ion-permeating one is frequently associated to global changes in response to different stimuli, that propagate conformational changes to the ion permeation pathway (reviewed by (Choe, 2002)).

TM4 has a gating function in voltage-gated K^+ channels, as depolarising voltage energetically favours an outward movement of TM4 that initiates channel opening (reviewed in (Miller, 2000)). After that, the transducer Box, which corresponds to the junction at which the transmembrane and the cytoplasmic domains meet, allows the coupling of conformational changes from different parts of the channel in response to different stimuli, which ends up leading to the opening and closing of the pore. The transducer box is formed by the membrane-facing side of T1, the loop between T1 and TM1, the inactivation-ball-binding loop between TM4 and TM5, and the gear near the C-terminus of TM6 (reviewed by (Choe, 2002)).

In terms of ***SLO channels***, they present, in addition to the VSD and the ion permeation pore, an extra transmembrane segment at the N-terminus, TM0, and four hydrophobic segments in the C-terminus cytosolic domain. These hydrophobic domains constitute two different regulators of K^+ conductance domains (RCK1 and RCK2), which present cation binding sites. Ion conduction is, therefore, regulated through both VSD and RCK domains. Whereas SLO1 and SLO3 are Ca^{2+}-sensitive, SLO2 is Na^+-gated. In addition, SLO3, which is exclusively

expressed in mammalian testis, is activated through intracellular alkalinisation, and the C-terminus is responsible for pH sensitivity (reviewed in (González et al., 2012).

Finally, ***SKCa channels*** are activated by an increase in intracellular calcium, but through a different mechanism to SLO channels. In this group of channels, a calmodulin binding domain at the C-terminus allows KCa channels to form a stable complex with calmodulin; this complex is involved in channel regulation. Moreover, despite presenting some positively charged residues in TM4, SKCa channels are voltage independent (reviewed in (González et al., 2012).

3.2 Implication of membrane channels in sperm physiology

In this section, the aforementioned groups of ion channels (i.e., AQPs, voltage-gated proton channels and potassium channels) are discussed in terms of the presence in mammalian sperm and their roles in sperm physiology.

3.2.1 Aquaporins in mammalian sperm

The presence and localisation of AQPs in sperm differ between species and cell domains. To date, the most investigated members of this protein family in mammalian sperm are AQP3, AQP7, AQP8 and AQP11, although AQP1 and AQP9 have also been identified in certain species (**Table 2**).

Table 2. Members of the family of aquaporins (AQPs) identified in sperm from different species of mammals. Different species, where the presence of each member of the AQPs family has been evaluated are detailed.

Aquaporin	Species	Strategy of Detection	Methodology	Reference
AQP1	Not in sheep	Protein	WB	(Curry et al., 1995)
	Not in human	mRNA, protein	RT-PCR, WB	(Liu et al., 1995; Yeung et al., 2010)
	Not in mouse	Protein	IHC	(Lu et al., 2008)
	Dog	mRNA, protein	RT-PCR, WB	(Ito et al., 2008)

(Cont.)

Aquaporin	Species	Strategy of Detection	Methodology	Reference
AQP3	Mouse	Protein	IF, IGEM	(Chen et al., 2011)
	Human	mRNA, protein	IF, WB, ICC, RT-PCR, FC	(Chen et al., 2011; Laforenza et al., 2017; Alyasin et al., 2020)
	Pig	Protein	WB, IF	(Prieto-Martínez et al., 2015)
	Horse	Protein	WB	(Bonilla-Correal et al., 2017)
	Cattle	Protein	WB, ICC	(Prieto-Martinez et al., 2017; Fujii et al., 2018)
AQP7	Rat	Protein	IF, WB	(Suzuki-Toyota et al., 1999; Calamita et al., 2001)
	Human	mRNA, protein	WB, ICC, IF, RT-PCR, FC	(Saito et al., 2004; Yeung et al., 2010; Moretti et al., 2012; Laforenza et al., 2017)
	Mouse	mRNA, protein	WB, RT-PCR	(Yeung et al., 2009)
	Pig	Protein	WB, ICC	(Prieto-Martínez et al., 2014; Vicente-Carrillo et al., 2016)
	Cattle	Protein	WB, ICC	(Prieto-Martinez et al., 2017; Fujii et al., 2018)
	Horse	Protein	WB	(Bonilla-Correal et al., 2017)
AQP8	Mouse	mRNA, protein	WB, RT-PCR	(Yeung et al., 2009)
	Human		WB, ICC, RT-PCR, FC	(Yeung et al., 2010; Laforenza et al., 2017)
AQP9	Not in mouse	Protein	WB	(Yeung et al., 2009)
	Not in human	mRNA, protein	WB, ICC, RT-PCR, FC	(Yeung et al., 2010)
	Pig	Protein	WB, ICC	(Vicente-Carrillo et al., 2016)

(Cont.)

Aquaporin	Species	Strategy of Detection	Methodology	Reference
AQP11	Mouse	Protein	IHC	(Yeung and Cooper, 2010)
	Rat		IHC	(Yeung and Cooper, 2010)
	Pig		WB, ICC	(Prieto-Martínez et al., 2014)
	Human		WB, ICC	(Laforenza et al., 2017)
	Horse		WB	(Bonilla-Correal et al., 2017)
	Cattle		IHC, WB	(Morató et al., 2018)

Abbreviations: WB, Western Blot; RT-PCR, real time-PCR; IHC, immunohistochemistry; sc-RNAseq, single cell RNA sequencing; IF, immunofluorescence; IGEM, immunogold and scanning and transmission electron microscopy; ICC, immunocytochemistry; FC, flow cytometry.

Aquaporin 3 (AQP3) has been identified in pig (Prieto-Martínez et al., 2015), cattle (Prieto-Martinez et al., 2017; Fujii et al., 2018), horse (Bonilla-Correal et al., 2017), mouse (Chen et al., 2011) and human sperm (Chen et al., 2011; Laforenza et al., 2017; Alyasin et al., 2020). The AQP3 localises in the sperm tail; it has been identified in the sperm midpiece in pigs and cattle, whereas in human and mouse sperm it is present in the principal piece. Aquaporin 7 (AQP7) has been identified in pig (Prieto-Martínez et al., 2014; Vicente-Carrillo et al., 2016), cattle (Prieto-Martinez et al., 2017; Fujii et al., 2018), horse (Bonilla-Correal et al., 2017), human (Saito et al., 2004; Yeung et al., 2010; Moretti et al., 2012; Laforenza et al., 2017), mouse (Yeung et al., 2009) and rat sperm (Suzuki-Toyota et al., 1999; Calamita et al., 2001). It is present in the tail of ejaculated sperm in the different mammalian species that have been studied thus far, and it has also been identified in certain regions of the head in human sperm (Moretti et al., 2012; Laforenza et al., 2017). Aquaporin 8 (AQP8) is present in the sperm tail in human (Yeung et al., 2010; Laforenza et al., 2017) and mouse sperm (Yeung et al., 2009). In humans, AQP8 has been suggested to localise in mitochondria from the midpiece (Laforenza et al., 2017). Aquaporin 11 (AQP11) is present in pig (Prieto-Martínez et al., 2014), horse (Bonilla-Correal et al., 2017), mouse (Yeung and Cooper, 2010), rat (Yeung and Cooper, 2010) and human sperm (Laforenza et al., 2017). It has been identified

in intracellular structures of the sperm tail; in humans it is also present in the sperm head (Laforenza et al., 2017) and, in rats, it is exclusively localised in the terminal piece of the sperm tail (Yeung and Cooper, 2010).

Aquaporin 1 (AQP1) was purported to be expressed in dog sperm (Ito et al., 2008); however, different studies have failed to identify it in other mammalian sperm, including those from sheep (Curry et al., 1995), humans (Liu et al., 1995; Yeung et al., 2010) and mice (Lu et al., 2008). Similarly, AQP9 has been identified in the head of pig sperm (Vicente-Carrillo et al., 2016) but it is absent from human (Yeung et al., 2010) and mouse sperm (Yeung et al., 2009).

3.2.1.1 Aquaporins are relevant for sperm osmoregulation

The most important role of AQPs in sperm is related to osmoregulation. After ejaculation, sperm undergo a severe osmotic stress when entering the female reproductive tract, because they experience a decrease in extracellular osmolality compared to the epididymis (reviewed in (Cooper and Yeung, 2003)). Osmoadaptability is acquired by sperm during their transit through the epididymis, as extracellular medium is progressively more hyperosmotic from the caput to the cauda. During this transit, and in order to counteract the lower osmolality in the female reproductive tract after insemination, sperm uptake osmolytes from the epidydimal fluid (reviewed in (Yeung et al., 2006)). Another change in extracellular medium that one must also consider is the interaction between sperm and seminal plasma, which takes place at the time of ejaculation. Strikingly, osmolality changes between cauda epididymis, seminal plasma and the female oviduct are species-specific in mammals. In sheep and cattle, the epididymis and uterine environments are hypertonic compared to the isotonic seminal plasma. In humans, mice, and rats, osmolality lowers progressively from the epididymis to the seminal plasma and then to the uterus (reviewed in (Lavanya et al., 2022)).

In response to hypotonic shock, sperm swell due to an excessive uptake of water. Sperm swelling impairs the normal movement of the tail, which becomes coiled, and plasma membrane function is highly compromised until the critical

volume is reached, when it may experience disruption (Drevius and Eriksson, 1966). In response to hypotonic stress, the signalling pathway involved in regulatory volume decrease (RVD) is initiated, and as a consequence it activates an osmolyte efflux that drives water outside of the cell, allowing the cell volume to restore (Ford et al., 2000). The rapid trafficking across the plasma membrane is possible due to the presence of AQPs, which favour cell volume regulation in response to osmotic stress (**Figure 2**).

Rather than being inert pores at the plasma membrane, some AQPs present different mechanisms of regulation of water permeability. Sperm from *Aqp3* knockout mice show progressive cell swelling after entering the uterus due to an impaired capacity to regulate their volume (Chen et al., 2011). Chen and Duan (2011), nevertheless, hypothesized that if AQP3 function was restricted to shorten the time required to reach the osmotic equilibrium, water flow should be diminished both into and out of the cell, and progressive cell swelling would not occur (Chen and Duan, 2011). In fact, according to the model of tetrameric structure of AQPs, an increase in plasma membrane tension would cause a decrease in water permeability of AQP tetramers because of pore channel distortion (reviewed in (Ozu et al., 2018)). Thus, (Chen and Duan, 2011) proposed that AQP3 in sperm might interact with other ion channels to trigger RVD events (**Figure 2**). Remarkably, this mechanosensory role of AQPs in volume regulation has been previously described in salivary gland cells, where AQP5 is coordinated with TRPV4 (Liu et al., 2006), and in astrocytes, where an AQP4/TRPV4 complex is involved in RVD signalling pathways (Benfenati et al., 2011). In this sense, it has been hypothesized that the distance between monomers would increase in response to membrane tension, thus activating the RVD signalling pathway through the interactions of AQPs with ion channels, which would evoke the driving force leading to water efflux (Chen and Duan, 2011).

In an *Aqp7* knockout (KO) mouse model, water transport in sperm was found to be faster than in sperm from wild-type animals previously exposed to quinine, an agent that blocks osmolyte efflux and, consequently, impairs RVD events and causes cell swelling (Yeung et al., 2009). In addition, sperm from *Aqp7* knockout

mice did not show morphological alterations indicative of cell swelling, like tail coiling (Sohara et al., 2007). These results suggest that in this KO model, the higher water transport and the absence of cell swelling could be the result of the functional compensation by other AQPs. In fact, these *Aqp7*-knockout mice presented higher levels of *Aqp8* transcripts in the testis (Yeung et al., 2009). These findings suggest that AQP7 does not play a relevant osmoregulatory role in mouse sperm. Variations in the localisation of AQP7 in human sperm, however, have been associated to sperm morphology alterations, including the presence of sperm with coiled tails, which is indicative of osmotic stress (Moretti et al., 2012).

Regarding AQP8, its levels in human sperm are inversely correlated to the presence of sperm with coiled tails in the ejaculate (Yeung et al., 2010). The inhibition of AQP8 through $HgCl_2$ blocks quinine-induced swelling in both human and mouse sperm (Callies et al., 2008; Yeung et al., 2009), which evidences the relevance of this protein for sperm osmoregulation in these species. In fact, (Yeung et al., 2009) described that the role of AQP8 is crucial for RVD mechanisms, since its inhibition reduces the volume response to osmolyte currents. It is worth noting, nonetheless, that mercury binds covalently to a cysteine residue that is conserved in all AQPs except AQP7 (Ishibashi et al., 1997; Hirano et al., 2010). Hence, although some studies using mercury compounds as AQP-inhibitors suggest that their observed results are an exclusive consequence of AQP8 blocking, water permeability through other AQPs is also impaired by mercury-derived agents.

3.2.1.2 Aquaporins and male fertility

Different studies have assessed the relationship between AQPs and sperm function. Essentially, cell swelling in response to osmotic stress causes tail coiling, which, in turn, impairs sperm motility and thus have a detrimental effect on fertility (reviewed in (Pellavio and Laforenza, 2021)). In spite of this, the hypotonic shock that sperm experience at their first contact with the female reproductive tract is essential to elicit sperm capacitation. On the one hand, sperm swelling in response to osmotic shock triggers a calcium influx through mechanosensitive calcium channels, which is one of the first events that occurs during capacitation

(Rossato et al., 1996). On the other hand, acrosome swelling that happens in response to this osmotic shock is essential for the preparation of a physiological acrosome reaction (Zanetti and Mayorga, 2009). Moreover, as aforementioned, a strict regulation of H_2O_2 concentration is essential during capacitation for motility hyperactivation and acrosome reaction, but the mechanism is still to be unveiled (Rivlin et al., 2004). Considering that some AQPs are peroxiporins, their potential involvement in the regulation of intracellular levels of H_2O_2 during capacitation can be speculated. In addition, the permeability of GLPs to glycerol has been proposed to be related to its entry and further use as a source of energy in sperm (Yeung et al., 2010).

In short, the role of AQPs in sperm fertility might be explained by their involvement in both motility and capacitation-associated events, which are crucial to ensure successful fertilisation.

3.2.1.2.1 Aquaporins in murine sperm physiology

Although sperm motility from an *Aqp3* knockout mouse model appeared to be normal after the first interaction with the female reproductive tract, progressive cell swelling started shortly after, and was found to cause tail coiling and alter sperm motility (Chen et al., 2011). As a consequence of motility alteration, the sperm ability to migrate into the oviduct was compromised and ended up with decreased fertilisation rates, causing male infertility (Chen et al., 2011). These results provide evidence that, in *Aqp3* knockout mice, detrimental motility is a direct consequence of inefficient osmoregulation after entering the female tract, but not of structural alterations derived from the absence of AQP3 during spermatogenesis. Other research, nevertheless, found that an *Aqp7* knockout mouse model did not show alterations in sperm production, motility or *in vitro* and *in vivo* fertilising ability (Sohara et al., 2007). These data suggest that, at least in mice, AQP3, but not AQP7, plays a relevant role for sperm motility activation via osmoregulation.

Glycerol was early reported as an energy source in rat sperm, because this molecule was found to be involved in sperm metabolism in the epididymis (Cooper

and Brooks, 1981). While, in other cell types, AQP7 is implicated in glycerol influx (Skowronski et al., 2007), further research is needed to elucidate whether, in mammalian sperm, AQP7 participates in glycerol uptake to produce energy.

3.2.1.2.2 Aquaporins in human sperm physiology

In certain infertile patients, AQP7 levels in sperm are lower than in fertile donors, and these levels are correlated to progressive motility (Saito et al., 2004; Yeung et al., 2010). Regarding AQP7, alterations in its localisation pattern in human sperm are detrimental to sperm motility and fertility (Moretti et al., 2012). This relationship with fertility has not been described in the case of AQP8 (Yeung et al., 2010). These alterations in sperm motility could be explained by an impaired osmoregulatory ability relying on AQP7 levels and its optimal distribution. It has also been suggested that AQP7 might be responsible for the intake of glycerol as an energy source in rat sperm (Yeung, 2010), which could also contribute to motility regulation. Moreover, inhibiting all AQPs but AQP7 through $HgCl_2$ causes a drastic decrease in sperm motility (Alyasin et al., 2020), which indicates that all AQPs, rather than only AQP7, are involved in its regulation.

When mercurial compounds are used to inhibit AQPs in human sperm, mitochondrial membrane potential is also impaired; hence, additional causes to structural alterations induced by cell swelling might be involved in motility disruption when AQP function is blocked (Alyasin et al., 2020). The use of mercury compounds to inhibit AQP3 and AQP8, which are peroxiporins (Miller et al., 2010; Laforenza et al., 2017), could hinder the efflux of the H_2O_2 generated in response to osmotic stress. In fact, the effect of mercury as a blocking agent of H_2O_2 efflux through AQPs has already been described (Laforenza et al., 2017). Because of the intracellular accumulation of ROS, different cellular organelles, such as mitochondria, might be damaged, which would explain the impairment in mitochondrial membrane potential (MMP) and, consequently, the decrease in sperm motility. The role of AQPs in sperm physiology, therefore, seems to be common in different species of mammals, including livestock, murine and human species.

With regard to AQP3, both mRNA and protein levels in sperm are known to be lower in some cases of asthenozoospermia compared to fertile controls (Mohammadi et al., 2021); this supports a relationship between this protein and sperm motility. In this group of infertile patients, AQP3 content is also negatively correlated to activated caspase-3 (CASP3) levels, which suggests that CASP3 could degrade AQP3 (Mohammadi et al., 2021). Because AQP3 also mediates H_2O_2 transport (Miller et al., 2010), it is reasonable to surmise that the correlation between this apoptosis marker and AQP3 levels could be related to the mitochondrial damage derived from intracellular accumulation of H_2O_2. In response to mitochondrial damage, disruption of MMP could lead to an increase in CASP3 levels. In fact, some cases of subfertility present a reduced permeability to both water and H_2O_2 (Laforenza et al., 2017), which would underpin the relationship between AQP levels, impairment of sperm mitochondrial function and fertility in humans.

The potential involvement of AQPs in the subfertility caused by human papillomavirus (HPV) infection was recently described (Pellavio et al., 2020). In patients infected by HPV, this virus was demonstrated to bind AQP8, but not AQP3 or AQP7, through immunolocalization and co-immunoprecipitation experiments. This virus might effectively decrease AQP8 permeability, causing an increase in osmotic and oxidative stresses, and thus, be the cause of the impaired sperm motility that has been described in infected patients (Pellavio et al., 2020).

To sum up, current evidence supports that all AQPs present in human sperm play a relevant role in the regulation of sperm motility, whereas AQP3 and AQP8 look to be also involved in ROS detoxification.

3.2.1.2.3 Aquaporins in sperm physiology from livestock

Studies evaluating the role of AQPs in livestock are scarce. In fresh pig semen, AQP11 but not AQP7 levels are positively correlated to sperm motility and different quality and functionality parameters, such as membrane lipid disorder or acrosome integrity (Prieto-Martínez et al., 2014). Considering the crucial role that different members of this group of channels have in murine and human sperm

physiology and the variability of their distribution in different species of mammals, studying the role of AQPs in sperm from livestock species may contribute to elucidate potential differences in sperm physiology between these species.

3.2.2 Voltage-gated proton channel HVCN1 in mammalian sperm

The presence and localisation of HVCN1 in sperm differ between species and cell domains (**Table 3**). It has been identified in human sperm, and it mainly localises in the principal piece (Lishko et al., 2010). It has also been identified in the principal piece of bovine sperm (Mishra et al., 2019), and it is also present in pig sperm (Yeste et al., 2020). The HVCN1 channel has not been identified in mouse sperm, where an alternative proton regulation mechanism, involving the Na^+-dependent (Cl^-/HCO_3^-) exchanger (NCB) and the sperm-specific Na^+/H^+ exchanger (sNHE), has been proposed (reviewed in (Lishko and Kirichok, 2010)).

Table 3. Species of mammals that present HVCN1. Different species, where the presence of this channel has been identified, are detailed.

Species	Strategy of Detection	Methodology	Reference
Human	mRNA, protein	RT-PCR, WB, ICC	(Lishko et al., 2010)
Cattle	mRNA, protein	WB, ICC	(Mishra et al., 2019)
Pig	Protein	WB	(Yeste et al., 2020)

Abbreviations: WB, Western Blot; RT-PCR, real time-PCR; ICC, immunocytochemistry.

3.2.2.1 The HVCN1 channel is relevant for sperm motility hyperactivation

Intracellular pH plays a crucial role in the regulation of capacitation-associated events, and depends on the transport of protons and bicarbonate across the plasma membrane. Proton transport across the sperm plasma membrane is carried out via two mechanisms: membrane transporters, such as sodium-hydrogen exchangers (NHEs), and the voltage-gated proton channel (HVCN1) (Bernardino et al., 2019).

3.2.2.2 HVCN1 and male fertility

Most studies exploring the impact of gene function on fertility are conducted in animal models. HVCN1 currents, however, are absent from mouse sperm, therefore it is not possible to evaluate the impact of null *HVCN1* mutations on

fertility using this model. In fact, *HVCN1* KO mice were generated and had normal fertility. While mutations in *HVCN1* are likely to result in men infertility, no studies have, to the best of the author's knowledge, been undertaken to date (Shukla et al., 2012). Further research is much warranted to assess the actual impact of HVCN1 function impairment and fertility.

3.2.2.2.1 HVCN1 in human sperm physiology

In human sperm, capacitated sperm with motility hyperactivation show enhanced HVCN1-mediated proton current (Lishko et al., 2010). In these cells, this channel is activated by membrane depolarization, extracellular alkaline environment, the presence of anandamide and the removal of Zn^{2+}, which is a potent blocker of HVCN1 (Lishko et al., 2010). Apart from the increase in pH that sperm experience when they interact with the female reproductive tract, Zn^{2+} concentration is much higher in seminal plasma than in the oviduct. This cation binds to both the activated and resting closed states of the HVCN1 channel, so that both sensor motion and gate opening are blocked (Qiu et al., 2016). Moreover, HVCN1 presents the same cell localisation as two channels involved in capacitation: CatSper, a pH-sensitive Ca^{2+} channel that participates in Ca^{2+} currents as a central signalling mechanism in capacitation; and SLO3, a pH-sensitive K^{+} channel that is crucial for membrane hyperpolarisation. This common localisation of the three channels and the regulatory role of pH supports the relevance of HVCN1 upstream in the signalling pathways leading to sperm capacitation (reviewed in (Ren, 2010)). In fact, inhibition of the HVCN1 channel using Zn^{2+} impairs sperm motility hyperactivation and abolishes progesterone-induced acrosome reaction (Keshtgar et al., 2018). The relevance of this channel in human sperm capacitation was also confirmed through the use of C6, a specific blocker (Zhao et al., 2018). Moreover, inhibition of HVCN1 abolishes alkalinisation specifically in the principal piece of sperm, which evidences a subcellular regulation of pH that, in the principal piece of the tail, is performed by HVCN1 (Matamoros-Volante and Treviño, 2020).

In addition to the previously mentioned regulatory mechanisms, (Zhao et al., 2021) described an albumin-dependent gating of this channel. In effect, albumin

directly binds and activates HVCN1 in human sperm, thus increasing the number of opened channels and the proton current. Precisely, albumin binds to the external residues linking TM3 and TM4, which comprise the voltage sensor, and favours the active "up" conformation of TM4. In human sperm, this albumin-mediated activation of HVCN1 can initiate capacitation. While albumin concentration in semen is too low to activate HVCN1, it is high enough to activate this channel in the female tract, which leads to an intracellular pH increase that subsequently triggers capacitation (Zhao et al., 2021). These data also offer a rationale for the higher efficiency of IVF when media are supplemented with albumin. Although albumin might also indirectly contribute to HVCN1 activation through Zn^{2+} chelation, which is an inhibitor of this channel, it also has similar stimulatory effects on HVCN1 mutants with low affinity to Zn^{2+} (Zhao et al., 2021).

3.2.2.2.2 HVCN1 in sperm physiology in livestock

Similar to humans, HVCN1 in bovine sperm is crucial for the regulation of motility activation. In this species, the inhibition of HVCN1 with Zn^{2+} prevents motility hyperactivation. HVCN1 and CatSper channels also interplay and regulate sperm motility through the cAMP/PKA signalling pathway, which could also be the cause of lower mitochondrial membrane potential as a downstream event. Moreover, blocking of HVCN1 channels causes an osmotic imbalance in terms of H^+, Na^+ and HCO_3^+, which then destabilises the plasma membrane (Mishra et al., 2019).

In pig sperm, inhibition of HVCN1 during sperm capacitation also impairs motility hyperactivation, which confirms the role of these channels in humans and cattle. As occurs in bovine sperm, mitochondrial membrane potential is lower when this channel is inhibited. Like in humans, sperm membrane is also destabilised, possibly because of the ion misbalance caused by the blocked proton efflux. In terms of calcium levels, the blocking of HVCN1 does not have an apparent effect on intracellular calcium levels in the sperm tail during capacitation, but after the addition of progesterone to trigger the acrosome reaction, sperm do not exhibit the increase in calcium levels that occurs when the channel is not inhibited (Yeste et al., 2020). These data suggest that, in pig sperm, HVCN1 might have a

more relevant role in calcium regulation during the events related to the acrosome reaction than in those linked to early capacitation. Current data, nevertheless, do not offer sufficient evidence to elucidate the regulation mechanisms through which HVCN1 modulates sperm physiology during capacitation.

3.2.3 Potassium channels in mammalian sperm

The presence and localisation of K^+ channels in sperm differ between species and cell domains (**Table 4**).

Table 4. Potassium channels identified in gametes from different species of mammals. Different species, where potassium channels have been identified, are detailed.

K^+ channels	Species	Strategy of Detection	Methodology	Reference
$K_{IR}5.1$	Mouse	Protein	ICC	(Poli et al., 2021)
$K_{2P}2.1$ (TREK-1)	Cattle	Protein	WB	(Hur et al., 2009)
$K_{2P}3.1$ (TASK-1)	Cattle	Protein	WB	(Hur et al., 2009)
$K_{2P}4.1$ (TRAAK)	Cattle	Protein	WB	(Hur et al., 2009)
$K_{2P}5.1$ (TASK-2)	Mouse	Protein	WB	(Barfield et al., 2005b)
	Human	Protein	ICC, WB	(Barfield et al., 2005a)
	Cattle	Protein	WB	(Blässe et al., 2012)
$K_{2P}9.1$ (TASK-3)	Cattle	Protein	WB	(Hur et al., 2009)
$K_{2P}10.1$ (TREK-2)	Cattle	Protein	WB	(Hur et al., 2009)
Kv1.1	Cattle	Protein	WB, IF	(Gupta et al., 2018)
Kv1.5	Mouse	Protein	WB	(Barfield et al., 2005b)
	Human	Protein	ICC, WB	(Barfield et al., 2005a)
Kv7.1	Human	Protein	ICC, WB	(Gao et al., 2021)
SLO1	Human	Protein	ICC, WB	(Mannowetz et al., 2013)
	Pig	Protein	ICC, WB	(Yeste et al., 2019)
SLO3	Mouse	mRNA	RT-PCR	(Schreiber et al., 1998)
	Human	Protein	ICC, WB	(Brenker et al., 2014)

Abbreviations: ICC, immunocytochemistry; WB, Western Blot; IF, immunofluorescence; RT-PCR, real time-PCR;.

In mouse sperm, the K^+ current that leads to membrane hyperpolarisation is pH-sensitive; before the channel involved in these currents was identified, it was

known as KSper (Navarro et al., 2007). SLO3, a member of the Ca^{2+}-activated SLO subfamily, was identified to be expressed exclusively in mouse testis; in sperm, its gating was found to be pH-dependent (Schreiber et al., 1998) and was explored as a good candidate for the regulation of KSper currents. Later, LRRC52 was identified as an auxiliary subunit of SLO3 (Yang et al., 2011). A member of the inward-rectifier K^+ channels family, $K_{IR}5.1$, has also been identified in mouse sperm (Poli et al., 2021). In addition, the voltage-gated K^+ channel Kv1.5 and a member of the two-pore domain K^+ channels family, $K_{2P}5.1$ (TASK-2), have also been described in mouse sperm (Barfield et al., 2005b).

In human sperm, SLO1, another member of the Ca^{2+}-activated SLO subfamily, is located in the sperm tail (Mannowetz et al., 2013). A variant of SLO3 (hSLO3) was also identified in human sperm, together with LRRC52, its auxiliary subunit, and was found to be expressed in the sperm tail (Brenker et al., 2014). Nevertheless, hSLO3 is a genetic variant that presents sequence variations to the mouse gene that alter the structure of the intracellular gating ring of this channel, that contains sensors to intracellular factors such as Ca^{2+} or pH (Geng et al., 2017). As a consequence, the pharmacology of hSLO3 presents differences with respect to the mouse variant, including its sensitivity to different inhibitors, Ca^{2+} and voltage (Sánchez-Carranza et al., 2015). In addition, a member of the two-pore domain K^+ channels family, $K_{2P}5.1$ (TASK-2), was identified in human sperm (Barfield et al., 2005a). Moreover, two different voltage-gated K^+ channels, Kv1.5 (Barfield et al., 2005a), and Kv7.1 (KCNQ1) and its regulatory subunit KCNE1 (Gao et al., 2021), were identified in human sperm. The latter study localised Kv7.1 in sperm head and tail, whereas KCNE1 was found in neck and tail regions (Gao et al., 2021), in accordance with previous studies (Yeung and Cooper, 2008).

In pig sperm, SLO1 was also found to be localised in acrosomal and post-acrosomal regions of the sperm head, as well as in the tail (Yeste et al., 2019).

Similar to the differences observed between human and mouse SLO3, this gene presents a high sequence variation between mice and bovine, which could underlie a distinct function between these two species (Santi et al., 2009). These differences in a gene that is specifically expressed in the testis account for a faster

evolution that is strictly related to male reproductive function (Swanson and Vacquier, 2002), and is much slower in nonsexual counterparts like SLO1. In bovine sperm, K_{2P}5.1 (TASK-2) (Blässe et al., 2012), K_{2P}2.1 (TREK-1), K_{2P}3.1 (TASK-1), K_{2P}4.1 (TRAAK), K_{2P}9.1 (TASK-3) and K_{2P}10.1 (TREK-2) channels are also present (Hur et al., 2009). Moreover, the voltage-gated potassium channel Kv1.1 was identified in bovine sperm, and it was found to be localised in the head, midpiece and principal piece of sperm (Gupta et al., 2018).

3.2.4 Potassium channels are crucial for sperm osmoregulation

The mechanism through which cells adapt to changes of osmolality, RVD, has already been described, with ion channels being crucial to restore cell volume. While different ion transport mechanisms may play a role in volume regulation, the most important ion currents in mammalian cells involve the opening of K^+ and Cl^- channels to create a driving force that permits water outflow (Pasantes-Morales, 2016). In sperm, K^+ channels have a crucial role as generators of this driving force (Barfield et al., 2005a, 2005b).

3.2.5 Potassium channels and sperm capacitation

Plasma membrane is hyperpolarised during capacitation. This event relies on an increase in the relative concentration of negative charges in the intracellular compartment in response to changes to ion permeability (reviewed in (Puga Molina et al., 2018)). Potassium, which is a positively charged ion, moves outside of the cell in response to different stimuli and contributes to membrane hyperpolarisation. In response to this change in membrane potential, different ion currents are activated through voltage-gated channels, among which calcium influx to the cytoplasm is essential. As a consequence of the increase in intracellular calcium concentration, sperm switch to hyperactivated motility and become prepared to undergo the acrosome reaction (reviewed in (Bailey, 2010)).

3.2.6 Potassium channels and fertility

3.2.6.1.1 Potassium channels in mice sperm physiology

When they must adapt to a hypertonic environment, sperm from *Slo3* KO mice present a higher percentage of morphological abnormalities and deficient motility than those from the wild type (Zeng et al., 2011). Moreover, a genetic KO of *Lrrc52*, the regulatory subunit of SLO3, also exhibits a severe fertility impairment (Zeng et al., 2015). This could be caused by the involvement of potassium channels in RVD. Furthermore, *Slo3* KO male mice are infertile, and neither their sperm plasma membrane undergoes hyperpolarisation – rather it remains depolarised during capacitation – nor does it exhibit pH-dependant K^+ currents.

In terms of physiology, sperm from a *Slo3* mutant model exhibit an impairment in motility hyperactivation, and are not able to undergo the AR. Even after removal of the zona pellucida, these sperm are not able to fertilise oocytes *in vitro* (Santi et al., 2010). To sum up, in mice, the pH-dependent K^+ current involved in sperm motility hyperactivation seems to be exclusively driven by SLO3. In addition, the use of clofilium, a specific inhibitor of SLO3 channels, extends the window of sperm capacitation, as it decreases the rate of premature acrosome reaction and prolongs the fertilizing competence of capacitated mouse sperm (Abi Nahed et al., 2018). All this evidence confirms the relevance of SLO3-mediated membrane hyperpolarisation in capacitation-associated events.

The mechanism through which the cAMP/PKA signalling pathway is related to membrane hyperpolarisation through SLO3 (Escoffier et al., 2015) is likely to involve cSrc kinase, a member of the Src family of kinases (SFK) that is activated downstream of PKA. The effects of cSrc inhibition in mouse sperm include a hampered responsiveness to progesterone and, thus, a reduced capability to undergo the acrosome reaction. These results evidence that SLO3-mediated hyperpolarisation, which is governed by cSrc, is necessary and sufficient to prepare sperm to trigger the acrosome reaction (Stival et al., 2015). An increase in extracellular pH, however, is also able to elicit K^+ currents through SLO3 causing plasma membrane hyperpolarisation, which suggests that the opening of these

channels can also occur independently from other events associated to mouse sperm capacitation, and potentially in direct response to an increase of intracellular pH (Chávez et al., 2013). In fact, it has been proposed that SLO3-dependant hyperpolarisation may activate a NHE and/or a bicarbonate transporter to achieve intracellular alkalinisation, and this higher pH may, in turn, trigger the opening of CatSper channels (Chávez et al., 2014). The differences on how SLO3 is regulated between species, nevertheless, restrict these conclusions to mice sperm until further research evaluates whether these mechanisms are conserved across the mammalian class. In fact, whereas there are different K^+ channels in human sperm that have been proven to be involved in plasma membrane hyperpolarisation, the deletion of *hSLO3* in sperm abolishes K^+ currents and the Ca^{2+} influx in response to hyperpolarisation (Zeng et al., 2013).

Concerning the $K_{IR}5.1$ channel, a recent study found that a significant proportion of KO mice were subfertile, and certain individuals experienced a premature loss of fertility. Moreover, these males presented smaller testes and higher percentages of morphologically abnormal sperm (Poli et al., 2021). Takin this into consideration, some detrimental effects of the absence of $K_{IR}5.1$ seem to occur before ejaculation, which suggests that this channel could be relevant for the acquisition of osmoadaptability. It must be considered, nevertheless, that separate types of K_{IR} present different regulatory mechanisms. On the one hand, cholesterol depletion increases K^+ currents through $K_{IR}2$, while it inhibits $K_{IR}4$ channels. Hence, there is a chance that certain members of the K_{IR} subfamily of channels have a relevant function during capacitation. On the other hand, while K_{IR} channels generally tend to move K^+ into the cell rather than out of it, which would cause plasma membrane depolarisation, their inhibition partially hampers both capacitation-associated hyperpolarisation and acrosome reaction in mouse sperm (reviewed in (Visconti et al., 2011)). Further research aiming to elucidate the role of this channel in sperm physiology is much warranted.

Finally, another inward rectifying K^+ channel with a relevant function in mice fertility is $K_{IR}3.2$ (GIRK2). Although a KO mouse model for this gene exhibits normal fertility, gain of function (GOF) mutations are known to lead to male

infertility (Yi et al., 2011). These GOF mutations result in a loss of selectivity for K^+ ions over Na^+ and a constitutive activity that is insensitive to G-protein regulation (Navarro et al., 1996; Tong et al., 1996).

3.2.6.1.2 Potassium channels in human sperm physiology

Potassium channels and osmoregulation

In human sperm, the unspecific inhibition of all K^+ channels using quinine causes an impairment of sperm motility because of cell swelling, and induces tail curling (Yeung and Cooper, 2001). Furthermore, TEA-insensitive, Ca^{2+}-independent K^+ channels are involved in RVD in human sperm (Yeung and Cooper, 2001), which suggests the presence of K_{2P} channels as they are TEA-insensitive and underlie K^+ leak currents (Alexander et al., 2011).

Membrane hyperpolarisation during capacitation and acrosome reaction rely on potassium channels

In human sperm, intracellular alkalisation has a mild regulatory effect on the K^+ current, which is activated by Ca^{2+} (Brenker et al., 2014). There are, nevertheless, inconsistencies in the literature regarding which specific channel is implicated in these currents. On the one hand, Mannowetz et al. proposed SLO1 as the main K^+ channel (KSper) in human sperm, because it is regulated by Ca^{2+} (Mannowetz et al., 2013). This is also supported by the fact that SLO1 inhibition abolishes K^+ current in human but not in mouse sperm, which are devoid of SLO1 channels. Moreover, the KSper current in human sperm originates in the sperm flagellum, which is in agreement with the subcellular localisation of SLO1 (Mannowetz et al., 2013). Another proof for the relevance of SLO1 channels is that KSper currents are blocked by progesterone, which leads to membrane depolarisation. This membrane depolarisation would then activate CatSper channels and cause an intracellular Ca^{2+} increase, thus triggering motility hyperactivation and acrosome reaction (Mannowetz et al., 2013).

On the other hand, (Brenker et al., 2014) suggested that hSLO3 channels rather than the SLO1 ones are involved in the Ca^{2+}-activated K^+ current in human

sperm. These authors observed that while unspecific inhibition of K^+ channels abolished K^+ currents, the specific blockade of SLO1 did not affect K^+ currents or the hyperpolarisation of sperm plasma membrane. Moreover, a heterologous expression system using Chinese hamster ovary (CHO) cells (Brenker et al., 2014) proved that the human hSLO3 channel is sensitive to Ca^{2+}. Finally, progesterone also showed the ability to inhibit K^+ currents and to stimulate an increase in Ca^{2+} levels in heterologously expressed hSLO3 (Brenker et al., 2014).

The different conclusions reached in these two works (i.e. Mannowetz et al., 2013 and Brenker et al., 2014) could be the consequence of different experimental conditions (for example, different intracellular and extracellular calcium concentrations). Furthermore, and because both SLO1 and hSLO3 channels are present in human sperm, a model considering these two channels have a certain role in Ca^{2+}-activated K^+ currents in these cells would be very reasonable. In support of this, López-González et al. observed alterations in the hyperpolarisation of human sperm plasmalemma when both SLO1 and SLO3 were inhibited, which would support this hybrid model of regulation (López-González et al., 2014). Yet, another study determined the physiological properties of hSLO3 channels in a heterologous expression system using *Xenopus* oocytes; these channels were found to be pH-sensitive, which would not exclude a Ca^{2+}-dependant activity that could be modulated through LRRC52 (Leonetti et al., 2012). Together, these studies unveiled that both SLO1 and hSLO3 channels seem to mediate Ca^{2+}-activated, pH-sensitive K^+ currents in sperm.

Gao et al. explored the potential role of KCNQ1 during capacitation through its inhibition with chromanol 293B (Gao et al., 2021). Inhibition of this channel causes an increased intracellular concentration of K^+ and membrane depolarisation, which confirms that it participates in sperm membrane hyperpolarisation during capacitation. Intracellular levels of Ca^{2+}, Cl^- and pH are also impaired in response to the inhibition of KCNQ1, probably because changes in membrane hyperpolarisation alter the permeability of other ion channels. In terms of sperm function, inhibition of KCNQ1 also impairs motility during capacitation as well as the ability to undergo a physiological AR, which suggests

that intracellular pathways involved in capacitation are impaired. In support of this hypothesis, inhibition of KCNQ1 alters the levels of tyrosine phosphorylation of sperm proteins, a feature of capacitation modulated by the cAMP/PKA pathway. Specifically, Gao et al. (2021) observed that while, as expected, control sperm showed high levels of tyrosine-phosphorylated proteins in the acrosomal region after *in vitro* capacitation, this was absent from sperm incubated with chromanol 293B (Gao et al., 2021).

3.2.6.1.3 Potassium channels in sperm physiology in livestock

Quinine has been used in both bovine and porcine sperm to elucidate the relevance of K^+ channels in osmoregulation. Although quinine does not affect cell volume when sperm are incubated in isotonic conditions, both cattle and pig sperm experience cell swelling when incubated in a hypotonic medium. This process is proportionally greater in bovine than in porcine sperm, which could result from the higher water conductivity of the plasma membrane of the former compared to the latter. In both species, however, the VRD process is relatively slower than in other cell types, such as lymphocytes (Petrunkina et al., 2001).

In bovine sperm, the K^+ current has been identified to be blocked by tetraethyl ammonium (TEA), an unspecific inhibitor of K^+ channels (Marconi et al., 2008). The effect of SLO3-inhibition on the fertilizing competence of *in vitro* capacitated bovine sperm was also assessed using clofilium, which, as aforementioned, is a specific blocker of SLO3 channels. Similar to the results observed in mouse, cattle sperm capacitated for 24 h in the presence of the inhibitor exhibited extended fertilising competence and motility, showed an increased fertilisation rate and led to greater blastocyst formation (Abi Nahed et al., 2018). These results confirmed the role of SLO3 in bovine sperm capacitation, including the modulation of sperm lifespan and fertilising competence.

The specific inhibition of Kv channels in bovine sperm using 4-aminopyridine (4-AP) (Rodríguez-Rangel et al., 2020) was found to cause cell swelling, a decrease in mitochondrial membrane potential and an impairment of sperm motility. These results, together with the identification of Kv1.1 in the sperm of this species,

suggest that this voltage-gated channel plays a relevant function in sperm physiology. Further evidence, however, is needed to confirm its potential role in sperm motility hyperactivation (Gupta et al., 2018).

The role of potassium channels during sperm capacitation has also been investigated in pigs (Yeste et al., 2019; Noto et al., 2021). The specific inhibition of the SLO1 channel through paxilline (PAX) during sperm capacitation was found not to cause drastic alterations in motility hyperactivation or total intracellular levels of Ca^{2+}, whereas the unspecific inhibition of all K^+ channels through tetraethyl ammonium (TEA) or quinine impaired these capacitation-associated changes (Yeste et al., 2019; Noto et al., 2021). After inducing the acrosomal reaction with progesterone, the presence of any of these inhibitors (PAX, TEA and quinine) led to lower percentages of acrosome-exocytosed sperm and intracellular levels of Ca^{2+} in the sperm head (Yeste et al., 2019; Noto et al., 2021). These findings suggest that while SLO1 channels in pig sperm are relevant for the signalling pathways that prepare sperm to undergo the acrosomal reaction during capacitation, some capacitation-associated changes can either be regulated or compensated by other K^+ channels.

3.3 Membrane channels as sperm cryotolerance biomarkers

Cryopreservation is the most efficient method for long-term storage of mammalian sperm. This procedure is used for the establishment of genetic banks for endangered domestic and wild species (Pickard and Holt, 2004). It is also relevant for storing sperm that are to be used later in assisted reproduction technology (ART), for male fertility preservation before undergoing certain treatments that may compromise it, or for social reasons (Di Santo et al., 2012). Furthermore, it is also important for livestock production, as cryopreserved sperm can be used for artificial insemination (AI) (reviewed in (Yánez-Ortiz et al., 2021)). When sperm cells are cryopreserved, nevertheless, they undergo a challenging process for their integrity because of the osmotic shock they must endure. During this process, the water outflow of the cell is crucial to avoid intracellular crystal formation. Some consequences of this procedure are the loss of integrity of the

nucleus, cytoskeleton and plasma membrane, the reduction in mitochondrial activity and motility, and the impairment of protein function (Sieme et al., 2008; Peña et al., 2011; Yeste, 2016), which result in decreased fertilizing ability. To minimize cryoinjuries, cryoprotecting agents, such as glycerol, are added to cryopreservation media (Curry, 2007). Yet, it is worth considering that sperm from different species present marked variations, not only in size and morphology but also in plasma membrane composition and metabolism, which are reflected on a high variability in their cryotolerance (also known as freezability). Moreover, within a given species, samples with a similar fresh semen quality present different cryotolerance, both intra- and inter-individually. Hence, ejaculates can be classified as with good (GFE) or poor freezability (PFE) depending on their post-thaw sperm quality (Hoffmann et al., 2011; Baishya et al., 2014; Rego et al., 2016). For this reason, and because freezability is only apparent after, but not before, freeze-thawing, the research aimed to identify cryotolerance biomarkers is highly relevant. In recent studies, differences between GFEs and PFEs have been evidenced in terms of transcriptomics (Fraser et al., 2020), metabolomics (Torres et al., 2021), lipidomics (Xin et al., 2018), proteomics (Vilagran et al., 2014; Llavanera et al., 2019), and antioxidant (Papas et al., 2019, 2020) and enzyme activities (Pinart et al., 2015) in fresh semen.

3.3.1 Aquaporins and sperm cryopreservation

Different studies have unveiled differences in AQPs levels between GFEs and PFEs, which has evidenced their potential as cryotolerance biomarkers in sperm from different mammalian species. On the one hand, in fresh bovine sperm, relative levels of AQP3 are positively related to motility after thawing (Fujii et al., 2018), and the content of AQP11 is correlated to both cryotolerance and AI outcomes of cryopreserved sperm (Morató et al., 2018). Also in fresh bovine semen, AQP7 levels are positively correlated to cryotolerance (Prieto-Martinez et al., 2017), and those of *AQP7* mRNA are positively associated to both osmoregulation ability and fertility after cryopreservation (Kasimanickam et al., 2017). On the other hand, in both pig and horse fresh sperm, AQP3 and AQP7, but not AQP11, are related to

their cryotolerance; in addition, in pig sperm, AQP7, but not AQP9, relocalises after freeze-thawing (Vicente-Carrillo et al., 2016; Bonilla-Correal et al., 2017; Prieto-Martínez et al., 2017).

3.3.2 Potassium channels and sperm cryopreservation

An increase in intracellular K^+ levels and decreased intracellular pH occurs in cryopreserved bull sperm (Blässe et al., 2012). Although relative levels of TASK-2 channels are not altered by cryopreservation, there is a change in ion homeostasis in frozen-thawed sperm. In fact, the impairment in K^+ permeability and its intracellular accumulation could lead to plasma membrane depolarisation (Navarro et al., 2007). In this context, where membrane destabilisation occurs together with depolarisation, a premature, degenerative acrosome exocytosis may occur (Blässe et al., 2012), as a physiological acrosome reaction can only be triggered when the plasma membrane is hyperpolarised (Ritagliati et al., 2018).

Objectives

Objectives

1. To evaluate the relevance of aquaporins (AQPs) during mammalian sperm capacitation, using the pig as a model.

2. To assess the role of different groups of aquaporins (AQPs) during pig and horse sperm cryopreservation.

3. To evaluate the relationship between the intrinsic ejaculate cryotolerance and the function of aquaporins (AQPs) during pig sperm cryopreservation.

4. To determine the general function of potassium channels and the specific role of SLO1 during pig sperm cryopreservation.

5. To assess the potential role of the HVCN1 channel during pig sperm cryopreservation.

Paper compendium

Paper I

Aquaporins are essential to maintain motility and membrane lipid architecture during mammalian sperm capacitation.

Ariadna Delgado-Bermúdez, Sandra Recuero, Marc Llavanera, Yentel Mateo-Otero, Andra Sandu, Isabel Barranco, Jordi Ribas-Maynou, Marc Yeste.

Frontiers in Cell Developmental Biology,

2021;9:656438

doi: 10.3389/fcell.2021.656438

frontiers in Cell and Developmental Biology

ORIGINAL RESEARCH
published: 01 September 2021
doi: 10.3389/fcell.2021.656438

Aquaporins Are Essential to Maintain Motility and Membrane Lipid Architecture During Mammalian Sperm Capacitation

*Ariadna Delgado-Bermúdez[1,2], Sandra Recuero[1,2], Marc Llavanera[1,2], Yentel Mateo-Otero[1,2], Andra Sandu[1,2], Isabel Barranco[1,2], Jordi Ribas-Maynou[1,2] and Marc Yeste[1,2]**

[1] Biotechnology of Animal and Human Reproduction (TechnoSperm), Institute of Food and Agricultural Technology, University of Girona, Girona, Spain, [2] Unit of Cell Biology, Department of Biology, Faculty of Sciences, University of Girona, Girona, Spain

OPEN ACCESS

Edited by:
Ana Josefa Soler,
University of Castilla-La Mancha, Spain

Reviewed by:
María Gracia Gervasi,
University of Massachusetts Amherst, United States
Felipe A. Navarrete,
University of Massachusetts Amherst, United States

***Correspondence:**
Marc Yeste
marc.yeste@udg.edu

Specialty section:
This article was submitted to Cell Growth and Division, a section of the journal Frontiers in Cell and Developmental Biology

Received: 20 January 2021
Accepted: 13 August 2021
Published: 01 September 2021

Citation:
Delgado-Bermúdez A, Recuero S, Llavanera M, Mateo-Otero Y, Sandu A, Barranco I, Ribas-Maynou J and Yeste M (2021) Aquaporins Are Essential to Maintain Motility and Membrane Lipid Architecture During Mammalian Sperm Capacitation. Front. Cell Dev. Biol. 9:656438. doi: 10.3389/fcell.2021.656438

Aquaporins are a family of ubiquitous transmembrane proteins that allow the transport of water and small molecules across the cell plasma membrane. The different members of this family present a characteristic distribution across different cell types, which is species-specific. In mammalian sperm, different AQPs, including AQP3, AQP7, and AQP11, have been identified; their main roles are related to osmoadaptation and sperm motility activation after ejaculation. Capacitation, which is a post-ejaculatory process that sperm must undergo to achieve fertilizing ability, is triggered by pH changes and different extracellular ions that are present in the female reproductive tract. Considering the function of AQPs and their influence on pH through the regulation of water flow, this study aimed to elucidate the potential role of different AQPs during *in vitro* sperm capacitation using three different transition metal compounds as AQP inhibitors. Cooper sulfate, a specific inhibitor of AQP3, caused a drastic increase in peroxide intracellular levels compared to the control. Mercury chloride, an unspecific inhibitor of all AQPs except AQP7 produced an increase in membrane lipid disorder and led to a decrease in sperm motility and kinetics parameters. Finally, the addition of silver sulfadiazine, an unspecific inhibitor of all AQPs, generated the same effects than mercury chloride, decreased the intracellular pH and altered tyrosine phosphorylation levels after the induction of the acrosome reaction. In the light of the aforementioned, (a) the permeability of AQP3 to peroxides does not seem to be crucial for sperm capacitation and acrosome reaction; (b) AQPs have a key role in preserving sperm motility during that process; and (c) AQPs as a whole seem to contribute to the maintenance of lipid membrane architecture during capacitation and may be related to the intracellular signaling pathways involved in the acrosome reaction. Hence, further research aimed to elucidate the mechanisms underlying the involvement of AQPs in mammalian sperm capacitation and acrosome reaction is warranted.

Keywords: aquaporins, spermatozoa, silver sulfadiazine, cooper sulfate, capacitation, mercury chloride

INTRODUCTION

Cell homeostasis relies on both the integrity and permeability of plasma membrane to water and electrolytes. Because of its amphipathic nature, additional mechanisms to simple diffusion are required in order for water and solutes to pass through the cell membrane (Watson, 2015). Aquaporins (AQPs) are ubiquitous transmembrane water proteins that allow the transport of water and small solutes across cell membranes (reviewed by Yeste et al., 2017). In mammalian cells, this family of channel proteins includes different members that are classified according to sequence similarity and solute permeability into: orthodox AQPs, aquaglyceroporins (GLPs) and superAQPs. The group of orthodox AQPs includes AQP0, AQP1, AQP2, AQP4, AQP5, AQP6, and AQP8, which are exclusively permeable to water. Aquaglyceroporins, which are permeable to water, glycerol, urea and other small electrolytes, include AQP3, AQP7, AQP9, and AQP10. Finally, the group of superAQPs comprises AQP11 and AQP12, which are localized in the membranes of intracellular organelles, present sequence variations to the other groups of AQPs and are involved in both water and glycerol transport.

Despite being ubiquitous, the distribution of AQPs across cell types and species is uneven and characteristic. Regarding mammalian sperm, AQP3, AQP7, and AQP11 have been identified in mouse (Yeung et al., 2009; Yeung and Cooper, 2010; Chen et al., 2011), human (Yeung et al., 2010; Laforenza et al., 2017), pig (Prieto-Martínez et al., 2014, 2015), cattle (Prieto-Martinez et al., 2016; Morató et al., 2018) and horse (Bonilla-Correal et al., 2017); AQP8 has been found in mouse (Yeung et al., 2009) and human spermatozoa (Yeung et al., 2010; Laforenza et al., 2017); and AQP9 has been reported to be present in pig sperm (Vicente-Carrillo et al., 2016). The main functions of AQPs in mammalian spermatozoa are volume regulation and osmoadaptation. In effect, AQP3 has a vital role in osmoregulation (Chen and Duan, 2011), which is of crucial importance in post-ejaculatory events, when sperm cells interact with the female tract. In addition, Prieto-Martínez et al. (2017) observed a positive correlation between relative AQP3-content and osmoadaptation during cryopreservation, which is a challenging process since sperm are exposed to significant osmolality changes. Moreover, AQP7 has been suggested to be related to sperm motility in humans (Saito et al., 2004), but not in mice (Sohara et al., 2007). As far as AQP9 is concerned, there is little evidence on its particular role, since despite having been observed in pig spermatozoa (Vicente-Carrillo et al., 2016), homozygous $Aqp9^{-/-}$ mice show preserved fertility and their spermatozoa are morphologically normal and motile (Rojek et al., 2007). Finally, and with regard to AQP11, while its relative content was found to be correlated with plasma membrane integrity and motility in pig spermatozoa (Prieto-Martínez et al., 2014), it was confirmed as a cryotolerance biomarker in cattle (Morató et al., 2018) but not in pig spermatozoa (Prieto-Martínez et al., 2017). It is worth mentioning that the specific role of each AQP appears to differ across species, and that the particular relevance of their functions evokes that certain members of the AQP family can be compensated by others. Nevertheless, since exposure to the female reproductive tract involves a major challenge to the ability of spermatozoa to adapt to drastic osmolality variations, the role of AQPs in osmoregulation is essential to ensure preservation of sperm function and the success of subsequent post-ejaculatory events, such as motility activation [reviewed by Yeste et al. (2017)].

Because of their exposure to the female reproductive tract, sperm cells meet constantly changing environments, from which they receive different chemical and thermal signals. This set of inputs drives a series of signaling events that are essential for sperm capacitation, which is the process that confers sperm the ability to fertilize an oocyte (Chang, 1951). Briefly, after entering the female tract, spermatozoa find higher bicarbonate and calcium levels, whose influx activates the cAMP-PKA pathway and increases tyrosine phosphorylation downstream, thus hyperactivating sperm motility (reviewed by Puga Molina et al., 2018). In addition, this ion flow through plasma membrane triggers lipid reorganization and cholesterol efflux; as a consequence, the sperm membrane is hyperpolarized and its fluidity rises, which is crucial to increase membrane fusogenicity (reviewed in Bailey, 2010). Thereafter, progesterone triggers the acrosome reaction through its interaction with a G protein-coupled receptor (GPCR) (Buffone et al., 2014). Given the importance of intracellular pH as a regulator of the sperm-specific, soluble adenylyl cyclase (sAC), which is the source of cAMP that allows the activation of the cAMP-PKA pathway, it is reasonable to posit that AQPs might have a relevant role during mammalian sperm capacitation.

High affinity inhibitors are a reasonably accurate strategy to study AQPs function, and transitional metals have been used as blockers of water permeability in different cell types (Haddoub et al., 2009). Different mercurial compounds were used at first to prove the existence of water channels in erythrocytes and renal proximal tubule cells (Smith and Agre, 1991), as well as in *Xenopus* oocytes (Preston et al., 1992). Silver compounds have also been used as AQP inhibitors (Niemietz and Tyerman, 2002), showing a higher affinity and specificity for this family of proteins. Finally, cooper was also identified as a reversible, rapid and specific inhibitor of AQP3 (Zelenina et al., 2004).

Considering all the aforementioned, this study aimed to elucidate the role of the different AQPs in mammalian sperm capacitation using the pig as a model, and through their inhibition with transition metal compounds.

MATERIALS AND METHODS

Animals and Ejaculates

A total of 32 ejaculates from separate Piétrain boars (n = 32) were used in this study. Boars were housed in a local farm (Grup Gepork SL, Masies de Roda, Spain) in controlled climatic conditions and fed with a standard diet. Sperm-rich fractions were manually collected and subsequently diluted to a final concentration of 33×10^6 sperm/mL in a commercial semen extender (Vitasem LD; Magapor SL, Zaragoza, Spain) and preserved at 17°C. Samples were transported to the laboratory within 2 h post-collection and, upon arrival, ejaculates were combined in pools of four for each experiment.

After that, each ejaculate pool was split into four different aliquots that were centrifuged (Universal 32R centrifuge; Hettich Zentrifugen; Tuttlingen, Germany) at 600 × *g* and 17°C for 5 min. Supernatants were discarded, and samples were then resuspended in pre-warmed, equilibrated capacitation medium [20 mM 4- (2-Hydroxyethyl) piperazine-1-ethanesulfonic acid (HEPES), 112 mM NaCl, 3.1 mM KCl, 5 mM glucose, 21.7 mM sodium L-lactate, 1 mM sodium pyruvate, 0.3 mM Na_2HPO_4, 0.4 mM $MgSO_4 \times 7H_2O$, 4.5 mM $CaCl_2 \times 2H_2O$, 5 mg/mL BSA and 15 mM bicarbonate; pH = 7.4 ± 0.1; osmolality = 0.300 Osm/Kg ± 0.01] to a final concentration of 25×10^6 sperm/mL. Thereafter, the corresponding inhibitors were added according to the treatment, and samples were kept in a Hera Cell 150 incubator at 38°C and 5% CO_2. In order to induce the acrosome reaction, progesterone (final concentration: 0.01 mg/mL) was added after 4 h of incubation and samples were incubated for an additional hour.

AQP Inhibitors

Three different AQP inhibitors were added to capacitation medium prior to incubation: cooper sulfate ($CuSO_4$; Sigma Aldrich; Saint Louis, MO, United States), mercury chloride ($HgCl_2$; Sigma Aldrich) and silver sulfadiazine (AgSDZ; Sigma Aldrich). The final concentrations of each inhibitor were set after preliminary experiments based on previous studies (Niemietz and Tyerman, 2002; Yeung et al., 2009; Reca et al., 2018). Each inhibitor was previously diluted in water. $CuSO_4$ (stock concentration: 400 mM) was added to samples at a final concentration of 100 μM; $HgCl_2$ (stock concentration: 40 mM) was added to a final concentration of 20 μM; and AgSDZ (stock concentration: 40 mM) was used at a final concentration of 5 μM.

Evaluation of Sperm Quality and Function

For the evaluation of sperm quality and function, sperm motility, flow cytometry, immunoblotting and ELISA analyses were performed after 0, 120, 240, 250, and 300 min of incubation in capacitation medium.

Motility

Sperm motility was assessed using a commercial computer-assisted sperm analysis (CASA) system, which consisted of a phase contrast microscope (Olympus BX41; Olympus, Tokyo, Japan) equipped with a video camera and ISAS software (Integrated Sperm Analysis System V1.0; Proiser SL, Valencia, Spain). With this purpose, a 5-μL drop of the sperm suspension was placed onto a Makler counting chamber (Sefi-Medical Instruments, Haifa, Israel) and observed under a negative phase-contrast field (Olympus 10 × 0.30 PLAN objective; Olympus). The following sperm motility parameters were recorded in each motility assessment: total motility (TMOT;%); progressive motility (PMOT,%); curvilinear velocity (VCL, μm/s); straight-line velocity (VSL, μm/s); average pathway velocity (VAP, μm/s); amplitude of lateral head displacement (ALH, μm); beat-cross frequency (BCF, Hz); linearity (LIN,%), that resulted from LIN = VSL/VCL × 100; straightness (STR,%), which was calculated as VSL/VAP × 100; and oscillation index (WOB,%), obtained from VAP/VCL × 100. A motile sperm was defined as having a VAP ≥ 10 μm/s, and a sperm cell was considered as progressively motile when its STR was at least 45%. In addition, the percentage of progressively motile spermatozoa among the population of motile sperm was calculated. For each sample, three replicates of at least 1,000 spermatozoa each were assessed. For each parameter, the corresponding mean and standard error of the mean (SEM) were calculated.

Flow Cytometry

Eight different parameters were assessed through flow cytometry in each time point and treatment: sperm plasma membrane integrity, membrane lipid disorder, acrosome membrane integrity, mitochondrial membrane potential (MMP), intracellular levels of calcium, superoxide ($O_2^{-}\bullet$) radicals and hydrogen peroxide (H_2O_2), and intracellular pH. All fluorochromes were obtained from ThermoFisher Scientific (Waltham, MA, United States) unless otherwise stated. Prior to the addition of the corresponding combination of fluorochromes, samples were diluted in phosphate-buffered saline (PBS) to a final concentration of 2×10^6 spermatozoa/mL. After staining, samples were incubated at 38°C in the dark. For each parameter, three replicates of at least 10,000 spermatozoa were assessed.

A Cell Lab Quanta™ SC cytometer (Beckman Coulter; Fullerton; CA, United States) was used to analyze sperm samples. Samples were excited with an argon ion laser (488 nm) at a power of 22 mW. Cell diameter/volume was assessed using the Coulter principle, which measures electrical resistance changes caused by suspended, non-conductive particles in an electrolyte solution. In this system, forward scatter (FS) was replaced by electronic volume (EV) and for EV-channel calibration, 10-μm Flow-Check fluorospheres (Beckman Coulter) were positioned at channel 200 on the EV-scale.

For fluorescence detection, three different optical filters were used: FL1 (Dichroic/Splitter, DRLP: 550 nm, BP filter: 525 nm, detection width 505–545 nm); FL2 (DRLP: 600 nm, BP filter: 575 nm, detection width: 560–590 nm); and FL3 (LP filter: 670 nm/730 nm, detection width: 655–685 nm). FL1 was used to detect green fluorescence from SYBR-14, YO-PRO-1, fluorescein isothiocyanate (FITC)-conjugated peanut agglutinin (PNA; PNA-FITC), JC-1 monomers ($JC\text{-}1_{mon}$), Fluo-3, 2′,7′-dichlorofluorescein (DCF^+) and 2′,7′-Bis-(2-Carboxyethyl)-5-(and-6)-Carboxyfluorescein, Acetoxymethyl (BCECF). FL2 was used to detect orange fluorescence from JC-1 aggregates ($JC\text{-}1_{agg}$). Finally, FL3 was used to detect red fluorescence from propidium iodide (PI), merocyanine 540 (M540) and ethidium (E^+). The signal was logarithmically amplified, and photomultiplier settings were adjusted according to particular staining methods.

The sheath flow rate was set at 4.17 μL/min, and EV and side scatter (SS) were measured and linearly recorded for all particles. Subcellular debris (particle diameter < 7 μm) and cell aggregates (particle diameter > 12 μm) were excluded through the adjustment of the analyzer threshold on the EV channel, and the sperm-specific events were positively gated on the basis of EV/SS distributions. For each sample and

parameter, three different replicates of a minimum of 10,000 events were evaluated.

Data analysis was performed using Flowing Software (Ver. 2.5.1; University of Turku, Finland), following the recommendations of the International Society for Advancement of Cytometry (ISAC). According to Petrunkina et al. (2010), the percentage of non-sperm debris particles from the SYBR-14$^-$/PI$^-$ population was used to correct the events corresponding to double-negative particles in the other protocols. For each sample and parameter, the corresponding mean and SEM were calculated.

Sperm plasma membrane integrity

The assessment of plasma membrane integrity was performed using the LIVE/DEAD sperm viability kit (Molecular Probes; Eugene, OR, United States) following the protocol of Garner and Johnson (1995). Briefly, spermatozoa were incubated in the presence of SYBR-14 (final concentration: 100 nmol/L) for 10 min, and PI (final concentration: 12 μmol/L) was subsequently added prior to an additional incubation of 5 min. Three different sperm populations were identified in flow cytometry dot-plots: (1) viable, green-stained spermatozoa (SYBR-14$^+$/PI$^-$); (2) non-viable, red-stained spermatozoa (SYBR-14$^-$/PI$^+$); and (3) non-viable, green- and red-stained spermatozoa (SYBR-14$^+$/PI$^+$). In addition, unstained, non-sperm particles (SYBR-14$^-$/PI$^-$) were not included for the calculation of the final percentages of the three previously mentioned populations. SYBR-14 fluorescence spill over into FL3 channel was compensated (2.45%).

Membrane lipid disorder

Co-staining with M540 and YO-PRO-1 was used to evaluate sperm membrane lipid disorder, following the protocol from Rathi et al. (2001) with minor modifications (Yeste et al., 2014). This protocol is based on the intercalation of M540 in the outer monolayer of the sperm plasma membrane when packing order of phospholipids decreases. In brief, samples were co-stained with M540 (final concentration: 2.6 μmol/L) and YO-PRO-1 (final concentration: 25 nmol/L) and then incubated for 10 min. Four different sperm populations were identified in flow cytometry dot-plots: (1) viable spermatozoa with low membrane lipid disorder (M540$^-$/YO-PRO-1$^-$); (2) viable sperm with high membrane lipid disorder (M540$^+$/YO-PRO-1$^-$); (3) non-viable sperm with low membrane lipid disorder (M540$^-$/YO-PRO-1$^+$); and (4) non-viable sperm with high membrane lipid disorder (M540$^+$/YO-PRO-1$^+$). The percentage of SYBR-14$^-$/PI$^-$ particles corresponding to non-sperm debris was used to correct the percentages of viable spermatozoa with low membrane lipid disorder (M540$^-$/YO-PRO-1$^-$); percentages of the other sperm populations were recalculated. Data were not compensated. Membrane lipid disorder was assessed through the calculation of the percentage of viable sperm with low membrane lipid disorder (M540$^-$/YO-PRO-1$^-$ sperm) from the population of viable spermatozoa (YO-PRO-1$^-$ sperm).

Acrosome membrane integrity

Samples were co-stained with fluorescein isothiocyanate (FITC)-conjugated peanut agglutinin (PNA; PNA-FITC) and PI in order to evaluate acrosome membrane integrity following the protocol from Nagy et al. (2003). PNA-FITC binds specifically to the outer acrosomal membrane. In brief, samples were co-incubated in the presence of PNA-FITC (final concentration: 2.5 μg/mL) and PI (final concentration: 12 μmol/L) for 10 min. As spermatozoa were not permeabilized, four different sperm populations were identified in flow cytometry dot-plots: (1) spermatozoa with an intact plasma membrane (PNA-FITC$^-$/PI$^-$); (2) spermatozoa with a damaged plasma membrane and an outer acrosome membrane that could not be fully intact (PNA-FITC$^+$/PI$^+$); (3) spermatozoa with a damaged plasma membrane and a non-intact acrosome membrane (PNA-FITC$^-$/PI$^+$); and (4) spermatozoa a with damaged plasma membrane (PNA-FITC$^+$/PI$^-$). The percentage of SYBR-14$^-$/PI$^-$ particles corresponding to non-sperm debris was used to correct the percentages of viable sperm with intact acrosome (PNA-FITC$^-$/PI$^-$), and the percentages of the other sperm populations were recalculated. PNA-FITC fluorescence spill over into FL3 channel was compensated (2.45%).

Intracellular levels of calcium

Sperm samples were co-stained with Fluo-3 AM and PI for the evaluation of intracellular calcium levels following the protocol from Harrison et al. (1993). Fluo-3 stains calcium that is located in the mid-piece, but it also stains faintly the calcium present in the sperm head (Yeste et al., 2015). In brief, samples were co-incubated with Fluo-3 (final concentration: 1 μmol/L) and PI (final concentration: 12 μmol/L) for 10 min. Four different sperm populations were identified in flow cytometry dot-plots: (1) viable sperm with low intracellular levels of calcium (Fluo-3$^-$/PI$^-$); (2) viable sperm with high intracellular levels of calcium (Fluo-3$^+$/PI$^-$); (3) non-viable sperm with low intracellular levels of calcium (Fluo-3$^-$/PI$^+$); and (4) non-viable sperm with high intracellular levels of calcium (Fluo-3$^+$/PI$^+$). The percentage of SYBR-14$^-$/PI$^-$ particles corresponding to non-sperm debris was used to correct the percentages of viable sperm with low intracellular levels of calcium (Fluo-3$^-$/PI$^-$), and the percentages of the other sperm populations were recalculated. Fluo-3 fluorescence spill over into FL3 channel was compensated (2.45%). Intracellular levels of calcium were assessed through the calculation of the percentage of viable sperm with high intracellular levels of calcium (Fluo-3$^+$/PI$^-$ sperm) within the population of viable spermatozoa (PI$^-$ sperm).

Mitochondrial membrane potential

Samples were stained with JC-1 in order to evaluate mitochondrial membrane potential following the protocol of Ortega-Ferrusola et al. (2008) with minor modifications. JC-1 molecules (5,5′,6,6′-tetrachloro-1,1′,3,3′tetraethyl-benzimidazolylcarbocyanine iodide) remain as monomers (JC-1$_{mon}$) in the presence of low MMP and emit green fluorescence, whereas in the presence of high MMP, these molecules form aggregates (JC-1$_{agg}$) that present orange fluorescence. Briefly, samples were incubated with JC-1 (final concentration: 0.3 μmol/L) for 30 min. Flow cytometry dot-plots allowed the identification of three different populations: (1) sperm with mitochondria presenting low MMP (JC-1$_{mon}$; FL1$^+$/FL2$^-$); (2) sperm with mitochondria showing high MMP

(JC-1_{agg}; $FL1^-/FL2^+$); and (3) sperm with heterogeneous mitochondria (JC-1_{mon} and JC-1_{agg}; $FL1^+/FL2^+$). The percentage of SYBR-$14^-/PI^-$ particles corresponding to non-sperm debris was used to correct the percentages of sperm with mitochondria presenting low MMP (JC-1_{mon}; $FL1^+/FL2^-$), and the percentages of the other sperm populations were recalculated. The sum of populations (2) and (3) corresponded to high MMP-spermatozoa. MMP was also assessed through the calculation of the ratio of the intensity of fluorescence JC-1_{agg}/JC-1_{mon} from each sperm population. $JC1_{mon}$ fluorescence spill-over into the FL2 channel was compensated (51.70%).

Intracellular levels of superoxide ($O_2^{-}\bullet$) radicals

Samples were co-stained with hydroethidine (HE) and YO-PRO-1 in order to evaluate the intracellular levels of superoxides ($O_2^{-}\bullet$) following the protocol from Guthrie and Welch (2006). In the presence of $O_2^{-}\bullet$ radicals, HE is oxidized into ethidium (E^+) and other products. Briefly, samples were incubated in the presence of HE (final concentration: 4 μmol/L) and YO-PRO-1 (final concentration: 25 nmol/L) for 20 min. As a result, flow cytometry dot-plots allowed the identification of four different sperm populations: (1) viable sperm with low intracellular levels of $O_2^{-}\bullet$ (E^-/YO-PRO-1^-); (2) viable sperm with high intracellular levels of $O_2^{-}\bullet$ (E^+/YO-PRO-1^-); (3) non-viable sperm with low intracellular levels of $O_2^{-}\bullet$ (E^-/YO-PRO-1^+); and (4) non-viable sperm with high intracellular levels of $O_2^{-}\bullet$ (E^+/YO-PRO-1^+). The percentage of SYBR-$14^-/PI^-$ particles corresponding to non-sperm debris was used to correct the percentages of viable sperm with low intracellular levels of $O_2^{-}\bullet$ (E^-/YO-PRO-1^-), and the percentages of the other sperm populations were recalculated. YO-PRO-1 spill-over into the FL3 channel was compensated (5.06%). Intracellular levels of superoxide radicals were assessed through the calculation of the percentage of viable sperm with high intracellular levels of superoxide (E^+/YO-PRO-1^- sperm) within the population of viable spermatozoa (YO-PRO-1^-sperm).

Intracellular levels of hydrogen peroxide (H_2O_2)

Intracellular levels of hydrogen peroxide (H_2O_2) were evaluated through co-staining with H_2DCFDA and PI following the protocol from Guthrie and Welch (2006). In the presence of H_2O_2, the non-fluorescent probe H_2DCFDA is intracellularly de-esterified and oxidized into highly fluorescent DCF^+. In brief, samples were co-incubated with H_2DCFDA (final concentration: 200 μmol/L) and PI (final concentration: 12 μmol/L) for 30 min. Four different sperm populations were identified in flow cytometry dot-plots: (1) viable sperm with low intracellular levels of H_2O_2 (DCF^-/PI^-); (2) viable sperm with high intracellular levels of H_2O_2 (DCF^+/PI^-); (3) non-viable sperm with low intracellular levels of H_2O_2 (DCF^-/PI^+); and (4) non-viable sperm with high intracellular levels of H_2O_2 (DCF^+/PI^+). The percentage of SYBR-$14^-/PI^-$ particles corresponding to non-sperm debris was used to correct the percentages of viable sperm with low intracellular levels of H_2O_2 (DCF^-/PI^-), and the percentages of the other sperm populations were recalculated. DCF^- spill-over into the FL3 channel was compensated (2.45%). Intracellular levels of hydrogen peroxide were assessed through the calculation of the percentage of viable sperm with high intracellular levels of peroxide (DCF^+/PI^- sperm) within the population of viable spermatozoa (PI^- sperm).

Intracellular pH

Intracellular pH was measured through staining with BCECF following the protocol from Pons-Rejraji et al. (2009) with minor modifications. BCECF is intracellularly modified by esterases, and its fluorescence excitation profile is pH-dependent. In brief, samples were incubated in the presence of BCECF (final concentration: 6 μmol/L) for 25 min. Data were not compensated. The intensity of fluorescence was measured for the different treatments and time points, and the intracellular pH was calculated as the variation compared to the control.

Immunoblotting

Tyrosine phosphorylation levels were assessed for the different treatments and time points through immunoblotting. With this purpose, samples were centrifuged at 600 × *g* and capacitation medium was discarded. Samples were subsequently stored at −80°C until analysis.

For cell lysis, samples were thawed on ice and resuspended in lysis buffer (xTractor® Buffer; Takara Bio, Mountain View, CA, United States) supplemented with 1% protease inhibitor cocktail, 1 mM sodium orthovanadate and 1 mM phenylmethanesulfonyl fluoride (PMSF). After incubation at 4°C for 30 min with shaking, samples were sonicated thrice for 30 s. Samples were then centrifuged at 4°C and 12,000 × *g* for 15 min, and supernatants were collected and stored at −80°C until analysis. Total protein was quantified by triplicate through a detergent compatible (DC) method (Bio-Rad, Hercules, CA, United States) using an Epoch™ microplate spectrophotometer (BioTek, Winooski, VT, United States).

For each sample, 10 μg of total protein was diluted in loading buffer, which consisted of 4 × Laemmli reductor (Bio-Rad) supplemented with 10% (v:v) 2-Mercaptoethanol. Then, samples were incubated at 95°C for 5 min and a total volume of 30 μL per sample was loaded onto a gradient (8–16%) polyacrylamide gel (Mini-PROTEAN® TGX Stain-Free™ Precast Gels, Bio-Rad). Electrophoresis ran at 150 V for approximately 1 h, and proteins from the gels were transferred onto polyvinylidene difluoride (PVDF) membranes using *Trans*-Blot® Turbo™ (Bio-Rad). Next, total protein content was visualized by UV exposition and acquisition using a G:BOX Chemi XL system (SynGene, Frederick, MD, United States). Membranes were subsequently incubated in blocking buffer [10 mM Tris, 150 mM NaCl, 0.05% (v:v) Tween-20 and 5% (w:v) bovine serum albumin (Roche Diagnostics, S.L., Basel, Switzerland); pH = 7.3] in agitation for 1 h at room temperature. Then, membranes were incubated overnight at 4°C with a 4G10® Platinum, Anti-Phosphotyrosine Antibody [mouse monoclonal cocktail IgG2b; Sigma Aldrich; 1:5,000; (v:v)]. Then, membranes were washed five times with TBS-Tween 20 1 × (10 mmol/L Tris, 150 mmol/L NaCl and 0.05% Tween-20; pH = 7.3) for 5 min before incubation with a rabbit anti-mouse, secondary antibody conjugated with HRP [ref. P0260; Agilent, Santa Clara, CA, United States; 1:10,000 (v:v)] for 1 h in agitation. Finally, membranes were

washed five times. For visualization, membranes were incubated in a chemiluminescence substrate (Immobilion^{TM} Western Detection Reagents, Millipore) for 5 min, and then revealed in G:BOX Chemi XL 1.4.

Two technical replicates per sample were evaluated, and band quantification was performed using the Image Studio^{TM} Lite Software (LI-COR Biosciences GmbH, Bad Homburg vor der Höhe, Germany). Band pattern quantifications were normalized using total protein values, and the corresponding mean ± SEM was calculated.

Enzyme-Linked Immunosorbent Assays

Concentrations of PKA in sperm samples were measured using a colorimetric activity kit (EIAPKA; Invitrogen, ThermoFisher Scientific) following the manufacturer's instructions. In brief, samples were centrifuged at 600 × *g*, capacitation medium was discarded and sperm cells were stored at −80°C until analysis. For cell lysis, samples were resuspended in cell lysis buffer, incubated for 30 min on ice with occasional vortexing, and then sonicated three times for 30 s each. After that, samples were centrifuged at 10,000 × *g* and 4°C for 10 min, and supernatants were recovered for analysis. Then, standards were diluted in kinase reaction buffer to obtain the standard curve (0.625, 1.25, 2.5, and 5 U/mL PKA), and samples were also diluted in this buffer (1:5,000). Then, 40 μL of the standards and diluted samples were added to the plate in duplicate, and 10 μL of ATP were also added to each well prior to a 90-min incubation at 30°C. After washing plate wells four times, 25 μL of the Donkey anti-Rabbit IgG HRP conjugate was added to each well followed by 25 μL of the Phospho PKA substrate antibody. Then, the plate was incubated at room temperature for 1 h. After washing the plate wells four times, 100 μL of TMB substrate was added to each well before incubating the plate at room temperature for 30 min. Finally, 50 μL of stop solution was added to all wells, and the plate was immediately read at 450 nm using an Epoch^{TM} microplate spectrophotometer (BioTek). Means were calculated for duplicate measurements of standards and samples, and average optical density from the blank was subtracted. The equation of the linear regression curve obtained through the interpolation of PKA concentration from absorbance reading was: (PKA) = 12.148 × Abs + 0.2793, R^2 = 0.9975 for one plate, and (PKA) = 6.5865 × Abs—0.0454, R^2 = 0.9962 for the other. This ELISA kit showed a sensitivity of 0.366 U/mL.

Concerning cAMP concentration, sperm samples were measured using a colorimetric competitive ELISA kit (ab133051; Abcam, Cambridge, United Kingdom) following the manufacturer's instructions. Briefly, samples were centrifuged at 600 × *g* to eliminate capacitation medium and sperm cells were stored at −80°C until analysis. Lysis buffer (0.1 mol/L HCl and 1% Triton X-100) was used to resuspend sperm cells, which were incubated at room temperature for 30 min with agitation. Next, samples were sonicated three times for 30 s and cell debris were pelleted through centrifugation at 10,000 × *g* and 4°C for 10 min. Supernatants were recovered for analysis. Then, standards were diluted in lysis buffer to obtain the standard curve (0.078, 0.312, 1.25, 5, and 20 pmol/mL cAMP), and samples were also diluted in this buffer (1:20; v:v). Then, acetylating reagent [acetic anhydride diluted and triethylamine; 1:2 (v:v)] was added to standards and samples [1:20 (v:v)] to achieve the maximum sensitivity of the kit (0.039 nmol/L). Apart from standards and samples, different controls were also loaded onto the plate: blank wells, that only contained pNpp substrate; total activity wells, which contained conjugate and pNpp substrate; non-specific binding control, with neutralizing reagent, lysis buffer, conjugate and substrate; and the zero standard, that contained neutralizing reagent, lysis buffer, conjugate, antibody and substrate. Fifty μL of neutralizing reagent was added to the plate wells, prior to the addition of 100 μL of standards and samples. After that, 50 μL of Cyclic AMP complete Alkaline Phosphatase conjugate was added, followed by 50 μL of cyclic AMP complete antibody. Thereafter, the plate was incubated at room temperature for 2 h with shaking. Next, 200 μL of pNpp substrate solution was added to every well and the plate was incubated at room temperature for 1 h. Finally, 50 μL of stop solution was added to every well and the plate was then read at 405 nm using an Epoch^{TM} microplate spectrophotometer (BioTek). Means were calculated for duplicate measurements of standards and samples, and average optical densities from the blank and the non-specific binding control were subtracted. The equation of the exponential regression curve obtained through the interpolation of cAMP concentration from absorbance reading was: (cAMP) 11.16942 × $e^{-11.30138 \times Abs}$, R^2 = 0.99001 for one plate, and (cAMP) = 29.322 × $e^{-24.69 \times Abs}$, R^2 = 0.9821 for the other.

Statistical Analyses

The results of this work were analyzed using a statistical package (IBM SPSS Statistics 25.0; Armonk, New York, United States). In order to assess the distribution of data and homogeneity of variances, Shapiro–Wilk and Levene tests were run, respectively. For each sperm parameter, a mixed model was subsequently conducted. The time point (i.e., 0, 120, 240, 250, or 300 min) was the intra-subjects factor, the treatment at a given concentration (i.e., control, CuSO, $HgCl_2$ or AgSDZ) was the fixed-effects factor (inter-subject), and the ejaculate pool (i.e., 1–8) was the random-effects factor. Pair-wise comparisons were evaluated through a *post hoc* Sidak test, and the level of significance was set at $P \leq 0.05$. Data are shown as mean ± standard error of the mean (SEM).

RESULTS

To determine the effects of AQP inhibitors during sperm capacitation, quality and function parameters of spermatozoa from the control and samples containing CuSO, $HgCl_2$ or AgSDZ were evaluated after 0, 120, 240, 250 and 300 min of incubation. No differences between treatments and the control ($P > 0.05$) were expected at 0 min for any parameter measured, since inhibitors were added immediately before starting incubation in capacitation medium. Therefore, sperm quality was exclusively measured in the control samples at 0 min (**Figures 1–6**).

Sperm Motility

Different motility and kinetics parameters were assessed in the presence of separate inhibitors and the control throughout

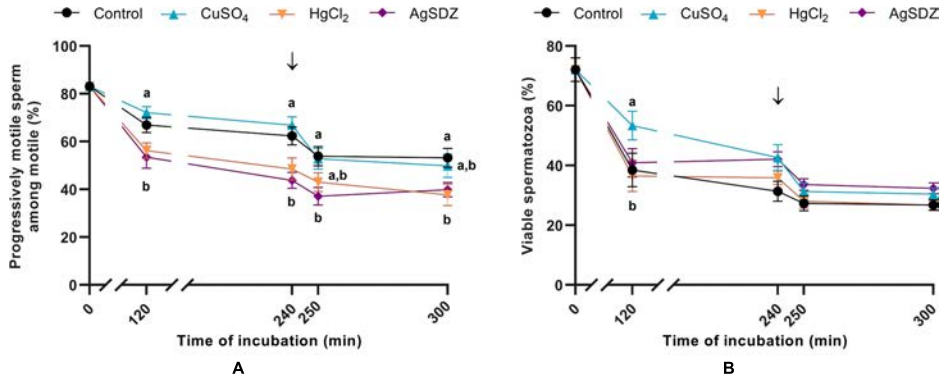

FIGURE 1 | Sperm motility and viability. **(A)** Percentages of progressively motile sperm within the population of motile cells (%) and **(B)** sperm viability measured as the percentage of spermatozoa with an intact plasma membrane (%) in samples exposed to the presence or absence of different AQP inhibitors in the capacitation medium: cooper sulfate ($CuSO_4$), mercury chloride ($HgCl_2$) and silver sulfadiazine (AgSDZ). Data were collected after 0, 120 and 240 min of incubation in capacitation medium. At this point, progesterone was added to capacitation medium (arrow) and data were collected after further 10 min and 60 min of incubation. Data are shown as mean ± SEM, and different letters (a,b) indicate significant differences ($P < 0.05$) between different treatments within a given time point.

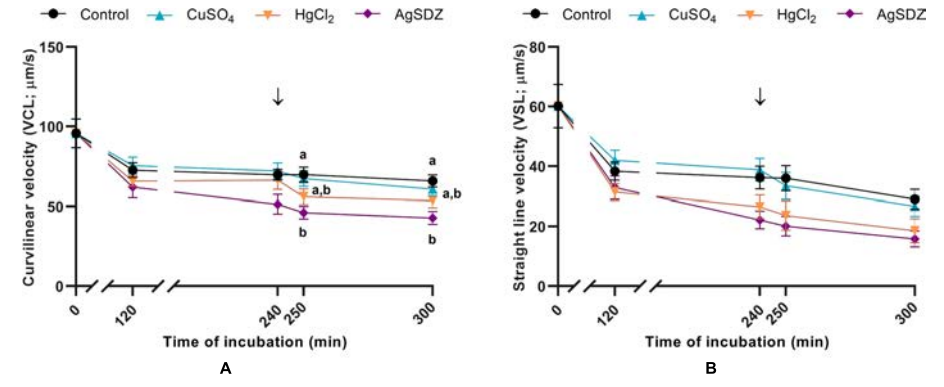

FIGURE 2 | Sperm kinetics parameters. **(A)** Curvilinear velocity (VCL, µm/s) and **(B)** straight-line velocity (VSL, µm/s) in samples exposed to the presence or absence of different AQP inhibitors in the capacitation medium: cooper sulfate ($CuSO_4$), mercury chloride ($HgCl_2$) and silver sulfadiazine (AgSDZ). Data were collected after 0, 120 and 240 min of incubation in capacitation medium. At this point, progesterone was added to capacitation medium (arrow) and data were collected after further 10 min and 60 min of incubation. Data are shown as mean ± SEM, and different letters (a,b) indicate significant differences ($P < 0.05$) between different treatments within a given time point.

incubation. From 120 min of incubation until the end of the period at 300 min, PMOT from the population of motile sperm (**Figure 1A**) was significantly lower in the treatments containing $HgCl_2$ and AgSDZ than in the control ($P < 0.05$). Nevertheless, TMOT was significantly lower than the control after 120 min of incubation only (**Table 1**).

Regarding kinetics parameters, VCL (**Figure 2A**) was significantly ($P < 0.05$) lower in the presence of AgSDZ than in control samples from 250 min of incubation in capacitation medium and until the end of the experiment. Similarly, samples containing AgSDZ presented lower ALH and BCF with respect to the control at 240, 250 and 300 min; whereas in the presence of $HgCl_2$ samples presented the same effect from 250 min of incubation ($P < 0.05$; **Table 1**). In addition, STR was lower than the control in the presence of $HgCl_2$ after 240 min and 300 min of incubation; in samples treated with AgSDZ, this effect was only observed after 300 min of incubation ($P < 0.05$; **Table 2**). Moreover, no significant differences between treatments/inhibitors and the control were observed in terms

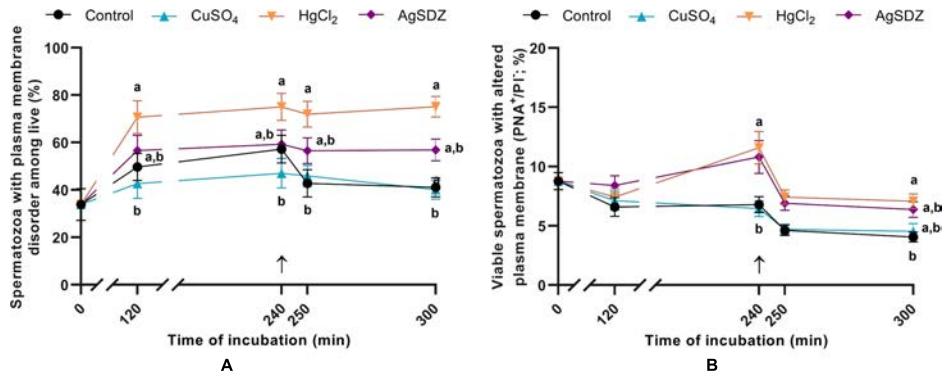

FIGURE 3 | Sperm plasma and acrosome membranes status. **(A)** Percentages of sperm cells with high membrane lipid disorder within the viable sperm population (%) and **(B)** percentages of viable spermatozoa with altered integrity of acrosome membrane (%) in samples exposed to the presence or absence of different AQP inhibitors in the capacitation medium: cooper sulfate ($CuSO_4$), mercury chloride ($HgCl_2$) and silver sulfadiazine (AgSDZ). Data were collected after 0, 120 and 240 min of incubation in capacitation medium. At this point, progesterone was added to capacitation medium (arrow) and data were collected after further 10 min and 60 min of incubation. Data are shown as mean ± SEM, and different letters (a,b) indicate significant differences ($P < 0.05$) between different treatments within a given time point.

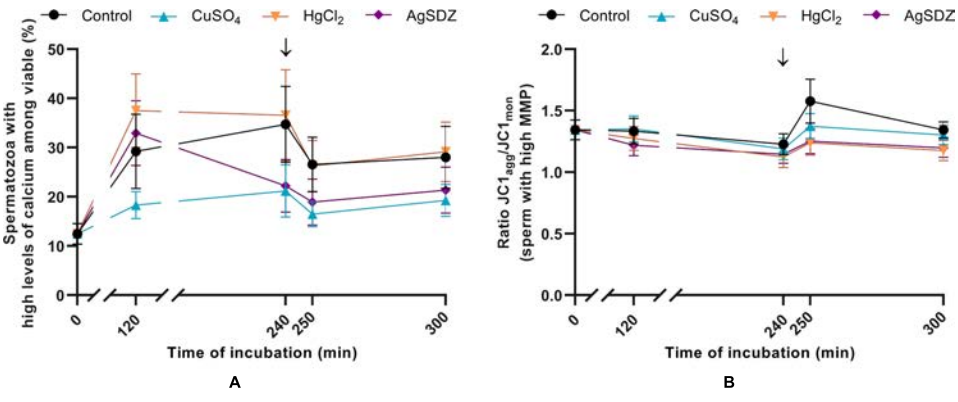

FIGURE 4 | Intracellular levels of calcium and mitochondrial membrane potential. **(A)** Percentages of spermatozoa with high levels of intracellular calcium within the viable sperm population (%) and **(B)** ratio of $JC1_{agg}/JC1_{mon}$ intensity of fluorescence in the population of spermatozoa with high MMP in samples exposed to the presence or absence of different AQP inhibitors in the capacitation medium: cooper sulfate ($CuSO_4$), mercury chloride ($HgCl_2$) and silver sulfadiazine (AgSDZ). Data were collected after 0, 120 and 240 min of incubation in capacitation medium. At this point, progesterone was added to capacitation medium (arrow) and data were collected after further 10 min and 60 min of incubation. Data are shown as mean ± SEM, and different letters (a,b) indicate significant differences ($P < 0.05$) between different treatments within a given time point.

of VSL (**Figure 2B**), VAP, LIN, or WOB ($P > 0.05$) at any time point (**Tables 1**, **2**).

Sperm Plasma Membrane Integrity and Membrane Lipid Disorder

As aforementioned, sperm plasma membrane integrity was evaluated through co-staining with SYBR-14 and PI in order to assess the effects of separate inhibitors at the different time points (**Figure 1B**). Sperm viability was higher in the presence of $CuSO_4$ than in the control after 120 min of incubation ($P > 0.05$).

Co-staining with M540 and YO-PRO-1 was used to evaluate the effects of the different inhibitors on plasma membrane lipid disorder during *in vitro* capacitation (**Figure 3A**). Percentages of spermatozoa exhibiting high levels of plasma membrane lipid disorder within the viable sperm population were significantly

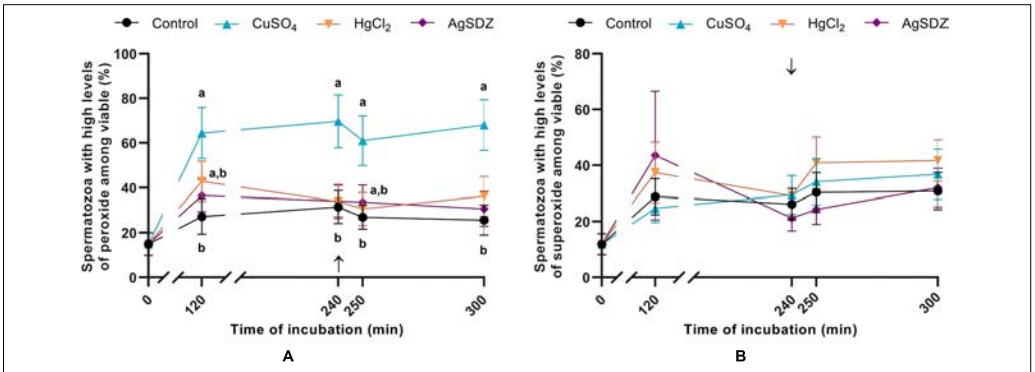

FIGURE 5 | Intracellular levels of ROS. **(A)** Percentages of spermatozoa with high intracellular levels of hydrogen peroxide within the viable sperm population (%) and **(B)** percentages of spermatozoa with high intracellular levels of superoxide within the viable sperm population (%) in samples exposed to the presence or absence of different AQP inhibitors in the capacitation medium: cooper sulfate ($CuSO_4$), mercury chloride ($HgCl_2$) and silver sulfadiazine (AgSDZ). Data were collected after 0, 120 and 240 min of incubation in capacitation medium. At this point, progesterone was added to capacitation medium (arrow) and data were collected after further 10 min and 60 min of incubation. Data are shown as mean ± SEM, and different letters (a,b) indicate significant differences ($P < 0.05$) between different treatments within a given time point.

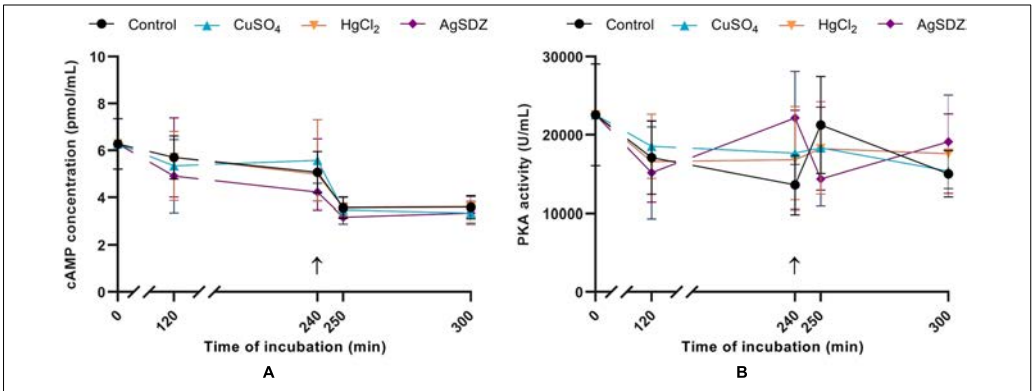

FIGURE 6 | Intracellular concentration of cAMP and PKA activity. **(A)** Intracellular concentration of cyclic AMP (cAMP) in sperm cells (pmol/mL) and **(B)** PKA intracellular activity (U/mL) in samples exposed to the presence or absence of different AQP inhibitors in the capacitation medium: cooper sulfate ($CuSO_4$), mercury chloride ($HgCl_2$) and silver sulfadiazine (AgSDZ). Data were collected after 0, 120, and 240 min of incubation in capacitation medium. At this point, progesterone was added to capacitation medium (arrow) and data were collected after further 10 and 60 min of incubation. Data are shown as mean ± SEM, and different letters (a,b) indicate significant differences ($P < 0.05$) between different treatments within a given time point.

higher in samples containing $HgCl_2$ than in the control after 250 and 300 min of incubation ($P < 0.05$). Nevertheless, a notable trend was observed from 120 min of incubation, since membrane lipid disorder was already higher in samples treated with $HgCl_2$ than in the control ($P = 0.062$).

Acrosome Membrane Integrity

Sperm were co-stained with PNA-FITC and PI to evaluate the effects of the different AQP inhibitors on acrosome membrane integrity during *in vitro* capacitation (**Figure 3B**). Samples treated with $HgCl_2$ and AgSDZ presented a higher percentage of spermatozoa with an altered plasma/acrosomal membrane after 240 min of incubation ($P < 0.05$). At the end of the experiment (300 min), this difference persisted in samples treated with $HgCl_2$ ($P < 0.05$).

Intracellular Levels of Calcium

Intracellular levels of calcium were evaluated through co-staining with Fluo-3 AM and PI in order to assess the effects of different AQP inhibitors during capacitation (**Figure 4A**). There were no

significant differences between the control and samples treated with inhibitors on the intracellular levels of calcium in the viable sperm population at any time point ($P > 0.05$).

Mitochondrial Membrane Potential

Mitochondrial membrane potential (MMP) was assessed through staining with JC1 in order to evaluate the effect of different inhibitors on this sperm function parameter during capacitation (**Figure 4B**). In the population of sperm with high MMP, the ratio of $JC1_{agg}/JC1_{mon}$ intensity presented no significant differences between the different treatments and the control at any time point ($P > 0.05$).

Intracellular Levels of ROS

The effects of different AQP inhibitors on the intracellular levels of ROS during capacitation were evaluated with two different co-staining protocols: H_2DCFDA/PI was used to assess peroxide levels and HE/YO-PRO-1 was used to determine $O_2^{-}\bullet$ levels. The addition of $CuSO_4$ to capacitation medium caused an increase in the percentage of viable spermatozoa with high intracellular levels of peroxides at any time point ($P < 0.05$; **Figure 5A**). No differences between the control and treated samples were observed in terms of $O_2^{-}\bullet$ levels at any time point ($P > 0.05$; **Figure 5B**).

Intracellular cAMP Levels and PKA Activity

Two different Enzyme-Linked Immunosorbent Assays were conducted to assess PKA intracellular activity and intracellular cAMP levels. No significant differences in terms of cAMP concentration (**Figure 6A**) or PKA activity (**Figure 6B**) were observed between the control and AQP inhibitors at any time point.

Intracellular pH

To assess the effects of inhibiting AQPs on intracellular pH, a BCECF staining protocol was used. The addition of AgSDZ caused a decrease in intracellular pH compared to the control after 250 min of incubation ($P < 0.05$; **Figure 7A**).

Tyrosine Phosphorylation

Levels of tyrosine phosphorylation were assessed through immunoblotting. A tyrosine phosphorylation band pattern was observed, and apart from total phosphorylation, four different bands were analyzed to assess the potential differences between

TABLE 1 | Sperm motility and kinetics parameters from direct measurement.

Time (min)	Control	$CuSO_4$	$HgCl_2$	AgSDZ
		TMOT (%)		
0	62.71% ± 2.33	62.71% ± 2.33	62.71% ± 2.33	62.71% ± 2.33
120	35.60% ± 3.73^{a}	40.13% ± 3.76^{a}	22.09% ± 2.05^{b}	19.29% ± 2.52^{b}
240	30.87% ± 3.15	35.27% ± 3.77	21.01% ± 2.81	13.54% ± 2.47
250	16.24% ± 2.28	17.11% ± 2.70	10.00% ± 1.15	7.67% ± 1.04
300	16.11% ± 2.64	14.96% ± 2.45	8.09% ± 1.07	7.65% ± 1.28
		VAP (μm/s)		
0	69.87 ± 8.56	69.87 ± 8.56	69.87 ± 8.56	69.87 ± 8.56
120	46.98 ± 3.64	50.00 ± 4.16	40.23 ± 3.08	40.45 ± 4.66
240	44.76 ± 3.90	46.83 ± 4.27	37.06 ± 3.98	29.24 ± 3.60
250	45.35 ± 4.32	42.77 ± 4.82	32.10 ± 4.75	27.63 ± 3.40
300	38.27 ± 3.31	35.48 ± 3.67	27.49 ± 4.04	22.49 ± 2.83
		ALH (μm)		
0	3.05 ± 0.15	3.05 ± 0.15	3.05 ± 0.15	3.05 ± 0.15
120	2.57 ± 0.09	2.61 ± 0.11	2.40 ± 0.11	2.17 ± 0.20
240	2.42 ± 0.07^{a}	2.51 ± 0.08^{a}	2.42 ± 0.20^{a,b}	1.84 ± 0.17^{b}
250	2.64 ± 0.11^{a}	2.41 ± 0.13^{a}	1.87 ± 0.12^{a,b}	1.53 ± 0.15^{b}
300	2.39 ± 0.10^{a}	2.04 ± 0.17^{a,b}	1.75 ± 0.18^{a,b}	1.46 ± 0.17^{b}
		BCF (Hz)		
0	11.06 ± 0.64	11.06 ± 0.64	11.06 ± 0.64	11.06 ± 0.64
120	9.92 ± 0.56^{a,b}	10.59 ± 0.47^{a}	8.44 ± 0.45^{a,b}	8.04 ± 0.74^{b}
240	9.18 ± 0.55^{a}	9.88 ± 0.52^{a}	7.97 ± 0.88^{a,b}	6.53 ± 0.89^{b}
250	9.12 ± 0.74^{a}	8.24 ± 0.63^{a}	5.33 ± 0.63^{b}	4.76 ± 0.63^{b}
300	7.98 ± 0.55^{a}	7.44 ± 0.74^{a}	4.75 ± 0.72^{b}	4.43 ± 0.68^{b}

Percentage of total motile spermatozoa (TMOT, %), average pathway velocity (VAP, μm/s), amplitude of lateral head displacement (ALH, μm) and beat-cross frequency (BCF, Hz) from samples exposed to the presence or absence of different AQP inhibitors in the capacitation medium: cooper sulfate ($CuSO_4$), mercury chloride ($HgCl_2$) and silver sulfadiazine (AgSDZ).
Data were collected after 0, 120, and 240 min of incubation in capacitation medium. At this point, progesterone was added to capacitation medium (arrow) and data were collected after further 10 min and 60 min of incubation.
Data are shown as mean ± SEM, and different letters (a,b) indicate significant differences ($P < 0.05$) between different treatments within a given time point.

TABLE 2 | Secondary sperm kinetics parameters.

Time (min)	Control	$CuSO_4$	$HgCl_2$	AgSDZ
		LIN (%)		
0	61.18 ± 3.02	61.18 ± 3.02	61.18 ± 3.02	61.18 ± 3.02
120	52.56 ± 2.28	55.43 ± 2.03	47.52 ± 3.05	49.28 ± 4.66
240	50.57 ± 3.82^{a,b}	53.45 ± 2.99^{a}	38.71 ± 4.69^{b}	41.22 ± 3.45^{a,b}
250	50.51 ± 3.62	47.81 ± 3.74	39.88 ± 4.78	41.98 ± 3.56
300	43.05 ± 3.47	42.47 ± 3.85	31.48 ± 4.79	33.51 ± 3.59
		STR (%)		
0	86.31 ± 1.09	86.31 ± 1.09	86.31 ± 1.09	86.31 ± 1.09
120	81.41 ± 1.52	84.26 ± 1.44	77.23 ± 1.74	75.04 ± 5.94
240	79.07 ± 2.34^{a}	82.30 ± 2.07^{a}	66.13 ± 4.46^{b}	71.72 ± 3.14^{a,b}
250	77.57 ± 2.54	76.27 ± 2.28	68.24 ± 3.15	69.08 ± 2.45
300	73.41 ± 2.62^{a}	72.58 ± 3.06^{a,b}	59.68 ± 4.45^{c}	62.38 ± 4.29^{b,c}
		WOB (%)		
0	70.69 ± 3.24	70.69 ± 3.24	70.69 ± 3.24	70.69 ± 3.24
120	64.34 ± 2.35	65.64 ± 2.03	60.92 ± 2.80	60.40 ± 5.31
240	62.93 ± 3.33	64.35 ± 2.65	52.17 ± 4.37	55.97 ± 3.14
250	61.00 ± 3.61	61.78 ± 3.31	55.87 ± 4.12	59.42 ± 3.25
300	57.40 ± 2.96	56.90 ± 3.21	48.47 ± 4.01	49.42 ± 3.11

Linearity (LIN, %), straightness (STR, %) and oscillation index (WOB, %) from samples exposed to the presence or absence of different AQP inhibitors in the capacitation medium: cooper sulfate ($CuSO_4$), mercury chloride ($HgCl_2$) and silver sulfadiazine (AgSDZ).
Data were collected after 0, 120, and 240 min of incubation in capacitation medium. At this point, progesterone was added to capacitation medium (arrow) and data were collected after additional 10 and 60 min of incubation.
Data are shown as mean ± SEM, and different letters (a,b) indicate significant differences ($P < 0.05$) between different treatments within a given time point.

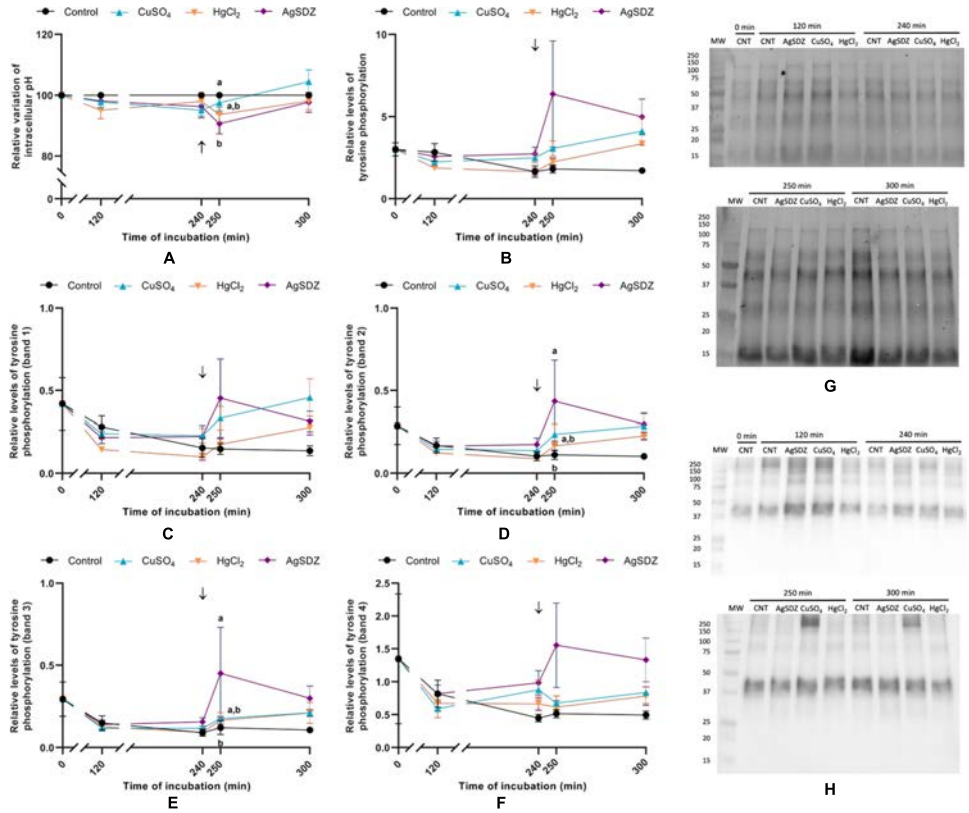

FIGURE 7 | Relative variation of pH and relative levels of tyrosine phosphorylation. **(A)** Intracellular variation of pH compared to the control sample; **(B)** relative levels of total tyrosine phosphorylation; **(C)** relative levels of total tyrosine phosphorylation from band 1 (∼200 kDa); **(D)** relative levels of total tyrosine phosphorylation from band 2 (∼175 kDa); **(E)** relative levels of total tyrosine phosphorylation from band 3 (∼75 kDa); **(F)** relative levels of total tyrosine phosphorylation from band 4 (∼40 kDa); **(G)** total protein measured through stain-free; and **(H)** immunoblotting showing the tyrosine phosphorylation pattern after the incubation with a 4G10® Platinum, mouse monoclonal Anti-Phosphotyrosine Antibody [1:5,000; (v:v)] and rabbit anti-mouse, secondary antibody conjugated with HRP [1:10,000; (v:v)]. All parameters were measured in samples exposed to the presence or absence of different AQP inhibitors in the capacitation medium: cooper sulfate ($CuSO_4$), mercury chloride ($HgCl_2$) and silver sulfadiazine (AgSDZ). Data were collected after 0, 120 and 240 min of incubation in capacitation medium. At this point, progesterone was added to capacitation medium (arrow) and data were collected after further 10 and 60 min of incubation. Data are shown as mean ± SEM, and different letters (a,b) indicate significant differences ($P < 0.05$) between different treatments within a given time point.

inhibitors and the control (**Figures 7B–H**). Despite no differences being observed in terms of total tyrosine phosphorylation of sperm proteins between different treatments and the control ($P > 0.05$), bands 2 and 3 from samples treated with AgSDZ presented a higher intensity than the control ($P < 0.05$), thus indicating higher levels of tyrosine phosphorylation.

DISCUSSION

Although several studies to address the function of ion channels during sperm capacitation were conducted (reviewed by Puga Molina et al., 2018), the potential role of water channels on this process is yet to be unveiled. Nevertheless, it is well known that soluble adenylate cyclase (sAC), which is regulated by pH, is crucial for the cAMP-PKA pathway triggered during capacitation (Chang and Oude-Elferink, 2014). Therefore, given the link between water flow and intracellular pH, it is reasonable to suggest that AQPs might be relevant in this process. For this reason, the aim of this study was to assess the role of the different groups of AQPs during mammalian sperm capacitation and acrosome reaction using the pig as a model. Three different salts of transition metals that have largely been demonstrated as AQP inhibitors (Haddoub et al., 2009)

were used: cooper sulfate ($CuSO_4$), mercury chloride ($HgCl_2$) and silver sulfadiazine (AgSDZ). $CuSO_4$ is a specific inhibitor of AQP3, since Cu^{2+} binds to three different extracellular residues of this protein, which correspond, in human AQP3, to Trp128, Ser152 and His241 (Zelenina et al., 2004). $HgCl_2$ is an unspecific and reversible inhibitor of AQPs; its blocking effect presumably occurs because of the Hg^{2+}-mediated, covalent modification of a Cys residue that is present in the pore of most AQPs. This modification either blocks the channel or causes conformational changes that avoid water transport (Hirano et al., 2010). Nevertheless, the fact that this Cys residue is not present in AQP7 could explain why previous studies demonstrated that AQP7 is Hg^{2+}-resistant (Ishibashi et al., 1997). Finally, AgSDZ is an unspecific, irreversible inhibitor of all AQPs, and is also thought to interact with this Cys residue of the AQP pore. Such an irreversibility suggests that its inhibitory mechanism might be different from that of Hg^{2+}. Niemietz and Tyerman (2002) surmised that, since the size of this ion (2.5 Å) matches the diameter of the AQP pore (2.8 Å), Ag^{2+} might block the AQP channel; thus, it is possible that this metal also inhibits AQP7 through that mechanism.

The effects of the aforementioned AQP inhibitors were evaluated in terms of sperm motility and kinetics parameters through a CASA system; flow cytometry was used to assess different sperm quality and function parameters; and tyrosine phosphorylation levels, PKA activity and intracellular levels of cAMP were evaluated as indicators of the intracellular pathways involved in capacitation. Briefly, the presence of $CuSO_4$ led to higher sperm viability than the control and increased intracellular levels of peroxides after 120 min of incubation; this effect persisted even after the addition of progesterone to trigger the acrosome reaction at 240 min. The addition of $HgCl_2$ augmented membrane lipid disorder from 120 min until the end of the experiment, caused a rise in the percentage of spermatozoa with an altered acrosome membrane from 240 min to the end of the experiment, and decreased progressive motility and other kinetics parameters from 120 min of incubation. Finally, the addition of AgSDZ caused a decrease in different parameters that evaluated sperm motility and kinetics during the entire incubation period, and the same effects on acrosome membrane integrity that were observed in the presence of $HgCl_2$. In addition, the presence of AgSDZ caused a decrease in intracellular pH, as well as an increase in tyrosine phosphorylation levels after the addition of progesterone (250 min of incubation).

Regarding the effects of $CuSO_4$, it became apparent from our results that AQP3 has not a key role in sperm capacitation or acrosome reaction. On the one hand, the higher percentages of sperm viability compared to the control after 120 min of incubation could be misleading. Considering the capacitation process leads to plasma membrane destabilization, it is possible that PI enters viable, membrane-destabilized sperm. Thus, while a population of sperm stained with both SYBR-14 and PI was observed, it could not be considered as strictly viable, since their viability was already compromised. In addition, the presence of $CuSO_4$ led to a lower (although not significant) membrane lipid disorder compared to the control. This could explain the higher rate of entrance of PI into live cells in the control compared to sperm treated with $CuSO_4$. These slight differences could lead to the small (but significant) difference in sperm viability between the control and the $CuSO_4$ treatment. On the other hand, the increase in intracellular levels of peroxides could be explained because of AQP3 permeability to this molecule (Miller et al., 2010). Therefore, AQP3-inhibition could block the outflow of peroxides to the extracellular medium, which would make them to accumulate intracellularly. In fact, Delgado-Bermúdez et al. (2019) also reported an increase of intracellular peroxides in pig spermatozoa in the presence of 1,3-propanediol, another inhibitor of AQPs. Surprisingly, and despite high extracellular peroxide levels having a detrimental effect upon sperm function (Laforenza et al., 2017), no sperm quality or function parameter was altered when peroxides were intracellularly accumulated. This suggests that sperm capacitation and acrosome reaction, at least in pigs, do not seem to be impaired by high intracellular H_2O_2 levels. Nevertheless, ROS have a central role as stimulators of capacitation that has been extensively described in other mammalian species (reviewed by Aitken, 2017). In fact, Rivlin et al. (2004) suggested that while relatively low concentrations of H_2O_2 are beneficial for sperm capacitation, too high ones inhibit that process. This report also concluded that H_2O_2 activates adenylyl cyclase to produce cAMP, leading to PKA-dependent protein tyrosine phosphorylation. In addition, H_2O_2 has been demonstrated to inhibit different tyrosine phosphatases (Hecht and Zick, 1992), and Aitken (2017) suggested that in sperm this inhibition could increase phosphorylation of cAMP-PKA pathway target proteins. In spite of this, in this work, high intracellular H_2O_2 levels did not seem to stimulate capacitation-associated changes, either in terms of acrosome membrane integrity or in terms of cAMP levels, PKA activity or tyrosine phosphorylation patterns. Therefore, it seems that the observed increase in intracellular peroxides was not sufficient either to impair or to enhance capacitation or acrosome reaction. Additional studies are needed to evaluate the relevance of H_2O_2 in pig sperm capacitation.

Concerning $HgCl_2$, it inhibits the different AQPs present in mammalian sperm except AQP7 (i.e., AQP3, AQP8, AQP9, and AQP11). Samples treated with $HgCl_2$ showed an increase in membrane lipid disorder and impaired kinetics parameters, which could result from cholesterol efflux and lipid reorganization, since this is a featured event that occurs during capacitation (reviewed by Aitken, 2017). In this context, one could posit that certain capacitation-associated events are enhanced when some AQPs are inhibited. Nevertheless, the absence of significant effects on acrosome membrane integrity and on intracellular calcium levels after the addition of progesterone suggests that plasma membrane alterations are not related to a higher sperm ability to elicit *in vitro* capacitation and the subsequent acrosome reaction. This is supported by the fact that neither tyrosine phosphorylation, nor cAMP levels or PKA activity were altered. Thus, while the presence of $HgCl_2$ seemed to induce an increase in membrane lipid disorder, likely increasing membrane fusogenicity, the observed changes were capacitation-like events that did not drive a proper, physiological sperm capacitation, as they did not lead to an increase in the percentage of spermatozoa undergoing the acrosome reaction. Considering all the aforementioned, these results suggest that AQP3 and AQP11 might exert some influence

on certain capacitation-associated changes, but do not have direct consequences on the ability of spermatozoa to undergo the acrosome reaction. A possible reason for the observed effects would be that the limitation of water flow through the plasma membrane resulting from AQPs blocking would compromise sperm osmoregulation ability, which is in turn crucial for the activation and maintenance of sperm motility (reviewed by Chen and Duan, 2011). In our experiment, blocking of AQPs during *in vitro* capacitation might have caused an alteration in sperm volume, which could have ended up with plasma membrane damage and motility impairment, without altering the intracellular pathways involved in sperm capacitation.

Finally, AgSDZ, an unspecific inhibitor of all AQPs had similar effects to those observed in the presence of $HgCl_2$. Nevertheless, an additional effect was observed, which suggests a relevant role of all AQPs as a whole during sperm capacitation and acrosome reaction. Samples treated with AgSDZ showed a lower intracellular pH compared to the control after the addition of progesterone to trigger the acrosome reaction, with a concomitant increase in tyrosine phosphorylation at the same time point (250 min of incubation). Nonetheless, cAMP levels and PKA activity were not impaired in the presence of this inhibitor. Therefore, either the concentration and activity changes were too subtle to be detected through the methods used in this study, or other signaling pathways were involved in the observed alteration of tyrosine phosphorylation patterns. According to Buffone et al. (2014), capacitation and acrosome reaction are driven through different signaling pathways. On the one hand, capacitation-associated changes are driven by phosphorylation of tyrosine residues as a downstream effect of the cAMP-PKA pathway, which relies upon cAMP synthesis by sAC. On the other hand, acrosome reaction is triggered by progesterone, which interacts with a GPCR coupled to a transmembrane adenylate cyclase (trAC) that is the source of the cAMP required in this process. It is important to highlight that, whilst sAC is regulated by pH, trAC activity does not. As the change in pH caused by the blockade of AQPs occurred after the addition of progesterone, it would be reasonable to suggest that sAC activity was unaltered, which would be in agreement with the lack of variations in PKA activity and cAMP levels. A potential candidate to explain the observed alteration in tyrosine phosphorylation levels would be PKC, which is involved in the intracellular signaling pathways that trigger the acrosome reaction (Teijeiro et al., 2017). Therefore, changes in osmoregulation during capacitation could induce latent alterations in sperm function that would become apparent upon triggering the acrosome reaction. The fact that these effects are only observed when all AQPs are inhibited as a whole might be the consequence of a functional compensation that is only possible when some AQPs remain unblocked. When a general inhibitor like AgSDZ is added and the function of all AQPs is suppressed, the absence of osmoregulation becomes an unbeatable challenge for the sperm cell that ends up altering its physiology, including the intracellular signaling pathways involved in the acrosome reaction. Additional experiments evaluating the mechanisms through which AQPs inhibition ends up with changes in intracellular pH and tyrosine phosphorylation patterns after triggering the acrosome reaction through progesterone are needed.

In conclusion, the relevance of AQPs during sperm capacitation is apparently related to their osmoregulatory ability. Whereas AQP3 is essential for H_2O_2 efflux, its inhibition does not seem to cause a toxic accumulation of this molecule at an intracellular level. Finally, the AQPs as a whole seem to have a relevant role for the intracellular signaling pathways involved in the acrosome reaction, thus suggesting that their blockade during the capacitation process has underlying effects that only become evident after the addition of progesterone.

DATA AVAILABILITY STATEMENT

The original contributions presented in the study are included in the article/supplementary material, further inquiries can be directed to the corresponding author/s.

AUTHOR CONTRIBUTIONS

AD-B and MY: conceptualization. AD-B, SR, and MY: methodology. AD-B, AS, and MY: formal analysis. AD-B, SR, ML, YM-O, AS, IB, and JR-M: investigation. MY: supervision and funding acquisition. AD-B: writing—original draft preparation and visualization. SR, ML, YM-O, AS, IB, JR-M, and MY: writing—review and editing. All authors have read and agreed to the published version of the manuscript.

FUNDING

This research was funded by the Ministry of Science and Innovation (Spain) (RYC-2014-15581, AGL2017-88329-R, and PRE2018-083488); and Regional Government of Catalonia, Spain (2017-SGR-1229).

ACKNOWLEDGMENTS

The authors would like to thank the technical support received from Jordi Soler (University of Girona, Spain).

REFERENCES

Aitken, R. J. (2017). Reactive oxygen species as mediators of sperm capacitation and pathological damage. *Mol. Reprod. Dev.* 84, 1039–1052. doi: 10.1002/mrd.22871

Bailey, J. L. (2010). Factors regulating sperm capacitation. *Syst. Biol. Reprod. Med.* 56, 334–348. doi: 10.3109/19396368.2010.512377

Bonilla-Correal, S., Noto, F., Garcia-Bonavila, E., Rodríguez-Gil, J. E., Yeste, M., and Miró, J. (2017). First evidence for the presence of aquaporins in stallion sperm. *Reprod. Domest. Anim.* 52, 61–64. doi: 10.1111/rda.13059

Buffone, M. G., Wertheimer, E. V., Visconti, P. E., and Krapf, D. (2014). Central role of soluble adenylyl cyclase and cAMP in sperm physiology. *Biochim. Biophys. Acta - Mol. Basis Dis.* 1842, 2610–2620. doi: 10.1016/j.bbadis.2014.07.013

Chang, J. C., and Oude-Elferink, R. P. J. (2014). Role of the bicarbonate-responsive soluble adenylyl cyclase in pH sensing and metabolic regulation. *Front. Physiol.* 5:42. doi: 10.3389/fphys.2014.00042

Chang, M. C. (1951). Fertilizing capacity of spermatozoa deposited into the fallopian tubes. *Nature* 168, 697–698. doi: 10.1038/168697b0

Chen, Q., and Duan, E. K. (2011). Aquaporins in sperm osmoadaptation: an emerging role for volume regulation. *Acta Pharmacol. Sin.* 32, 721–724. doi: 10.1038/aps.2011.35

Chen, Q., Peng, H., Lei, L., Zhang, Y., Kuang, H., Cao, Y., et al. (2011). Aquaporin 3 is a sperm water channel essential for postcopulatory sperm osmoadaptation and migration. *Cell Res.* 21, 922–933. doi: 10.1038/cr.2010.169

Delgado-Bermúdez, A., Llavanera, M., Fernández-Bastit, L., Recuero, S., Mateo, Y., Bonet, S., et al. (2019). Aquaglyceroporins but not orthodox aquaporins are involved in the cryotolerance of pig spermatozoa. *J. Anim. Sci. Biotechnol.* 10:77. doi: 10.1186/s40104-019-0388-388

Garner, D. L., and Johnson, L. A. (1995). Viability assessment of mammalian sperm using SYBR-14 and propidium Iodide1. *Biol. Reprod.* 53, 276–284. doi: 10.1095/biolreprod53.2.276

Guthrie, H. D., and Welch, G. R. (2006). Determination of intracellular reactive oxygen species and high mitochondrial membrane potential in Percoll-treated viable boar sperm using fluorescence-activated flow cytometry. *J. Anim. Sci.* 84, 2089–2100. doi: 10.2527/jas.2005-2766

Haddoub, R., Rützler, M., Robin, A., and Flitsch, S. L. (2009). "Design, synthesis and assaying of potential aquaporin inhibitors," in *Aquaporins. Handbook of Experimental Pharmacology*, ed. E. Beitz (Berlin: Springer-Verlag), 385–402. doi: 10.1007/978-3-540-79885-9_19

Harrison, R. A. P., Mairet, B., and Miller, N. G. A. (1993). Flow cytometric studies of bicarbonate-mediated Ca2+ influx in boar sperm populations. *Mol. Reprod. Dev.* 35, 197–208. doi: 10.1002/mrd.1080350214

Hecht, D., and Zick, Y. (1992). Selective inhibition of protein tyrosine phosphatase activities by H2O2 and vanadate *In vitro*. *Biochem. Biophys. Res. Commun.* 188, 773–779. doi: 10.1016/0006-291X(92)91123-8

Hirano, Y., Okimoto, N., Kadohira, I., Suematsu, M., Yasuoka, K., and Yasui, M. (2010). Molecular mechanisms of how mercury inhibits water permeation through aquaporin-1: understanding by molecular dynamics simulation. *Biophys. J.* 98, 1512–1519. doi: 10.1016/j.bpj.2009.12.4310

Ishibashi, K., Kuwahara, M., Gu, Y., Tanaka, Y., Marumo, F., and Sasaki, S. (1997). Cloning and functional expression of a new water channel abundantly expressed in the testis permeable to water glycerol, and urea. *J. Biol. Chem.* 272, 20782–20786. doi: 10.1006/bbrc.1998.8252

Laforenza, U., Pellavio, G., Marchetti, A., Omes, C., Todaro, F., and Gastaldi, G. (2017). Aquaporin-Mediated water and hydrogen peroxide transport is involved in normal human spermatozoa functioning. *Int. J. Mol. Sci.* 18:E66. doi: 10.3390/ijms18010066

Miller, E. W., Dickinson, B. C., and Chang, C. J. (2010). Aquaporin-3 mediates hydrogen peroxide uptake to regulate downstream intracellular signaling. *Proc. Natl. Acad. Sci. U S A.* 107, 15681–15686. doi: 10.1073/pnas.1005776107

Morató, R., Prieto-Martínez, N., Muiño, R., Hidalgo, C. O., Rodríguez-Gil, J. E., Bonet, S., et al. (2018). Aquaporin 11 is related to cryotolerance and fertilising ability of frozen–thawed bull spermatozoa. *Reprod. Fertil. Dev.* 30, 1099–1108. doi: 10.1071/rd17340

Nagy, S., Jansen, J., Topper, E. K., and Gadella, B. M. (2003). A triple-stain flow cytometric method to assess plasma- and acrosome-membrane integrity of cryopreserved bovine sperm immediately after thawing in presence of egg-yolk particles. *Biol. Reprod.* 68, 1828–1835. doi: 10.1095/biolreprod.102.011445

Niemietz, C. M., and Tyerman, S. D. (2002). New potent inhibitors of aquaporins: silver and gold compounds inhibit aquaporins of plant and human origin. *FEBS Lett.* 531, 443–447. doi: 10.1016/S0014-5793(02)03581-3580

Ortega-Ferrusola, C., Sotillo-Galán, Y., Varela-Fernández, E., Gallardo-Bolaños, J. M., Muriel, A., González-Fernández, L., et al. (2008). Detection of "Apoptosis-Like" changes during the cryopreservation process in equine sperm. *J. Androl.* 29, 213–221. doi: 10.2164/jandrol.107.003640

Petrunkina, A. M., Waberski, D., Bollwein, H., and Sieme, H. (2010). Identifying non-sperm particles during flow cytometric physiological assessment: a simple approach. *Theriogenology* 73, 995–1000. doi: 10.1016/j.theriogenology.2009.12.006

Pons-Rejraji, H., Bailey, J. L., and Leclerc, P. (2009). Cryopreservation affects bovine sperm intracellular parameters associated with capacitation and acrosome exocytosis. *Reprod. Fertil. Dev.* 21, 525–537. doi: 10.1071/RD07170

Preston, G. M., Carroll, T. P., Guggino, W. B., and Agre, P. (1992). Appearance of water channels in *Xenopus oocytes* expressing red cell CHIP28 protein. *Science* 256, 385–387. doi: 10.1126/science.256.5055.385

Prieto-Martinez, N., Morato, R., Muino, R., Hidalgo, C. O., Rodriguez-Gil, J. E., Bonet, S., et al. (2016). Aquaglyceroporins 3 and 7 in bull spermatozoa: identification, localisation and their relationship with sperm cryotolerance. *Reprod. Fertil. Dev.* 29, 1249–1259. doi: 10.1071/RD16077

Prieto-Martínez, N., Morató, R., Vilagran, I., Rodríguez-Gil, J. E., Bonet, S., and Yeste, M. (2015). Aquaporins in boar spermatozoa. Part II: detection and localisation of aquaglyceroporin 3. *Reprod. Fertil. Dev.* 29, 703–711. doi: 10.1071/rd15164

Prieto-Martínez, N., Vilagran, I., Morató, R., Rivera, del, Álamo, M. M., et al. (2017). Relationship of aquaporins 3 (AQP3), 7 (AQP7), and 11 (AQP11) with boar sperm resilience to withstand freeze-thawing procedures. *Andrology* 5, 1153–1164.

Prieto-Martínez, N., Vilagran, I., Morató, R., Rodríguez-Gil, J. E., Yeste, M., Bonet, S., et al. (2014). Aquaporins 7 and 11 in boar spermatozoa: detection, localisation and relationship with sperm quality. *Reprod. Fertil. Dev.* 28, 663–672. doi: 10.1071/rd14237

Puga Molina, L. C., Luque, G. M., Balestrini, P. A., and Marín-briggiler, C. I. (2018). Molecular basis of human sperm capacitation. *Front. Cell Dev. Biol.* 6:72. doi: 10.3389/fcell.2018.00072

Rathi, R., Colenbrander, B., Bevers, M. M., and Gadella, B. M. (2001). Evaluation of *in vitro* capacitation of stallion spermatozoa. *Biol. Reprod.* 65, 462–470. doi: 10.1095/biolreprod65.2.462

Reca, A., Szpilbarg, N., and Damiano, A. E. (2018). The blocking of aquaporin-3 (AQP3) impairs extravillous trophoblast cell migration. *Biochem. Biophys. Res. Commun.* 499, 227–232. doi: 10.1016/j.bbrc.2018.03.133

Rivlin, J., Mendel, J., Rubinstein, S., Etkovitz, N., and Breitbart, H. (2004). Role of hydrogen peroxide in sperm capacitation and acrosome reaction. *Biol. Reprod.* 70, 518–522. doi: 10.1095/biolreprod.103.020487

Rojek, A. M., Skowronski, M. T., Füchtbauer, E. M., Füchtbauer, A. C., Fenton, R. A., Agre, P., et al. (2007). Defective glycerol metabolism in aquaporin 9 (AQP9) knockout mice. *Proc. Natl. Acad. Sci. U S A.* 104, 3609–3614. doi: 10.1073/pnas.0610894104

Saito, K., Kageyama, Y., Okada, Y., Kawakami, S., Kihara, K., Ishibashi, K., et al. (2004). Localization of aquaporin-7 in human testis and ejaculated sperm: possible involvement in maintenance of sperm quality. *J. Urol.* 172, 2073–2076. doi: 10.1097/01.ju.0000141499.08650.ab

Smith, B. L., and Agre, P. (1991). Erythrocyte Mr 28,000 transmembrane protein exists as a multisubunit oligomer similar to channel proteins. *J. Biol. Chem.* 266, 6407–6415.

Sohara, E., Ueda, O., Tachibe, T., Hani, T., Jishage, K., Rai, T., et al. (2007). Morphologic and functional analysis of sperm and testes in aquaporin 7 knockout mice. *Fertil. Steril.* 87, 671–676. doi: 10.1016/j.fertnstert.2006.07.1522

Teijeiro, J. M., Marini, P. E., Bragado, M. J., and Garcia-Marin, L. J. (2017). Protein kinase C activity in boar sperm. *Andrology* 5, 381–391. doi: 10.1111/andr.12312

Vicente-Carrillo, A., Ekwall, H., Alvarez-Rodriguez, M., Rodriguez-Martinez, H., Álvarez-Rodríguez, M., and Rodríguez-Martínez, H. (2016). Membrane stress during thawing elicits redistribution of aquaporin 7 but not of aquaporin 9 in boar spermatozoa. *Reprod. Domest. Anim.* 51, 665–679. doi: 10.1111/rda.12728

Watson, H. (2015). Biological membranes. *Essays Biochem.* 59, 43–70. doi: 10.1063/1.2913788

Yeste, M., Estrada, E., Rivera Del, Álamo, M. M., Bonet, S., Rigau, T., et al. (2014). The increase in phosphorylation levels of serine residues of protein HSP70 during holding time at 17°C is concomitant with a higher cryotolerance of boar spermatozoa. *PLoS One* 9:e90887. doi: 10.1371/journal.pone.0090887

Yeste, M., Fernández-Novell, J. M., Ramió-Lluch, L., Estrada, E., Rocha, L. G., Cebrián-Pérez, J. A., et al. (2015). Intracellular calcium movements of boar spermatozoa during '*in vitro*' capacitation and subsequent acrosome exocytosis follow a multiple-storage place, extracellular calcium-dependent model. *Andrology* 3, 729–747. doi: 10.1111/andr.12054

Yeste, M., Morató, R., Rodríguez-Gil, J. E., Bonet, S., and Prieto-Martínez, N. (2017). Aquaporins in the male reproductive tract and sperm: functional implications and cryobiology. *Reprod. Domest. Anim.* 52, 12–27. doi: 10.1111/rda.13082

Yeung, C. H., Callies, C., Rojek, A., Nielsen, S., and Cooper, T. G. (2009). Aquaporin isoforms involved in physiological volume regulation of murine spermatozoa. *Biol. Reprod.* 80, 350–357. doi: 10.1095/biolreprod.108.071928

Yeung, C. H., Callies, C., Tüttelmann, F., Kliesch, S., and Cooper, T. G. (2010). Aquaporins in the human testis and spermatozoa - identification, involvement in sperm volume regulation and clinical relevance. *Int. J. Androl.* 33, 629–641. doi: 10.1111/j.1365-2605.2009.00998.x

Yeung, C. H., and Cooper, T. G. (2010). Aquaporin AQP11 in the testis: molecular identity and association with the processing of residual cytoplasm of elongated spermatids. *Reproduction* 139, 209–216. doi: 10.1530/REP-09-0298

Zelenina, M., Tritto, S., Bondar, A. A., Zelenin, S., and Aperia, A. (2004). Copper inhibits the water and glycerol permeability of aquaporin-3. *J. Biol. Chem.* 279, 51939–51943. doi: 10.1074/jbc.M407645200

Conflict of Interest: The authors declare that the research was conducted in the absence of any commercial or financial relationships that could be construed as a potential conflict of interest.

Paper II

Aquaglyceroporins but not orthodox aquaporins are involved in the cryotolerance of pig spermatozoa.

Ariadna Delgado-Bermúdez, Marc Llavanera, Leira Fernández-Bastit, Sandra Recuero, Yentel Mateo-Otero, Sergi Bonet, Isabel Barranco, Beatriz Fernández-Fuertes, Marc Yeste.

Journal of Animal Science and Biotechnology

2019;10:77

doi: 10.1186/s40104-019-0388-8

Delgado-Bermúdez et al. Journal of Animal Science and Biotechnology (2019) 10:77
https://doi.org/10.1186/s40104-019-0388-8

Journal of Animal Science and Biotechnology

RESEARCH Open Access

Aquaglyceroporins but not orthodox aquaporins are involved in the cryotolerance of pig spermatozoa

Ariadna Delgado-Bermúdez, Marc Llavanera, Leira Fernández-Bastit, Sandra Recuero, Yentel Mateo-Otero, Sergi Bonet, Isabel Barranco, Beatriz Fernández-Fuertes and Marc Yeste*

Abstract

Background: Aquaporins (AQPs) are a family of transmembrane water channels that includes orthodox AQPs, aquaglyceroporins (GLPs) and superAQPs. AQP3, AQP7, AQP9 and AQP11 have been identified in boar sperm, and they are crucial for sperm maturation and osmoregulation. Water exchange is an important event in cryopreservation, which is the most efficient method for long-term storage of sperm. However, the freeze-thaw process leads to sperm damage and a loss of fertilizing potential. Assuming that the quality of frozen-thawed sperm partially depends on the regulation of osmolality variations during this process, AQPs might play a crucial role in boar semen freezability. In this context, the aim of this study was to unravel the functional relevance of the different groups of AQPs for boar sperm cryotolerance through three different inhibitors.

Results: Inhibition of different groups of AQPs was found to have different effects on boar sperm cryotolerance. Whereas the use of 1,3-propanediol (PDO), an inhibitor of orthodox AQPs and GLPs, decreased total motility ($P < 0.05$), it increased post-thaw sperm viability, lowered membrane lipid disorder and increased mitochondrial membrane potential (MMP) ($P < 0.05$). When acetazolamide (AC) was used as an inhibitor of orthodox AQPs, the effects on post-thaw sperm quality were restricted to a mild increase in MMP in the presence of the intermediate concentration at 30 min post-thaw and an increase in superoxide levels ($P < 0.05$). Finally, the addition of phloretin (PHL), a GLP inhibitor, had detrimental effects on post-thaw total and progressive sperm motilities, viability and lipid membrane disorder ($P < 0.05$).

Conclusions: The effects of the different inhibitors suggest that GLPs rather than orthodox AQPs are relevant for boar sperm freezability. Moreover, the positive effect of PDO on sperm quality suggests a cryoprotective role for this molecule.

Keywords: Acetazolamide, Aquaporins, Boar, Phloretin, Propanediol, Sperm

Introduction

Cell function and survival are strictly related to metabolite concentration, which, in turn, depends on plasma membrane permeability to water and solutes. Considering plasma membrane hydrophobicity, mechanisms other than simple diffusion are required to allow water transport across the plasma membrane in certain cell functions [1]. Aquaporins (AQPs) are a family of ubiquitous integral transmembrane proteins that allow the passive transport of water through cell membranes. Moreover, some AQPs also facilitate the transport of small solutes, such as glycerol or hydrogen peroxide [2]. Mammalian AQPs are classified according to their sequence similarity and substrate affinity into orthodox AQPs, aquaglyceroporins (GLPs) and superaquaporins (superAQPs). Orthodox AQPs are permeable to water, and this group is formed by AQP0, AQP1, AQP2, AQP4, AQP5, AQP6 and AQP8. Concerning the group of GLPs, it comprises AQP3, AQP7, AQP9 and AQP10, which are permeable to water, but also to glycerol, urea and other small electrolytes.

* Correspondence: marc.yeste@udg.edu
Biotechnology of Animal and Human Reproduction (TechnoSperm), Unit of Cell Biology, Department of Biology, Faculty of Sciences, Institute of Food and Agricultural Technology, University of Girona, C/Maria Aurèlia Campany, 69, Campus Montilivi, E-17003 Girona, Spain

Finally, AQP11 and AQP12 belong to the superAQPs group, which are specifically localized in the membrane of intracellular organelles and regulate organelle volume and intravesicular homeostasis while being involved in both water and glycerol transport [2].

AQPs have been identified in mammalian sperm cells with differences between species. While AQP3, AQP7 and AQP11 have been identified in sperm from boar [3, 4], mouse [5–7], human [8, 9], cattle [10, 11] and stallion [12], AQP8 has only been observed in mouse [6] and human [8, 9] sperm, and AQP9 has been identified in boar sperm [13]. In mammalian sperm, AQPs play an important role in the adaptation to the osmotic variation caused by the exposure to the female reproductive tract, which is also involved in sperm motility activation upon ejaculation (reviewed in [2]). In addition, AQPs play a key role during spermatogenesis [14], since they contribute to cytoplasm reduction from spermatids to spermatozoa.

Cryopreservation is the most efficient method for the long-term storage of sperm. However, the freeze-thawing process damages spermatozoa in terms of plasma membrane destabilization, nuclear alterations, reduction of mitochondrial activity, changes in sperm proteins and a decrease in sperm motility [15, 16]. Cryoinjury is mainly inflicted during the processes of freezing and thawing, when extracellular water freezes and intracellular water is lost. In this context, the penetration of permeating cryoprotective agents (CPAs), such as glycerol, is essential to minimize cryoinjuries [15, 17, 18]. The resilience of sperm cells to cryopreservation is also known as freezability or cryotolerance, which differs between species according to differences in membrane composition [15, 17, 18]. Among the AQPs identified in boar sperm cells, AQP3 and AQP7 are associated to sperm cryotolerance, which suggests that they could be used as freezability biomarkers [19].

GLPs substrate affinity and their role in volume regulation is the potential mechanism through which AQP3 and AQP7 appear to be related to sperm cryotolerance. Therefore, it is reasonable to suggest that the inhibition of sperm AQPs would impair their resilience to freeze-thawing procedures. Different AQP inhibitors have previously been tested in other cell types, such as 1,3-propanediol (PDO), acetazolamide (AC) and phloretin (PHL). PDO occludes the pore channel of orthodox AQPs, such as AQP1, AQP2, AQP4 and AQP5 [20, 21] from the outer side of the plasma membrane, but it is also able to penetrate through *Plasmodium falciparum* PfAQP (which is an analogue of AQP3, AQP7 and AQP9) and to inhibit this GLP analogue from the inner part of the plasma membrane [21]. AC has inhibitory effects on the orthodox AQPs, AQP1 and AQP4 [22, 23], whereas PHL inhibits AQP3 and AQP9, which are both GLPs [24, 25]. Against this background, this study aims to elucidate the functional relevance of orthodox AQPs and GLPs during boar sperm cryopreservation, through their inhibition by the aforementioned agents.

Methods

Boars and ejaculates

A total of 20 ejaculates from separate Piétrain boars ($n = 20$) were used in this study. The boars were housed in a local farm (Semen Cardona, Cardona, Barcelona, Spain) with controlled climatic conditions, and were fed a standard diet. Sperm-rich fractions were collected manually, and subsequently diluted 1:1 (*v*:*v*) in a commercial semen extender (Vitasem LD; Magapor S.L., Zaragoza, Spain). After collection, ejaculates were stored in bags at 17 °C and transported to the laboratory within 5 h after extraction. Once in the laboratory, the ejaculates were pooled in pairs, and each pool was split into two different fractions. The first one was used to evaluate the quality parameters in fresh semen; the second one was divided into seven different sub-fractions, which were cryopreserved with or without different concentrations of the three AQP inhibitors.

AQP inhibitors

Prior to cryopreservation, three AQP inhibitors were added to the semen samples: 1,3-propanediol (PDO, Sigma-Aldrich, St. Louis, MO, USA), acetazolamide (AC, Sigma-Aldrich), and phloretin (PHL, Sigma-Aldrich). PDO was diluted in cryopreservation medium (LEYGO medium, see composition in the following section) to a working concentration of 100 mmol/L, AC was diluted in dimethyl sulfoxide (DMSO, Sigma-Aldrich) to a working concentration of 450 mmol/L, and PHL was diluted in methanol (Fisher Chemical, ThermoFisher Scientific; Waltham, Massachusetts, USA) to a working concentration of 365 mmol/L. For each inhibitor, three different concentrations were tested: 0.1, 1 and 10 mmol/L for PDO; and 250, 500 and 1000 μmol/L for AC and PHL. It is worth mentioning that in the case of treatments containing PDO and AC, samples were exposed to methanol or DMSO at concentrations lower than 0.5% (*v*/*v*). These concentrations showed no detrimental effects on the sperm quality parameters (data not shown).

Boar sperm cryopreservation

Cryopreservation of boar sperm was performed to determine whether the three AQP inhibitors affected their cryotolerance. The fraction of the pool intended for cryopreservation was divided into 50-mL aliquots and centrifuged at 15 °C and 2400×*g* for 3 min. After discarding the supernatants, pellets were resuspended to a final concentration of 1.5×10^9 spermatozoa/mL in β-lactose-egg yolk freezing medium (LEY), which consisted of 80% (*v*/*v*) lactose (Sigma-Aldrich) and 20% (*v*/*v*) egg yolk. Subsequently, sperm were cooled down to 5 °C with a cooling

ramp of − 0.1 °C/min (180 min) in a programmable, controlled-rate freezer (Icecube14S-B; Minitüb Ibérica SL; Tarragona, Spain). Sperm were then diluted to a final concentration of 1×10^9 spermatozoa/mL in LEYGO medium, which consisted of LEY medium supplemented with 6% (*v*/*v*) glycerol (Sigma-Aldrich) and 1.5% Orvus ES Paste (Equex STM; Nova Chemical Sales Inc., Scituate, MA, USA). At this point, the suspension was divided into seven sub-fractions: one for each concentration and inhibitor, and a non-treated control. Samples were packed into distinct 0.5 mL plastic straws (Minitüb Ibérica, S.L.). Afterwards, straws were placed in a controlled-rate, programmable freezer (Icetube 14S-B; Minitub Ibérica, S.L), using the following cooling rates [26]: − 6 °C/min from 5 to − 5 °C (100 s); − 39.82 °C/min from − 5 to − 80 °C (113 s); hold at − 80 °C for 30 s; and cooled at − 60 °C/min from − 80 to − 150 °C (70 s). Finally, straws were plunged into liquid nitrogen (− 196 °C) for storage.

Analysis of sperm quality parameters was performed after thawing. With this purpose, two straws per treatment and pool were immersed and agitated in a water bath at 38 °C for 15 s. Thereafter, sperm samples were diluted 1:3 (*v*:*v*) in pre-warmed Beltsville Thawing Solution (BTS) [27]. Diluted, frozen-thawed samples were incubated at 38 °C for 240 min, and sperm quality was evaluated at two different time points: 30 min and 240 min.

Sperm motility

Sperm motility was evaluated in both fresh and frozen-thawed semen samples through a computer-assisted sperm analysis (CASA) system, which consisted of a phase contrast microscope (Olympus BX41; Olympus, Tokyo, Japan) equipped with a video camera and ISAS software (Integrated Sperm Analysis System V1.0; Proiser SL, Valencia, Spain). Extended samples were incubated at 38 °C for 15 min before sperm motility assessment, whereas frozen-thawed samples were directly examined after 30 min and 240 min of incubation. Following incubation, 5 μL of the sperm suspension were placed onto a pre-warmed Makler counting chamber (Sefi-Medical Instruments, Haifa, Israel) and observed under a negative phase-contrast field (Olympus 10× 0.30 PLAN objective; Olympus). At least 1000 sperm were examined per replicate, and three replicates were evaluated per sample.

In each motility assessment, the following parameters were recorded: total (TMOT, %) and progressive sperm motility (PMOT, %); curvilinear velocity (VCL, μm/s); straight line velocity (VSL, μm/s); average path velocity (VAP, μm/s); amplitude of lateral head displacement (ALH, μm); beat cross frequency (BCF, Hz); linearity (LIN, %), which was calculated assuming that LIN=VSL/VCL × 100; straightness (STR, %), resulting from VSL/VAP × 100; and motility parameter wobble (WOB, %), obtained from VAP/VCL × 100. A sperm cell was considered to be motile when its VAP was equal to or higher than 10 μm/s and progressively motile when its STR was equal to or higher than 45%. The corresponding mean ± standard error of the mean (SEM) was calculated for each parameter.

Flow cytometry

As mentioned above, five different parameters were assessed through flow cytometry in both fresh and frozen-thawed semen samples: viability, membrane lipid disorder, mitochondrial membrane potential (MMP), intracellular levels of superoxide ($O_2^{-}\bullet$) radicals and intracellular levels of hydrogen peroxide (H_2O_2). All fluorochromes used were purchased from ThermoFisher Scientific. For proper staining, all samples were diluted to a final concentration of 1×10^6 spermatozoa/mL, and after the addition of the corresponding fluorochromes, they were incubated at 38 °C in the dark. A total of three replicates per sample were assessed for each parameter.

Samples were evaluated using a Cell Laboratory QuantaSC™ cytometer (Beckman Coulter; Fullerton, CA, USA). All samples were excited with an argon ion laser (488 nm) set at a power of 22 mW. Cell diameter/volume was assessed employing the Coulter principle for volume assessment using the Cell Lab Quanta™ SC cytometer, which is based on measuring changes in electrical resistance produced in an electrolyte solution by suspended, non-conductive particles. In this system, forward scatter (FS) is replaced by electronic volume (EV). Furthermore, 10-μm Flow-Check fluorospheres (Beckman Coulter) were used for EV-channel calibration, by positioning this size of bead at channel 200 on the EV-scale.

Three optical filters were used: FL1 (Dichroic/Splitter, DRLP: 550 nm, BP filter: 525 nm, detection width: 505–545 nm), FL2 (DRLP: 600 nm, BP filter: 575 nm, detection width: 560–590 nm) and FL3 (LP filter: 670 nm/730 nm, detection width: 655–685 nm). The first one was used to detect green fluorescence from SYBR-14, YO-PRO-1, JC-1 monomers ($JC\text{-}1_{mon}$) and 2′,7′-dichlorofluorescein (DCF^+); the second one was used to detect orange fluorescence from JC-1 aggregates ($JC\text{-}1_{agg}$); and the third one was used to detect red fluorescence from propidium iodide (PI), merocyanine 540 (M540) and ethidium (E^+). The signal was logarithmically amplified, and the adjustment of photomultiplier settings was performed according to particular staining methods.

For all particles, EV and side scatter (SS) were measured and linearly recorded. The sheath flow rate was set at 4.17 μL/min and a minimum of 10,000 events were evaluated per replicate. On the EV channel, the analyzer threshold was adjusted to exclude subcellular debris (particle diameter < 7 μm) and cell aggregates (particle

diameter > 12 μm). Therefore, on the basis of EV and SS distributions, the sperm-specific events were positively gated, whereas the others were gated out.

Subsequent data analysis was performed using Flowing Software (Ver. 2.5.1; University of Turku, Finland) and according to the recommendations of the International Society for Advancement of Cytometry (ISAC). The corresponding mean ± SEM was calculated for each parameter.

Plasma membrane integrity

Sperm viability was evaluated by the assessment of membrane integrity using the LIVE/DEAD Sperm Viability Kit (Molecular Probes, Eugene, OR, USA), following the protocol of Garner and Johnson [28]. In brief, sperm were incubated with SYBR-14 (final concentration: 100 nmol/L) for 10 min, PI was subsequently added (final concentration of 12 μmol/L) and sperm were incubated for an additional 5 min. In flow cytometry dot plots, three sperm populations were observed: 1) viable, green-stained sperm ($SYBR\text{-}14^+/PI^-$); 2) non-viable, red-stained sperm ($SYBR\text{-}14^-/PI^+$); 3) non-viable, both red- and green-stained sperm ($SYBR\text{-}14^+/PI^+$). The fourth dot population corresponded to unstained, non-sperm particles ($SYBR\text{-}14^-/PI^-$). Viable green-stained sperm were used to assess sperm viability, and SYBR-14 fluorescence spill over into FL3-channel was compensated (2.45%).

Sperm membrane lipid disorder

The evaluation of membrane lipid disorder was performed with M540 and YO-PRO-1 fluorochromes following a modification of the protocol from Rathi et al. [29] with minor modifications by Yeste et al. [30]. M540 detects a decrease in packing order of phospholipids in the outer monolayer of the plasma membrane. Sperm were incubated with M540 at a final concentration of 2.6 μmol/L, and with YO-PRO-1 at a final concentration of 25 nmol/L for 10 min. Four populations were identified in flow cytometry dot plots: 1) non-viable sperm with low membrane lipid disorder ($M540^-/YO\text{-}PRO\text{-}1^+$); 2) non-viable sperm with high membrane lipid disorder ($M540^+/YO\text{-}PRO\text{-}1^+$); 3) viable sperm with low membrane lipid disorder ($M540^-/YO\text{-}PRO\text{-}1^-$); and 4) viable sperm with high membrane lipid disorder ($M540^+/YO\text{-}PRO\text{-}1^-$). The percentage of viable sperm with low membrane lipid disorder ($M540^-/YO\text{-}PRO\text{-}1^-$) was corrected using the non-sperm particles from the SYBR-14/PI co-staining. Data were not compensated.

Mitochondrial membrane potential (MMP)

Determination of mitochondrial membrane potential (MMP) was performed with JC-1 following the procedure of Ortega-Ferrusola et al. [31] with minor modifications. Sperm were incubated with 0.3 μmol/L JC-1 for 30 min. Whereas high MMP causes JC-1 aggregate ($JC\text{-}1_{agg}$) formation, in sperm cells with low MMP, JC-1 remains as a monomer ($JC\text{-}1_{mon}$). Particles showing no fluorescence (either green or orange) were gated out. Flow cytometry dot plots allowed the identification of two different sperm populations: 1) sperm with low MMP ($JC\text{-}1_{mon}$); and 2) sperm with high MMP ($JC\text{-}1_{agg}$). Data were compensated, as green fluorescence from FL1-channel was subtracted from FL2-channel (51.70%).

Intracellular levels of superoxide ($O_2^-\bullet$)

Intracellular levels of superoxide ($O_2^-\bullet$) radicals were determined with hydroethidine (HE) and YO-PRO-1 fluorochromes following a modification of the procedure from Guthrie and Welch [32]. Sperm were incubated with 4 μmol/L HE and 40 nmol/L YO-PRO-1 for 20 min. HE permeates the sperm plasma membrane and is oxidized by $O_2^-\bullet$ to ethidium (E^+) among other products. Flow cytometry dot plots allowed the identification of four different sperm populations: 1) non-viable sperm with low superoxide levels ($E^-/YO\text{-}PRO\text{-}1^+$); 2) non-viable sperm with high superoxide levels ($E^+/YO\text{-}PRO\text{-}1^+$); 3) viable sperm with low superoxide levels ($E^-/YO\text{-}PRO\text{-}1^-$); and 4) viable sperm with high superoxide levels ($E^+/YO\text{-}PRO\text{-}1^-$). The percentage of viable sperm with low superoxide levels ($E^-/YO\text{-}PRO\text{-}1^-$) was corrected using the non-sperm particles from the SYBR-14/PI co-staining. The percentages of sperm in the other three populations were recalculated and YO-PRO-1 spill over into the FL3-channel was compensated (5.06%).

Intracellular levels of hydrogen peroxide (H_2O_2)

Intracellular levels of hydrogen peroxide (H_2O_2) were determined with 2′,7′-dichlorodihydrofluorescein diacetate (H_2DCFDA) and PI fluorochromes, following the procedure from Guthrie and Welch [32] with minor modifications. Sperm were incubated with 200 μmol/L H_2DCFDA and 12 μmol/L PI for 30 min. H_2DCFDA is a non-fluorescent probe that, after penetrating the sperm cell membrane, is intracellularly de-esterified and converted into highly fluorescent, 2′,7′-dichlorofluorescein (DCF^+) upon oxidation. Flow cytometry dot plots allowed the identification of four different sperm cell populations: 1) viable sperm with high peroxide levels (DCF^+/PI^-); 2) non-viable sperm with high peroxide levels (DCF^+/PI^+); 3) viable sperm with low peroxide levels (DCF^-/PI^-); and 4) non-viable sperm with low peroxide levels (DCF^-/PI^+). DCF^+-spill over into FL3-channel was compensated (2.45%). The percentage of viable sperm with high peroxide levels (DCF^+/PI^-) was corrected using the non-sperm particles from the SYBR-14/PI co-staining.

Statistical analyses

Data were analyzed using a statistical package (IBM SPSS Statistics 25.0; Armonk, New York, USA). Distribution of data and homogeneity of variances were tested through Shapiro-Wilk and Levene tests, respectively. A mixed model was subsequently run for each sperm parameter. The intra-subjects factor was the cryopreservation step (i.e. fresh, frozen-thawed at 30 min, frozen-thawed at 240 min), the fixed-effects factor (inter-subjects) was the treatment (C, and different concentrations of PDO, AC or PHL), and the random-effects factor was the ejaculate pool. A post-hoc Sidak test was used for pair-wise comparisons and the level of significance was set at $P \leq 0.05$. Data are shown as mean ± SEM.

Results

As mentioned above, sperm quality parameters were evaluated in both fresh and frozen-thawed samples to determine the effects of the AQP inhibition during cryopreservation. Because inhibitors were added immediately before cryopreservation, no effect of treatment was observed in fresh samples in any of the variables analyzed ($P > 0.05$; Figs. 1, 2, 3 and Tables 1, 2, 3).

Effects of PDO on sperm quality

Figure 1 and Table 1 show sperm quality parameters before and after freeze-thawing and the effects of PDO-mediated AQP inhibition during cryopreservation.

Regardless of its concentration, PDO induced a decrease in total sperm motility ($P < 0.05$) at 240 min post-thaw (Fig. 1a), but there were no differences ($P > 0.05$) between the treatments and the control in terms of progressive sperm motility at any post-thaw time point (Table 1). At 30 min post-thaw, the sperm viability (percentage of SYBR-14$^+$/PI$^-$ spermatozoa) of all PDO treatments was higher than in control samples ($P < 0.05$), but at 240 min post-thaw this difference only persisted in the 1 mmol/L treatment (Fig. 1b). Whereas the percentage of viable sperm with low membrane lipid disorder (percentage of M540$^-$/YO-PRO-1$^-$ spermatozoa) was significantly ($P < 0.05$) higher than in the control at 30 min post-thaw in the presence of all PDO concentrations, only the 0.1 mmol/L and 1 mmol/L PDO concentrations elicited this effect at 240 min post-thaw ($P < 0.05$; Table 1).

Moreover, addition of 0.1 mmol/L and 1 mmol/L PDO led to a higher MMP (percentage of JC-1$_{agg}^+$ spermatozoa) with respect to the other treatments and the control at both time points after thawing ($P < 0.05$; Table 1).

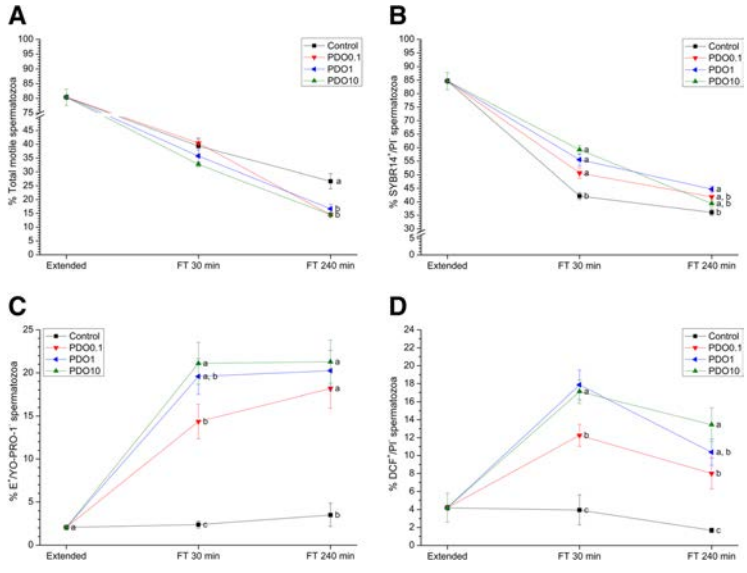

Fig. 1 Sperm quality parameters in the presence of 1,3-propanediol (PDO) at three different concentrations (0.1 mmol/L, 1 mmol/L and 10 mmol/L) compared to samples exposed to extender alone. **a** Percentage of total motile spermatozoa (TMOT); **b** Percentage of viable sperm (SYBR-14$^+$/PI$^-$); **c** Superoxide levels (percentage of spermatozoa E$^+$/YO-PRO-1$^-$); **d** Peroxide levels (percentage of spermatozoa DCF$^+$/PI$^-$). Data were collected from fresh (extended) and frozen-thawed (FT) samples 30 and 240 min after thawing. Data reported as mean ± SEM. Different letters (**a-c**) indicate significant differences ($P < 0.05$) between treatments within a given time point

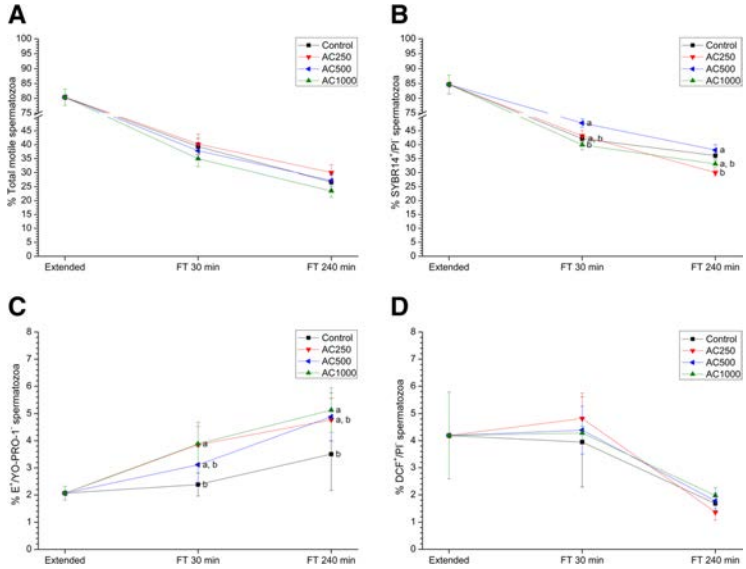

Fig. 2 Sperm quality parameters in the presence of acetazolamide (AC) at three different concentrations (250 μmol/L, 500 μmol/L and 1000 μmol/L) compared to samples exposed to extender alone. **a** Percentage of total motile spermatozoa (TMOT); **b** Percentage of viable sperm (SYBR-14$^+$/PI$^-$); **c** Superoxide levels (percentage of spermatozoa E$^+$/YO-PRO-1$^-$); **d** Peroxide levels (percentage of spermatozoa DCF$^+$/PI$^-$). Data were collected from fresh (extended) and frozen-thawed (FT) samples 30 and 240 min after thawing. Data reported as mean ± SEM. Different letters (**a**, **b**) indicate significant differences ($P < 0.05$) between treatments within a given time point

The percentage of viable spermatozoa showing high levels of $O_2^-\bullet$ (percentage of E$^+$/YO-PRO-1$^-$ spermatozoa) was higher in PDO-supplemented samples than the control, at both 30 and 240 min post-thaw ($P < 0.05$; Fig. 1c). Similarly, samples treated with different concentrations of PDO presented a higher percentage of viable sperm cells with high peroxide levels (percentage of DCF$^+$/PI$^-$ spermatozoa) than the control at both 30 and 240 min post-thaw ($P < 0.05$; Fig. 1d).

Effects of AC on sperm quality

Figure 2 and Table 2 show sperm quality parameters before and after freeze-thawing and the effects of AC-mediated AQP inhibition during cryopreservation.

Neither total nor progressive sperm motility differed between treatments containing AC and the control ($P > 0.05$) (Fig. 2a; Table 2). Regarding viability, it decreased when sperm were exposed to 250 μmol/L AC at 240 min post-thaw ($P < 0.05$; Fig. 2b). Treatment of sperm with AC did not induce changes ($P > 0.05$) in membrane lipid disorder in any of the studied time points compared to the control (Table 2).

In the treatment containing 500 μmol/L AC, the percentage of sperm cells with high MMP was higher than in the control at 30 min post-thaw ($P < 0.05$; Table 2).

In addition, 250 and 1000 μmol/L AC induced an increase in the percentage of viable sperm cells with high $O_2^-\bullet$ levels at 30 min post-thaw ($P < 0.05$), but this difference only persisted for the 1000 μmol/L at 240 min post-thaw ($P < 0.05$; Fig. 2c). In contrast, AC had no effect on the percentage of viable spermatozoa with high peroxide levels (Fig. 2d).

Effects of PHL on sperm quality

Figure 3 and Table 3 show sperm quality parameters before and after freeze-thawing and the effects of PHL-mediated AQP inhibition during cryopreservation.

Concerning PHL, 500 μmol/L concentration reduced total sperm motility at 240 min post-thaw (Fig. 3a; $P < 0.05$). Moreover, PHL at 1000 μmol/L caused a significant ($P < 0.05$) decrease in both total and progressive sperm motilities at any time point after thaw (Fig. 3a, Table 3). Similarly, 1000 μmol/L PHL lowered both sperm viability at 240 min post-thaw ($P < 0.05$; Fig. 3b) and the percentage of viable spermatozoa with low membrane lipid disorder at any time point after thaw ($P < 0.05$; Table 3).

With regard to MMP, no significant differences ($P > 0.05$) were observed in this sperm parameter between treatments and the control (Table 3).

Finally, PHL had no effect either on the percentage of viable spermatozoa with high superoxide levels or on the

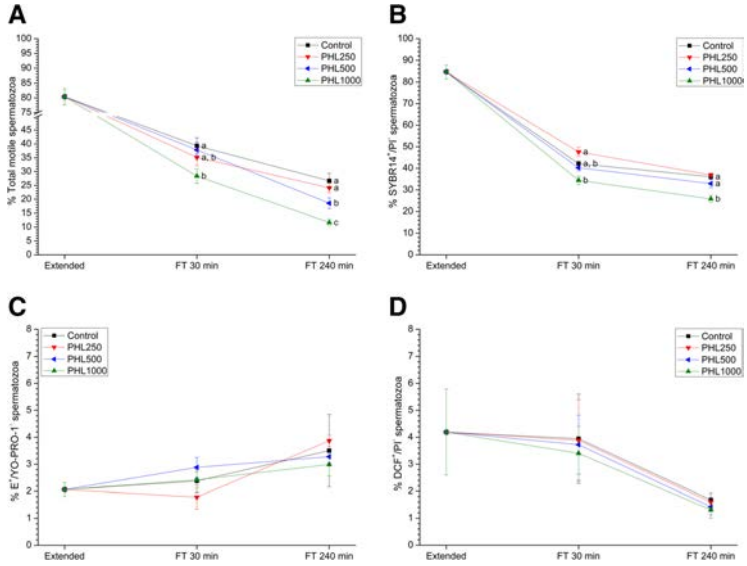

Fig. 3 Sperm quality parameters in the presence of phloretin (PHL) at three different concentrations (250 μmol/L, 500 μmol/L and 1000 μmol/L) compared to samples exposed to extender alone. **a** Percentage of total motile spermatozoa (TMOT); **b** Percentage of viable sperm (SYBR-14$^+$/PI$^-$); **c** Superoxide levels (percentage of spermatozoa E$^+$/YO-PRO-1$^-$); **d** Peroxide levels (percentage of spermatozoa DCF$^+$/PI$^-$). Data were collected from fresh (extended) and frozen-thawed (FT) samples 30 and 240 min after thawing. Data reported as mean ± SEM. Different letters (**a-c**) indicate significant differences ($P < 0.05$) between treatments within a given time point

Table 1 Sperm quality parameters from samples exposed to extender alone (control), or in the presence of 1,3-propanediol (PDO) at three different concentrations (0.1 mmol/L, 1 mmol/L and 10 mmol/L). The evaluated parameters were: percentage of progressively motile spermatozoa (PMOT), percentage of spermatozoa with low membrane lipid disorder (%M540$^-$/YO-PRO-1$^-$ sperm cells) and percentage of spermatozoa with high mitochondrial membrane potential (MMP; %$JC1_{agg}$ spermatozoa). Determinations were performed in fresh (extended) and frozen-thawed (FT) spermatozoa after 30 and 240 min of thawing. Data reported as mean ± SEM

Variable	PDO concentration	Time point		
		Extended	FT-30 min	FT-240 min
%PMOT	CNT	69.87 ± 3.20	23.38 ± 2.74^a	10.96 ± 1.12^{a,b}
	0.1 mmol/L		26.62 ± 2.10^a	7.60 ± 0.42^b
	1 mmol/L		22.80 ± 2.12^a	11.71 ± 1.07^a
	10 mmol/L		24.94 ± 2.20^a	8.48 ± 0.45^{a,b}
%M540$^-$/ YO-PRO-1$^-$	CNT	80.83 ± 2.79	39.03 ± 1.49^a	31.25 ± 1.06^a
	0.1 mmol/L		48.12 ± 1.75^b	37.56 ± 1.50^{b,c}
	1 mmol/L		53.28 ± 2.10^b	42.93 ± 1.38^c
	10 mmol/L		56.02 ± 2.32^b	36.50 ± 1.23^{a,b}
%$JC1_{agg}$	CNT	82.79 ± 2.41	31.95 ± 1.89^a	26.01 ± 1.44^a
	0.1 mmol/L		48.76 ± 1.85^b	38.67 ± 1.58^b
	1 mmol/L		40.95 ± 2.07^c	34.39 ± 1.54$^{b,\ c}$
	10 mmol/L		35.89 ± 2.06$^{a,\ c}$	30.56 ± 1.29$^{a,\ c}$

Different letters ($^{a-c}$) indicate significant differences ($P < 0.05$) between treatments within a given time point for each parameter

Table 2 Sperm quality parameters from samples exposed to extender alone (control), or in the presence of acetazolamide (AC) at three different concentrations (250 μmol/L, 500 μmol/L and 1000 μmol/L). The evaluated parameters were: percentage of progressively motile spermatozoa (PMOT), percentage of spermatozoa with low membrane lipid disorder (%M540$^-$/YO-PRO-1$^-$ sperm cells) and percentage of spermatozoa with high mitochondrial membrane potential (MMP; %$JC1_{agg}$ spermatozoa). Determinations were performed in fresh (extended) and frozen-thawed (FT) spermatozoa after 30 and 240 min of thawing. Data reported as mean ± SEM

Variable	AC concentration	Time point		
		Extended	FT-30 min	FT-240 min
%PMOT	CNT	69.87 ± 3.20	23.38 ± 2.74^{a}	10.96 ± 1.12$^{a, b}$
	250 μmol/L		25.34 ± 2.83^{a}	13.47 ± 2.19^{a}
	500 μmol/L		22.99 ± 2.57^{a}	12.94 ± 1.98$^{a, b}$
	1000 μmol/L		20.77 ± 2.29^{a}	8.93 ± 1.30^{b}
%M540$^-$/ YO-PRO-1$^-$	CNT	80.83 ± 2.79	39.03 ± 1.49$^{a, b}$	31.25 ± 1.06$^{a, b}$
	250 μmol/L		40.26 ± 1.73$^{a, b}$	27.01 ± 0.98^{a}
	500 μmol/L		46.39 ± 1.30^{a}	35.28 ± 1.71^{b}
	1000 μmol/L		36.03 ± 1.58^{b}	30.52 ± 1.18$^{a, b}$
%$JC1_{agg}$	CNT	82.79 ± 2.41	31.95 ± 1.89^{a}	26.01 ± 1.44$^{a, b}$
	250 μmol/L		29.30 ± 1.63^{a}	23.70 ± 1.24$^{a, b}$
	500 μmol/L		40.84 ± 2.11^{b}	31.98 ± 1.89^{a}
	1000 μmol/L		30.20 ± 1.72^{a}	21.92 ± 1.35^{b}

Different letters ($^{a, b}$) indicate significant differences ($P < 0.05$) between treatments within a given time point for each parameter

percentage of viable spermatozoa with high peroxide levels ($P > 0.05$; Fig. 3c, d).

Discussion

Despite studies conducted in the last decade identifying the presence of AQPs in sperm cells of several mammalian species (reviewed in [17]), neither their precise function nor their mechanism of action have been fully addressed. To this end, this study has used different AQP inhibitors to unveil the relevance of orthodox AQPs and GLPs during cryopreservation. Three different inhibitors were added at three concentrations each: 1,3-propanediol (PDO; 0.1, 1 and 10 mmol/L), acetazolamide (AC; 250, 500 and 1000 μmol/L) and phloretin

Table 3 Sperm quality parameters from samples exposed to extender alone (control), or in the presence of phloretin (PHL) at three different concentrations (250 μmol/L, 500 μmol/L and 1000 μmol/L). The evaluated parameters were: percentage of progressively motile spermatozoa (PMOT), percentage of spermatozoa with low membrane lipid disorder (%M540$^-$/YO-PRO-1$^-$ sperm cells) and percentage of spermatozoa with high mitochondrial membrane potential (MMP; %$JC1_{agg}$ spermatozoa). Determinations were performed in fresh (extended) and frozen-thawed (FT) spermatozoa after 30 and 240 min of thawing. Data reported as mean ± SEM

Variable	PHL concentration	Time point		
		Extended	FT-30 min	FT-240 min
%PMOT	CNT	69.87 ± 3.20	23.38 ± 2.74^{a}	10.96 ± 1.12^{a}
	250 μmol/L		20.52 ± 0.98^{a}	8.61 ± 0.93^{a}
	500 μmol/L		22.16 ± 0.75^{a}	7.62 ± 0.89^{a}
	1000 μmol/L		10.38 ± 0.90^{b}	3.82 ± 0.92^{b}
%M540$^-$/ YO-PRO-1$^-$	CNT	80.83 ± 2.79	39.03 ± 1.49$^{a, b}$	31.25 ± 1.06^{a}
	250 μmol/L		44.53 ± 1.99^{a}	34.19 ± 1.29^{a}
	500 μmol/L		37.92 ± 1.37^{b}	30.20 ± 1.10^{a}
	1000 μmol/L		31.01 ± 1.60^{c}	21.42 ± 1.05^{b}
%$JC1_{agg}$	CNT	82.79 ± 2.41	31.95 ± 1.89^{a}	26.01 ± 1.44^{a}
	250 μmol/L		38.21 ± 2.08^{a}	22.49 ± 1.21^{a}
	500 μmol/L		34.98 ± 2.09^{a}	29.29 ± 1.74^{a}
	1000 μmol/L		31.93 ± 1.88^{a}	25.18 ± 1.29^{a}

Different letters (a–c) indicate significant differences ($P < 0.05$) between treatments within a given time point for each parameter

(PHL; 250, 500 and 1000 μmol/L). PDO has been proven to inhibit orthodox AQPs (AQP1, AQP2, AQP5 and AQP4) with high efficiency, and GLPs (the family to which AQP3, AQP7 and AQP9 belong) with low intensity [20, 21]. With regard to AC, it inhibits AQP1 and AQP4 [22, 23], whereas PHL inhibits both AQP3 and AQP7 [33–35]. The concentrations were based on preliminary experiments conducted to determine the minimum concentration at which an effect was observed, and the maximum concentration at which cytotoxic effects appeared. The assessment of how each inhibitor affected sperm function and survival during cryopreservation was made on the basis of sperm motility, sperm viability, membrane lipid disorder, MMP, and intracellular levels of superoxide and peroxides.

Compared to the control, PDO tended to maintain better post-thaw sperm viability and lower levels of membrane lipid disorder; however, total sperm motility decreased, whereas percentages of spermatozoa with high MMP and with high levels of ROS (including superoxides and peroxides) increased at some concentrations. As far as AC is concerned, there was a lack of consistent effects, and only the percentage of spermatozoa with high MMP and intracellular levels of $O_2^-\bullet$ changed at some concentrations and time points. Finally, PHL had detrimental effects on total and progressive sperm motilities, viability and membrane lipid disorder.

The different effects observed between inhibitors might be due to their specificity for different AQPs and the collateral effects on other proteins that are present in the sperm cell. In this context, PDO inhibits a great number of AQPs, especially orthodox AQPs, and, with less efficiency, GLPs. Whereas PDO remains inside the pore of orthodox AQPs because of its narrow diameter, it is able to freely permeate through the GLP pore [20, 21]. Relate to this, it is worth mentioning that Cooper et al. [36] assessed the ability of PDO to penetrate epididymal murine sperm. PDO may disrupt the transport of water and also that of small solutes, including glycerol. Since glycerol is present in many cryopreservation extenders, including the one used in this study, it is possible that its entry to sperm cells and, as a consequence, its function as a CPA, are partially impaired through GLP inhibition. Nevertheless, this hypothesis would not explain why post-thaw sperm viability and the percentage of spermatozoa with low membrane lipid disorder were higher in those samples containing PDO. In this context, one could suggest that PDO could mitigate the negative effects of the lower intracellular concentration of glycerol inside the sperm cell by acting as a CPA itself. In addition, it is widely known that glycerol, much like other CPAs, presents certain toxic effects for sperm cells (reviewed in [15]), and reducing its intracellular concentration could decrease its toxicity. Considering the aforementioned, our results could be explained by PDO lowering the toxic effect of glycerol, and acting as a CPA itself. Consequently, PDO should be further studied as a potential CPA in combination with other agents, as its positive effects on frozen-thawed sperm warrant further research and its impact on sperm viability observed in the current work is coincident with that observed by Widiasih et al. [37] in human sperm. Moreover, PDO has also been used in cryopreservation protocols for canine ovarian cortices [38] and in human multipotent stromal cells [39].

On the other hand, the increase of MMP and ROS levels in PDO-treatments is noteworthy. To the best of our knowledge, the potential effects of PDO on oxidative stress have not been previously reported. Our results suggest that the increase in sperm viability observed when this inhibitor is present in the cryopreservation medium is at the expense of an increase in the percentage of sperm cells with high levels of ROS, and therefore, with potential DNA damage [40]. It is worth mentioning that some studies have unraveled the fact that AQP3 and AQP9 are permeable to H_2O_2 [41, 42], and that H_2O_2 transport through these proteins does play a vital role in human sperm function [9]. Since the increase of MMP causes an increase in ROS production, including H_2O_2, one could suggest that the inhibition of AQP3 and AQP9 by PDO would block H_2O_2-efflux. That being said, the aforementioned increase in MMP does not have an apparent cause. A possible explanation could be an interaction of PDO with AQP11, which localizes in the mitochondrial membrane of boar sperm [3]. However, since the inhibiting capacity of PDO with regard to superAQPs has not been previously tested, further studies are needed to unravel the mechanism behind the PDO-mediated increase in MMP.

Regarding the inhibitory mechanism of PHL, it permeates the sperm plasma membrane thanks to its hydrophobic nature [43], and it inhibits GLPs through an internal binding site [44]. Considering its proven inhibitory effect on GLPs, detrimental effects on sperm quality in its presence could be a consequence of the decrease in glycerol permeability, which is consistent with the effects observed in the presence of PDO. In fact, total sperm motility is similarly affected by both inhibitors. Moreover, the detrimental effects on sperm viability and membrane lipid disorder support the hypothesis that PDO rather than PHL exerts a cryoprotective effect. Nevertheless, it is worth highlighting that PHL has inhibitory effects on other sperm proteins, such as SLC2A2 (also known as GLUT2), protein kinase C (PKC), and volume-sensitive and cAMP-activated Cl^- channels [45]. All of these proteins can play an

important role in the regulation of sperm function: SLC2A2 is involved in the uptake of monosaccharides, which are the main energy source for sperm cells [46]; PKC is implicated in the regulation of sperm motility through phosphorylation of other sperm proteins; and chloride-dependent transport mechanisms are relevant for different sperm cell pathways, such as cAMP-protein kinase A (PKA), which plays a vital role during sperm capacitation [16]. Therefore, not only could PHL mediate the decrease in sperm motility, viability and MMP through the inhibition of GLPs, but also through the inhibition of other sperm proteins.

Concerning AC and its specificity for orthodox AQPs, one would expect that this inhibitor would not affect CPA transport, which could explain why sperm viability and membrane lipid disorder were not affected. Moreover, the fact that AC inhibits AQP1 and AQP4, which have not been previously identified in boar spermatozoa, supports the absence of effects when this inhibitor is added before cryopreservation. In spite of this, some sperm parameters were altered in the presence of AC. While this impact did not appear to depend on the AC concentration, we suggest that it is not directly related to AQP inhibition. Indeed, AC is known to inhibit carbonic anhydrase (CA), and therefore it blocks the conversion of CO_2 and H_2O into bicarbonate and protons [47]. Since bicarbonate together with Ca^{2+} stimulates PKA, and complex IV of the electron transport chain is activated via a PKA-mediated phosphorylation, inhibition of CA through AC could cause uncoupling of the electron transport chain [48]. This uncoupling is likely to be responsible for the increase in percentages of spermatozoa with high MMP and with high superoxide levels in AC treatments. Nevertheless, while the intermediate concentration of AC causes an increase in MMP, the highest one has no effect in this parameter compared to the control. Even if no significant differences were found in sperm viability when AC treatments and the control were compared, samples treated with the intermediate concentration of AC showed a significantly ($P < 0.05$) higher viability than those treated with the highest concentration of AC at 30 min post-thaw. Therefore, the absence of differences in MMP in the presence of the highest concentration of AC could be a consequence of mitochondrial alterations that would compromise the integrity of this organelle. In this case, AC would have a hormetic effect on MMP: namely, MMP would have a biphasic response to AC, which would be characterized by a response effect consisting of an increase at low doses, and a decrease at the high ones. Finally, the lack of a concomitant increase in H_2O_2 levels might be explained by the normal efflux of this molecule, since rather than targeting GLPs, which present oxygen peroxide permeability, AC inhibit orthodox AQPs only.

Conclusion

In conclusion, AQP-inhibition effects are highly reliant upon the specificity of the inhibitor and its ability to affect other sperm proteins. In this work, PDO has been found to improve post-thaw sperm survival at the expense of an increase in the percentages of viable spermatozoa with high ROS levels, which suggests its potential role as a CPA. Further research is, however, required to confirm this hypothesis. Based on the observed effects after AC supplementation, which mainly targets orthodox AQPs, it seems that orthodox AQPs are not involved in the response to osmolality variations during freeze-thawing of boar sperm, since the observed changes compared to the control seem to result from collateral effects of this inhibitor upon the sperm cell. Finally, the dramatic impairment observed in post-thaw sperm quality parameters when PHL was added to the cryopreservation media supports the crucial role of GLPs – and not of orthodox AQPs – during boar sperm cryopreservation.

Abbreviations

AC: Acetazolamide; ALH: Amplitude of lateral head displacement; AQP: Aquaporin; BCF: Beat cross frequency; BTS: Beltsville Thawing Solution; CA: Carbonic anhydrase; cAMP: cyclic AMP; CASA: Computer-assisted sperm analysis; CPA: Cryoprotective agent; DCF^{+}: 2′,7′-dichlorofluorescein; E^{+}: Ethidium; EV: Electronic volume; FS: Forward scatter; GLP: Aquaglyceroporins; H_2DCFDA: 2′,7′-dichlorodihydrofluorescein diacetate; H_2O_2: Hydrogen peroxide; HE: Hydroethidine; ISAC: International Society for Advancement of Cytometry; JC-1: 5,5′,6,6′-tetrachloro-1,1′,3,3′tetraethylbenzimidazolylcarbocyanine iodide; $JC\text{-}1_{agg}$: JC-1 aggregates; $JC\text{-}1_{mon}$: JC-1 monomers; LEY: β-Lactose -Egg yolk -Glycerol; LEYGO: β-Lactose -Egg yolk -Glycerol -Orvus Es Paste; LIN: Linearity; M540: Merocyanine 540; MMP: Mitochondrial membrane potential; $O_2^{-}\cdot$: Superoxide; PDO: 1,3-propanediol; PfAQP: *Plasmodium falciparum* aquaporin; PHL: Phloretin; PI: Propidium iodide; PKA: cAMP dependent protein kinase; PKC: Protein kinase C; PMOT: Progressive motility; ROS: Reactive oxygen species; SEM: Standard error of the mean; SLC2A2: Solute carrier family 2, facilitated glucose transporter member 2; SS: Side scatter; STR: Straightness; TMOT: Total motility; VAP: Average path velocity; VCL: Curvilinear velocity; VSL: Straight line velocity; WOB: Motility parameter wobble

Acknowledgements

The authors acknowledge the technical support received from Estela Garcia (University of Girona, Spain).

Authors' contributions

ADB performed the experiments, undertook flow cytometry and statistical analyses and wrote the draft. ML and LFB contributed to performing CASA and flow cytometry evaluations. IB, SR, YM, SB and BFF contributed to the critical revision of the Manuscript. MY conceived the study and help conduct data analysis. All authors read and approved the final manuscript.

Funding

The authors acknowledge the support from the European Commission (H2020-MSCA-IF-79212), the Ministry of Science, Innovation and Universities, Spain (Grants: RYC-2014-15581, AGL2016–81890-REDT, AGL2017–88329-R and FJCI-2017-31689), and the Regional Government of Catalonia, Spain (2017-SGR-1229).

Availability of data and materials

The datasets and/or analyzed during the current study are available from the corresponding author on reasonable request.

Ethics approval and consent to participate
Not applicable.

Consent for publication
Not applicable.

Competing interests
The authors declare that the research was conducted in the absence of any commercial or financial relationships that could be construed as a potential conflict of interest.

Received: 17 April 2019 Accepted: 8 August 2019
Published online: 14 October 2019

References

1. Watson H. Biological membranes. Essays Biochem. 2015;59:43–70.
2. Yeste M, Morató R, Rodríguez-Gil JE, Bonet S, Prieto-Martínez N. Aquaporins in the male reproductive tract and sperm: functional implications and cryobiology. Reprod Domest Anim. 2017;52:12–27.
3. Prieto-Martínez N, Vilagran I, Morató R, Rodríguez-Gil JE, Yeste M, Bonet S. Aquaporins 7 and 11 in boar spermatozoa: detection, localisation and relationship with sperm quality. Reprod Fertil Dev. 2014;28:663–72.
4. Prieto-Martínez N, Morató R, Vilagran I, Rodríguez-Gil JE, Bonet S, Yeste M. Aquaporins in boar spermatozoa. Part II: detection and localisation of aquaglyceroporin 3. Reprod Fertil Dev. 2015;29:703–11.
5. Chen Q, Peng H, Lei L, Zhang Y, Kuang H, Cao Y, et al. Aquaporin 3 is a sperm water channel essential for postcopulatory sperm osmoadaptation and migration. Cell Res. 2011;21:922–33.
6. Yeung CH, Callies C, Rojek A, Nielsen S, Cooper TG. Aquaporin isoforms involved in physiological volume regulation of murine spermatozoa. Biol Reprod. 2009;80:350–7.
7. Yeung CH, Cooper TG. Aquaporin AQP11 in the testis: molecular identity and association with the processing of residual cytoplasm of elongated spermatids. Reproduction. 2010;139:209–16.
8. Yeung CH, Callies C, Tüttelmann F, Kliesch S, Cooper TG. Aquaporins in the human testis and spermatozoa - identification, involvement in sperm volume regulation and clinical relevance. Int J Androl. 2010;33:629–41.
9. Laforenza U, Pellavio G, Marchetti A, Omes C, Todaro F, Gastaldi G. Aquaporin-mediated water and hydrogen peroxide transport is involved in Normal human spermatozoa functioning. Int J Mol Sci. 2017;18:E66.
10. Prieto-Martínez N, Morató R, Muiño R, Hidalgo CO, Rodríguez-Gil JE, Bonet S, et al. Aquaglyceroporins 3 and 7 in bull spermatozoa: identification, localisation and their relationship with sperm cryotolerance. Reprod Fertil Dev. 2016;29:1249–59.
11. Morató R, Prieto-Martínez N, Muiño R, Hidalgo CO, Rodríguez-Gil JE, Bonet S, et al. Aquaporin 11 is related to cryotolerance and fertilising ability of frozen–thawed bull spermatozoa. Reprod Fertil Dev. 2018;30:1099–108.
12. Bonilla-Correal S, Noto F, Garcia-Bonavila E, Rodríguez-Gil JE, Yeste M, Miró J. First evidence for the presence of aquaporins in stallion sperm. Reprod Domest Anim. 2017;52:61–4.
13. Vicente-Carrillo A, Ekwall H, Álvarez-Rodríguez M, Rodríguez-Martínez H. Membrane stress during thawing elicits redistribution of aquaporin 7 but not of aquaporin 9 in boar spermatozoa. Reprod Domest Anim. 2016;51:665–79.
14. Huang HF, He RH, Sun CC, Zhang Y, Meng QX, Ma YY. Function of aquaporins in female and male reproductive systems. Hum Reprod Update. 2006;12:785–95.
15. Yeste M. Sperm cryopreservation update: Cryodamage, markers, and factors affecting the sperm freezability in pigs. Theriogenology. 2016;85:47–64.
16. Bonet S, Casas I, Holt WV. Boar reproduction: fundamentals and new biotechnological trends. 1st ed. London: Springer; 2013.
17. Yeste M. Recent advances in boar sperm cryopreservation: state of the art and current perspectives. Reprod Domest Anim. 2015;50:71–9.
18. Yeste M, Rodríguez-Gil JE, Bonet S. Artificial insemination with frozen-thawed boar sperm. Mol Reprod Dev. 2017;84:802–13.
19. Prieto-Martínez N, Vilagran I, Morató R, Rivera del Álamo MM, Rodríguez-Gil JE, Bonet S, et al. Relationship of aquaporins 3 (AQP3), 7 (AQP7), and 11 (AQP11) with boar sperm resilience to withstand freeze-thawing procedures. Andrology. 2017;5:1153–64.
20. Yu L, Villarreal OD, Chen LL, Chen LY. 1,3-Propanediol binds inside the water-conducting pore of aquaporin 4: does this efficacious inhibitor have sufficient potency? J Syst Integr Neurosci. 2016;2:91–8.
21. Yu L, Rodriguez RA, Chen LL, Chen LY, Perry G, McHardy SF, et al. 1,3-Propanediol binds deep inside the channel to inhibit water permeation through Aquaporins. Protein Sci. 2016;25:433–41.
22. Gao J, Wang X, Chang Y, Zhang J, Song Q, Yu H, et al. Acetazolamide inhibits osmotic water permeability by interaction with aquaporin-1. Anal Biochem. 2006;350:165–70.
23. Tanimura Y, Hiroaki Y, Fujiyoshi Y. Acetazolamide reversibly inhibits water conduction by aquaporin-4. J Struct Biol. 2009;166:16–21.
24. Tsukaguchi H, Shayakul C, Berger UV, Mackenzie B, Devidas S, Guggino WB, et al. Molecular characterization of a broad selectivity neutral Solute Channel. J Biol Chem. 1998;273:24737–43.
25. Cheung KH, Leung CT, Leung GPH, Wong PYD. Synergistic effects of cystic fibrosis transmembrane conductance regulator and Aquaporin-9 in the rat epididymis. Biol Reprod. 2003;68:1505–10.
26. Casas I, Sancho S, Briz M, Pinart E, Bussalleu E, Yeste M, et al. Freezability prediction of boar ejaculates assessed by functional sperm parameters and sperm proteins. Theriogenology. 2009;72:930–48.
27. Pursel VG, Johnson LA. Freezing of boar spermatozoa: fertilizing capacity with concentrated semen and a new thawing procedure. J Anim Sci. 1975; 40:99–102.
28. Garner DL, Johnson LA. Viability assessment of mammalian sperm using SYBR-14 and propidium iodide. Biol Reprod. 1995;53:276–84.
29. Rathi R, Colenbrander B, Bevers MM, Gadella BM. Evaluation of in vitro capacitation of stallion spermatozoa. Biol Reprod. 2001;65:462–70.
30. Yeste M, Estrada E, Rivera Del Álamo MM, Bonet S, Rigau T, Rodríguez-Gil JE. The increase in phosphorylation levels of serine residues of protein HSP70 during holding time at 17°C is concomitant with a higher cryotolerance of boar spermatozoa. PLoS One. 2014;9:e90887.
31. Ortega-Ferrusola C, Sotillo-Galán Y, Varela-Fernández E, Gallardo-Bolaños JM, Muriel A, González-Fernández L, et al. Detection of 'apoptosis-like' changes during the cryopreservation process in equine sperm. J Androl. 2008;29:213–21.
32. Guthrie HD, Welch GR. Determination of intracellular reactive oxygen species and high mitochondrial membrane potential in Percoll-treated viable boar sperm using fluorescence-activated flow cytometry. J Anim Sci. 2006;84:2089–100.
33. Rezk BM, Haenen GRMM, van der Vijgh WJF, Bast A. The antioxidant activity of phloretin: the disclosure of a new antioxidant pharmacophore in flavonoids. Biochem Biophys Res Commun. 2002;295:9–13.
34. Barreca D, Currò M, Bellocco E, Ficarra S, Laganà G, Tellone E, et al. Neuroprotective effects of phloretin and its glycosylated derivative on rotenone-induced toxicity in human SH-SY5Y neuronal-like cells. BioFactors. 2017;43:549–57.
35. Przybylo M, Procek J, Hof M, Langner M. The alteration of lipid bilayer dynamics by phloretin and 6-ketocholestanol. Chem Phys Lipids. 2014;178:38–44.
36. Cooper TG, Barfield JP, Yeung CH. The tonicity of murine epididymal spermatozoa and their permeability towards common cryoprotectants and epididymal osmolytes. Reproduction. 2008;135:625–33.
37. Widiasih D, Yeung CH, Junaidi A, Cooper TG. Multistep and single-step treatment of human spermatozoa with cryoprotectants. Fertil Steril. 2009;92:382–9.
38. Lopes CA, Alves AM, Jewgenow K, Báo SN, de Figueiredo JR. Cryopreservation of canine ovarian cortex using DMSO or 1,3-propanediol. Theriogenology. 2016;86:1165–74.
39. Pogozhykh D, Prokopyuk V, Pogozhykh O, Mueller T, Prokopyuk O. Influence of factors of cryopreservation and hypothermic storage on survival and functional parameters of multipotent stromal cells of placental origin. PLoS One. 2015;10:e0139834.
40. Aitken RJ. Reactive oxygen species as mediators of sperm capacitation and pathological damage. Mol Reprod Dev. 2017;84:1039–52.
41. Miller EW, Dickinson BC, Chang CJ. Aquaporin-3 mediates hydrogen peroxide uptake to regulate downstream intracellular signaling. Proc Natl Acad Sci. 2010;107:15681–6.
42. Watanabe S, Moniaga CS, Nielsen S, Hara-Chikuma M. Aquaporin-9 facilitates membrane transport of hydrogen peroxide in mammalian cells. Biochem Biophys Res Commun. 2016;471:191–7.
43. Pohl P, Rokitskaya TI, Pohl EE, Saparov SM. Permeation of phloretin across bilayer lipid membranes monitored by dipole potential and microelectrode measurements. Biochim Biophys Acta. 1997;1323:163–72.
44. Wacker SJ, Aponte-Santamaría C, Kjellbom P, Nielsen S, De Groot BL, Rützler M. The identification of novel, high affinity AQP9 inhibitors in an intracellular binding site. Mol Membr Biol. 2013;30:246–60.

45. Fan H, Morishima S, Kida H, Okada Y. Phloretin differentially inhibits volume-sensitive and cyclic AMP-activated, but not ca-activated, cl- channels. Br J Pharmacol. 2001;133:1096–106.
46. Bucci D, Isani G, Spinaci M, Tamanini C, Mari G, Zambelli D, et al. Comparative Immunolocalization of GLUTs 1, 2, 3 and 5 in boar, stallion and dog spermatozoa. Reprod Domest Anim. 2010;45:315–22.
47. Van Berkel MA, Pharm D. Evaluating off-label uses of acetazolamide. Am J Health Syst Pharm. 2018;75:524–31.
48. Jakobsen E, Lange SC, Andersen JV, Desler C, Kihl HF, Hohnholt MC, et al. The inhibitors of soluble adenylate cyclase 2-OHE, KH7, and bithionol compromise mitochondrial ATP production by distinct mechanisms. Biochem Pharmacol. 2018;155:92–101.

Paper III

Effect of AQP inhibition on boar sperm cryotolerance depends on the intrinsic freezability of the ejaculate.

Ariadna Delgado-Bermúdez, Marc Llavanera, Sandra Recuero, Yentel Mateo-Otero, Sergi Bonet, Isabel Barranco, Beatriz Fernandez-Fuertes, Marc Yeste.

International Journal of Molecular Sciences,

2019;20(24):6255

doi: 10.3390/ijms20246255

International Journal of
Molecular Sciences

MDPI

Article

Effect of AQP Inhibition on Boar Sperm Cryotolerance Depends on the Intrinsic Freezability of the Ejaculate

Ariadna Delgado-Bermúdez, Marc Llavanera, Sandra Recuero, Yentel Mateo-Otero, Sergi Bonet, Isabel Barranco, Beatriz Fernandez-Fuertes and Marc Yeste *

Biotechnology of Animal and Human Reproduction (TechnoSperm), Unit of Cell Biology, Department of Biology, Institute of Food and Agricultural Technology, Faculty of Sciences, University of Girona, E-17003 Girona, Spain; ariadna.delgado@udg.edu (A.D.-B.); marc.llavanera@udg.edu (M.L.); sandra.recuero@udg.edu (S.R.); yentel.mateo@udg.edu (Y.M.-O.); sergi.bonet@udg.edu (S.B.); isabel.barranco@udg.edu (I.B.); beatriz.fernandez@udg.edu (B.F.-F.)

* Correspondence: marc.yeste@udg.edu

Received: 19 November 2019; Accepted: 10 December 2019; Published: 11 December 2019

Abstract: Aquaporins (AQPs) are transmembrane channels with permeability to water and small solutes that can be classified according to their structure and permeability into orthodox AQPs, aquaglyceroporins (GLPs), and superAQPs. In boar spermatozoa, AQPs are related to osmoregulation and play a critical role in maturation and motility activation. In addition, their levels differ between ejaculates with good and poor cryotolerance (GFE and PFE, respectively). The aim of this work was to elucidate whether the involvement of AQPs in the sperm response to cryopreservation relies on the intrinsic freezability of the ejaculate. With this purpose, two different molecules: phloretin (PHL) and 1,3-propanediol (PDO), were used to inhibit sperm AQPs in GFE and PFE. Boar sperm samples were treated with three different concentrations of each inhibitor prior to cryopreservation, and sperm quality and functionality parameters were evaluated in fresh samples and after 30 and 240 min of thawing. Ejaculates were classified as GFE or PFE, according to their post-thaw sperm viability and motility. While the presence of PHL caused a decrease in sperm quality and function compared to the control, samples treated with PDO exhibited better quality and function parameters than the control. In addition, the effects of both inhibitors were more apparent in GFE than in PFE. In conclusion, AQP inhibition has more notable consequences in GFE than in PFE, which can be related to the difference in relative levels of AQPs between these two groups of samples.

Keywords: aquaporins; boar; phloretin; propanediol; spermatozoa

1. Introduction

The amphipathic nature of the plasma membrane is a limiting factor for simple diffusion of water molecules at high rates. In contrast, proper cell function and homeostasis strictly depend on the permeability of the plasma membrane to water and solutes [1]. Aquaporins (AQPs), a family of transmembrane proteins ubiquitously present in mammalian cells, facilitate the diffusion of water and some small solutes through the plasma membrane [2]. Mammalian AQPs are classified into three different groups according to their sequence similarity and their solute permeability: orthodox AQPs, aquaglyceroporins (GLPs) and superAQPs; that include a total of 13 members (AQP0-AQP12). Orthodox AQPs are exclusively permeable to water and include AQP0, AQP1, AQP2, AQP4, AQP5, AQP6, and AQP8. GLPs include AQP3, AQP7, AQP9, and AQP10, which are permeable to water, glycerol and other small molecules. Finally, AQP11 and AQP12 are members of the superAQPs group, and are involved in the transport of both water and glycerol, presenting deep structural differences with the members of the other groups. Even if ubiquitous, the presence of AQPs differs between

species and also between cell types. Concerning mammalian spermatozoa, AQP3, AQP7, and AQP11 have been identified in the pig [3,4], horse [5], mouse [6–8], human [9,10], and bull [11,12]; AQP8 has been found in mouse [7] and human spermatozoa [9,10]; and AQP9 is present in pig spermatozoa [13]. The importance of AQPs in spermatozoa relies on their ability to regulate cell volume and osmotic balance, thus having a key role in spermatogenesis [14] and post-ejaculatory events, such as the activation of sperm motility and the adaptation to the female environment (reviewed by [2]).

To date, sperm cryopreservation is the most efficient method for long-term storage of boar spermatozoa [15]. Nevertheless, this procedure is a source of osmotic stress causing damage to the sperm nucleus, intracellular organelles, and plasma membrane, and reducing sperm survival and fertilizing capacity [15,16]. Cryotolerance, which can be defined as the ability of sperm to withstand the detrimental effects of the cryopreservation process, is highly variable between different mammalian species, and it depends, among other factors, on differences in membrane composition [16–20]. Moreover, within a given species, males with similar fresh sperm quality present highly variable cryotolerance, both intra- and inter-individually [21–23]. For this reason, ejaculates can be classified as having good (GFE) or poor freezability (PFE), depending on their post-thaw sperm quality and functional parameters, mainly viability and motility [21]. Because the levels of some proteins differ between GFE and PFE, they can be used as biomarkers of cryotolerance in fresh samples [24]. The key role of AQPs in osmoregulation is a potential mechanism through which these proteins might be involved in sperm cryopreservation, which has previously been confirmed in bull [11,12], boar [25,26], and stallion [5], since spermatozoa from GFE and PFE present different levels of some AQPs. In effect, AQP3 and AQP7 are related to the cryotolerance of boar spermatozoa [25], AQP7 [3] and AQP11 [12] are associated with that of bull spermatozoa, and AQP3 and AQP11 are related to stallion sperm freezability [5]. Moreover, inhibition of AQPs alters boar and stallion sperm cryotolerance [26,27].

Different AQP inhibitors have been previously tested in other cell types, such as 1,3-propanediol (PDO) and phloretin (PHL). PDO has been proven to occlude, with high affinity, the pore channel of orthodox AQPs from the outer side of the plasma membrane and with high affinity [28,29]. In addition, PDO is able to penetrate through *Plasmodium falciparum Pf* AQP (which is an analogue of AQP3, AQP7, and AQP9) and to mildly inhibit this GLP analogue from the inner part of the plasma membrane [28]. PHL inhibits AQP3 and AQP9, which are both GLPs [30,31]. Considering the differences on AQP levels between GFE and PFE [25] and the impact of AQP inhibition on sperm cryotolerance [26], it is reasonable to suggest that the effects of AQP inhibition might vary between GFE and PFE. Therefore, this study aims to elucidate whether the sperm response to AQP inhibition (through incubation with PDO and PHL) prior to cryopreservation differs between GFE and PFE.

2. Results

2.1. Classification of Boar Ejaculates in GFE and PFE Groups

Classification of ejaculate pools by cluster analysis resulted in 11 GFE and 10 PFE. In fresh samples, no differences were identified in any of the parameters measured between groups ($p > 0.05$). However, sperm total and progressive motility, viability, percentage of viable cells with low membrane lipid disorder and percentage of cells with high mitochondrial membrane potential were higher in GFE than in PFE at both 30 min and 240 min post-thaw ($p < 0.05$).

2.2. Effects of AQP Inhibition on Cryopreserved Sperm Quality Parameters

To determine the effects of AQP inhibitors during cryopreservation, quality and function parameters of both fresh and frozen-thawed spermatozoa from GFE and PFE samples were evaluated. No differences were observed in fresh samples for any parameter measured between treatments and the control ($p > 0.05$), since inhibitors were added immediately before cryopreservation (Figures 1–7). After thawing, samples from the PFE group presented significantly ($p < 0.05$) lower values of all sperm quality and function parameters than GFE in the presence of all treatments and in the control group.

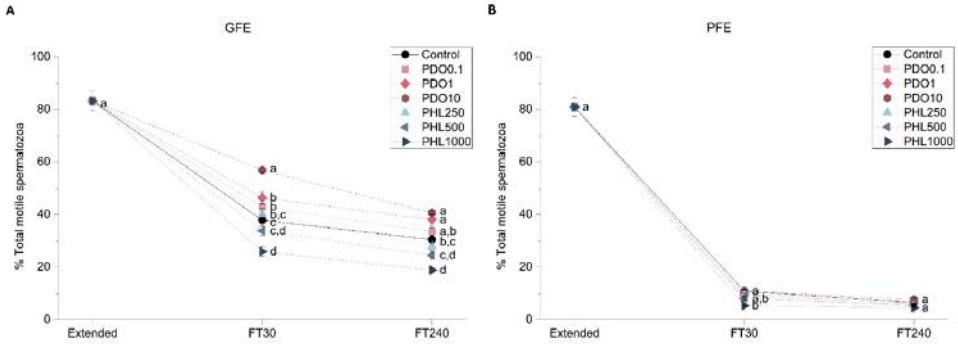

Figure 1. Percentages of total motile spermatozoa (TMOT) in good freezability ejaculates (GFE; (**A**)) and poor freezability ejaculates (PFE; (**B**)) exposed to AQP inhibitors in the extender: 0.1 mmol/L, 1 mmol/L and 10 mmol/L 1,3-propanediol (PHL) or 250 µmol/L, 500 µmol/L and 1000 µmol/L phloretin (PHL); or not (control). Data were collected from fresh (extended) and frozen-thawed (FT) samples at 30 and 240 min post-thaw, and are shown as mean ± SEM. Different letters (a, b, c, d) indicate a significant difference ($p < 0.05$) between treatments within a given time point.

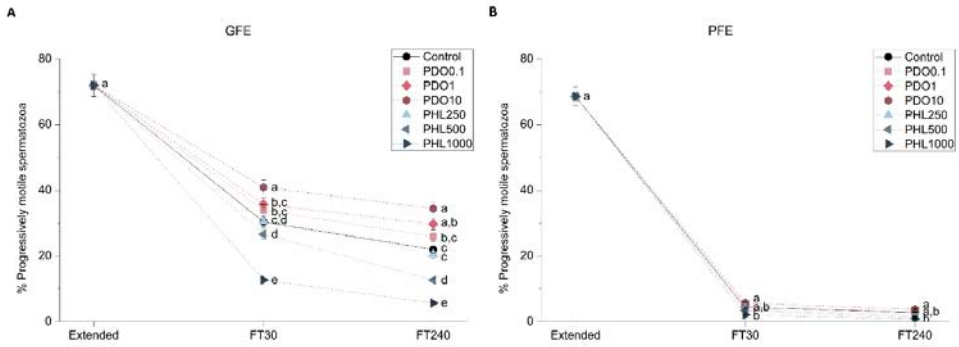

Figure 2. Percentages of progressively motile spermatozoa (PMOT) in good freezability ejaculates (GFE; (**A**)) and poor freezability ejaculates (PFE; (**B**)) exposed to AQP inhibitors in the extender: 0.1 mmol/L, 1 mmol/L, and 10 mmol/L 1,3-propanediol (PHL) or 250 µmol/L, 500 µmol/L, and 1000 µmol/L phloretin (PHL); or not (control). Data were collected from fresh (extended) and frozen-thawed (FT) samples at 30 and 240 min post-thaw, and are shown as mean ± SEM. Different letters (a, b, c, d, e) indicate a significant difference ($p < 0.05$) between treatments within a given time point.

2.2.1. Sperm Motility

Figures 1 and 2 show the percentage of total motility (TMOT, %) and progressive motility (PMOT, %) in fresh and frozen-thawed samples exposed to different AQP inhibitors during cryopreservation. In GFE, TMOT was higher when samples were treated with PDO than in the control ($p < 0.05$), whereas in PFE there were no differences with regard to the control when exposed to different PDO concentrations ($p > 0.05$). On the other hand, in the presence of 1000 µmol/L PHL, TMOT was lower than in the control at 30 min post-thaw ($p < 0.05$) in both GFE and PFE, whereas, at 240 min post-thaw, this difference was only observed in GFE ($p < 0.05$). At 30 min post-thaw, treatment with 10 mmol/L PDO caused an increase in PMOT, whereas at 240 min this change was observed at both 1 and 10 mmol/L concentrations in GFE ($p < 0.05$). Concerning samples treated with PHL, PMOT was lower than in the control at the 1000 µmol/L concentration at 30 min post-thaw, whereas at 240 min post-thaw this effect was observed at both 500 and 1000 µmol/L concentrations in GFE ($p < 0.05$). PMOT was not affected by any inhibitor in PFE ($p > 0.05$).

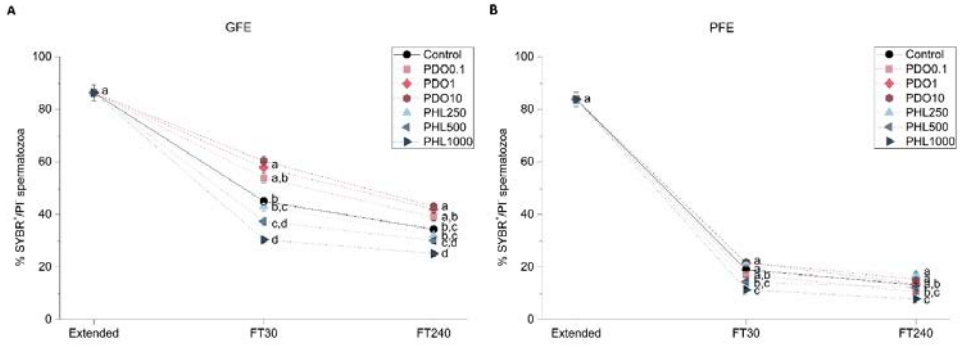

Figure 3. Percentages of SYBR14^{+}/PI^{-} spermatozoa in good freezability ejaculates (GFE; (**A**)) and poor freezability ejaculates (PFE; (**B**)) exposed to AQP inhibitors in the extender: 0.1 mmol/L, 1 mmol/L, and 10 mmol/L 1,3-propanediol (PHL) or 250 µmol/L, 500 µmol/L, and 1000 µmol/L phloretin (PHL); or not (control). Data were collected from fresh (extended) and frozen-thawed (FT) samples at 30 and 240 min post-thaw, and are shown as mean ± SEM. Different letters (a, b, c, d) indicate a significant difference ($p < 0.05$) between treatments within a given time point.

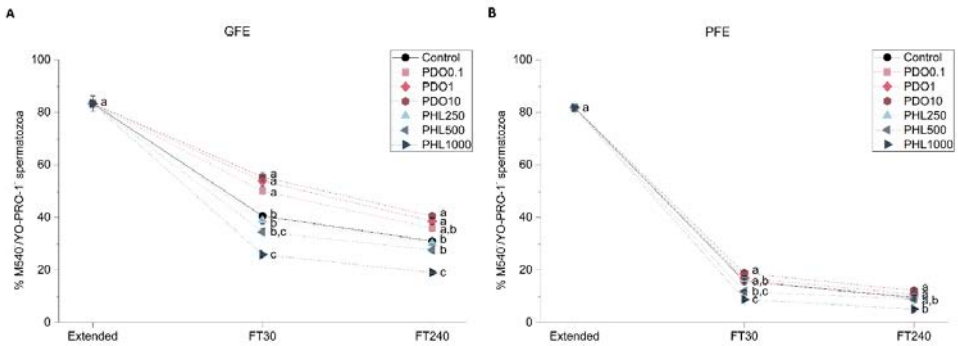

Figure 4. Percentages of viable spermatozoa with low membrane lipid disorder (M540^{-}/YO-PRO-1^{-}) in good freezability ejaculates (GFE; (**A**)) and poor freezability ejaculates (PFE; (**B**)) exposed to AQP inhibitors in the extender: 0.1 mmol/L, 1 mmol/L, and 10 mmol/L 1,3-propanediol (PHL) or 250 µmol/L, 500 µmol/L, and 1000 µmol/L phloretin (PHL); or not (control). Data were collected from fresh (extended) and frozen-thawed (FT) samples at 30 and 240 min post-thaw, and are shown as mean ± SEM. Different letters (a, b, c) indicate a significant difference ($p < 0.05$) between treatments within a given time point.

2.2.2. Sperm Viability

Sperm viability was assessed with the SYBR14/propidium iodide (PI) test in order to determine the effects of different concentrations of the inhibitors during cryopreservation (Figure 3). Sperm viability was higher in GFE treated with 1 mmol/L and 10 mmol/L PDO at both 30 and 240 min post-thaw ($p < 0.05$). However, PDO had no effect in sperm viability in PFE, as evidenced by a lack of differences between PDO-exposed sperm samples and the control ($p > 0.05$). Concerning the PHL treatments, sperm viability in both GFE and PFE was lower in the presence of both 500 and 1000 µmol/L PHL at 30 min post-thaw ($p < 0.05$). Nevertheless, at 240 min post-thaw, sperm viability was only lower than the control in the presence of the highest concentration of PHL ($p < 0.05$).

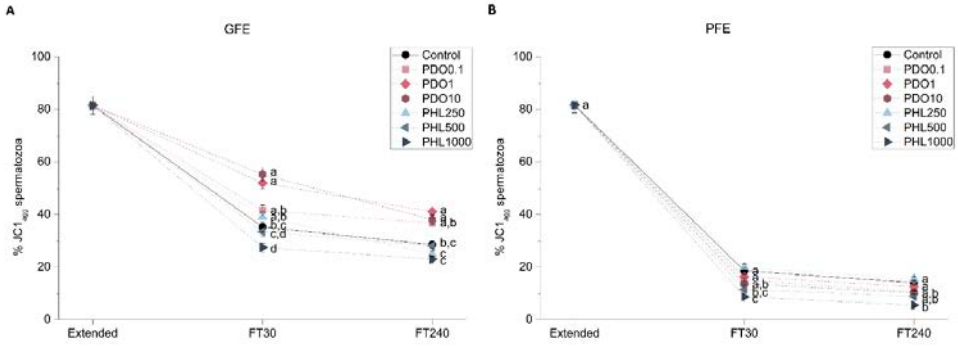

Figure 5. Percentages of spermatozoa with high mitochondrial membrane potential ($JC1_{agg}$) in good freezability ejaculates (GFE; (**A**)) and poor freezability ejaculates (PFE; (**B**)) exposed to AQP inhibitors in the extender: 0.1 mmol/L, 1 mmol/L, and 10 mmol/L 1,3-propanediol (PHL) or 250 µmol/L, 500 µmol/L, and 1000 µmol/L phloretin (PHL); or not (control). Data were collected from fresh (extended) and frozen-thawed (FT) samples at 30 and 240 min post-thaw, and are shown as mean ± SEM. Different letters (a, b, c, d) indicate a significant difference ($p < 0.05$) between treatments within a given time point.

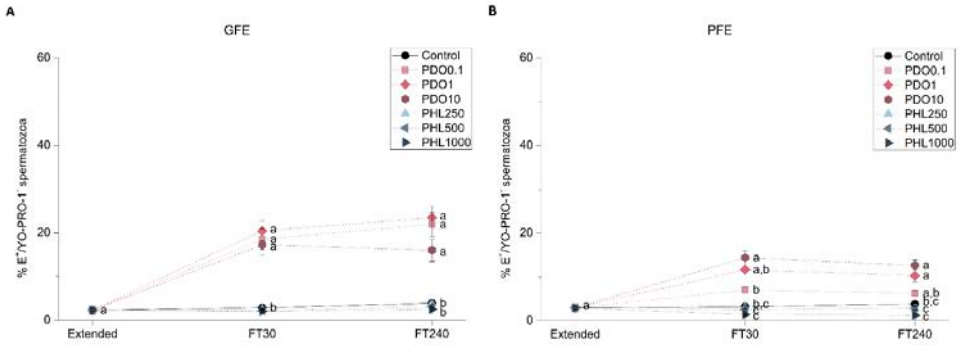

Figure 6. Percentages of viable spermatozoa with high levels of superoxides (E^+/YO-PRO-1^-) in good freezability ejaculates (GFE; (**A**)) and poor freezability ejaculates (PFE; (**B**)) exposed to AQP inhibitors in the extender: 0.1 mmol/L, 1 mmol/L, and 10 mmol/L 1,3-propanediol (PHL) or 250 µmol/L, 500 µmol/L, and 1000 µmol/L phloretin (PHL); or not (control). Data were collected from fresh (extended) and frozen-thawed (FT) samples at 30 and 240 min post-thaw, and are shown as mean ± SEM. Different letters (a, b, c) indicate a significant difference ($p < 0.05$) between treatments within a given time point.

2.2.3. Sperm Membrane Lipid Disorder

Sperm membrane lipid disorder was evaluated through the merocyanine 540 and YO-PRO-1 co-staining test (Figure 4). When PDO was added to GFE samples, there was an increase in the percentage of spermatozoa with low membrane lipid disorder at 30 min post-thaw ($p < 0.05$), whereas this effect did not persist at 240 min post-thaw in the 0.1 mmol/L group ($p > 0.05$). No effect was observed when PDO was added to PFE samples ($p > 0.05$). Addition of 1000 µmol/L PHL to GFE samples caused a decrease in the percentage of spermatozoa with low membrane lipid disorder at both 30 and 240 min post-thaw ($p < 0.05$). However, in PFE samples, this same PHL concentration caused a decrease at 30 min after-thaw ($p < 0.05$), which was not observed at 240 min post-thaw ($p > 0.05$).

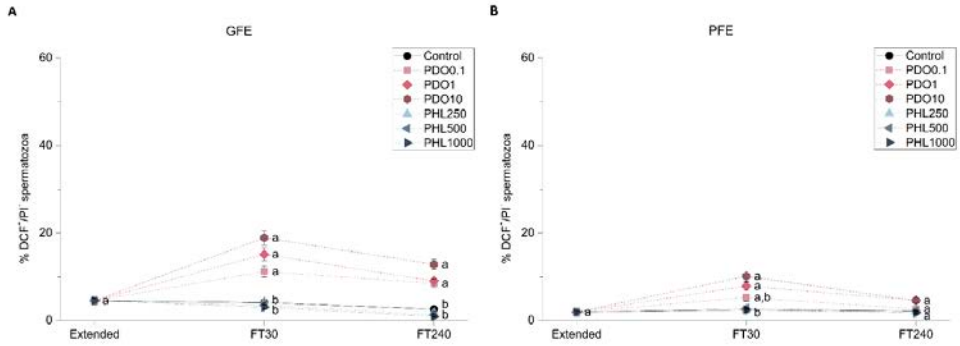

Figure 7. Percentages of viable spermatozoa with high levels of peroxides (DCF^+/PI^-) in good freezability ejaculates (GFE; (**A**)) and poor freezability ejaculates (PFE; (**B**)) exposed to AQP inhibitors in the extender: 0.1 mmol/L, 1 mmol/L, and 10 mmol/L 1,3-propanediol (PHL) or 250 µmol/L, 500 µmol/L, and 1000 µmol/L phloretin (PHL); or not (control). Data were collected from fresh (extended) and frozen-thawed (FT) samples at 30 and 240 min post-thaw, and are shown as mean ± SEM. Different letters (a, b) indicate a significant difference ($p < 0.05$) between treatments within a given time point.

2.2.4. Mitochondrial Membrane Potential (MMP)

Mitochondrial membrane potential (MMP) was evaluated through JC1-staining to determine the effects of AQP inhibition on GFE and PFE (Figure 5). The addition of PDO to GFE samples caused an increase in the percentage of spermatozoa with high MMP (spermatozoa with JC1 aggregates, $JC1_{agg}$) at the highest concentrations, at both 30 min and 240 min post-thaw ($p < 0.05$). Nevertheless, no effect was observed in PDO-treated PFE samples ($p > 0.05$). When PHL was added to GFE samples, MMP decreased in the presence of the highest concentration at 30 min post-thaw ($p < 0.05$), but this difference did not persist at 240 min post-thaw ($p > 0.05$). Concerning PFE samples, MMP decreased at 30 min post-thaw when PHL was added at final concentrations of 500 µmol/L and 1000 µmol/L ($p < 0.05$), and this effect only persisted at 240 min post-thaw in the presence of PDO at the highest concentration ($p < 0.05$).

2.2.5. Intracellular Levels of Superoxides ($O_2^-\bullet$)

Intracellular levels of superoxides were evaluated through a co-staining with hydroethidine and YO-PRO-1 in GFE and PFE samples in order to determine the effects of AQP inhibition on sperm function (Figure 6). Intracellular levels of superoxides increased post-thaw in the presence of PDO, regardless of its concentration in GFE ($p < 0.05$). Regarding PFE, the percentage of spermatozoa with high intracellular levels of $O_2^-\bullet$ increased in the presence of the highest concentration at 30 min post-thaw ($p < 0.05$), whereas at 240 min post-thaw this effect was observed in the presence of both 1 and 10 mmol/L PDO ($p < 0.05$). There were no differences between PHL-treated samples and the control in terms of $O_2^-\bullet$ levels in the PFE group ($p > 0.05$).

2.2.6. Intracellular Levels of Hydrogen Peroxides (H_2O_2)

Intracellular levels of hydrogen peroxides were assessed through co-staining with 2′,7′-dichlorodihydrofluorescein diacetate (H_2DCFDA) and PI fluorochromes in order to determine the effect of AQP inhibitors on this sperm functional parameter (Figure 7). When GFE samples were treated with PDO, intracellular levels of hydrogen peroxides were higher than in the control at both post-thaw time points ($p < 0.05$). In the PFE group, this effect was observed in the presence of both 1 and 10 mmol/L PDO at 30 min post-thaw ($p < 0.05$), whereas at 240 min post-thaw there were no differences between the control and any of the PDO treatments ($p > 0.05$). Regarding treatments with

PHL, no variations in the intracellular levels of hydrogen peroxides were observed at any time point or concentration, either in GFE or in PFE group ($p > 0.05$).

3. Discussion

Despite several studies conducted in the last decade to identify the presence of AQPs in sperm of different mammalian species (reviewed in [18]), neither their precise function nor their mechanism of action have been fully addressed. In this context, sperm cryotolerance has been correlated with relative levels of AQP3 and AQP7 (which are both GLPs) [25]. Moreover, there is recent evidence suggesting that GLPs have a more relevant role than orthodox AQPs in the cryotolerance of boar and stallion spermatozoa [26,27]. Thus, this study has used different AQP inhibitors to unveil the functional relevance of AQPs during cryopreservation, comparing ejaculates with good (GFE) and poor (PFE) freezability. To this end, two inhibitors were added to the extender at three different concentrations: PDO at 0.1, 1 and 10 mmol/L, and PHL at 250, 500, and 1000 µmol/L. Whereas PDO inhibits orthodox AQPs (AQP1, AQP2, AQP5, and AQP4) with high efficiency, it is less efficient as a GLPs inhibitor (the family to which AQP3, AQP7, and AQP9 belong) is lower [28,29]. PHL, on the other hand, inhibits both AQP3 and AQP7 [32–34]. The effects of each inhibitor on sperm function and survival during cryopreservation were evaluated in terms of sperm motility, viability, membrane lipid disorder, MMP, and intracellular levels of ROS (reactive oxygen species). With regard to PDO, its presence in GFE samples increased total and progressive motility and sperm viability, decreased membrane lipid disorder, and increased MMP and ROS levels. In PFE samples, however, only the increase in ROS levels was observed. On the other hand, when PHL was added to extender, a decrease in TMOT, PMOT, sperm viability, and in the percentage of spermatozoa with low membrane lipid disorder and with high MMP was observed. In PFE, the effect on sperm viability was less evident than in GFE, the effect on MMP was more drastic and, whereas TMOT and membrane lipid disorder were transitionally lower at 30 min post-thaw, this difference with regard to the control was less apparent than in GFE and did not persist at 240 min post-thaw.

Differences between the effects of each AQP inhibitor are potentially caused by their different affinity for GLPs and the collateral effects on other sperm structures and molecules. In this context, PHL is able to freely permeate the plasma membrane due to its hydrophobicity [35], and it binds to GLPs through an internal binding site [36]. Therefore, GLP inhibition through PHL decreases the permeability to both water and other small solutes, which suggests that the detrimental effects observed might be a consequence of the impairment in this transport. The fact that sperm quality and function are less affected in PFE than in GFE, either because there is no effect in PFE or because that effect is less dramatic in PFE than in GFE, is in agreement with the different levels of GLPs (AQP3 and AQP7) between these groups, which, as described by Prieto-Martinez et al. (2017), are higher in samples with better cryotolerance. Moreover, the transitional decrease in total motility and in membrane lipid disorder at 30 min post-thaw in PFE could be masked at 240 min post-thaw because of the poor quality of these samples. Finally, the higher impairment of MMP in PFE than in GFE does not have an apparent cause, but it could be a consequence of collateral effects of PHL on other sperm proteins, such as SLC2A2 (solute carrier family 2, also known as GLUT2) [37]. Since this protein is involved in the uptake of monosaccharides, which are the main source of energy for sperm [38], this could be the reason of the lower MMP observed in the presence of PHL. Considering all the aforementioned, it can be suggested that the detrimental effect of GLP inhibition by PHL depends on the intrinsic freezability of the ejaculate.

Regarding PDO, it remains inside the pore of orthodox AQPs, whereas the broader pore of GLPs allows its free permeability [29]. One could expect the effect of GLP inhibition through PDO on sperm quality and function to be similar to the effect of PHL treatments, but our group recently showed that the inhibition of GLPs through PDO does not seem to be as efficient as through PHL, and that PDO is a potential cryoprotective agent [26]. Moreover, we showed that the inhibition of orthodox AQPs during cryopreservation does not seem to have detrimental effects on sperm quality and function after

thaw and thus, the effects of PDO supplementation seems an exclusive consequence of the interactions with GLPs and of its cryoprotective effects on spermatozoa [26]. The present work evidenced that the effects of PDO treatments were more apparent in GFE than in PFE, as was also observed in the PHL treatments, and the consequences of PDO supplementation were consistent to the ones from previous works [26]. Concerning the GFE group, the addition of PDO seemed to better preserve the overall quality and function of sperm in terms of TMOT, PMOT, viability, and membrane lipid disorder, which might be a consequence of the expected cryoprotective effect. In this context, PDO has been used as a cryoprotective agent in cryopreservation protocols for canine ovarian cortices [39], and Widiasih et al. [40] demonstrated that PDO has milder detrimental effects on human sperm quality than glycerol. Moreover, even if the increase in MMP does not have an apparent cause, it is also a good sperm quality indicator and it might be the cause of the higher percentage of viable spermatozoa with high levels of ROS, since mitochondria are the main source of these molecules. Even if, to the best of our knowledge, the effects of PDO on oxidative stress have not been previously reported, AQP3 participates in H_2O_2 transport [41]. Therefore, PDO inhibition of H_2O_2-efflux might contribute to the increase in H_2O_2 intracellular concentration, which has a relevant role in mammalian sperm function [10]. In fact, ROS play a crucial role in the activation of the molecular pathways that are associated with sperm capacitation but, when generated in excess, oxidative stress can alter the maintenance of sperm function through both the induction of lipid peroxidation and DNA damage (reviewed in [42]). While the increase in ROS, which can be considered to have a negative effect on sperm quality, was more evident in GFE than in PFE, the positive effects on sperm quality and function were only detected in the GFE group. Therefore, it seems that both positive and negative effects of PDO rely upon the intrinsic ejaculate freezability.

4. Materials and Methods

4.1. Boars and Ejaculates

In this study, 42 ejaculates from separate Piétrain boars (n = 27) were used. Boars (aged between 15 and 24 months old) were housed with controlled climatic conditions and were fed a standard diet in a local farm (Semen Cardona, Cardona, Barcelona, Spain). Manual collection of sperm-rich fractions was performed twice a week with an interval of three days between collections. Samples were subsequently diluted 1:1 (v/v) in a commercial semen extender (Vitasem LD; Magapor S.L., Zaragoza, Spain), and then packaged in bags and stored at 17 °C. Within 5 h post-extraction, samples were transported to the laboratory. Ejaculates were then pooled in pairs (n = 21) and were subsequently divided into two different fractions. The first fraction was used to assess sperm quality parameters in fresh samples. The second one was divided into seven different sub-fractions, one of which was the control and the remaining six were treated with three different concentrations of two AQP inhibitors and subsequently cryopreserved. Sperm quality evaluation was also performed in cryopreserved samples after thawing.

4.2. AQP Inhibitors

Two AQP inhibitors, 1,3-propanediol (PDO, Sigma-Aldrich, St. Louis, MO, USA) and phloretin, (PHL, Sigma-Aldrich) were added to the freezing medium before sample cryopreservation. For each inhibitor, a stock solution was prepared; whereas PDO was diluted at 100 mmol/L in cryopreservation medium (LEYGO medium, composition detailed in the following section), PHL was diluted at 365 mmol/L in methanol (Fisher Chemical, ThermoFisher Scientific; Waltham, MA, USA). Samples were supplemented with three different concentrations of each inhibitor: 0.1, 1, and 10 mmol/L of PDO; and 250, 500, and 1000 µmol/L of PHL. Preliminary experiments were conducted to determine the minimum concentration of each inhibitor at which an effect was observed, and the maximum concentration at which cytotoxic effects appeared.

Concerning PHL-treated samples, concentrations of methanol to which spermatozoa were exposed were lower than 0.5% (v/v). We confirmed that, at these concentrations, sperm quality parameters evaluated were not altered (data not shown).

4.3. Boar Sperm Cryopreservation

Samples were cryopreserved to determine the effects of AQP inhibition on the cryotolerance of ejaculates. Fifty-mL aliquots of the fraction of each ejaculate pool that was intended for cryopreservation were centrifuged at 2400× *g* for 3 min at 15 °C. After discarding supernatants, β-lactose-egg yolk freezing medium (LEY), which consisted of 80% (v/v) lactose (Sigma-Aldrich) and 20% (v/v) egg yolk, was used to resuspend pellets at a final concentration of 1.5×10^9 spermatozoa/mL. Sample cooling was performed in a programmable, controlled-rate freezer (Icecube14S-B; Minitüb Ibérica SL; Tarragona, Spain), with a cooling rate of −0.1 °C/min (180 min) and a final temperature of 5 °C. At this point, LEYGO medium, consisting of LEY medium supplemented with 6% (v/v) glycerol (Sigma-Aldrich) and 1.5% Orvus ES Paste (Equex STM; Nova Chemical Sales Inc., Scituate, MA, USA), was used to dilute samples to a final concentration of 1×10^9 spermatozoa/mL. Seven sub-fractions were subsequently obtained from this fraction: a non-treated control and one for each concentration and inhibitor. Sample packaging was carried out in 0.5 mL plastic straws (Minitüb Ibérica, S.L.); filled straws were placed in a programmable, controlled-rate freezer and exposed to the following cooling rates [20]: −6 °C/min from 5 to −5 °C (100 s); −39.82 °C/min from −5 to −80 °C (113 s); hold at −80 °C for 30 s; and cooled at −60 °C/min from −80 to −150 °C (70 s). Samples were then plunged and stored in liquid nitrogen (−196 °C).

Sample thawing was performed in order to evaluate sperm quality parameters in cryopreserved samples. Two straws per treatment from each pool were immersed in a water bath at 38 °C for 15 s and subsequently diluted 1:3 (v/v) in pre-warmed (38 °C) Beltsville Thawing Solution (BTS) [27]. Sperm samples were then incubated at 38 °C for 240 min, and sperm quality was evaluated at two different time points: 30 min and 240 min. These time points are consistent with the protocols from Vilagran et al. [24] and Prieto-Martínez et al. [25] for the evaluation of sperm function and survival in cryopreserved boar semen. The evaluation at 30 min post-thaw allows the stabilization of spermatozoa after both thermal and osmotic stresses that occur upon thawing, but it is also at this time point that the short-term detrimental effects of cryopreservation are evident. Regarding the analysis at 240 min post-thaw, it was set to assess the quality and function of frozen-thawed spermatozoa within the insemination-to-ovulation interval recommended for cryopreserved doses [43]. In addition, this time period is coincident with the time that boar spermatozoa need to capacitate, and therefore, it corresponds to the time at which capacitation-like changes are apparent [44]. Therefore, the evaluation of sperm function and survival at 240 min post-thaw is performed in order to ensure that the insemination-to-ovulation interval recommended for cryopreserved boar semen is covered, and to assess capacitation-like changes, which correspond to the long-term detrimental effects of cryopreservation.

4.4. Sperm Motility

Sperm motility evaluation was performed with a computer-assisted sperm analysis (CASA) system, consisting of a negative phase-contrast microscope (Olympus BX41; Olympus, Tokyo, Japan), a video camera and ISAS software (Integrated Sperm Analysis System V1.0; Proiser SL, Valencia, Spain), in both fresh (extended) and frozen-thawed samples. Before sperm motility assessment, extended samples required 15 min of incubation at 38 °C, whereas frozen-thawed samples were directly examined after their respective incubation times at 38 °C: 30 min or 240 min. Once incubated, 5 µL of each sample was examined in a pre-warmed (38 °C) Makler counting chamber (Sefi-Medical Instruments, Haifa, Israel), under a negative phase-contrast field (Olympus 10× 0.30 PLAN objective; Olympus). Three replicates of at least 1000 spermatozoa were examined for each treatment.

The following parameters were recorded in each motility assessment: TMOT (%) and PMOT (%); curvilinear velocity (VCL, µm/s); straight line velocity (VSL, µm/s); average path velocity (VAP, µm/s);

amplitude of lateral head displacement (ALH, μm); beat cross frequency (BCF, Hz); linearity (LIN, %), which was calculated as LIN = VSL/VCL×100; straightness (STR, %), resulting from VSL/VAP×100; and motility parameter wobble (WOB, %), obtained from VAP/VCL×100 [45]. Spermatozoa considered as motile were those presenting a VAP value equal to or higher than 10 μm/s; progressively motile spermatozoa presented an STR value equal to or higher than 45% [46]. The corresponding mean ± standard error of the mean (SEM) was calculated for each parameter.

4.5. Flow Cytometry

Flow cytometry was used to evaluate five different sperm quality and functionality parameters in both fresh and frozen-thawed samples: sperm viability, membrane lipid disorder, MMP, intracellular levels of superoxides and intracellular levels of peroxides. All fluorochromes were purchased from ThermoFisher Scientific (Waltham, MA, USA). Prior to the addition of the corresponding fluorochromes, samples were diluted to a final concentration of 1×10^6 spermatozoa/mL. Once stained, samples were incubated at 38 °C. A total of three replicates per sample were assessed for each parameter.

Samples were analyzed in a Cell Lab Quanta^{TM} SC cytometer (Beckman Coulter; Fullerton, CA, USA). Samples were excited at a power of 22 mW through an argon ion laser (488 nm). The Coulter principle, which measures changes of electrical resistance in an electrolyte solution by suspended, non-conductive particles, allowed cell diameter/volume assessment. In this system, forward scatter (FS) is replaced by electronic volume (EV). For EV-channel calibration, 10-μm Flow-Check fluorospheres (Beckman Coulter) were positioned at channel 200 on the EV-scale.

Three optical filters were used for fluorescence detection: FL1 (Dichroic/Splitter, DRLP: 550 nm, BP filter: 525 nm, detection width: 505–545 nm), FL2 (DRLP: 600 nm, BP filter: 575 nm, detection width: 560–590 nm), and FL3 (LP filter: 670 nm/730 nm, detection width: 655–685 nm). FL1 detected green fluorescence from SYBR14, YO-PRO-1, JC-1 monomers (JC-1_{mon}), and 2′,7′-dichlorofluorescein (DCF^+); FL2 detected orange fluorescence from JC-1 aggregates (JC-1_{agg}); and FL3 was used to detect red fluorescence from PI, M540, and ethidium (E^+). The signal was logarithmically amplified, and particular staining methods were considered for photomultiplier setting.

EV and side scatter (SS) were measured and linearly recorded for all particles, and the sheath flow rate was set at 4.17 μL/min. On the EV channel, the analyzer threshold was adjusted to exclude subcellular debris (particle diameter <7 μm) and cell aggregates (particle diameter >12 μm). Therefore, on the basis of EV/SS distributions, the sperm-specific events were positively gated. A minimum of 10,000 events were evaluated per replicate, and three replicates were analyzed per sample.

Flowing Software (Ver. 2.5.1; University of Turku, Finland) was used for data analysis, according to the recommendations of the International Society for Advancement of Cytometry (ISAC). Following Petrunkina et al. [47], the percentage of non-sperm debris particles of the $SYBR14^-/PI^-$ population was used to correct the events corresponding to double-negative particles of all protocols. For each parameter, the corresponding mean ± SEM was calculated.

4.5.1. Sperm Viability

Sperm viability was evaluated through the LIVE/DEAD sperm viability kit (Molecular Probes, Eugene, OR, USA) following the protocol of Garner and Johnson [48]. Briefly, sperm were incubated with a final concentration of 100 nmol/L SYBR14 for 10 min, and with PI at a final concentration of 12 μmol/L for 5 min. Flow cytometry dot-plots showed three different sperm populations: (1) viable, green-stained spermatozoa ($SYBR14^+/PI^-$); (2) non-viable, red-stained spermatozoa ($SYBR14^-/PI^+$); (3) non-viable spermatozoa stained in both green and red ($SYBR14^+/PI^+$). The unstained, non-sperm particles ($SYBR14^-/PI^-$) were not included for the calculation of the final percentages of the three aforementioned populations. SYBR14 fluorescence spill over into FL3 channel was compensated (2.45%).

4.5.2. Sperm Membrane Lipid Disorder

Samples were co-stained with M540 and YO-PRO-1 to evaluate sperm membrane lipid disorder, according to the protocol from Rathi et al. [49] with minor modifications [50]. Decreases in packing order of phospholipids from the outer monolayer of the plasma membrane are detected by M540, which is the basis of this protocol. M540 was added to samples at a final concentration of 2.6 µmol/L, and YO-PRO-1 at a final concentration of 25 nmol/L, prior to 10 min of incubation. Four different populations were identified in flow cytometry dot plots: (1) viable spermatozoa presenting low membrane lipid disorder ($M540^-$/YO-PRO-1^-); (2) viable spermatozoa presenting high membrane lipid disorder ($M540^+$/YO-PRO-1^-); (3) non-viable spermatozoa presenting low membrane lipid disorder ($M540^-$/YO-PRO-1^+); and (4) non-viable spermatozoa presenting high membrane lipid disorder ($M540^+$/YO-PRO-1^+). The percentage of $SYBR14^-/PI^-$ particles corresponding to non-sperm debris particles was used to correct the percentages of viable spermatozoa presenting low membrane lipid disorder ($M540^-$/YO-PRO-1^-), the percentages of the other populations were recalculated. Data were not compensated.

4.5.3. Mitochondrial Membrane Potential (MMP)

Samples were stained with JC1 following the protocol of Ortega-Ferrusola et al. [51] with minor modifications in order to evaluate MMP. JC1 molecules (5,5′,6,6′-tetrachloro-1,1′,3,3′tetraethyl-benzimidazolylcarbocyanine iodide) remain as monomers ($JC1_{mon}$) in the presence of low MMP, whereas, in the presence of high MMP, they form aggregates ($JC1_{agg}$). Briefly, samples were incubated with JC1 at a final concentration of 0.3 µmol/L for 30 min. Three different populations were observed in flow cytometry dot-plots: (1) low MMP-spermatozoa ($JC1_{mon}$; $FL1^+/FL2^-$); (2) high MMP-spermatozoa ($JC1_{agg}$; $FL1^-/FL2^+$); and (3) spermatozoa with heterogeneous mitochondria in the same cell ($JC1_{agg}$ and $JC1_{mon}$; $FL1^+/FL2^+$). The percentage of $SYBR14^-/PI^-$ particles was used to correct the percentages of double-negative particles ($FL1^-/FL2^-$), and the percentages of the other three populations were recalculated. The sum of populations (2) and (3) corresponded to high MMP-spermatozoa. FL1 spill-over into the FL2 channel was compensated (51.70%).

4.5.4. Intracellular Levels of Superoxides ($O_2^-\bullet$)

Samples were co-stained with HE and YO-PRO-1 in order to evaluate the levels of intracellular superoxides ($O_2^-\bullet$), following the protocol from Guthrie & Welch [52]. HE is oxidized at an intracellular level by $O_2^-\bullet$ radicals to E^+ and other products. In brief, samples were incubated with HE at a final concentration of 4 µmol/L and YO-PRO-1 at a final concentration of 40 nmol/L for 20 min. Flow cytometry dot-plots allowed the identification of four different sperm populations: (1) viable spermatozoa with low $O_2^-\bullet$levels (E^-/YO-PRO-1^-); (2) viable spermatozoa with high $O_2^-\bullet$levels (E^+/YO-PRO-1^-); (3) non-viable spermatozoa with low $O_2^-\bullet$ levels (E^-/YO-PRO-1^+); and (4) non-viable spermatozoa with high $O_2^-\bullet$ levels (E^+/YO-PRO-1^+). The proportions of non-sperm debris particles ($SYBR14^-/PI^-$ particles) were used to correct the percentages of viable spermatozoa with low $O_2^-\bullet$levels (E^-/YO-PRO-1^-). YO-PRO-1 spill over into the FL3-channel was compensated (5.06%).

4.5.5. Intracellular Levels of Hydrogen Peroxide (H_2O_2)

Spermatozoa were co-stained with H_2DCFDA and PI following the protocol set by Guthrie & Welch [52] with minor modifications to assess intracellular levels of hydrogen peroxide (H_2O_2). The non-fluorescent probe H_2DCFDA is de-esterified and oxidized at an intracellular level into highly fluorescent DCF^+. Briefly, samples were incubated with H_2DCFDA at a final concentration of 200 µmol/L and PI at a final concentration of 12 µmol/L for 30 min. Four different sperm populations were identified in flow cytometry dot-plots: (1) viable spermatozoa with low levels of peroxides (DCF^-/PI^-); (2) viable spermatozoa with high levels of peroxides (DCF^+/PI^-); (3) non-viable spermatozoa with

low levels of peroxides (DCF^-/PI^+); and (4) non-viable spermatozoa with high levels of peroxides (DCF^+/PI^+). The proportions of non-sperm debris particles from the $SYBR14^-/PI^-$ quadrant were used to correct the percentages of live spermatozoa with low levels of peroxides (DCF^-/PI^-); the percentages of the other populations were recalculated. DCF-spill over into FL3-channel was compensated (2.45%).

4.6. Statistical Analyses

A statistical package (IBM SPSS Statistics 25.0; Armonk, New York, USA) was used to analyze the results obtained in this work. Shapiro–Wilk and Levene tests were run to assess the distribution of data and homogeneity of variances, respectively. Thereafter, ejaculate pools were classified as good (GFE) or poor (PFE) freezability based on their total and progressive sperm motilities, and sperm viability (% $SYBR14^+/PI^-$ spermatozoa) at 30 min post-thaw through a two-step hierarchical cluster analysis using the log-likelihood distance and the Bayesian–Schwarz criterion. For each sperm parameter, a mixed model was subsequently run. The cryopreservation step was the intra-subjects factor (i.e., fresh, frozen-thawed at 30 min, frozen-thawed at 240 min), the treatment at a given concentration (C, PDO, or PHL) and the ejaculate group (GFE or PFE) were the fixed-effects factors (inter-subject), and the ejaculate pool was the random-effects factor. Pair-wise comparisons were tested through a post-hoc Sidak test, and the level of significance was set at $p \leq 0.05$. Data are shown as mean ± standard error of the mean (SEM).

5. Conclusions

In conclusion, the inhibition of AQPs through two different inhibitors has more detrimental effects on ejaculates with good cryotolerance than in those with poor cryotolerance. Moreover, the improvement of post-thaw sperm quality and functionality with PDO as a supplementary CPA is exclusively evident in GFE.

Author Contributions: Conceptualization, A.D.-B. and M.Y.; Investigation, A.D.-B. and M.L.; Formal analysis, A.D.-B. and M.Y.; Writing—original draft preparation, A.D.-B.; Writing—review and editing, S.B., I.B., B.F.-F. and M.Y.; Visualization, S.R. and Y.M.-O.; Supervision, M.Y.

Funding: The authors acknowledge the support from the European Commission (H2020-MSCA-IF-79212), the Ministry of Science, Innovation and Universities, Spain (grant nos. RYC-2014-15581, AGL2017-88329-R, FJCI-2017-31689, and PRE2018-083488), and the Regional Government of Catalonia, Spain (2017-SGR-1229).

Acknowledgments: The authors acknowledge the technical support received from Estela Garcia (University of Girona, Spain).

Conflicts of Interest: The authors declare no conflict of interest.

Abbreviations

AQP	Aquaporin
ALH	Amplitude of lateral head displacement
BCF	Beat cross frequency
BTS	Beltsville Thawing Solution
CASA	Computer-assisted sperm analysis
CPA	Cryoprotective agent
DCF^+	2′,7′-dichlorofluorescein
E^+	Ethidium
EV	Electronic volume
FS	Forward scatter
GFE	Good freezability ejaculates
GLP	Aquaglyceroporins
H_2DCFDA	2′,7′-dichlorodihydrofluorescein diacetate
H_2O_2	Hydrogen peroxide
HE	Hydroethidine
ISAC	International Society for Advancement of Cytometry

JC-1	5,5′,6,6′-tetrachloro-1,1′,3,3′tetraethyl-benzimidazolylcarbocyanine iodide
$JC\text{-}1_{agg}$	JC-1 aggregates
$JC\text{-}1_{mon}$	JC-1 monomers
LEY	β-Lactose–egg yolk–glycerol
LEYGO	β-Lactose–egg yolk–glycerol–Orvus ES Paste
LIN	Linearity
M540	Merocyanine 540
MMP	Mitochondrial membrane potential
$O_2^{-}\bullet$	Superoxide
PDO	1,3-propanediol
PfAQP	Plasmodium falciparum aquaporin
PFE	Poor freezability ejaculates
PHL	Phloretin
PI	Propidium iodide
PMOT	Progressive motility
ROS	Reactive oxygen species
SEM	Standard error of the mean
SLC2A2	Solute carrier family 2, facilitated glucose transporter member 2
SS	Side scatter
STR	Straightness
TMOT	Total motility
VAP	Average path velocity
VCL	Curvilinear velocity
VSL	Straight line velocity
WOB	Motility parameter wobble
PMOT	Progressive motility
ROS	Reactive oxygen species
SEM	Standard error of the mean
SLC2A2	Solute carrier family 2, facilitated glucose transporter member 2
SS	Side scatter
STR	Straightness

References

1. Watson, H. Biological membranes. *Essays Biochem.* **2015**, *59*, 43–70. [CrossRef]
2. Yeste, M.; Morató, R.; Rodríguez-Gil, J.E.; Bonet, S.; Prieto-Martínez, N. Aquaporins in the male reproductive tract and sperm: Functional implications and cryobiology. *Reprod. Domest. Anim.* **2017**, *52*, 12–27. [CrossRef] [PubMed]
3. Prieto-Martínez, N.; Vilagran, I.; Morató, R.; Rodríguez-Gil, J.E.; Yeste, M.; Bonet, S. Aquaporins 7 and 11 in boar spermatozoa: Detection, localisation and relationship with sperm quality. *Reprod. Fertil. Dev.* **2014**, *28*, 663–672. [CrossRef] [PubMed]
4. Prieto-Martínez, N.; Morató, R.; Vilagran, I.; Rodríguez-Gil, J.E.; Bonet, S.; Yeste, M. Aquaporins in boar spermatozoa. Part II: Detection and localisation of aquaglyceroporin 3. *Reprod. Fertil. Dev.* **2015**, *29*, 703–711. [CrossRef] [PubMed]
5. Bonilla-Correal, S.; Noto, F.; Garcia-Bonavila, E.; Rodríguez-Gil, J.E.; Yeste, M.; Miró, J. First evidence for the presence of aquaporins in stallion sperm. *Reprod. Domest. Anim.* **2017**, *52*, 61–64. [CrossRef]
6. Chen, Q.; Peng, H.; Lei, L.; Zhang, Y.; Kuang, H.; Cao, Y.; Shi, Q.; Ma, T.; Duan, E. Aquaporin 3 is a sperm water channel essential for postcopulatory sperm osmoadaptation and migration. *Cell Res.* **2011**, *21*, 922–933. [CrossRef]
7. Yeung, C.H.; Callies, C.; Rojek, A.; Nielsen, S.; Cooper, T.G. Aquaporin Isoforms Involved in Physiological Volume Regulation of Murine Spermatozoa. *Biol. Reprod.* **2009**, *80*, 350–357. [CrossRef]
8. Yeung, C.H.; Cooper, T.G. Aquaporin AQP11 in the testis: Molecular identity and association with the processing of residual cytoplasm of elongated spermatids. *Reproduction* **2010**, *139*, 209–216. [CrossRef]

9. Yeung, C.H.; Callies, C.; Tüttelmann, F.; Kliesch, S.; Cooper, T.G. Aquaporins in the human testis and spermatozoa - identification, involvement in sperm volume regulation and clinical relevance. *Int. J. Androl.* **2010**, *33*, 629–641. [CrossRef]
10. Laforenza, U.; Pellavio, G.; Marchetti, A.; Omes, C.; Todaro, F.; Gastaldi, G. Aquaporin-Mediated Water and Hydrogen Peroxide Transport Is Involved in Normal Human Spermatozoa Functioning. *Int. J. Mol. Sci.* **2017**, *18*, 66. [CrossRef]
11. Prieto-Martínez, N.; Morató, R.; Muiño, R.; Hidalgo, C.O.; Rodríguez-Gil, J.E.; Bonet, S.; Yeste, M. Aquaglyceroporins 3 and 7 in bull spermatozoa: Identification, localisation and their relationship with sperm cryotolerance. *Reprod. Fertil. Dev.* **2016**, *29*, 1249–1259. [CrossRef] [PubMed]
12. Morató, R.; Prieto-Martínez, N.; Muiño, R.; Hidalgo, C.O.; Rodríguez-Gil, J.E.; Bonet, S.; Yeste, M. Aquaporin 11 is related to cryotolerance and fertilising ability of frozen–thawed bull spermatozoa. *Reprod. Fertil. Dev.* **2018**, *30*, 1099–1108. [CrossRef] [PubMed]
13. Vicente-Carrillo, A.; Ekwall, H.; Alvarez-Rodriguez, M.; Rodriguez-Martinez, H. Membrane Stress During Thawing Elicits Redistribution of Aquaporin 7 But Not of Aquaporin 9 in Boar Spermatozoa. *Reprod. Domest. Anim.* **2016**, *51*, 665–679. [CrossRef] [PubMed]
14. Huang, H.F.; He, R.H.; Sun, C.C.; Zhang, Y.; Meng, Q.X.; Ma, Y.Y. Function of aquaporins in female and male reproductive systems. *Hum. Reprod. Update* **2006**, *12*, 785–795. [CrossRef]
15. Bonet, S.; Casas, I.; Holt, W.V. *Boar Reproduction: Fundamentals and New Biotechnological Trends*, 1st ed.; Springer: London, UK, 2013; ISBN 9783642350481.
16. Yeste, M. Sperm cryopreservation update: Cryodamage, markers, and factors affecting the sperm freezability in pigs. *Theriogenology* **2016**, *85*, 47–64. [CrossRef]
17. Yeste, M.; Rodríguez-Gil, J.E.; Bonet, S. Artificial insemination with frozen-thawed boar sperm. *Mol. Reprod. Dev.* **2017**, *84*, 802–813. [CrossRef]
18. Yeste, M. Recent advances in boar sperm cryopreservation: State of the art and current perspectives. *Reprod. Domest. Anim.* **2015**, *50*, 71–79. [CrossRef]
19. Kuisma, P.; Andersson, M.; Koskinen, E.; Katila, T. Fertility of frozen-thawed stallion semen cannot be predicted by the currently used laboratory methods. *Acta Vet. Scand.* **2006**, *48*, 14. [CrossRef]
20. Peña, F.J.; Macías García, B.; Samper, J.C.; Aparicio, I.M.; Tapia, J.A.; Ortega Ferrusola, C. Dissecting the molecular damage to stallion spermatozoa: The way to improve current cryopreservation protocols? *Theriogenology* **2011**, *76*, 1177–1186. [CrossRef]
21. Casas, I.; Sancho, S.; Briz, M.; Pinart, E.; Bussalleu, E.; Yeste, M.; Bonet, S. Freezability prediction of boar ejaculates assessed by functional sperm parameters and sperm proteins. *Theriogenology* **2009**, *72*, 930–948. [CrossRef]
22. Yeste, M.; Estrada, E.; Casas, I.; Bonet, S.; Rodríguez-Gil, J.E. Good and bad freezability boar ejaculates differ in the integrity of nucleoprotein structure after freeze-thawing but not in ROS levels. *Theriogenology* **2013**, *79*, 929–939. [CrossRef]
23. Yeste, M.; Estrada, E.; Pinart, E.; Bonet, S.; Miró, J.; Rodríguez-Gil, J.E. The improving effect of reduced glutathione on boar sperm cryotolerance is related with the intrinsic ejaculate freezability. *Cryobiology* **2014**, *68*, 251–261. [CrossRef] [PubMed]
24. Vilagran, I.; Yeste, M.; Sancho, S.; Casas, I.; Rivera del Álamo, M.M.; Bonet, S. Relationship of sperm small heat-shock protein 10 and voltage-dependent anion channel 2 with semen freezability in boars. *Theriogenology* **2014**, *82*, 418–426. [CrossRef]
25. Prieto-Martínez, N.; Vilagran, I.; Morató, R.; Rivera del Álamo, M.M.; Rodríguez-Gil, J.E.; Bonet, S.; Yeste, M. Relationship of aquaporins 3 (AQP3), 7 (AQP7), and 11 (AQP11) with boar sperm resilience to withstand freeze-thawing procedures. *Andrology* **2017**, *5*, 1153–1164. [CrossRef]
26. Delgado-Bermúdez, A.; Llavanera, M.; Fernández-Bastit, L.; Recuero, S.; Mateo, Y.; Bonet, S.; Barranco, I.; Fernández-Fuertes, B.; Yeste, M. Aquaglyceroporins but not orthodox aquaporins are involved in the cryotolerance of pig spermatozoa. *J. Anim. Sci. Biotechnol.* **2019**, in press.
27. Delgado-Bermúdez, A.; Noto, F.; Bonilla-Correal, S.; Garcia-Bonavila, E.; Catalán, J.; Papas, M.; Bonet, S.; Miró, J.; Yeste, M. Cryotolerance of stallion spermatozoa relies on GLPs rather than orthodox AQPs. *Biology (Basel)* **2019**, *8*, 85.

28. Yu, L.; Rodriguez, R.A.; Chen, L.L.; Chen, L.Y.; Perry, G.; McHardy, S.F.; Yeh, C.K. 1,3-Propanediol Binds Deep Inside the Channel To Inhibit Water Permeation Through Aquaporins. *Protein Sci.* **2016**, *25*, 433–441. [CrossRef]
29. Yu, L.; Villarreal, O.D.; Chen, L.L.; Chen, L.Y. 1,3-Propanediol binds inside the water-conducting pore of aquaporin 4: Does this efficacious inhibitor have sufficient potency? *J. Syst. Integr. Neurosci.* **2016**, *2*, 91–98. [CrossRef]
30. Tsukaguchi, H.; Shayakul, C.; Berger, U.V.; Mackenzie, B.; Devidas, S.; Guggino, W.B.; van Hoek, A.N.; Hediger, M.A. Molecular Characterization of a Broad Selectivity Neutral Solute Channel. *J. Biol. Chem.* **1998**, *273*, 24737–24743. [CrossRef]
31. Cheung, K.H.; Leung, C.T.; Leung, G.P.H.; Wong, P.Y.D. Synergistic Effects of Cystic Fibrosis Transmembrane Conductance Regulator and Aquaporin-9 in the Rat Epididymis. *Biol. Reprod.* **2003**, *68*, 1505–1510. [CrossRef]
32. Rezk, B.M.; Haenen, G.R.M.M.; van der Vijgh, W.J.F.; Bast, A. The antioxidant activity of phloretin: The disclosure of a new antioxidant pharmacophore in flavonoids. *Biochem. Biophys. Res. Commun.* **2002**, *295*, 9–13. [CrossRef]
33. Barreca, D.; Currò, M.; Bellocco, E.; Ficarra, S.; Laganà, G.; Tellone, E.; Giunta, M.L.; Visalli, G.; Caccamo, D.; Galtieri, A.; et al. Neuroprotective effects of phloretin and its glycosylated derivative on rotenone-induced toxicity in human SH-SY5Y neuronal-like cells. *BioFactors* **2017**, *43*, 549–557. [CrossRef] [PubMed]
34. Przybylo, M.; Procek, J.; Hof, M.; Langner, M. The alteration of lipid bilayer dynamics by phloretin and 6-ketocholestanol. *Chem. Phys. Lipids* **2014**, *178*, 38–44. [CrossRef] [PubMed]
35. Pohl, P.; Rokitskaya, T.I.; Pohl, E.E.; Saparov, S.M. Permeation of phloretin across bilayer lipid membranes monitored by dipole potential and microelectrode measurements. *Biochim. Biophys. Acta-Biomembr.* **1997**, *1323*, 163–172. [CrossRef]
36. Wacker, S.J.; Aponte-Santamaría, C.; Kjellbom, P.; Nielsen, S.; De Groot, B.L.; Rützler, M. The identification of novel, high affinity AQP9 inhibitors in an intracellular binding site. *Mol. Membr. Biol.* **2013**, *30*, 246–260. [CrossRef]
37. Fan, H.; Morishima, S.; Kida, H.; Okada, Y. Phloretin differentially inhibits volume-sensitive and cyclic AMP-activated, but not Ca-activated, Cl- channels. *Br. J. Pharmacol.* **2001**, *133*, 1096–1106. [CrossRef]
38. Bucci, D.; Isani, G.; Spinaci, M.; Tamanini, C.; Mari, G.; Zambelli, D.; Galeati, G. Comparative Immunolocalization of GLUTs 1, 2, 3 and 5 in Boar, Stallion and Dog Spermatozoa. *Reprod. Domest. Anim.* **2010**, *45*, 315–322. [CrossRef]
39. Lopes, C.A.; Alves, A.M.; Jewgenow, K.; Báo, S.N.; de Figueiredo, J.R. Cryopreservation of canine ovarian cortex using DMSO or 1,3-propanediol. *Theriogenology* **2016**, *86*, 1165–1174. [CrossRef]
40. Widiasih, D.; Yeung, C.H.; Junaidi, A.; Cooper, T.G. Multistep and single-step treatment of human spermatozoa with cryoprotectants. *Fertil. Steril.* **2009**, *92*, 382–389. [CrossRef]
41. Miller, E.W.; Dickinson, B.C.; Chang, C.J. Aquaporin-3 mediates hydrogen peroxide uptake to regulate downstream intracellular signaling. *Proc. Natl. Acad. Sci.* **2010**, *107*, 15681–15686. [CrossRef]
42. Aitken, R.J. Reactive oxygen species as mediators of sperm capacitation and pathological damage. *Mol. Reprod. Dev.* **2017**, *84*, 1039–1052. [CrossRef] [PubMed]
43. Casas, I.; Sancho, S.; Briz, M.; Pinart, E.; Bussalleu, E.; Yeste, M.; Bonet, S. Fertility after post-cervical artificial insemination with cryopreserved sperm from boar ejaculates of good and poor freezability. *Anim. Reprod. Sci.* **2010**, *118*, 69–76. [CrossRef] [PubMed]
44. Ramió, L.; Rivera, M.M.; Ramírez, A.; Concha, I.I.; Peña, A.; Rigau, T.; Rodríguez-Gil, J.E. Dynamics of motile-sperm subpopulation structure in boar ejaculates subjected to "in vitro" capacitation and further "in vitro" acrosome reaction. *Theriogenology* **2008**, *69*, 501–512. [CrossRef] [PubMed]
45. Verstegen, J.; Iguer-Ouada, M.; Onclin, K. Computer assisted semen analyzers in andrology research and veterinary practice. *Theriogenology* **2002**, *57*, 149–179. [CrossRef]
46. Maes, D.G.D.; Mateusen, B.; Rijsselaere, T.; de Vliegher, S.; van Soom, A.; de Kruif, A. Motility characteristics of boar spermatozoa after addition of prostaglandin F2a. *Theriogenology* **2003**, *60*, 1435–1443. [CrossRef]
47. Petrunkina, A.M.; Waberski, D.; Bollwein, H.; Sieme, H. Identifying non-sperm particles during flow cytometric physiological assessment: A simple approach. *Theriogenology* **2010**, *73*, 995–1000. [CrossRef]
48. Garner, D.L.; Johnson, L.A. Viability assessment of mammalian sperm using SYBR-14 and propidium iodide. *Biol. Reprod.* **1995**, *53*, 276–284. [CrossRef]

49. Rathi, R.; Colenbrander, B.; Bevers, M.M.; Gadella, B.M. Evaluation of in vitro capacitation of stallion spermatozoa. *Biol. Reprod.* **2001**, *65*, 462–470. [CrossRef]
50. Yeste, M.; Estrada, E.; Rivera Del Álamo, M.M.; Bonet, S.; Rigau, T.; Rodríguez-Gil, J.E. The increase in phosphorylation levels of serine residues of protein HSP70 during holding time at 17 °C is concomitant with a higher cryotolerance of boar spermatozoa. *PLoS ONE* **2014**, *9*, e90887. [CrossRef]
51. Ortega-Ferrusola, C.; Sotillo-Galán, Y.; Varela-Fernández, E.; Gallardo-Bolaños, J.M.; Muriel, A.; González-Fernández, L.; Tapia, J.A.; Peña, F.J. Detection of "Apoptosis-Like" Changes During the Cryopreservation Process in Equine Sperm. *J. Androl.* **2008**, *29*, 213–221. [CrossRef]
52. Guthrie, H.D.; Welch, G.R. Determination of intracellular reactive oxygen species and high mitochondrial membrane potential in Percoll-treated viable boar sperm using fluorescence-activated flow cytometry. *J. Anim. Sci.* **2006**, *84*, 2089–2100. [CrossRef]

Paper IV

Cryotolerance of stallion spermatozoa relies on aquaglyceroporins rather than orthodox aquaporins.

Ariadna Delgado-Bermúdez, Federico Noto, Sebastian Bonilla-Correal, Estela Garcia-Bonavila, Jaime Catalán, Marion Papas, Sergi Bonet, Jordi Miró, Marc Yeste.

Biology-Basel,

2019;8(4):85

doi: 10.3390/biology8040085

biology

MDPI

Article

Cryotolerance of Stallion Spermatozoa Relies on Aquaglyceroporins rather than Orthodox Aquaporins

Ariadna Delgado-Bermúdez [1], Federico Noto [1], Sebastián Bonilla-Correal [2], Estela Garcia-Bonavila [1], Jaime Catalán [2], Marion Papas [2], Sergi Bonet [1], Jordi Miró [2,†] and Marc Yeste [1,†,*]

[1] Biotechnology of Animal and Human Reproduction (TechnoSperm), Unit of Cell Biology, Department of Biology, Institute of Food and Agricultural Technology, Faculty of Sciences, University of Girona, 17003 Girona, Spain; ariadna.delgado@udg.edu (A.D.-B.); fnoto83@gmail.com (F.N.); estela.garcia@udg.edu (E.G.-B.); sergi.bonet@udg.edu (S.B.)

[2] Equine Reproduction Service, Department of Animal Medicine and Surgery, Faculty of Veterinary Sciences, Autonomous University of Barcelona, 08193 Bellaterra (Cerdanyola del Vallès), Spain; sebastian.bonilla@e-campus.uab.cat (S.B.-C.); dr.jcatalan@gmail.com (J.C.); papas.marion@gmail.com (M.P.); jordi.miro@uab.cat (J.M.)

* Correspondence: marc.yeste@udg.edu

† These authors contributed equally to this work.

Received: 2 October 2019; Accepted: 11 November 2019; Published: 12 November 2019

Abstract: Aquaporins (AQPs), a family of ubiquitous water channels divided into orthodox AQPs, aquaglyceroporins (GLPs), and superAQPs, are present in stallion spermatozoa. The aim of this study was to elucidate the functional relevance of each group of AQPs during stallion sperm cryopreservation through the use of three different inhibitors: acetazolamide (AC), phloretin (PHL) and propanediol (PDO). Sperm quality and function parameters were evaluated in the presence or absence of each inhibitor in fresh and frozen–thawed samples. In the presence of AC, different parameters were altered ($p < 0.05$), but not in a concentration- or time-depending manner. PHL was found to decrease sperm motility, viability, acrosome integrity, and the percentages of spermatozoa with low membrane lipid disorder, high mitochondrial membrane potential (MMP) and high intracellular levels of calcium and superoxides ($p < 0.05$). Finally, the sperm motility, viability, acrosome integrity, the percentages of spermatozoa with low membrane lipid disorder, high MMP and high intracellular calcium levels were higher ($p < 0.05$) in PDO treatments than in the control. The sperm response to AC, PHL and PDO indicates that GLPs, rather than orthodox AQPs, play a crucial role during stallion sperm cryopreservation. Furthermore, post-thaw sperm quality was higher in PDO treatments than in the control, suggesting that this molecule is a potential permeable cryoprotectant.

Keywords: acetazolamide; aquaporins; phloretin; propanediol; sperm; stallion

1. Introduction

The permeability of the plasma membrane to water and solutes is crucial for proper cell function and homeostasis. Because of the amphipathic nature of the plasma membrane, the simple diffusion of water molecules does not occur at high rates [1]. Aquaporins (AQPs) are a family of ubiquitous transmembrane proteins that allow for the facilitated diffusion of water. Some AQPs are also permeable to small solutes [2]. To date, 13 AQPs (AQP0–AQP12) have been identified in mammalian cells and have been classified into three different groups (orthodox AQPs, aquaglyceroporins (GLPs), and superAQPs), which differ in their sequence and solute permeability. The orthodox AQP group includes AQP0, AQP1, AQP2, AQP4, AQP5, AQP6, and AQP8, which are exclusively permeable

to water. The group of GLPs that is permeable to water, glycerol, urea and other small electrolytes comprises AQP3, AQP7, AQP9 and AQP10. Finally, AQP11 and AQP12 are members of the superAQPs group, which are localized in the membranes of intracellular organelles and are involved in the transport of water and glycerol. Even if ubiquitous, the presence of AQPs varies between cell types and species. In mammalian spermatozoa, AQP1 has been identified in porcine [3]; AQP3, AQP7 and AQP11 in equine [4], porcine [5,6], murine [7–9], human [10,11] and bovine species [12,13]; AQP8 has been found in mouse [8] and human spermatozoa [10,11]; and AQP9 is present in boar spermatozoa [14]. In the male gamete, AQPs are involved in the regulation of cell volume and osmotic balance, which are crucial for spermatogenesis [15] and post-ejaculation events, including the activation of sperm motility upon ejaculation and sperm adaptation to the female environment (reviewed in [2]).

Cryopreservation, which is the most efficient method for the long-term storage of stallion spermatozoa, causes a drastic impairment in sperm quality at both lethal and sub-lethal temperature levels. The hyperosmotic shock during freezing and the following hypotonic stress during thawing induce a dramatic modification of the sperm cell volume that injuries the cytoskeleton, the mitochondria and the plasma membrane (reviewed in [16]). Mitochondria are the most sensitive organelle to osmotic stress and, when damaged, these organelles are a major source of oxidative stress through the generation of reactive oxygen species (ROS) [17]. Moreover, alterations in the plasma membrane affect embedded and membrane-associated proteins. This, in turn, affects specific signaling pathways and may detrimentally impact sperm fertilizing ability [18].

It is worth mentioning that there is a high variability between and within stallions in the ability of their ejaculates to withstand cryopreservation, i.e., cryotolerance or freezability. This inter- and intra-individual variability has also been described in other mammalian species [19–21]. Good (GFE) and poor freezability ejaculates (PFE) differ in their post-thaw sperm quality and function parameters, such as sperm membrane integrity, motility [22], ROS production and mitochondrial membrane potential (MMP) [23], all of which may ultimately affect the fertilizing capacity [24].

During the last decade, the efforts to improve the efficiency of sperm cryopreservation protocols have been focused on the use of alternative cryoprotectant agents (CPAs) and antioxidants to reduce osmotic and oxidative stresses, respectively (reviewed in [16]). In addition, the presence of damaged and non-viable sperm cells after thawing, which releases factors that have deleterious effects on viable spermatozoa, has evidenced the importance of selecting stallion spermatozoa after cryopreservation [25]. In spite of these advances, increasing cryopreservation efficiency in stallion spermatozoa still needs further optimization through the prediction of sperm cryotolerance (i.e., identification of GFE). In this context, AQPs are potential freezability biomarkers, since their permeability to water and small molecules are crucial for sperm's response to osmotic stress. In fact, the AQP involvement in sperm cryopreservation has previously been confirmed in bull [12,13], boar [26,27] and stallion spermatozoa [4]. In effect, AQP3 and AQP7 are related to the cryotolerance of boar spermatozoa [28], AQP7 [5] and AQP11 [13] are associated with that of bull spermatozoa, and AQP3, AQP7, and AQP11 are related to stallion sperm freezability [4]. As one may assume that the inhibition of these AQPs may affect the sperm's ability to withstand cryopreservation, the present study aimed to elucidate the functional relevance of orthodox AQPs and GLPs during stallion sperm cryopreservation by using three separate inhibitors (phloretin (AC), phloretin (PHL) and propanediol (PDO)). The sperm response to AQP-inhibition indicates that GLPs, rather than orthodox AQPs, play a crucial role during stallion sperm cryopreservation. Moreover, post-thaw sperm quality is higher in the presence of PDO than in the control, suggesting that this molecule could be added to cryopreservation media as a permeable cryoprotectant.

2. Materials and Methods

2.1. Stallions and Ejaculates

A total of 12 ejaculates coming from different stallions (n = 12) were used. Animals were housed at the Equine Reproduction Service, Autonomous University of Barcelona (Spain), which is a European Union (EU)-approved equine semen collection center (Authorization code: ES09RS01E) that operates under strict protocols of animal welfare and health control. Since all stallions used in this study were semen donors and were housed at the Equine Reproduction Service, the local ethics committee at our University indicated that no further ethics authorization was required.

Semen samples were collected using a Hannover-type artificial vagina (Minitüb GmbH, Tiefenbach, Germany) with an in-line nylon mesh filter to separate the gel fraction. Gel-free semen ere subsequently diluted 1:5 (v:v) in a Kenney extender [29], previously warmed at 37 °C. Sperm concentration was assessed with a Neubauer chamber (Paul Marienfeld GmbH & Co. KG, Lauda-Königshofen, Germany), and each sample was split into two different fractions. The first one was used to assess the quality of the fresh semen, whereas the other was divided into nine different sub-fractions that were cryopreserved in the presence or absence of different concentrations of the three AQP-inhibitors.

2.2. AQP Inhibitors

Prior to cryopreservation, three AQP inhibitors were added to semen samples: 1,3-propanediol (PDO, Sigma-Aldrich, St. Louis, MO, USA), acetazolamide (AC, Sigma-Aldrich), and phloretin (PHL, Sigma-Aldrich). PDO was diluted in the commercial freezing extender used for cryopreservation (see next section) to a working concentration of 100 mmol/L; AC was diluted in dimethyl sulfoxide (DMSO, Sigma-Aldrich) to a working concentration of 450 mmol/L, and PHL was diluted in methanol (Fisher Chemical, ThermoFisher Scientific; Waltham, MA, USA) to a working concentration of 365 mmol/L. Each inhibitor was assayed at the following concentrations, which were chosen according to preliminary experiments conducted in our laboratory and previous studies [27]: 0.1, 1 and 10 mmol/L for PDO; 250, 500 and 1000 µmol/L for AC; and 350 and 800 µmol/L for PHL. It is worth mentioning that, in the case of treatments containing PDO and AC, samples were exposed to methanol or DMSO at concentrations lower than 0.5% (v/v). These concentrations showed no detrimental effects on sperm quality parameters (data not shown).

2.3. Stallion Sperm Cryopreservation

The cryopreservation of stallion spermatozoa was performed in order to assess how the inhibition of AQPs from different groups affected sperm cryotolerance. The fraction of the ejaculate intended for cryopreservation was centrifuged in a programmable centrifuge (Medifriger BL-S; JP Selecta S.A., Barcelona, Spain) at 600× *g* and 20 °C for 15 min, and the supernatants were discarded. Pellets were subsequently resuspended in 2 mL of a BotuCRYO™ commercial extender (Botupharma, Botucatu, Brazil), and sperm concentration, motility and membrane integrity were evaluated for the subsequent adjustment of sperm concentration to 2×10^6 viable spermatozoa per mL. In this step, eight aliquots of 1 mL of semen each were added with AQP inhibitors (see Section 2.2), and the remaining semen was used as a control. Treatments were as follows: AC at 250 µmol/L (AC250); AC at 500 µmol/L (AC500); AC at 1000 µmol/L (AC1000); PDO at 0.1 mmol/L (PDO0.1); PDO at 1 mmol/L (PDO1); PDO at 10 mmol/L (PDO10); PHL at 350 µmol/L (PHL350); and PHL at 800 µmol/L (PHL800). Samples were subsequently packaged into 0.5 mL straws (Minitüb) and frozen in a controlled-rate freezer (Ice-Cube 14S-B; Minitüb), using the following cooling rates: i) −0.25 °C/min from 20 to 5 °C (60 min), ii) −4.75 °C/min from 5 to −90 °C (20 min), and iii) −11.11 °C/min from −90 to −120 °C (2.7 min). Finally, straws were plunged into liquid nitrogen (−196 °C) for storage.

Frozen–thawed sperm quality was evaluated after thawing. Two straws per ejaculate were thawed at 37 °C by immersion in a water bath for 20 s. The content of these straws was then diluted 1:3 (v:v) in a pre-warmed Kenney medium. After that, samples were incubated at 37 °C for 2 h, and sperm quality was assessed twice: at 10 min (0 h) and 2 h post-thaw.

2.4. Sperm Motility

Sperm motility was evaluated before and after freeze–thawing through a computer-assisted sperm analysis (CASA) system that consisted of a phase-contrast microscope (Olympus BX41; Olympus, Tokyo, Japan) equipped with a video camera and ISAS software (Integrated Sperm Analysis System V1.0; Proiser SL, Valencia, Spain). The assessment of sperm motility in extended samples was performed after 15 min of incubation at 37 °C; frozen–thawed samples were evaluated after 10 min (0 h) and 2 h of thawing. Three replicates of 1000 spermatozoa per sample and time points were evaluated using a pre-warmed (at 37 °C) Makler counting chamber (Sefi-Medical Instruments, Haifa, Israel) and observed under a negative phase-contrast field (Olympus 10 × 0.30 PLAN objective, Olympus).

For each motility assessment, the evaluation of the following parameters was performed: total motility (TMOT, %), progressive sperm motility (PMOT, %); curvilinear velocity (VCL, $\mu m \cdot s^{-1}$); straight line velocity (VSL, $\mu m \cdot s^{-1}$); average path velocity (VAP, $\mu m \cdot s^{-1}$); amplitude of lateral head displacement (ALH, μm); beat cross frequency (BCF, Hz); linearity (LIN, %), which was calculated assuming that LIN = VSL/VCL × 100; straightness (STR, %), resulting from VSL/VAP × 100; and motility parameter wobble (WOB, %), obtained from VAP/VCL × 100. A sperm cell was considered to be motile when its VAP was higher than 10 μm/s, and it was considered to be progressively motile when its STR was higher than 75%. For each parameter, the corresponding mean ± standard error of the mean (SEM) was calculated.

2.5. Flow Cytometry Analyses

Flow cytometry analyses were performed in order to evaluate different sperm quality parameters in both fresh and frozen–thawed sperm samples: viability, acrosome integrity, membrane lipid disorder, MMP, intracellular calcium levels, and intracellular levels of superoxide ($O_2^{\bullet -}$) and peroxides (H_2O_2). Samples were diluted to a final concentration of 1×10^6 sperm/mL with 4-(2-hydroxyethyl)-1-piperazineethanesulfonic acid (HEPES) buffered saline solution (10 mmol/L HEPES, 150 mmol/L NaCl, 10% BSA; pH = 7.4) prior to staining with the corresponding fluorochromes (ThermoFisher Scientific, Waltham, MA, USA). After that, samples were incubated at 38 °C in the dark, and a total of three replicates per sample and parameter were evaluated.

Flow cytometry analyses were performed using a Cell Laboratory QuantaSC™ cytometer (Beckman Coulter; Fullerton, CA, USA), and samples were excited with an argon ion laser (488 nm) set at a power of 22 mW. Cell diameter/volume was determined using the Cell Lab Quanta™ SC cytometer through the Coulter principle for volume assessment, which is based on the changes in electrical resistance produced in an electrolyte solution by suspended, non-conductive particles. In this system, forward scatter (FS) is replaced by electronic volume (EV). The EV-channel was calibrated using 10 μm flow-check fluorospheres (Beckman Coulter), and this size of beads was positioned at channel 200 on the EV scale.

Three different optical filters were used: FL1 (Dichroic/Splitter, DRLP (dichroic long pass): 550 nm, BP (band pass) filter: 525 nm, detection width: 505–545 nm), FL2 (DRLP: 600 nm, BP filter: 575 nm, detection width: 560–590 nm) and FL3 (LP (long pass) filter: 670 nm/730 nm, detection width: 655–685 nm). While FL1 allowed for the detection of green fluorescence from SYBR14, *Arachis hypogaea* lectin—peanut agglutinin—conjugated with fluorescein isothiocyanate (PNA-FITC), YO-PRO-1, JC1 (5,5′,6,6′-tetrachloro-1,1′,3,3′tetraethyl-benzimidazolylcarbocyanine iodide) monomers ($JC1_{mon}$), Fluo3 and 2′,7′-dichlorofluorescein (DCF); FL2 was used to detect orange fluorescence from JC1 aggregates ($JC1_{agg}$); and FL3 allowed for the detection of red fluorescence from propidium iodide (PI), merocyanine

540 (M540), Rhod5 and ethidium (E). Signals were logarithmically amplified, and the adjustment of photomultiplier settings was performed according to particular staining methods.

The sheath flow rate was set at 4.17 µL/min, and EV and side scatter (SS) were measured and linearly recorded for all particles. The analyzer threshold on the EV channel was adjusted to exclude subcellular debris (particle diameter <7 µm) and cell aggregates (particle diameter >12 µm), and the sperm-specific events were positively gated on the basis of EV/SS distributions.

Data obtained from flow cytometry evaluations were analyzed with Flowing Software (Ver. 2.5.1; University of Turku, Turku, Finland), and the recommendations of the International Society for Advancement of Cytometry (ISAC) were adhered. Following Petrunkina et al. [30], the events corresponding to the double negative-stained particles of all protocols except SYBR14/PI were corrected using the percentage of non-sperm debris particles of the SYBR14$^-$/PI$^-$ population. The percentages of all the other sperm populations were recalculated. Finally, the corresponding mean ± SEM was calculated for each parameter.

2.5.1. Plasma Membrane and Acrosome Integrity

Plasma membrane and acrosome integrity were evaluated through two different tests: SYBR14/PI and PNA-FITC/PI.

On the one hand, the LIVE/DEAD sperm viability kit (Molecular Probes, Eugene, OR, USA) was used following the protocol of Garner and Johnson [31]. In brief, sperm were incubated with SYBR14 at a final concentration of 100 nmol/L for 10 min, and PI was added at a final concentration of 12 µmol/L prior to an additional incubation of 5 min. Three different sperm populations were observed: 1) viable, green-stained spermatozoa (SYBR14$^+$/PI$^-$); 2) non-viable, red-stained spermatozoa (SYBR14$^-$/PI$^+$); and 3) non-viable spermatozoa stained in both green and red (SYBR14$^+$/PI$^+$). The remaining population in the dot-plots, which corresponded to unstained, non-sperm particles (SYBR14$^-$/PI$^-$), was not included in the calculation of the final percentages of each sperm population (SYBR14$^+$/PI$^-$, SYBR14$^-$/PI$^+$, and SYBR14$^+$/PI$^+$). The SYBR14 fluorescence spill over into the FL3 channel was compensated for (2.45%).

In the second case, spermatozoa were co-stained with PNA-FITC and PI, following the procedure described by Nagy et al. [32] with minor modifications. Briefly, spermatozoa were incubated with PNA-FITC (final concentration: 2.5 µg/mL) and with PI (12 µmol/L) for 10 min. Flow cytometry dot-plots allowed for the identification of four different populations: 1) spermatozoa with an intact plasma membrane (PNA-FITC$^-$/PI$^-$); 2) spermatozoa with a damaged plasma membrane (PNA-FITC$^+$/PI$^-$); 3) spermatozoa with a damaged plasma membrane and a partially altered outer acrosome membrane (PNA-FITC$^+$/PI$^+$); and 4) spermatozoa with a damaged plasma membrane and a lost outer acrosome membrane (PNA-FITC$^-$/PI$^+$). Thereafter, spermatozoa were classified into two different categories: (a) spermatozoa with an intact plasma membrane and acrosome (Population 1; PNA-FITC$^-$/PI$^-$); and (b) spermatozoa with acrosome and/or plasma membrane damage, which included Populations 2, 3 and 4. Events appearing in the PNA-FITC$^-$/PI$^-$ quadrant were corrected using the percentages of non-sperm debris particles found in the SYBR14$^-$/PI$^-$ quadrant; the percentages of the other three populations were recalculated. PNA-FITC fluorescence spill over into the FL3 channel was compensated for (2.45%).

2.5.2. Sperm Membrane Lipid Disorder

The evaluation of sperm membrane lipid disorder was performed according the protocol from Rathi et al. [33] with minor modifications [34], using M540 and YO-PRO-1. M540 detected the decrease in packing order of phospholipids in the outer monolayer of the plasma membrane. Samples were incubated with M540 (final concentration: 2.6 µmol/L) and YO-PRO-1 (final concentration: 25 nmol/L) for 10 min. Four populations were observed in flow cytometry dot-plots: 1) non-viable spermatozoa with low membrane lipid disorder (M540$^-$/YO-PRO-1$^+$); 2) non-viable spermatozoa with high membrane lipid disorder (M540$^+$/YO-PRO-1$^+$); 3) viable spermatozoa with low membrane lipid disorder (M540$^-$/YO-PRO-1$^-$); and 4) viable spermatozoa with high membrane lipid disorder

($M540^+$/YO-PRO-1^-). The percentages of viable spermatozoa with low membrane lipid disorder ($M540^-$/YO-PRO-1^-) were corrected using proportions of non-sperm debris particles found in the SYBR-14^-/PI^- quadrant; the percentages of the other three populations were recalculated. Data were not compensated for.

2.5.3. Mitochondrial Membrane Potential (MMP)

JC1-staining was used for the assessment of MMP, following the protocol of Ortega-Ferrusola et al. [35] with minor modifications. In brief, samples were incubated in the presence of JC1 at a final concentration of 0.3 µmol/L for 30 min. JC1 molecules form aggregates ($JC1_{agg}$) in the presence of high MMP, whereas JC1 molecules remain monomers in the presence of low MMP ($JC1_{mon}$). Three different populations were identified in flow cytometry dot-plots: 1) spermatozoa with low MMP ($JC1_{mon}$; $FL1^+$/$FL2^-$); 2) spermatozoa with high MMP ($JC1_{agg}$; $FL1^-$/$FL2^+$; and 3) spermatozoa with heterogeneous mitochondria ($JC1_{agg}$ and $JC1_{mon}$; $FL1^+$/$FL2^+$) in the same cell. The percentages of double-negative particles ($FL1^-$/$FL2^-$) were corrected using the proportions of SYBR14^-/PI^-; the percentages of the other populations were recalculated. Spermatozoa with high MMP resulted from the sum of Populations 2 and 3. FL1 spill-over into the FL2 channel was compensated for (70.29%).

2.5.4. Intracellular Calcium Levels

For the evaluation of intracellular calcium levels, two different co-staining tests were performed: Fluo3-AM (acetoxymethyl, ester form)/PI and Rhod5-N/YO-PRO-1.

In the first test, intracellular calcium levels were evaluated with Fluo3-AM, which penetrates cell membranes and has more affinity for the calcium residing in the sperm mid-piece [36]. This test was performed according to the protocol of Harrison et al. [37] that was modified by Kadirvel et al. [38]. In brief, spermatozoa were incubated in the presence of 1 µmol/L of Fluo3-AM and 12 µmol/L of PI for 10 min. Four different sperm populations were identified in dot-plots: 1) non-viable spermatozoa with low intracellular calcium levels (Fluo3^-/PI^+); 2) non-viable spermatozoa with high intracellular calcium levels (Fluo3^+/PI^+); 3) viable spermatozoa with low intracellular calcium levels (Fluo3^-/PI^-); and 4) viable spermatozoa with high intracellular calcium levels (Fluo3^+/PI^-). The percentages of viable spermatozoa with low intracellular calcium levels (Fluo3^-/PI^-) were corrected using proportions of non-sperm debris particles found in the SYBR14^-/PI^- quadrant; the percentages of the other three populations were recalculated. The spillover of PI into the FL1-channel and Fluo3 spill over into the FL3-channel were compensated for (28.72% and 2.45%, respectively).

Intracellular calcium levels were also assessed through Rhod-5N staining following the protocol described by Yeste et al. [36], in which Rhod-5N was found to have more affinity for the calcium residing in the sperm head. Briefly, samples were incubated with Rhod-5N at a final concentration of 5 µmol/L and YO-PRO-1 at a final concentration of 25 nmol/L for 10 min. Four different populations were identified in flow cytometry dot-plots: 1) non-viable spermatozoa with low levels of intracellular calcium (Rhod5^-/YO-PRO-1^+); 2) non-viable spermatozoa with high levels of intracellular calcium (Rhod5^+/YO-PRO-1^+); 3) viable spermatozoa with low levels of intracellular calcium (Rhod5^-/YO-PRO-1^-); and 4) viable spermatozoa with high levels of intracellular calcium (Rhod5^+/YO-PRO-1^-). The percentages of viable spermatozoa with low intracellular calcium levels (Rhod5N$^-$/YO-PRO-1^-) were corrected using the percentages of non-sperm debris particles found in the SYBR14^-/PI^- quadrant; the percentages of the other three populations were recalculated. Rhod5 spill over into the FL1-channel was compensated for (3.16%).

2.5.5. Intracellular Superoxide Levels (O_2^-)

The evaluation of intracellular superoxide (O_2^-) radical levels was performed following a modification of the protocol from Guthrie and Welch [39] through hydroethidine (HE) and YO-PRO-1 co-staining. HE is able to penetrate the sperm plasma membrane, and it is oxidized by O_2^- to ethidium (E^+) and other products at the intracellular environment. In brief, samples were incubated with HE (final concentration: 4 μmol/L) and YO-PRO-1 (final concentration: 40 nmol/L) for 20 min. Four different sperm populations were identified in flow cytometry dot-plots: 1) non-viable spermatozoa with low superoxide levels (E^-/YO-PRO-1^+); 2) non-viable spermatozoa with high superoxide levels (E^+/YO-PRO-1^+); 3) viable spermatozoa with low superoxide levels (E^-/YO-PRO-1^-); and 4) viable spermatozoa with high superoxide levels (E^+/YO-PRO-1^-). The percentages of viable spermatozoa with low superoxide levels (E^-/YO-PRO-1^-) were corrected using the percentages of non-sperm debris particles found in the SYBR14^-/PI^- quadrant; the percentages of the other three populations were recalculated. YO-PRO-1 spill over into the FL3-channel was compensated for (5.06%).

2.5.6. Intracellular Hydrogen Peroxide Levels (H_2O_2)

The determination of the intracellular levels of hydrogen peroxide (H_2O_2) through co-staining with 2′,7′-dichlorodihydrofluorescein diacetate (H_2DCFDA) and PI fluorochromes was performed following the protocol from Guthrie and Welch [39] with minor modifications. H_2DCFDA is a non-fluorescent probe that penetrates the sperm plasma membrane and is intracellularly de-esterified and converted into highly fluorescent, 2′,7′-dichlorofluorescein (DCF^+) upon oxidation. In brief, samples were incubated with H_2DCFDA (final concentration: 200 μmol/L) and PI (final concentration: 12 μmol/L) for 30 min. Four different populations were identified in flow cytometry dot-plots: 1) viable spermatozoa with high peroxide levels (DCF^+/PI^-); 2) non-viable spermatozoa with high peroxide levels (DCF^+/PI^+); 3) viable spermatozoa with low peroxide levels (DCF^-/PI^-); and 4) non-viable spermatozoa with low peroxide levels (DCF^-/PI^+). The percentages of viable spermatozoa with low peroxide levels (DCF^-/PI^-) were corrected using the percentages of non-sperm debris particles found in the SYBR14^-/PI^- quadrant; the percentages of the other three populations were recalculated. DCF-spill over into the FL3-channel was compensated for (2.45%).

2.6. Statistical Analyses

All data were analyzed using a statistical package (IBM SPSS Statistics 25.0; Armonk, New York, NY, USA). Data were first tested for normal distribution (Shapiro–Wilk test) and homogeneity of variances (Levene test). Following this, the effects of each inhibitor and cryopreservation step (i.e. fresh, frozen–thawed at 0 h, and frozen–thawed at 2 h) were tested through a mixed model followed by the post-hoc Sidak test for pair-wise comparisons. The intra-subjects factor (i.e., repeated measures) was the cryopreservation step (i.e., fresh, frozen–thawed at 0 h, frozen–thawed at 2 h), and the inter-subjects factor was the treatment (C, and different concentrations of PDO, AC or PHL). The level of significance was set at $p \leq 0.05$, and data are shown as mean ± SEM.

3. Results

As previously mentioned, sperm quality and function parameters were evaluated in both fresh and frozen–thawed samples in order to determine the effects of AQP inhibition during sperm cryopreservation. Regarding fresh samples, the absence of differences between controls and treated samples in any sperm parameter was due to the fact that inhibitors were added immediately before cryopreservation ($p > 0.05$; Table 1).

Table 1. Sperm quality and function parameters (mean ± SEM) in fresh stallion semen. SYBR14$^+$/propidium iodide (PI$^-$) spermatozoa, viable cells; peanut agglutinin conjugated with fluorescein isothiocyanate (PNA-FITC$^-$)/PI$^-$ spermatozoa, cells with an intact plasma membrane and acrosome; merocyanine 540 (M540$^-$)/YO-PRO-1$^-$ spermatozoa, live cells with low mitochondrial membrane disorder; JC1$_{agg}$ spermatozoa, cells with high mitochondrial membrane potential (MMP); Fluo3$^+$/PI$^-$ spermatozoa, live cells with high intracellular calcium levels, mainly in the sperm mid-piece; Rhod5$^+$/YO-PRO-1$^-$ spermatozoa, live cells with high intracellular calcium levels, mainly in the sperm head; E$^+$/YO-PRO-1$^-$ spermatozoa, live cells with high superoxide (O_2^-) levels; 2′,7′-dichlorofluorescein (DCF$^+$)/PI$^-$ spermatozoa, live cells with high peroxide (H_2O_2) levels.

Sperm Parameter	Mean ± SEM
% Total motile spermatozoa (TMOT)	78.4 ± 3.6
% Progressively motile spermatozoa (PMOT)	57.9 ± 2.4
% SYBR14$^+$/PI$^-$ spermatozoa	80.5 ± 3.2
% PNA-FITC$^-$/PI$^-$ spermatozoa	79.1 ± 3.0
% M540$^-$/YO-PRO-1$^-$ spermatozoa	76.2 ± 3.2
% JC1$_{agg}$ spermatozoa	73.6 ± 3.1
% Fluo3$^+$/PI$^-$ spermatozoa	14.3 ± 0.9
% Rhod5$^+$/YO-PRO-1$^-$ spermatozoa	20.8 ± 1.4
% E$^+$/YO-PRO-1$^-$ spermatozoa	8.7 ± 0.7
% DCF$^+$/PI$^-$ spermatozoa	4.5 ± 0.4

3.1. Sperm Motility

The total and progressive motilities of frozen–thawed spermatozoa are shown in Figure 1. The percentages of total motile spermatozoa were significantly ($p < 0.05$) higher in PDO treatments than in the control at both 0 and 2 h post-thaw (Figure 1A), whereas the two PHL concentrations caused a significant ($p < 0.05$) decrease in total motility at both post-thaw time points; the presence of AC did not cause any significant effect ($p > 0.05$).

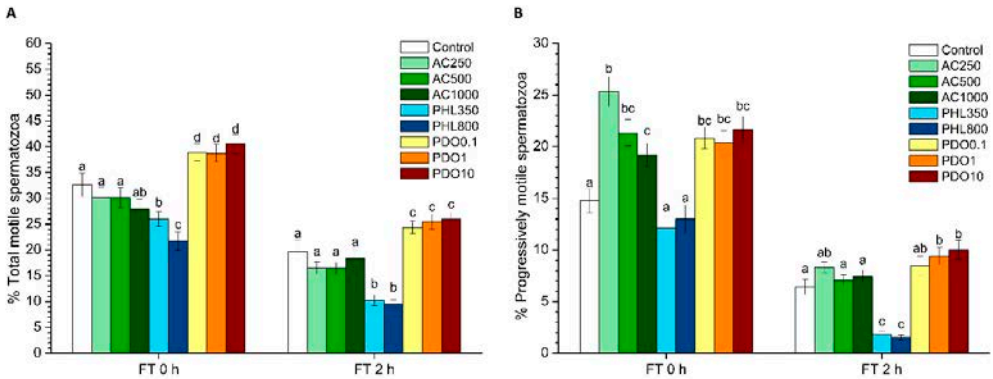

Figure 1. Sperm motility of samples after cryopreservation with a standard freezing medium (control) or with a freezing medium supplemented with acetazolamide (AC) at three different concentrations (250, 500, and 1000 µmol/L), with phloretin (PHL) at two different concentrations (350 and 800 µmol/L), or with 1,3-propanediol (PDO) at three concentrations (0.1, 1, and 10 mmol/L). (**A**) The percentages of total motile spermatozoa (TMOT). (**B**) The percentages of progressively motile spermatozoa (PMOT). Data, shown as mean ± SEM, correspond to 0 and 2 h post-thaw. Different letters (a–d) indicate significant differences ($p < 0.05$) between treatments within a given time point.

Progressive sperm motility (Figure 1B) significantly ($p < 0.05$) increased in the presence of both AC and PDO immediately after thawing, whereas PHL did not have any significant effect ($p > 0.05$). Two hours after thawing, there were no significant differences between controls and samples treated

with either AC or the lowest concentration of PDO ($p > 0.05$). In contrast, progressive sperm motility in the treatments containing 1 and 10 mmol/L of PDO was significantly ($p < 0.05$) higher than in the control. Moreover, the progressive sperm motility in the treatments containing PHL was significantly ($p < 0.05$) lower than in the control.

3.2. Sperm Viability: SYBR14/PI Test

The percentages of viable spermatozoa (SYBR14$^+$/PI$^-$) did not differ between AC treatments and the control immediately after thawing (0 h), but the presence of this inhibitor induced a significant ($p < 0.05$) decrease at 2 h post-thaw (Figure 2A). While the percentages of viable spermatozoa in PHL treatments were significantly ($p < 0.05$) lower than in the control at 0 and 2 h post-thaw, all PDO treatments showed significantly ($p < 0.05$) higher percentages of viable spermatozoa than the control.

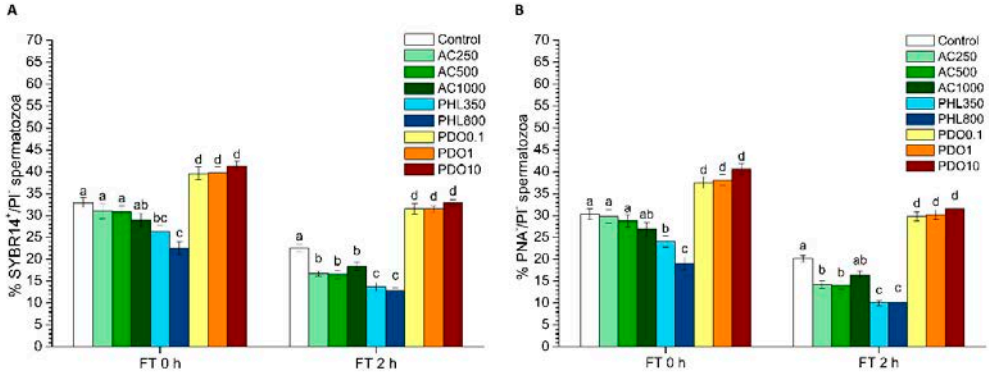

Figure 2. Sperm viability (SYBR14/PI) and acrosome integrity (PNA-FITC/PI) after cryopreservation with a standard freezing medium (control) or with a freezing medium supplemented with acetazolamide (AC) at three different concentrations (250, 500 and 1000 μmol/L), with phloretin (PHL) at two different concentrations (350 and 800 μmol/L), or with 1,3-propanediol (PDO) at three concentrations (0.1, 1 and 10 mmol/L). (**A**) The percentages of viable spermatozoa (SYBR-14$^+$/PI$^-$ spermatozoa). (**B**) The percentage of viable spermatozoa with an intact acrosome (PNA-FITC$^-$/PI$^-$ spermatozoa). Data, shown as mean ± SEM, correspond to 0 and 2 h post-thaw. Different letters (a–d) indicate significant differences ($p < 0.05$) between treatments within a given time point.

3.3. Acrosome Integrity: PNA-FITC/PI Test

The PNA-FITC/PI test was carried out to determine the integrity of both acrosome and plasma membranes, and PNA-FITC$^-$/PI$^-$ spermatozoa were those that had an intact acrosome and plasma membrane (Figure 2B). Samples treated with AC did not show significant differences to the control at any concentration immediately after thawing ($p > 0.05$), but there was a significant ($p < 0.05$) decrease in the percentage of spermatozoa that presented an intact plasma and acrosome membrane in the samples treated with the lowest concentrations of AC at 2 h post-thaw. The percentages of spermatozoa with an intact plasma and acrosome membrane were significantly ($p < 0.05$) lower in PHL treatments than in the control at both 0 and 2 h post-thaw. In contrast, all treatments containing PDO showed significantly ($p < 0.05$) higher percentages of spermatozoa with an intact plasma and acrosome membrane at both 0 and 2 h post-thaw.

3.4. Membrane Lipid Disorder: M540/YO-PRO-1 Test

The M540/YO-PRO-1 test allowed for the evaluation of sperm membrane lipid disorder, the population of M540$^-$/YO-PRO-1$^-$ spermatozoa corresponding to those viable cells with low membrane lipid disorder (Figure 3A). While right after thawing, samples treated with 1000 μmol/L AC showed significantly ($p < 0.05$) lower percentages of viable spermatozoa with low membrane lipid

disorder than the control, the treatments containing 250 and 500 µmol/L AC also showed reduced ($p < 0.05$) percentages of viable spermatozoa with low membrane lipid disorder than the control at 2 h post-thaw. The percentages of viable spermatozoa with low membrane lipid disorder at the highest PHL concentration were significantly ($p < 0.05$) lower than the control immediately after thawing. At 2 h post-thaw, both 350 and 800 µmol/L concentrations showed significantly ($p < 0.05$) lower percentages of viable spermatozoa with low membrane lipid disorder than the control. Finally, the percentages of viable spermatozoa with low membrane lipid disorder were significantly ($p < 0.05$) higher than the control in all PDO treatments, both at 0 and 2 h post-thaw.

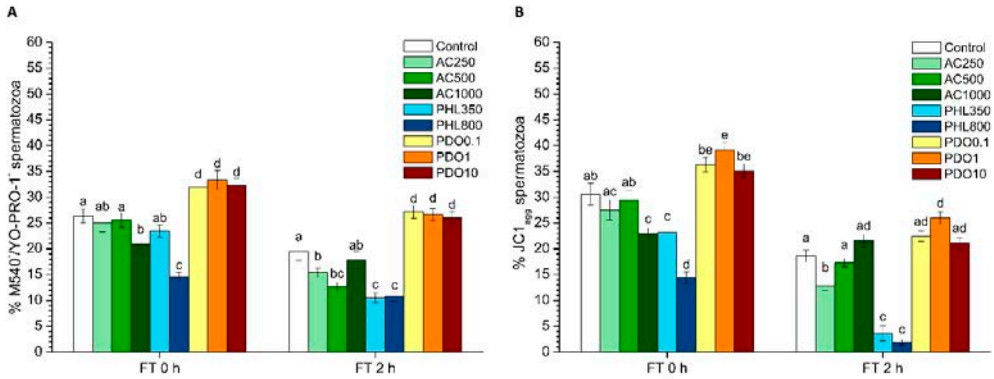

Figure 3. Sperm membrane lipid disorder (M540/YO-PRO-1) and mitochondrial membrane potential (JC1) after cryopreservation with a standard freezing medium (control) or with a freezing medium supplemented with acetazolamide (AC) at three different concentrations (250, 500 and 1000 µmol/L), with phloretin (PHL) at two different concentrations (350 and 800 µmol/L), or with 1,3-propanediol (PDO) at three concentrations (0.1, 1 and 10 mmol/L). (**A**) The percentages of viable spermatozoa with low membrane lipid disorder ($M540^-/YO\text{-}PRO\text{-}1^-$ spermatozoa). (**B**) The percentages of spermatozoa with high mitochondrial membrane potential ($JC1_{agg}$ spermatozoa). Data, shown as mean ± SEM, correspond to 0 and 2 h post-thaw. Different letters (a–e) indicate significant differences ($p < 0.05$) between treatments within a given time point.

3.5. Mitochondrial Membrane Potential (MMP): JC1 Test

The percentages of spermatozoa with high MMP were significantly ($p < 0.05$) lower in the treatment containing AC at 1000 µmol/L than in the control immediately after thawing and in the treatment containing AC at 250 µmol/L at 2 h post-thaw (Figure 3B). When treated with PHL, samples showed a decrease in MMP at any time point after thaw ($p < 0.05$). In contrast, the percentages of spermatozoa with high MMP in the treatment containing 1 mmol/L PDO were significantly ($p < 0.05$) higher than in the control both at 0 and 2 h post-thaw.

3.6. Intracellular Calcium of Spermatozoa: Fluo3/PI Test

Intracellular calcium levels were assessed through the Fluo3/PI test, and the population of $Fluo3^+/PI^-$ spermatozoa corresponded to viable cells with high intracellular calcium levels (Figure 4A). While, compared to the control, samples treated with any concentration of AC showed a significant ($p < 0.05$) decrease in the percentage of viable spermatozoa with high levels of intracellular calcium immediately after thawing, no significant ($p > 0.05$) differences between AC treatments and the control were found after 2 h of thawing. Treatments containing any concentration of PHL showed significantly ($p < 0.05$) lower percentages of spermatozoa with high levels of intracellular calcium at both 0 and 2 h post-thaw. In contrast, the percentages of viable spermatozoa with high levels of intracellular calcium were significantly ($p < 0.05$) higher in all PDO concentrations than in the control right after thawing

(0 h) and were significantly ($p < 0.05$) higher than the control at the two highest PDO concentrations after 2 h of thawing.

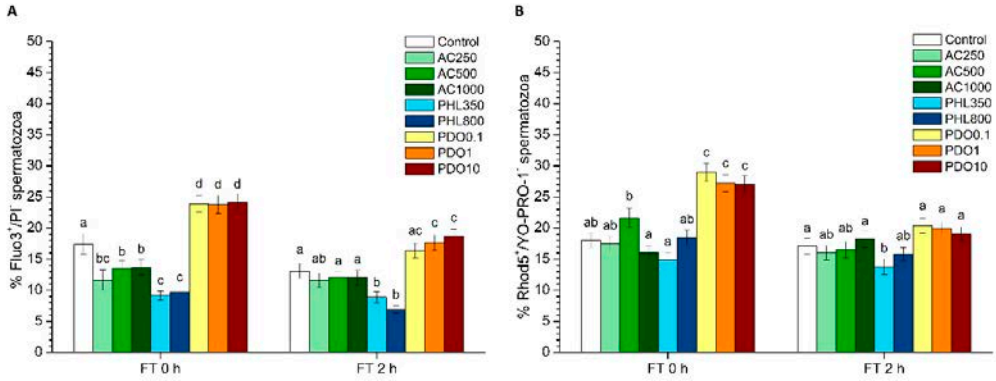

Figure 4. Intracellular calcium levels (Fluo3/PI and Rhod5/YO-PRO-1) after cryopreservation with a standard freezing medium (control) or with a freezing medium supplemented with acetazolamide (AC) at three different concentrations (250, 500 and 1000 μmol/L), with phloretin (PHL) at two different concentrations (350 and 800 μmol/L), or with 1,3-propanediol (PDO) at three concentrations (0.1, 1 and 10 mmol/L). (**A**) The percentages of viable spermatozoa with high levels of intracellular calcium levels ($Fluo3^+/PI^-$ spermatozoa). (**B**) The percentages of viable spermatozoa with high levels of intracellular calcium levels ($Rhod5^+$/YO-PRO-1^- spermatozoa). Data, shown as mean ± SEM, correspond to 0 and 2 h post-thaw. Different letters (a–d) indicate significant differences ($p < 0.05$) between treatments within a given time point.

3.7. Intracellular Calcium of Spermatozoa: Rhod5/YO-PRO-1 Test

The Rhod5/YO-PRO-1 test was also performed to determine intracellular calcium levels, and the population of $Rhod5^+$/YO-PRO-1^- spermatozoa corresponded to viable cells with high intracellular calcium levels (Figure 4B). When AC was present, no significant ($p > 0.05$) differences with regard to the control were observed either at 0 or 2 h post-thaw. The treatments containing PHL showed no significant differences compared to the control at 0 h post-thaw, but those containing the lowest PHL concentration showed significantly ($p > 0.05$) lower percentages of viable spermatozoa with high intracellular calcium levels after 2 h of thawing. In contrast, the percentages of viable spermatozoa with high intracellular calcium levels were significantly ($p < 0.05$) higher in PDO treatments than in the control at 0 h but not at 2 h post-thaw.

3.8. Intracellular Superoxide Levels (O_2^-): HE/YO-PRO-1 Test

Intracellular O_2^- levels were evaluated through the HE/YO-PRO-1 test, in which the population of E^+/YO-PRO-1^- spermatozoa corresponded to viable cells with high intracellular levels of O_2^-. The percentages of viable spermatozoa with high intracellular levels of O_2^- did not differ ($p > 0.05$) between AC treatments and the control, either at 0 or at 2 h post-thaw (Figure 5A). In contrast, the treatment containing 800 μmol/L PHL showed significantly ($p < 0.05$) lower percentages of viable spermatozoa with high intracellular levels of O_2^- both at 0 and 2 h post-thaw ($p < 0.05$). Concerning samples treated with PDO, the single change that was observed was a significant ($p < 0.05$) increase in the percentages of viable spermatozoa with high intracellular levels of O_2^- at 1 mmol/L immediately after thawing.

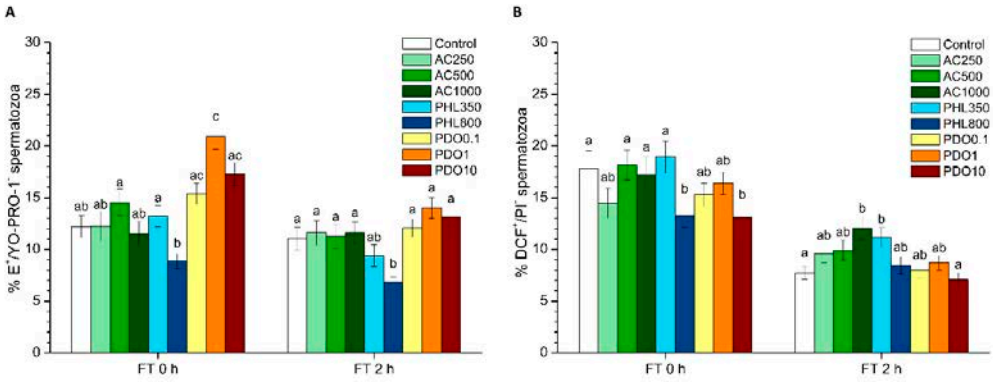

Figure 5. Intracellular levels of reactive oxygen species (ROS) after cryopreservation with a standard freezing medium (control) or with a freezing medium supplemented with acetazolamide (AC) at three different concentrations (250, 500 and 1000 µmol/L), with phloretin (PHL) at two different concentrations (350 and 800 µmol/L), or with 1,3-propanediol (PDO) at three concentrations (0.1, 1 and 10 mmol/L). (**A**) The percentages of viable spermatozoa with high levels of superoxide (E^+/YO-PRO-1^- spermatozoa). (**B**) The percentages of viable spermatozoa with high levels of peroxide (DCF^+/PI^- spermatozoa). Data, shown as mean ± SEM, correspond to 0 and 2 h post-thaw. Different letters (a–d) indicate significant differences ($p < 0.05$) between treatments within a given time point.

3.9. Intracellular Peroxide Levels (H_2O_2): H_2DCFDA/PI Test

Intracellular H_2O_2 levels were assessed through the H_2DCFDA/PI test, and the DCF^+/PI^- sperm population corresponded to viable spermatozoa with high intracellular levels of peroxides. The percentages of viable spermatozoa with high intracellular levels of peroxides were significantly ($p < 0.05$) higher than the control in the treatment with 1000 µmol/L AC after 2 h of thawing (Figure 5B). While the percentages of viable spermatozoa with high intracellular levels of peroxides were significantly ($p < 0.05$) lower in the 800 µmol/L PHL treatment than in the control at 0 h post-thaw, those percentages in the treatment containing 350 µmol/L PHL were significantly ($p < 0.05$) higher than in the control after 2 h of thawing. Finally, the treatment containing 10 mmol/L PDO showed significantly ($p < 0.05$) lower percentages of viable spermatozoa with high intracellular levels of peroxides at 0 h post-thaw.

4. Discussion

While AQPs have been identified in sperm cells from different mammalian species in the last decade (reviewed in [2]), their precise function and mechanism of action are yet to be fully addressed. In the case of horses, AQP3, AQP7 and AQP11 have been identified in stallion spermatozoa [4]. Taking this into account, this study aimed to unveil the relevance of each group of AQPs during stallion sperm cryopreservation. With this purpose, three different inhibitors were added at different concentrations: AC, which is known to inhibit AQP1 and AQP4 [40,41]; PHL, which inhibits both AQP3 and AQP7 [42–44]; PDO, which has been proven to inhibit orthodox AQPs (AQP1, AQP2, AQP5 and AQP4) with high efficiency; and GLPs (the family to which AQP3, AQP7 and AQP9 belong) with low intensity [45,46]. The effects of each AQP-inhibitor on sperm function and survival after cryopreservation were assessed on the basis of sperm motility, sperm viability, acrosome integrity, membrane lipid disorder, MMP, intracellular calcium levels, and intracellular levels of ROS. Upon thawing, samples treated with AC showed higher PMOT and lower percentages of $Fluo3^+/PI^-$ than the control, and the highest AC concentration increased membrane lipid disorder and decreased MMP. At 2 h post-thaw, AC reduced sperm viability and the percentages of viable spermatozoa with low membrane lipid disorder at all concentrations. While the lowest AC concentrations reduced the percentage of acrosome-intact spermatozoa and MMP, the highest concentration of this inhibitor caused an increase in intracellular H_2O_2 levels. PHL decreased in all the studied parameters at

almost any concentration and time point. In contrast, in the presence of PDO, samples showed higher percentages of TMOT, PMOT, viable and acrosome-intact spermatozoa, viable spermatozoa with low membrane lipid disorder, spermatozoa with high MMP, and viable spermatozoa with high intracellular calcium levels.

Differences between the effects of these three inhibitors appeared to result from their specificity for separate AQPs and from the collateral effects on other proteins that are present in the sperm cell. Considering the function of orthodox AQPs as water transporters and, as a consequence, their crucial role in osmoregulation, the expected effect of their inhibition through AC would be a drastic impairment of sperm quality and function. Since water outflow is crucial to avoid the formation of water crystals inside spermatozoa, the inhibition of water transport during cryopreservation could have dramatic consequences for the structure of sperm membranes and organelles, thereby compromising sperm membrane integrity and, thus, their function. In spite of this, there was an absence of clear effects immediately after thawing in the presence of AC, which is consistent with the fact that AQP1 and AQP4 have not been previously identified in stallion spermatozoa (reviewed in [2]). Nevertheless, AQP1 has been identified in boar spermatozoa [3]; therefore, while the few alterations in sperm function parameters that were observed in the presence of AC could be a consequence of this inhibition, future studies are necessary to assess whether this protein is present in stallion spermatozoa. Moreover, some of the changes observed in the presence of AC did not appear to depend on the concentration of the inhibitor or on the post-thaw incubation time. In this context, it is worth mentioning that not only does AC inhibit some AQPs but also carbonic anhydrase, whose function is to convert CO_2 and H_2O to bicarbonate and protons [47]. Therefore, the inhibition of carbonic anhydrase through AC could decrease the concentration of intracellular bicarbonate. Bicarbonate, together with Ca^{2+}, is crucial for the activation of the soluble adenylate cyclase (sAC) which, in turn, produces cAMP that triggers protein kinase A (PKA). Protein kinase A activates different complexes of the electron transport chain, and the inhibition of PKA has been reported to reduce the electron flow passing through complex I [48]. This mechanism could explain the reduction of the mitochondrial membrane potential observed in the presence of some AC concentrations. In addition, the decrease in the percentages of spermatozoa with intracellular calcium levels observed in the presence of AC could be related to the lack of activation of the CatSper calcium channel. The CatSper channel is responsible for the increase of intracellular calcium levels that mediate sperm capacitation (reviewed in [49,50]), and a lower activation of this channel would also be related to the decreased levels of bicarbonate via the AC-inhibition of carbonic anhydrase. Since sperm motility is also mediated by the increase of intracellular bicarbonate and calcium levels, the higher sperm progressive motility observed right after thawing cannot be explained by these previous interactions. Thus, further research is needed to understand why sperm motility data observed in this work did not match with the decreased MMP and intracellular calcium levels observed immediately after thawing. Finally, while neither sperm viability nor acrosome integrity were altered at 0 h, both parameters decreased at 2 h post-thaw. This suggests that the aforementioned collateral effects of AC induce sub-lethal alterations that are not only apparent at 2 h post-thaw but not right after thawing.

The hydrophobic nature of PHL allows for its penetration through the sperm plasma membrane [51] and its binding to an internal site of GLPs [52]. This internal binding specifically inhibits GLPs, which in turn disrupts the transport of water and small solutes, such as glycerol. As glycerol, which is the most used permeating CPA in stallion sperm cryopreservation, was present in the freezing medium used in this study, it is reasonable to suggest that the addition of PHL decreased the transport of this CPA, which had detrimental effects on sperm quality and function parameters. The reduced influx of glycerol together with a limited water efflux through PHL-inhibition of GLPs could cause extreme osmotic stress to spermatozoa, thus compromising membrane integrity (including the membranes of intracellular organelles) and increasing membrane lipid disorder. Related with this, sperm motility and survival were lower than in the control after thawing, which could match with this hypothesis. In addition, an impairment in the sperm membrane integrity could also explain the drop in the

intracellular calcium levels which, in turn, could be related to the compromised mitochondrial function that we observed through the decrease of spermatozoa with high MMP. While the reduction in the percentages of viable spermatozoa with high superoxide and peroxide levels immediately after thawing could be related to the decrease of MMP, the observed increase in the percentage of viable spermatozoa with high peroxide levels at 2 h post-thaw could be due to the inhibition of H_2O_2 efflux through AQP3 [53]. Related with this, some studies have unraveled that H_2O_2 efflux through AQP3 and AQP9 plays a vital role for human sperm function [11].

Regarding PDO, it strongly inhibits orthodox the AQPs remaining inside their pore [45,46]. PDO also inhibits GLPs, though less efficiently, since the pore diameter of GLPs is broader than that of orthodox AQPs. This broader diameter of GLPs allows PDO to pass through these channels [45,54]. Therefore, PDO would be able to impair the cell permeability to both water and small solutes, including glycerol, so that the expected effects should be a combination of those observed in the presence of AC and PHL. However, neither the cryodamage-related effects caused by the inhibition of GLPs that were observed in the presence of PHL nor the potential cryodamage that could occur as a consequence of the high-affinity inhibition of orthodox AQPs (if present in stallion spermatozoa) were observed in the presence of PDO. In fact, our results showed that the addition of PDO to the freezing medium had a positive effect on sperm quality and function parameters (motility, viability, acrosome integrity and membrane lipid disorder). On the one hand, the absence of a detrimental impact is consistent with the lack of negative effects observed in samples treated with AC; taking altogether, these results support—or, at least suggest—that orthodox AQPs are not relevant for stallion sperm cryotolerance. On the other hand, it is worth recalling that the affinity of PDO for GLPs is lower than for orthodox AQPs. Thus, its inhibitory efficiency might also be lower on orthodox AQPs, and, therefore, it might not be able to completely block water and solutes transport through the pore of this group of AQPs. Nevertheless, this absence of transport blockage does not explain the improving effect on the overall sperm quality and function in the presence of PDO. In this context, it could be hypothesized that PDO could function as a CPA itself, thereby mitigating the potential cryodamage that one would have expected to observe as a consequence of the lower intracellular concentration of glycerol. In fact, Widiasih et al. [55] observed that, when the impact of different cryoprotectants was evaluated, PDO yielded higher motility and viability in human spermatozoa than glycerol. Moreover, PDO has also been used as a CPA for the cryopreservation of canine ovarian cortex [56] and human multipotent stromal cells [57]. Considering all the aforementioned information, one could consider that the combination of two different CPAs at low concentrations could restrict the widely known collateral toxic effects of each CPA, including glycerol (reviewed in [50]). In fact, a less toxic and more efficient combination of CPAs would limit cryodamage and thus membrane alterations, which would yield higher post-thaw sperm viability and motility. The rise in the percentages of viable spermatozoa with high intracellular calcium levels could be related to a better maintenance of sperm survival rather than to the specific effect of PDO on the calcium transport (reviewed in [49,50]). In this context, while the increase in both total and progressive motilities and in MMP could be due to this calcium increase, the cause of this augmented calcium levels remains unexplained, since sperm membranes were intact according to the results of separate tests (SYBR14/PI, PNA-FITC/PI and M540/YO-PRO-1). Finally, the increase in superoxide levels might be a direct consequence of the increased MMP, since mitochondria are the main source of ROS. Considering all the aforementioned information, it can be hypothesized that PDO is not an effective inhibitor of GLPs and that the absence of negative effects is consistent with the results observed in the presence of AC. This suggests that orthodox AQPs might not be present in stallion spermatozoa or, if present, this group of AQPs is not relevant for stallion sperm cryotolerance. Moreover, further studies are needed to elucidate whether the use of PDO as a CPA alone or in combination with other agents might lead to obtaining frozen–thawed stallion spermatozoa of better quality.

5. Conclusions

In conclusion, the effects of AQP inhibition rely on the specificity of each inhibitor for each AQPs group and its collateral effects on other sperm proteins. The observed effects when samples were supplemented with AC, which mainly inhibits orthodox AQPs, suggest that these proteins are not involved in the response to osmolality changes produced during stallion sperm cryopreservation, and the observed changes seem to be caused by the side-effects on other sperm proteins. The absence of orthodox AQPs in stallion spermatozoa is consistent with the absence of detrimental effects in the presence of PDO, which is also a high-affinity inhibitor of orthodox AQPs. On the other hand, the dramatic impairment of post-thaw sperm quality observed in the presence of PHL suggests that GLPs play a crucial role in the response of stallion sperm to the osmolality changes that occur during cryopreservation. Finally, the improvement of overall sperm quality and function parameters in the presence of PDO evidences it might not be an efficient GLPs inhibitor and supports its role as a permeable CPA, whether alone or in combination with other cryoprotectants.

Author Contributions: A.D.-B. performed the experiments, undertook sperm quality and statistical analyses and wrote the draft. F.N. and E.G.-B. contributed to performing CASA and flow cytometry evaluations. S.B.-C., J.C. and M.P. collected the sperm samples and provided help evaluating sperm quality parameters. S.B., J.M. and M.Y. conceived the study, help conduct data analysis and contributed to the critical revision of the Manuscript. All authors read and approved the final manuscript.

Funding: This research was funded by the Ministry of Science, Innovation and Universities, Spain (Grants: RYC-2014-15581, AGL2017-88329-R and PRE2018-083488), and the Regional Government of Catalonia, Spain (2017-SGR-1229).

Acknowledgments: The authors acknowledge the technical support from Sandra Recuero, Marc Llavanera, Yentel Mateo-Otero, Beatriz Fernandez-Fuertes and Isabel Barranco (University of Girona, Spain).

Conflicts of Interest: The authors declare that the research was conducted in the absence of any commercial or financial relationships that could be construed as a potential conflict of interest.

References

1. Watson, H. Biological membranes. *Essays Biochem.* **2015**, *59*, 43–70. [CrossRef] [PubMed]
2. Yeste, M.; Morató, R.; Rodríguez-Gil, J.E.; Bonet, S.; Prieto-Martínez, N. Aquaporins in the male reproductive tract and sperm: Functional implications and cryobiology. *Reprod. Domest. Anim.* **2017**, *52*, 12–27. [CrossRef] [PubMed]
3. Feugang, J.M.; Liao, S.F.; Willard, S.T.; Ryan, P.L. In-depth proteomic analysis of boar spermatozoa through shotgun and gel-based methods. *BMC Genom.* **2018**, *19*, 62. [CrossRef] [PubMed]
4. Bonilla-Correal, S.; Noto, F.; Garcia-Bonavila, E.; Rodríguez-Gil, J.E.; Yeste, M.; Miró, J. First evidence for the presence of aquaporins in stallion sperm. *Reprod. Domest. Anim.* **2017**, *52*, 61–64. [CrossRef] [PubMed]
5. Prieto-Martínez, N.; Vilagran, I.; Morató, R.; Rodríguez-Gil, J.E.; Yeste, M.; Bonet, S. Aquaporins 7 and 11 in boar spermatozoa: Detection, localisation and relationship with sperm quality. *Reprod. Fertil. Dev.* **2014**, *28*, 663–672. [CrossRef] [PubMed]
6. Prieto-Martínez, N.; Morató, R.; Vilagran, I.; Rodríguez-Gil, J.E.; Bonet, S.; Yeste, M. Aquaporins in boar spermatozoa. Part II: Detection and localisation of aquaglyceroporin 3. *Reprod. Fertil. Dev.* **2015**, *29*, 703–711. [CrossRef] [PubMed]
7. Chen, Q.; Peng, H.; Lei, L.; Zhang, Y.; Kuang, H.; Cao, Y.; Shi, Q.; Ma, T.; Duan, E. Aquaporin 3 is a sperm water channel essential for postcopulatory sperm osmoadaptation and migration. *Cell Res.* **2011**, *21*, 922–933. [CrossRef] [PubMed]
8. Yeung, C.H.; Callies, C.; Rojek, A.; Nielsen, S.; Cooper, T.G. Aquaporin Isoforms Involved in Physiological Volume Regulation of Murine Spermatozoa. *Biol. Reprod.* **2009**, *80*, 350–357. [CrossRef] [PubMed]
9. Yeung, C.H.; Cooper, T.G. Aquaporin AQP11 in the testis: Molecular identity and association with the processing of residual cytoplasm of elongated spermatids. *Reproduction* **2010**, *139*, 209–216. [CrossRef] [PubMed]

10. Yeung, C.H.; Callies, C.; Tüttelmann, F.; Kliesch, S.; Cooper, T.G. Aquaporins in the human testis and spermatozoa—Identification, involvement in sperm volume regulation and clinical relevance. *Int. J. Androl.* **2010**, *33*, 629–641. [CrossRef] [PubMed]
11. Laforenza, U.; Pellavio, G.; Marchetti, A.; Omes, C.; Todaro, F.; Gastaldi, G. Aquaporin-Mediated Water and Hydrogen Peroxide Transport Is Involved in Normal Human Spermatozoa Functioning. *Int. J. Mol. Sci.* **2017**, *18*, E66. [CrossRef] [PubMed]
12. Prieto-Martínez, N.; Morató, R.; Muiño, R.; Hidalgo, C.O.; Rodríguez-Gil, J.E.; Bonet, S.; Yeste, M. Aquaglyceroporins 3 and 7 in bull spermatozoa: Identification, localisation and their relationship with sperm cryotolerance. *Reprod. Fertil. Dev.* **2016**, *29*, 1249–1259. [CrossRef] [PubMed]
13. Morató, R.; Prieto-Martínez, N.; Muiño, R.; Hidalgo, C.O.; Rodríguez-Gil, J.E.; Bonet, S.; Yeste, M. Aquaporin 11 is related to cryotolerance and fertilising ability of frozen–thawed bull spermatozoa. *Reprod. Fertil. Dev.* **2018**, *30*, 1099–1108. [CrossRef] [PubMed]
14. Vicente-Carrillo, A.; Ekwall, H.; Alvarez-Rodriguez, M.; Rodriguez-Martinez, H. Membrane Stress During Thawing Elicits Redistribution of Aquaporin 7 But Not of Aquaporin 9 in Boar Spermatozoa. *Reprod. Domest. Anim.* **2016**, *51*, 665–679. [CrossRef] [PubMed]
15. Huang, H.F.; He, R.H.; Sun, C.C.; Zhang, Y.; Meng, Q.X.; Ma, Y.Y. Function of aquaporins in female and male reproductive systems. *Hum. Reprod. Update* **2006**, *12*, 785–795. [CrossRef] [PubMed]
16. Peña, F.J.; Macías García, B.; Samper, J.C.; Aparicio, I.M.; Tapia, J.A.; Ortega Ferrusola, C. Dissecting the molecular damage to stallion spermatozoa: The way to improve current cryopreservation protocols? *Theriogenology* **2011**, *76*, 1177–1186. [CrossRef] [PubMed]
17. Ball, B.A.; Vo, A.T.; Baumber, J. Generation of reactive oxygen species by equine spermatozoa. *Am. J. Vet. Res.* **2001**, *62*, 508–515. [CrossRef] [PubMed]
18. Sieme, H.; Harrison, R.A.P.; Petrunkina, A.M. Cryobiological determinants of frozen semen quality, with special reference to stallion. *Anim. Reprod. Sci.* **2008**, *107*, 276–292. [CrossRef] [PubMed]
19. Casas, I.; Sancho, S.; Briz, M.; Pinart, E.; Bussalleu, E.; Yeste, M.; Bonet, S. Freezability prediction of boar ejaculates assessed by functional sperm parameters and sperm proteins. *Theriogenology* **2009**, *72*, 930–948. [CrossRef] [PubMed]
20. Yeste, M.; Estrada, E.; Casas, I.; Bonet, S.; Rodríguez-Gil, J.E. Good and bad freezability boar ejaculates differ in the integrity of nucleoprotein structure after freeze-thawing but not in ROS levels. *Theriogenology* **2013**, *79*, 929–939. [CrossRef] [PubMed]
21. Yeste, M.; Estrada, E.; Pinart, E.; Bonet, S.; Miró, J.; Rodríguez-Gil, J.E. The improving effect of reduced glutathione on boar sperm cryotolerance is related with the intrinsic ejaculate freezability. *Cryobiology* **2014**, *68*, 251–261. [CrossRef] [PubMed]
22. Kuisma, P.; Andersson, M.; Koskinen, E.; Katila, T. Fertility of frozen-thawed stallion semen cannot be predicted by the currently used laboratory methods. *Acta Vet. Scand.* **2006**, *48*, 14. [CrossRef] [PubMed]
23. Yeste, M.; Estrada, E.; Rocha, L.G.; Marín, H.; Rodríguez-Gil, J.E.; Miró, J. Cryotolerance of stallion spermatozoa is related to ROS production and mitochondrial membrane potential rather than to the integrity of sperm nucleus. *Andrology* **2015**, *3*, 395–407. [CrossRef] [PubMed]
24. Katila, T. In Vitro Evaluation of Frozen-Thawed Stallion Semen: A Review. *Acta Vet. Scand.* **2001**, *42*, 199–217. [CrossRef] [PubMed]
25. Macías García, B.; Morrell, J.M.; Ortega-ferrusola, C.; González-fernández, L.; Tapia, J.A.; Rodríguez-Martínez, H.; Peña, F.J. Centrifugation on a single layer of colloid selects improved quality spermatozoa from frozen-thawed stallion semen. *Anim. Reprod. Sci.* **2009**, *114*, 193–202. [CrossRef] [PubMed]
26. Prieto-Martínez, N.; Mateo, E.; Puig-Timonet, A.; Rodríguez-Gil, J.E.; Bonet, S.; Morató, R.; Yeste, M. Aquaporins 3 and 7 as cryotolerance markers in boar semen. *Reprod. Domest. Anim.* **2016**, *51* (Suppl. 2), 132.
27. Delgado-Bermúdez, A.; Llavanera, M.; Fernández-Bastit, L.; Recuero, S.; Mateo, Y.; Bonet, S.; Barranco, I.; Fernández-Fuertes, B.; Yeste, M. Aquaglyceroporins but not orthodox aquaporins are involved in the cryotolerance of pig spermatozoa. *J. Anim. Sci. Biotechnol.* **2019**, *10*, 77. [CrossRef] [PubMed]
28. Prieto-Martinez, N.; Vilagran, I.; Morato, R.; Rivera Del Alamo, M.M.; Rodriguez-Gil, J.E.; Bonet, S.; Yeste, M. Relationship of aquaporins 3 (AQP3), 7 (AQP7), and 11 (AQP11) with boar sperm resilience to withstand freeze-thawing procedures. *Andrology* **2017**, *5*, 1153–1164. [CrossRef] [PubMed]

29. Kenney, R.M.; Bergman, R.V.; Cooper, W.L.; Morse, F.W. Minimal contamination techniques for breeding mares: Techniques and preliminary findings. *Proc. Am. Assoc. Equine Pract.* **1975**, *21*, 327–336.
30. Petrunkina, A.M.; Waberski, D.; Bollwein, H.; Sieme, H. Identifying non-sperm particles during flow cytometric physiological assessment: A simple approach. *Theriogenology* **2010**, *73*, 995–1000. [CrossRef] [PubMed]
31. Garner, D.L.; Johnson, L.A. Viability assessment of mammalian sperm using SYBR-14 and propidium iodide. *Biol. Reprod.* **1995**, *53*, 276–284. [CrossRef] [PubMed]
32. Nagy, S.; Jansen, J.; Topper, E.K.; Gadella, B.M. A Triple-Stain Flow Cytometric Method to Assess Plasma- and Acrosome-Membrane Integrity of Cryopreserved Bovine Sperm Immediately after Thawing in Presence of Egg-Yolk Particles. *Biol. Reprod.* **2003**, *68*, 1828–1835. [CrossRef] [PubMed]
33. Rathi, R.; Colenbrander, B.; Bevers, M.M.; Gadella, B.M. Evaluation of in vitro capacitation of stallion spermatozoa. *Biol. Reprod.* **2001**, *65*, 462–470. [CrossRef] [PubMed]
34. Yeste, M.; Estrada, E.; Rivera Del Álamo, M.M.; Bonet, S.; Rigau, T.; Rodríguez-Gil, J.E. The increase in phosphorylation levels of serine residues of protein HSP70 during holding time at 17 °C is concomitant with a higher cryotolerance of boar spermatozoa. *PLoS ONE* **2014**, *9*, e90887. [CrossRef] [PubMed]
35. Ortega-Ferrusola, C.; Sotillo-Galán, Y.; Varela-Fernández, E.; Gallardo-Bolaños, J.M.; Muriel, A.; González-Fernández, L.; Tapia, J.A.; Peña, F.J. Detection of "Apoptosis-Like" Changes During the Cryopreservation Process in Equine Sperm. *J. Androl.* **2008**, *29*, 213–221. [CrossRef] [PubMed]
36. Yeste, M.; Fernández-Novell, J.M.; Ramió-Lluch, L.; Estrada, E.; Rocha, L.G.; Cebrián-Pérez, J.A.; Muiño-Blanco, T.; Concha, I.I.; Ramírez, A.; Rodríguez-Gil, J.E. Intracellular calcium movements of boar spermatozoa during 'in vitro' capacitation and subsequent acrosome exocytosis follow a multiple-storage place, extracellular calcium-dependent model. *Andrology* **2015**, *3*, 729–747. [CrossRef] [PubMed]
37. Harrison, R.A.P.; Mairet, B.; Miller, N.G.A. Flow Cytometric Studies of Bicarbonate-Mediated Ca2+ Influx in Boar Sperm Populations. *Mol. Reprod. Dev.* **1993**, *35*, 197–208. [CrossRef] [PubMed]
38. Kadirvel, G.; Kumar, S.; Kumaresan, A.; Kathiravan, P. Capacitation status of fresh and frozen-thawed buffalo spermatozoa in relation to cholesterol level, membrane fluidity and intracellular calcium. *Anim. Reprod. Sci.* **2009**, *116*, 244–253. [CrossRef] [PubMed]
39. Guthrie, H.D.; Welch, G.R. Determination of intracellular reactive oxygen species and high mitochondrial membrane potential in Percoll-treated viable boar sperm using fluorescence-activated flow cytometry. *J. Anim. Sci.* **2006**, *84*, 2089–2100. [CrossRef] [PubMed]
40. Gao, J.; Wang, X.; Chang, Y.; Zhang, J.; Song, Q.; Yu, H.; Li, X. Acetazolamide inhibits osmotic water permeability by interaction with aquaporin-1. *Anal. Biochem.* **2006**, *350*, 165–170. [CrossRef] [PubMed]
41. Tanimura, Y.; Hiroaki, Y.; Fujiyoshi, Y. Acetazolamide reversibly inhibits water conduction by aquaporin-4. *J. Struct. Biol.* **2009**, *166*, 16–21. [CrossRef] [PubMed]
42. Rezk, B.M.; Haenen, G.R.M.M.; van der Vijgh, W.J.F.; Bast, A. The antioxidant activity of phloretin: The disclosure of a new antioxidant pharmacophore in flavonoids. *Biochem. Biophys. Res. Commun.* **2002**, *295*, 9–13. [CrossRef]
43. Barreca, D.; Currò, M.; Bellocco, E.; Ficarra, S.; Laganà, G.; Tellone, E.; Giunta, M.L.; Visalli, G.; Caccamo, D.; Galtieri, A.; et al. Neuroprotective effects of phloretin and its glycosylated derivative on rotenone-induced toxicity in human SH-SY5Y neuronal-like cells. *BioFactors* **2017**, *43*, 549–557. [CrossRef] [PubMed]
44. Przybylo, M.; Procek, J.; Hof, M.; Langner, M. The alteration of lipid bilayer dynamics by phloretin and 6-ketocholestanol. *Chem. Phys. Lipids* **2014**, *178*, 38–44. [CrossRef] [PubMed]
45. Yu, L.; Rodriguez, R.A.; Chen, L.L.; Chen, L.Y.; Perry, G.; McHardy, S.F.; Yeh, C.K. 1,3-Propanediol Binds Deep Inside the Channel to Inhibit Water Permeation Through Aquaporins. *Protein Sci.* **2016**, *25*, 433–441. [CrossRef] [PubMed]
46. Yu, L.; Villarreal, O.D.; Chen, L.L.; Chen, L.Y. 1,3-Propanediol binds inside the water-conducting pore of aquaporin 4: Does this efficacious inhibitor have sufficient potency? *J. Syst. Integr. Neurosci.* **2016**, *2*, 91–98. [CrossRef] [PubMed]
47. Jakobsen, E.; Lange, S.C.; Andersen, J.V.; Desler, C.; Kihl, H.F.; Hohnholt, M.C.; Stridh, M.H.; Rasmussen, L.J.; Waagepetersen, H.S.; Bak, L.K. The inhibitors of soluble adenylate cyclase 2-OHE, KH7, and bithionol compromise mitochondrial ATP production by distinct mechanisms. *Biochem. Pharmacol.* **2018**, *155*, 92–101. [CrossRef] [PubMed]

48. Lark, D.S.; Reese, L.R.; Ryan, T.E.; Torres, M.J.; Smith, C.D.; Lin, C.; Neufer, P.D. Protein Kinase A Governs Oxidative Phosphorylation Kinetics and Oxidant Emitting Potential at Complex I. *Front. Physiol.* **2015**, *6*, 332. [CrossRef] [PubMed]
49. Nishigaki, T.; José, O.; González-Cota, A.L.; Romero, F.; Treviño, C.L.; Darszon, A. Intracellular pH in Sperm Physiology. *Biochem. Biophys. Res. Commun.* **2014**, *450*, 1149–1158. [CrossRef] [PubMed]
50. Yeste, M. Sperm cryopreservation update: Cryodamage, markers, and factors affecting the sperm freezability in pigs. *Theriogenology* **2016**, *85*, 47–64. [CrossRef] [PubMed]
51. Pohl, P.; Rokitskaya, T.I.; Pohl, E.E.; Saparov, S.M. Permeation of phloretin across bilayer lipid membranes monitored by dipole potential and microelectrode measurements. *Biochim. Biophys. Acta Biomembr.* **1997**, *1323*, 163–172. [CrossRef]
52. Wacker, S.J.; Aponte-Santamaría, C.; Kjellbom, P.; Nielsen, S.; De Groot, B.L.; Rützler, M. The identification of novel, high affinity AQP9 inhibitors in an intracellular binding site. *Mol. Membr. Biol.* **2013**, *30*, 246–260. [CrossRef] [PubMed]
53. Miller, E.W.; Dickinson, B.C.; Chang, C.J. Aquaporin-3 mediates hydrogen peroxide uptake to regulate downstream intracellular signaling. *Proc. Natl. Acad. Sci. USA* **2010**, *107*, 15681–15686. [CrossRef] [PubMed]
54. Cooper, T.G.; Barfield, J.P.; Yeung, C.H. The tonicity of murine epididymal spermatozoa and their permeability towards common cryoprotectants and epididymal osmolytes. *Reproduction* **2008**, *135*, 625–633. [CrossRef] [PubMed]
55. Widiasih, D.; Yeung, C.H.; Junaidi, A.; Cooper, T.G. Multistep and single-step treatment of human spermatozoa with cryoprotectants. *Fertil. Steril.* **2009**, *92*, 382–389. [CrossRef] [PubMed]
56. Lopes, C.A.; Alves, A.M.; Jewgenow, K.; Báo, S.N.; de Figueiredo, J.R. Cryopreservation of canine ovarian cortex using DMSO or 1,3-propanediol. *Theriogenology* **2016**, *86*, 1165–1174. [CrossRef] [PubMed]
57. Pogozhykh, D.; Prokopyuk, V.; Pogozhykh, O.; Mueller, T.; Prokopyuk, O. Influence of factors of cryopreservation and hypothermic storage on survival and functional parameters of multipotent stromal cells of placental origin. *PLoS ONE* **2015**, *10*, e0139834. [CrossRef] [PubMed]

Paper V

HVCN1 but not potassium channels are related to mammalian sperm cryotolerance.

Ariadna Delgado-Bermúdez, Yentel Mateo-Otero, Marc Llavanera, Sergi Bonet, Marc Yeste, Elisabeth Pinart.

International Journal of Molecular Sciences,

2021;22(4):1646

doi: 10.3390/ijms22041646

International Journal of
Molecular Sciences

MDPI

Article

HVCN1 but Not Potassium Channels Are Related to Mammalian Sperm Cryotolerance

Ariadna Delgado-Bermúdez [1,2], Yentel Mateo-Otero [1,2], Marc Llavanera [1,2], Sergi Bonet [1,2], Marc Yeste [1,2] and Elisabeth Pinart [1,2,*]

[1] Biotechnology of Animal and Human Reproduction (TechnoSperm), Institute of Food and Agricultural Technology, University of Girona, E-17003 Girona, Spain; ariadna.delgado@udg.edu (A.D.-B.); yentel.mateo@udg.edu (Y.M.-O.); marc.llavanera@udg.edu (M.L.); sergi.bonet@udg.edu (S.B.); marc.yeste@udg.edu (M.Y.)
[2] Unit of Cell Biology, Department of Biology, Faculty of Sciences, University of Girona, E-17003 Girona, Spain
* Correspondence: elisabeth.pinart@udg.edu; Tel.: +34-972-419-514

Abstract: Little data exist about the physiological role of ion channels during the freeze–thaw process in mammalian sperm. Herein, we determined the relevance of potassium channels, including SLO1, and of voltage-gated proton channels (HVCN1) during mammalian sperm cryopreservation, using the pig as a model and through the addition of specific blockers (TEA: tetraethyl ammonium chloride, PAX: paxilline or 2-GBI: 2-guanidino benzimidazole) to the cryoprotective media at either 15 °C or 5 °C. Sperm quality of the control and blocked samples was performed at 30- and 240-min post-thaw, by assessing sperm motility and kinematics, plasma and acrosome membrane integrity, membrane lipid disorder, intracellular calcium levels, mitochondrial membrane potential, and intracellular $O_2^{\bullet -}$ and H_2O_2 levels. General blockade of K^+ channels by TEA and specific blockade of SLO1 channels by PAX did not result in alterations in sperm quality after thawing as compared to control samples. In contrast, HVCN1-blocking with 2-GBI led to a significant decrease in post-thaw sperm quality as compared to the control, despite intracellular $O_2^{\bullet -}$ and H_2O_2 levels in 2-GBI blocked samples being lower than in the control and in TEA- and PAX-blocked samples. We can thus conclude that HVCN1 channels are related to mammalian sperm cryotolerance and have an essential role during cryopreservation. In contrast, potassium channels do not seem to play such an instrumental role.

Keywords: cryopreservation; sperm; HVCN1 channels; SLO1 channels; potassium channels; pigs

Citation: Delgado-Bermúdez, A.; Mateo-Otero, Y.; Llavanera, M.; Bonet, S.; Yeste, M.; Pinart, E. HVCN1 but Not Potassium Channels Are Related to Mammalian Sperm Cryotolerance. *Int. J. Mol. Sci.* **2021**, 22, 1646. https://doi.org/10.3390/ijms22041646

Academic Editor: Felipe Martinez-Pastor
Received: 30 December 2020
Accepted: 28 January 2021
Published: 6 February 2021

1. Introduction

Ion channels are essential for sperm physiology during spermatogenesis, epididymal maturation, and storage, transit throughout the female reproductive tract and interaction with the oocyte [1]. Since the first identification of cation sperm channels (CatSper) in the plasma membrane of mouse spermatozoa in 2001 [2], several studies have investigated different ion channels and their relevance for sperm function (reviewed in [3]). These studies were usually performed in mouse and human sperm and focused on the physiological role of these ion channels during sperm capacitation. In contrast, little data exist about the types of ion channels present in the sperm of other mammalian species, as well as on their functional significance in sperm differentiation, maturation and adaptation to the surrounding medium, and their relationship with sperm cryotolerance.

Cryopreservation is the most efficient method for long-term storage of sperm. In humans, it is crucial for fertility preservation strategies [4,5], and in domestic animals it is frequently used as a technique to accelerate the rate of genetic improvement [6]. However, the freeze–thaw process induces destabilization of plasma membrane, nuclear alterations, changes in sperm proteins and the lateral phase separation of lipid membrane components; alters the permeability of plasma membrane to water and ions; and impairs mitochondrial activity [7–10]. Proteins and lipids in cryoprotective media provide a partial protection

from these deleterious effects (reviewed in [7]). Freezability or cryotolerance refers to the resilience of sperm cells to cryopreservation and shows great variability between species, mainly due to differences in membrane composition [8,11,12]. Cryotolerance is lower in pig than in bovine and human sperm; this low ability of pig sperm to withstand freeze–thaw damage is related to the low content of cholesterol [13] and high content of polyunsaturated fatty acids [14] of the plasma membrane. Moreover, great variability in sperm cryotolerance has been observed between breeds, between individuals of the same breed, and even between ejaculates from the same animal [7,10,15].

Recent research has been focused on the identification of cryotolerance markers for sperm of different species, including the pig [9,10,15]. A wide variety of proteins have been proposed as candidate biomarkers of sperm freezability, ranging from membrane transporters and receptors to enzymes [9,10,15–19]. Several membrane transporters exert a crucial role during sperm cryopreservation, among them to highlight hexose transporters [16,20] and aquaporins and aquaglyceroporins [9,21]. Nevertheless, few data exist about the role of ion channels during sperm cryopreservation, not only in pigs but also in other mammalian species, including humans.

While previous studies have immunolocalized both SLO1 potassium channels and voltage-gated proton channels (HVCN1) in the plasma membrane of mammalian spermatozoa (human [22–24], cattle [1], and pig [25,26]) and support a role for them during sperm capacitation, none has investigated whether they are involved in sperm cryotolerance. Therefore, the main objective of the present research is to elucidate the physiological role of SLO1 and HVCN1 channels during mammalian sperm cryopreservation. The study uses the pig as a model, as the presence and functional relevance of these channels during sperm capacitation have been previously reported in this species [25,26].

This functional approach was performed pharmacologically by the addition of specific SLO1- and HVCN1-blockers to cryopreservation media and further analysis of sperm quality in frozen–thawed samples. Three different blockers were used: (1) Paxilline (PAX), a fungal indole alkaloid that acts as a potent and specific inhibitor of SLO1 channels [27,28]; (2) tetraethyl ammonium chloride (TEA), a quaternary ammonium compound with a broad inhibiting effect on several K^+ transporters [27,29]; and (3) 2-guanidino benzimidazole (2-GBI), a specific inhibitor of HVCN1 channels [30,31]. As aforementioned, all these blockers have been previously used to analyze the function of SLO1 [25] and HVCN1 channels [26] during in vitro capacitation of pig spermatozoa.

2. Results

To understand the general role of K^+ channels and the specific role SLO1 and HVCN1 channels during sperm cryopreservation, two experiments were designed. In Experiment 1, sperm samples were cryopreserved in the presence of TEA, PAX, or 2-GBI blockers which were added to LEY medium at 15 °C. In Experiment 2, blockers were added to LEYGO medium at 5 °C.

2.1. Sperm Viability

Post-thaw sperm viability, expressed as the percentage of spermatozoa with an intact plasma membrane, did not differ significantly between the control and samples blocked with TEA and PAX in Experiment 1 ($P > 0.05$) and Experiment 2 ($P > 0.05$). In contrast, the addition of 2-GBI to LEY medium at 15 °C (Experiment 1) and to LEYGO medium at 5 °C (Experiment 2) led to a significant decrease in sperm viability at both 30 min and 240 min post-thaw ($P < 0.05$) as compared to the control and TEA- and PAX-blocked samples (Figure 1).

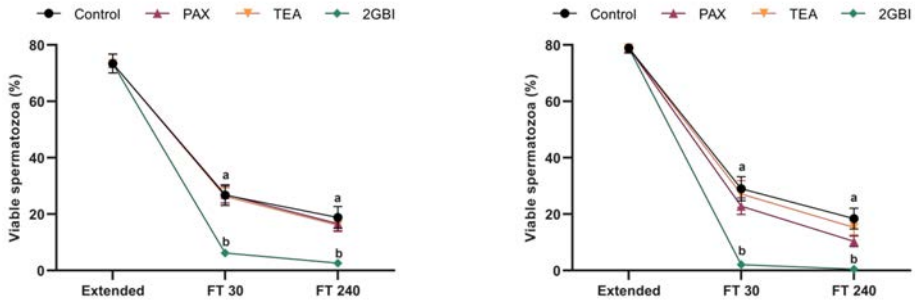

(**a**) (**b**)

Figure 1. Percentages of viable spermatozoa (SYBR14$^+$/PI$^-$) in extended and frozen–thawed (FT) samples at 30 min and 240 min post-thaw. In Experiment 1 (n = 8), TEA, PAX, and 2-GBI blockers were added to LEY medium at 15 °C (**a**), whereas in Experiment 2 (n = 9), they were added to LEYGO medium at 5 °C (**b**). Different superscripts indicate significant differences ($P < 0.05$) between samples within the same time point. Results are given as mean ± SEM.

2.2. Sperm Motility

In Experiment 1, percentages of total and progressively motile spermatozoa did not differ between the control and samples blocked with TEA and PAX at either 30- or 240-min post-thaw ($P > 0.05$; Figure 2a,c). The addition of 2-GBI resulted in a significant decrease in total motility at 30 min post-thaw ($P < 0.05$), but not in progressive motility ($P > 0.05$). After 240 min of thawing, sperm motility did not differ between the control and blocked samples ($P > 0.05$). The analysis of sperm kinematics showed a lack of significant differences between the control and samples blocked with TEA and PAX in post-thaw curvilinear (VCL) and straight-line (VSL) velocities ($P > 0.05$). In contrast, HVCN1-blocking with 2-GBI led to a significant decrease in VCL at 30 min post-thaw ($P < 0.05$) and in VSL at both 30 min and 240 min post-thaw ($P < 0.05$) (Figure 3a,c). Other kinematics parameters that were evaluated showed similar trends (data not shown).

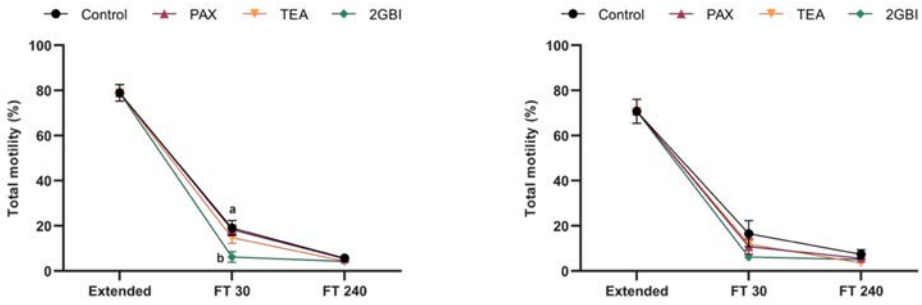

(**a**) (**b**)

Figure 2. *Cont.*

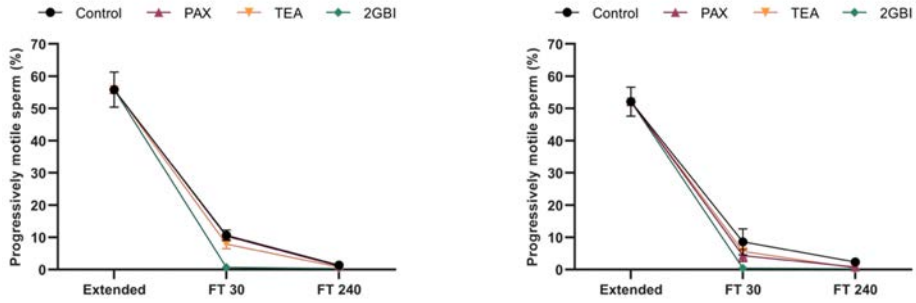

Figure 2. Percentages of total (**a**,**b**) and progressive (**c**,**d**) motile spermatozoa in extended and frozen–thawed (FT) samples at 30 min and 240 min post-thaw. In Experiment 1 (n = 8), TEA, PAX, and 2-GBI blockers were added to LEY medium at 15 °C (**a**,**c**), whereas in Experiment 2 (n = 9), they were added to LEYGO medium at 5 °C (**b**,**d**). Different superscripts indicate significant differences ($P < 0.05$) between samples within the same time point. Results are given as mean ± SEM.

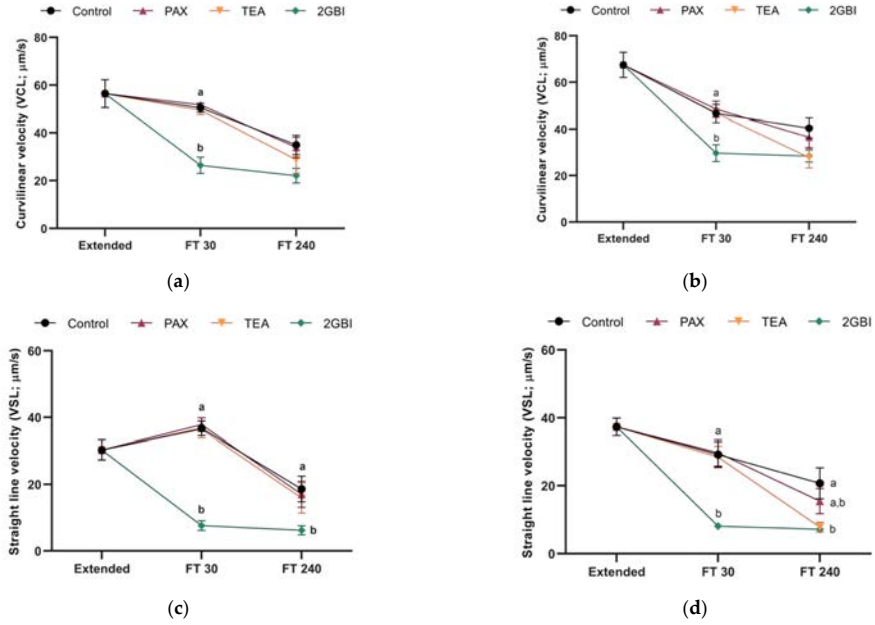

Figure 3. Curvilinear velocity (VCL; **a**,**b**) and straight-line velocity (VSL; **c**,**d**) in extended and frozen–thawed (FT) samples at 30 min and 240 min post-thaw. In Experiment 1 (n = 8), TEA, PAX, and 2-GBI blockers were added to LEY medium at 15 °C (**a**,**c**), whereas in Experiment 2 (n = 9), they were added to LEYGO medium at 5 °C (**b**,**d**). Different superscripts indicate significant differences ($P < 0.05$) between samples within the same time point. Results are given as mean ± SEM.

In experiment 2, post-thaw sperm motility did not differ significantly between the control and blocked samples, regardless of the inhibitor ($P > 0.05$; Figure 2b,d). The comparative analysis of sperm kinematics showed a different effect depending on the blocker. Therefore, as compared to the control, blocking samples with TEA led to a

significant decrease in VSL at 240 min post-thaw ($P < 0.05$). In addition, while samples blocked with PAX did not show changes in VCL or VSL ($P > 0.05$), inhibition of HVCN1 channels with 2-GBI led to a significant decrease in VCL at 30 min post-thaw ($P < 0.05$) and in VSL at both 30 min and 240 min post-thaw ($P < 0.05$; Figure 3b,d). Other parameters evaluated in kinematics analysis showed similar trends (data not shown).

2.3. Acrosome Integrity

Post-thaw acrosome integrity, expressed as percentages of viable spermatozoa with an intact acrosome, was not affected by the addition of TEA or PAX to LEY medium at 15 °C (Experiment 1; $P > 0.05$) or to LEYGO medium at 5 °C (Experiment 2; $P > 0.05$). In contrast, the addition of 2-GBI to LEY and LEYGO media led to a significant decrease of acrosome integrity at 30- and 240-min post-thawing ($P < 0.05$; Figure 4).

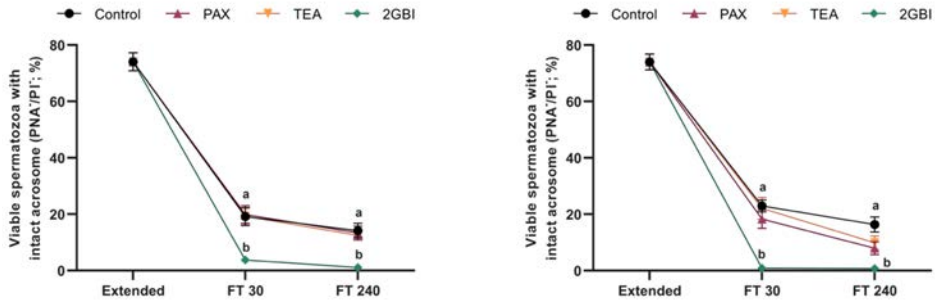

Figure 4. Percentages of viable spermatozoa with an intact acrosome in extended and frozen-thawed (FT) samples at 30 min and 240 min post-thaw. In experiment 1 ($n = 8$), TEA, PAX, and 2-GBI blockers were added to LEY medium at 15 °C (**a**), whereas in experiment 2 ($n = 9$), they were added to LEYGO medium at 5 °C (**b**). Different superscripts indicate significant differences ($P < 0.05$) between samples within the same time point. Results are given as mean ± SEM.

2.4. Membrane Lipid Disorder

In Experiment 1, percentages of viable spermatozoa with high membrane lipid disorder at post-thaw did not differ between the control and samples blocked with TEA and PAX ($P > 0.05$). 2-GBI blockade resulted in a significant increase in this percentage at 30 min post-thaw ($P < 0.05$). However, at 240 min post-thaw, this parameter did not differ significantly between the control and TEA- and PAX-blocked samples ($P > 0.05$; Figure 5).

In Experiment 2, the percentage of viable spermatozoa with high membrane disorder was significantly higher in 2-GBI blocked samples than in the control and samples blocked with TEA and PAX ($P < 0.05$).

2.5. Intracellular Levels of Calcium

Addition of TEA and PAX blockers at either LEY medium at 15 °C (Experiment 1) or LEYGO medium at 5 °C (Experiment 2) did not alter the percentage of viable spermatozoa with high calcium levels in comparison to control samples ($P > 0.05$). In contrast, blocking HVCN1 channels with 2-GBI resulted in a significant decrease in this parameter when added to LEY and LEYGO media ($P < 0.05$; Figure 6).

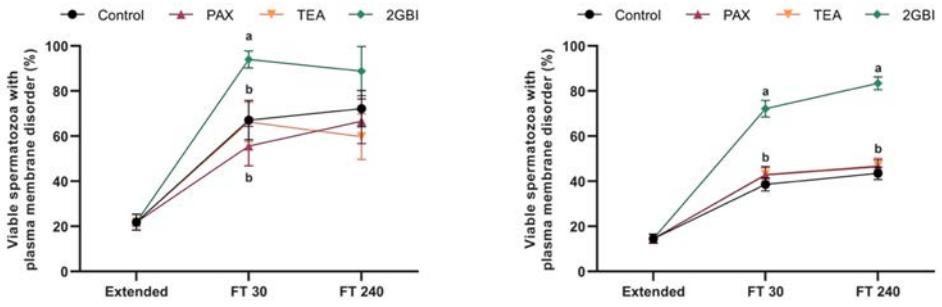

Figure 5. Percentages of viable spermatozoa with high membrane lipid disorder in extended and frozen–thawed (FT) samples at 30 min and 240 min post-thaw. In Experiment 1 (n = 8), TEA, PAX, and 2-GBI blockers were added to LEY medium at 15 °C (**a**), whereas in Experiment 2 (n = 9), they were added to LEYGO medium at 5 °C (**b**). Different superscripts indicate significant differences ($P < 0.05$) between samples within the same time point. Results are given as mean ± SEM.

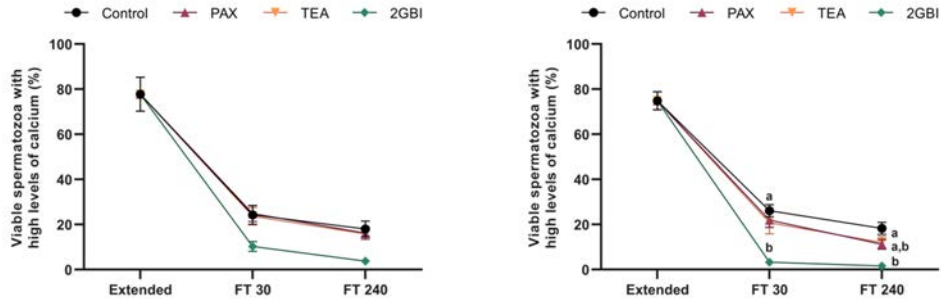

Figure 6. Percentages of viable spermatozoa with high levels of intracellular calcium in extended samples and frozen—30 min and 240 min post-thaw. In Experiment 1 (n = 8), TEA, PAX, and 2-GBI blockers were added to LEY medium at 15 °C (**a**), whereas in Experiment 2 (n = 9), they were added to LEYGO medium at 5 °C (**b**). Different superscripts indicate significant differences ($P < 0.05$) between samples within the same time point. Results are given as mean ± SEM.

2.6. Mitochondrial Membrane Potential

$JC1_{agg}/JC1_{mon}$ fluorescence ratio in the population of sperm with intermediate MMP ($JC1_{agg}{}^{+}/JC1_{mon}{}^{+}$ spermatozoa) did not differ between frozen–thawed control samples or samples blocked with PAX and TEA in either Experiment 1 ($P > 0.05$) or Experiment 2 ($P > 0.05$). In contrast, this parameter was significantly higher in 2-GBI blocked samples than in the control and samples blocked with TEA and PAX at 240 min post-thaw when added to LEYGO medium ($P < 0.05$; Figure 7b). This effect was also observed when 2-GBI was added to LEY medium, but differences were not significant ($P > 0.05$; Figure 7a).

2.7. Intracellular Levels of Mitochondrial Superoxide ($O_2{}^{\bullet -}$)

In Experiment 1 and Experiment 2, the pattern of variation in the percentage of viable spermatozoa with high levels of mitochondrial superoxide did not differ between the control and samples blocked with TEA and PAX ($P > 0.05$). In contrast, the addition of 2-GBI to LEYGO medium (Experiment 2) resulted in a significant decrease in this percentage

as compared to both the control and samples blocked with TEA or PAX ($P < 0.05$; Figure 8b). These differences were not significant in Experiment 1 ($P > 0.05$; Figure 8a).

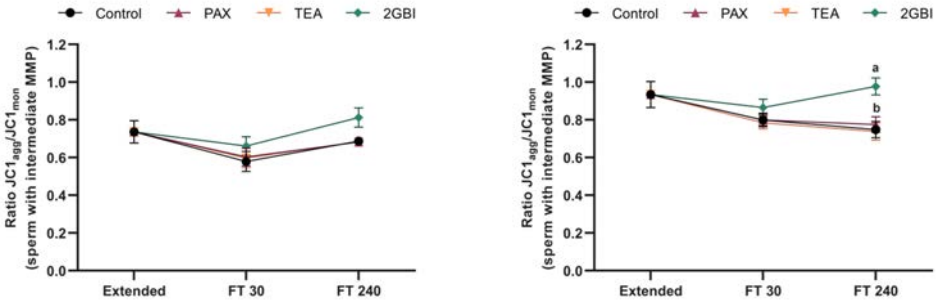

Figure 7. $JC1_{agg}/JC1_{mon}$ ratios in extended and frozen–thawed (FT) samples at 30 min and 240 min post-thaw. In Experiment 1 ($n = 8$), TEA, PAX, and 2-GBI blockers were added to LEY medium at 15 °C (**a**), whereas in Experiment 2 ($n = 9$), they were added to LEYGO medium at 5 °C (**b**). Different superscripts indicate significant differences ($P < 0.05$) between samples within the same time point. Results are given as mean ± SEM.

2.8. Intracellular Levels of Hydrogen Peroxide (H_2O_2)

In Experiment 1, percentages of viable spermatozoa with high levels of H_2O_2 did not differ between the control and samples blocked with PAX and TEA at 30 min and 240 min post-thaw. In samples blocked with 2-GBI, this percentage tended to be lower than in the control and in samples blocked with TEA and PAX, but differences were not significant ($P > 0.05$; Figure 8c).

In Experiment 2, a blocking effect was observed on the percentage of viable spermatozoa with high levels of H_2O_2. In contrast, TEA blocker did not alter this percentage as compared to control samples at either 30 min or 240 min post-thaw ($P > 0.05$). This parameter tended to decrease in the presence of PAX blocker at 240 min post-thaw, but differences were not significant ($P > 0.05$). In contrast, in the case of the 2-GBI blocker differences became significant from 30 min post-thaw ($P < 0.05$; Figure 8d).

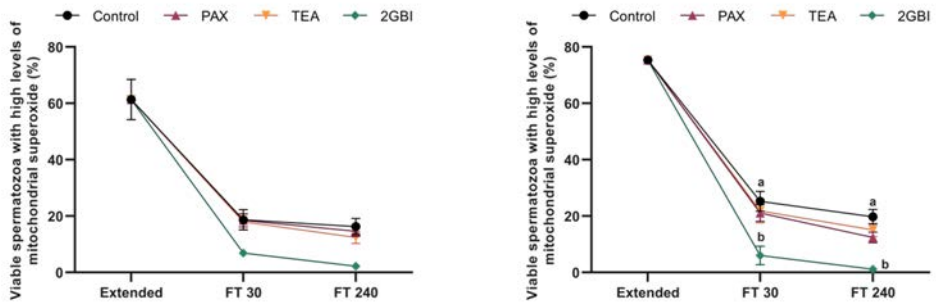

Figure 8. *Cont.*

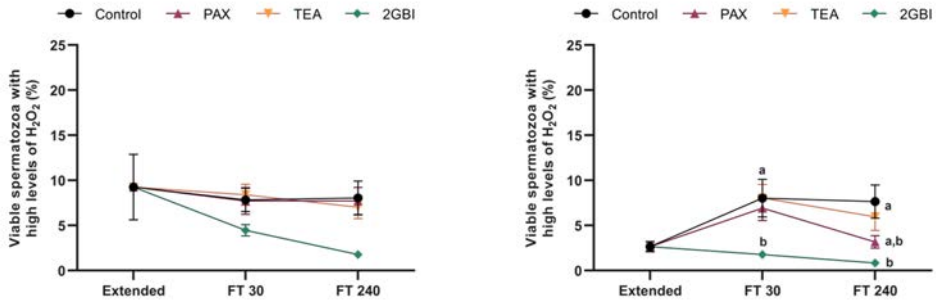

Figure 8. Mitochondrial superoxide levels expressed as percentages of viable spermatozoa Mito-E^+/YO-PRO-1^- (**a**,**b**), and peroxide levels expressed as percentages of viable spermatozoa DCF^+/PI^-, (**c**,**d**) in extended and frozen–thawed (FT) samples at 30 min and 240 min post-thaw. In Experiment 1 (n = 8), TEA, PAX, and 2-GBI blockers were added to LEY medium at 15 °C (**a**,**c**), whereas in Experiment 2 (n = 9), they were added to LEYGO medium at 5 °C (**b**,**d**). Different superscripts indicate significant differences ($P < 0.05$) between samples within the same time point. Results are given as mean ± SEM.

3. Discussion

Sperm cryopreservation has been extensively studied in different mammalian species, given its potential applications for safeguarding fertility. Due to the great sensitivity of sperm to freeze–thawing, previous research has been focused on both the changes in plasma membrane permeability to water and cryoprotectants [9,21] and the identification of biological markers to predict sperm cryotolerance [4,5,9,10,15,32–35]. Previous studies have also demonstrated the critical role of aquaporins (AQPs) in regulating the transport of water and cryoprotectants across cell membranes and in preventing osmotic damage [9,36–38]. While ion channels have been reported to be involved in sperm adaptation to changes in the osmolality of the surrounding medium [2], their physiological role during sperm cryopreservation has been less studied.

The present study analyses the general role of K^+ channels and the specific role of SLO1 and HVCN1 channels during sperm cryopreservation. This functional approach was performed by adding distinct inhibitors (TEA, PAX, or 2-GBI) to LEY medium at 15 °C or to LEYGO medium at 5 °C; and used the pig as a model. The concentration of these three inhibitors was determined in previous studies [25,26]. The results obtained herein indicate that blocking K^+- and HVCN1-channels during sperm cryopreservation has a different impact upon sperm quality after thawing. In effect, while TEA and PAX, which are inhibitors of K^+ channels, did not alter post-thaw sperm function and survival as compared to the control at either 30 min or 240 min post-thaw, blocking HVCN1 channels with 2-GBI resulted in a dramatic impairment of post-thaw sperm quality.

Unexpectedly, the general blockade of K^+ channels and the specific blockade of SLO1, either when samples were kept at 15 °C or after being cooled down to 5 °C, did not induce alterations in plasma and acrosome membrane integrity, sperm motility, and kinematics, membrane lipid disorder, intracellular calcium levels, mitochondrial membrane potential or $O_2^{\bullet -}$ and H_2O_2 production. To the best of the authors' knowledge, neither the physiological role of K^+ channels nor that of the HVCN1 ones during sperm cryopreservation has been previously studied. On the other hand, little data exist about the nature, distribution, and function of K^+- and HVCN1-channels in mammalian sperm. SLO channels are the main K^+ channels in human and mouse sperm, and they are involved in the regulation of sperm volume and capacitation [39–41]. However, both species differ in the types and regulation mechanisms of SLO channels; in mouse sperm the predominant form is SLO3, which localizes in the principal piece [3,42–45], whereas the plasma membrane of human

sperm contains SLO1 channels, which are localized in the principal piece, and SLO3 channels, which are distributed throughout the whole flagellum [40,46]. SLO1 channels are activated by both increased membrane voltage and intracellular Ca^{2+} levels [27,47], and SLO3 channels are highly sensitive to intracellular alkalinization [41]. SLO1 channels have also been identified in the acrosomal and post-acrosomal region of the sperm head, and in the mid-, principal, and terminal pieces of the flagellum of pig sperm [25]. Despite this wide distribution, some studies suggest that not only SLO1 channels but also other K^+ channels are involved in K^+ conductance over the pig sperm flagellum [25]. In bovine sperm, two different types of K^+ channels have been identified, the chloride and potassium ion channel 3 (CLC-3) and the two-pore domain channel (TASK-2) [48].

Considering the physiological role of K^+ channels during spermatogenesis, sperm maturation and capacitation [2,25], the biological significance of our present results is uncertain. Lack of differences between the control and samples blocked with TEA and PAX suggest that either K^+ channels are not relevant for osmolar adaptation of pig sperm during cryopreservation, or that alterations in K^+ conductance have a modest impact on post-thaw sperm quality. In this regard, further studies must be oriented towards determining the effects of cryopreservation on the relative content, functional activity, and conductance of K^+ channels in pig sperm. Interestingly, cryopreservation of bovine sperm does not alter the amount of CLC-3 and TASK-2 channels, but it is associated to an increase of intracellular potassium levels [48]. As not only do the types of K^+ channels differ between species but also their regulatory mechanisms, research in this field is much warranted.

K^+ efflux is essential for sperm capacitation as it underlies the changes in motility patterns during sperm hyperactivation, plasma membrane hyperpolarization, calcium influx, and acrosome exocytosis [3,25,46,49]. The biological significance of these differences between sperm cryopreservation and capacitation remain unclear, but they seem to be related with differences in the composition of the surrounding environment. In this regard, the activation of K^+ channels in human sperm has been strongly related with presence of divalent cations in the extracellular medium [40]. Nevertheless, further research is necessary to understand the physiological regulation of K^+ channels in sperm cells.

The alteration of nearly all sperm parameters after 2-GBI blockade supports the physiological relevance of HVCN1 channels and of H^+ conductance during sperm cryopreservation. HVCN1 channels have an essential regulating role in several cell types (reviewed in [50]) by driving protons unidirectionally to the extracellular medium [30], despite their functional significance in mammalian sperm being poorly understood. While HVCN1 channels are present in the plasma membrane of human, macaque, cattle and pig sperm, they are absent from mouse sperm [1,23,24,46,51]. Remarkably, in macaques, sperm cryopreservation results in a decreased content of HVCN1 channels in the plasma membrane [48].

Blockade of HVCN1 channels during cryopreservation led to reduced sperm viability, expressed as spermatozoa exhibiting an intact plasma membrane integrity, and reduced sperm motility and kinematics after thawing. In previous studies, inactivation of HVCN1 channels has been reported to result in decreased sperm viability in ejaculated human [52] and bovine sperm [1], since this makes these cells unable to regulate their inner pH [23]. Nevertheless, little data exist about the changes in the intracellular pH throughout the cryopreservation procedure. Only a single study reported a slight decrease of inner pH in cryopreserved bovine sperm [48]. Blocking HVCN1 channels also leads to a decrease in the motility and velocity of in vitro capacitated sperm from pigs [26] and humans [22]. In bovine [1] and human sperm [23], these channels are essential for activation of progressive motility upon ejaculation and for hyperactivation during capacitation. Moreover, in humans, HVCN1 activity is higher in capacitated than in non-capacitated sperm due to the phosphorylation of this channel during capacitation [22,23].

After thawing, samples blocked with 2-GBI showed reduced percentages of viable spermatozoa with high calcium levels in the sperm tail, which were determined by Fluo3 staining. These reduced intracellular calcium levels in the flagellum could be related with

the low sperm motility and velocity in HVCN1-blocked samples as compared to the control. Only few data exist regarding the relationship between H^+ and Ca^{2+} conductance. In spite of that, and in the same line of our results, Yeste et al. [26] also observed a decrease in intracellular calcium levels in the flagellum during acrosome reaction when 2-GBI was added to pig spermatozoa. Therefore, further studies are needed to elucidate the potential interaction between this inhibitor and calcium channels present in the sperm tail.

Cryopreservation has been extensively related to capacitation-like processes or cryocapacitation, which manifest in premature acrosomal exocytosis and altered plasma membrane permeability, and result in diminished sperm lifespan and the appearance of apoptotic-like changes (reviewed in [7]). As compared to control samples, blocking HVCN1 channels with 2-GBI led to a reduced percentage of viable spermatozoa with an intact acrosome and an increased percentage of viable spermatozoa with high membrane lipid disorder after thawing. In contrast, these percentages did not differ between the control and samples blocked with TEA (K^+ channel blockade) or PAX (SLO1 channel blockade). In agreement with these findings, previous studies in pig and human sperm also demonstrated that HVCN1 blockade during in vitro capacitation induces premature acrosomal exocytosis, high plasma membrane lipid disorder and increased Ca^{2+} levels in the sperm head [26,52], whereas K^+ channel blockade does not trigger such a sequence of events [25]. Together, these results strongly suggest that in pigs HVCN1 channels are essential for sperm homeostasis during in vitro capacitation and cryopreservation and for preventing premature sperm activation.

In control samples, cryopreservation resulted in an increase of ROS production associated to high mitochondrial membrane potential, as being extensively reported in previous studies investigating sperm cryopreservation [6,9,10]. Moreover, we also found that while blocking HVCN1 channels with 2-GBI led to increased mitochondrial membrane potential at 240 min post-thaw, it unexpectedly reduced $O_2^{\bullet -}$ and H_2O_2 levels at both 30- and 240-min post-thaw. In contrast, the blockade of aquaporin channels prior to pig sperm cryopreservation results in an increase of both mitochondrial membrane potential and intracellular ROS levels [9]. This increase in intracellular ROS levels seems to be a direct consequence of the blocking of these channels, since aquaglyceroporins are not exclusively permeable to water, but also to other small molecules, such as H_2O_2, which might accumulate intracellularly [9]. It must be considered that sperm cytoplasm contains a set of antioxidant enzymes, such as glutathione peroxidase (GPx), superoxide dismutase (SOD), glutathione S-transferase Mu 3 (GSTM3), and AMP-activated protein kinase (AMPK), which are damaged during cryopreservation, thus resulting in a low ability of sperm to scavenge ROS [6,10]. Nevertheless, in pig sperm, the protective effect against ROS damage of antioxidative agents added to freezing media is associated to an increased activity of antioxidant enzymes [6]. Taken all the aforementioned into account and considering that HVCN1 channels are involved in the generation of superoxide radicals from mitochondrial membrane chain by activation of NADPH oxidase [53,54], one could surmise that the decrease in ROS levels might be a direct consequence of HVCN1 blockade during sperm cryopreservation.

4. Materials and Methods

4.1. Materials

Chemicals and fluorochromes were provided by either Sigma-Aldrich Química (Madrid, Spain) or ThermoFisher Scientific (Waltham, MA, USA). In case of another supplier, it is specified next to the product.

4.2. Semen samples

The present study included ejaculates from 17 Piétrain boars from an artificial insemination program, and an age range between 18 and 24 months. Boars were randomly distributed into two groups, one per experiment, of 8 and 9 males, respectively. According to the Animal Welfare Regulations of the Regional Government of Catalonia (Spain), ani-

mals were hosted in standard conditions of temperature and humidity. Feed was provided once daily and water ad libitum. Semen samples were obtained twice a week following the standard protocols for commercial seminal doses in a local farm (Semen Cardona, Cardona, Barcelona, Spain). Considering that authors did not manipulate any animal, specific approval from an Ethics Committee was not needed.

Immediately after collection, the sperm-rich fraction of each ejaculate was filtered through gauze, and diluted 1:1 (v:v) in a long-term extender (Vitasem, Magapor, S.L., Zaragoza, Spain) at 37 °C inside a collecting recipient. Diluted sperm-rich fraction was cooled to 17 °C and were transported to the lab in a thermal insulated box. Time between semen extraction and dose arrival to the lab never exceeded five hours. Before sample processing, diluted sperm-rich fraction was divided into two fractions, a fresh fraction and a fraction intended to cryopreservation. After assessing the sperm quality in the fresh fraction, the other fraction was processed for cryopreservation either in the absence or presence of inhibitors.

4.3. Sperm cryopreservation

Th fraction intended to cryopreservation was divided into 50-mL aliquots and centrifuged at 15 °C and 2400× *g* for 3 min. The procedure included five steps [6,7]: (1) Pellet resuspension in β-lactose-egg yolk freezing medium (LEY medium: 80% (*v*/*v*) lactose and 20% (*v*/*v*) egg yolk) at 15 °C to a final concentration of 1.5×10^9 spermatozoa/mL; (2) sample dilution in LEY and cooling down to 5 °C at a ratio of −0.1 °C/min (180 min) in a programmable freezer (Icecube 14S-B; Minitüb Ibérica SL; Tarragona, Spain); (3) sample cooling at 5 °C and dilution in LEYGO medium (LEY medium supplemented with 6% (*v*/*v*) glycerol and 1.5% Orvus ES Paste; Equex STM; Nova Chemical Sales Inc., Scituate, MA, USA) to 1×10^9 spermatozoa/mL; (4) packaging of cooled and diluted samples into 0.5-mL plastic straws (Minitüb Ibérica, S.L.) and frozen in a programmable freezer (Icetube 14S-B; Minitub Ibérica, S.L), with the freezing ramp [17]: −6 °C/min from 5 °C to −5 °C (100 s), −39.82 °C/min from −5 °C to −80 °C (113 s), holding at −80 °C for 30 s, and cooling at −60 °C/min from −80 °C to −150 °C (70 s); and (5) plunging of frozen straws into liquid nitrogen (−196 °C) for long-term storage.

4.4. Experimental Design

To determine the involvement of HVCN1 and SLO1 channels on sperm cryotolerance, samples were cryopreserved in the presence or the absence of either paxilline (PAX), tetraethyl ammonium chloride (TEA), or 2-guanidinobenzimidazole (2-GBI). Two sets of experiments were designed.

In the first experiment, inhibitors were added to aliquots containing sperm resuspended with LEY at 15 °C (Step 1). For this purpose, aliquots diluted with LEY were distributed into four subfractions, one for each inhibitor (i.e., PAX, TEA, and 2-GBI) and a non-treated control. In the second experiment, inhibitors were added to aliquots containing LEYGO at 5 °C (Step 3). Again, aliquots were split into four subfractions, one for each inhibitor plus a non-treated control. In both experiments, the final inhibitor concentration was 100 nM for PAX, 20 mM for TEA, and 10 mM for 2-GBI. The concentration of each inhibitor was established according to previous studies [25,26].

The analyze the effects of channel blocking during sperm cryopreservation, three straws per sample and inhibitor were thawed by drowning and agitating in a water bath at 38 °C for 15 s. Thawed samples were then diluted 1:3 (*v*/*v*) in pre-warmed Beltsville Thawing Solution (BTS) [55] and incubated at 38 °C for 240 min. Throughout incubation the sperm quality was analyzed at two critical points: 30 min and 240 min.

4.5. Sperm Motility

In fresh and frozen–thawed samples, the analysis of sperm motility was performed in a computer-assisted sperm analysis (CASA) system, formed by a phase contrast microscope (Olympus BX41; Olympus, Tokyo, Japan) with a video camera and an ISAS software

(Integrated Sperm Analysis System V1.0; Proiser SL, Valencia, Spain). Before motility assessment, fresh samples were incubated at 38 °C for 15 min; since thawed samples were incubated at 38 °C, they were directly examined at 30 min and 240 min post-thaw. For both fresh and thawed samples, a 5 µL-volume were placed onto a pre-warmed (38 °C) Makler counting chamber (Sefi-Medical Instruments, Haifa, Israel) and observed under a negative phase-contrast field objective (Olympus 10× 0.30 PLAN). Sperm motility was assessed from the count of at least 1,000 sperm per replicate, being three replicates per sample analyzed.

For each sperm sample and inhibitor, different motility and kinematics parameters were evaluated: Total (TMOT, %), progressive sperm motility (PMOT, %) curvilinear velocity (VCL, µm/s); straight line velocity (VSL, µm/s); average path velocity (VAP, µm/s); amplitude of lateral head displacement (ALH, µm); beat cross frequency (BCF, Hz); linearity (LIN=VSL/VCL × 100, %); and straightness (STR = VSL/VAP × 100, %); wobble (WOB:VAP/VCL × 100, %). Only those spermatozoa with VAP equal to or higher than 10 µm/s were considered motile, and those with STR equal to or higher than 45% were considered as progressively motile. Each motility and kinematic sperm parameter was expressed as the mean ± standard error of the mean (SEM).

4.6. Flow Cytometry

Flow cytometry was used to assess the plasma and acrosome membrane integrity, membrane lipid disorder, intracellular calcium levels, mitochondrial membrane potential (MMP), intracellular levels of superoxide ($O_2^{\bullet -}$) radicals and intracellular levels of hydrogen peroxide (H_2O_2). Each assay required pre-dilution of both fresh and frozen–thawed samples to a final concentration of 1×10^6 spermatozoa/mL, as well as an appropriate fluorochrome combination and further incubation at 38 °C in darkness. For each sample and sperm parameter analyses were performed per triplicate.

All cytometric analyses were performed in a Cell Laboratory QuantaSC™ cytometer (Beckman Coulter; Fullerton, CA, USA), using an argon ion laser (488 nm) at 22 mW. Cell diameter/volume was assessed using the Coulter principle for volume assessment of the cytometer, which measured the changes in electrical resistance produced in an electrolyte solution by non-conductive particles. In this system, forward scatter (FS) is replaced by electronic volume (EV). EV-channel calibration was performed using 10-µm Flow-Check fluorospheres (Beckman Coulter), by positioning this size of bead at channel 200 on the EV-scale.

Three optical filters were used: FL1 filter (Dichroic/Splitter, DRLP: 550 nm, BP filter: 525 nm, detection width: 505–545 nm) to detect green emission from SYBR-14, Fluo3, PNA-FITC, YO-PRO-1, JC-1 monomers (JC-1_{mon}) and 2′,7′-dichlorofluorescein (DCF^+) fluorochromes; FL2 filter (DRLP: 600 nm, BP filter: 575 nm, detection width: 560–590 nm) to detect orange emission from JC-1 aggregates (JC-1_{agg}); and FL3 (LP filter: 670 nm/730 nm, detection width: 655–685 nm), to detect red emission from propidium iodide (PI), merocyanine 540 (M540) and Mito-ethidium (Mito-E^+). The signal was logarithmically amplified, and the adjustment of photomultiplier settings was performed according to the staining method.

EV and side scatter (SS) were measured and linearly recorded for all particles. The sheath flow rate was of 4.17 µL/min, and the number of events counted per replicate of 10,000. The analyzer threshold of the EV channel was adjusted to exclude both subcellular debris and cell aggregates, with a diameter < 7 µm and > 12 µm, respectively. According to EV and SS distributions, only sperm-specific events were positively gated, whereas other events were gated out.

Cytometric data analysis was performed using the Flowing Software (Ver. 2.5.1; University of Turku, Finland), following the recommendations of the International Society for Advancement of Cytometry (ISAC). For each parameter, the results are expressed as the mean ± SEM.

4.6.1. Plasma and Acrosome Membrane Integrity

Plasma membrane integrity was used as an indicator of sperm viability. The assay was performed with the LIVE/DEAD Sperm Viability Kit (Molecular Probes, Eugene, OR, USA), which consisted in two consecutive staining steps [56]: (1) Incubation of sperm samples with SYBR-14 (final concentration: 100 nmol/L) for 10 min, and (2) incubation with PI (final concentration of 12 µmol/L) for 5 min. Two different sperm populations were differentiated according to the staining pattern: (1) Viable sperm, with a staining pattern of SYBR-14$^+$/PI$^-$ and green fluorescence emission, and (2) non-viable sperm, which could stain either SYBR-14$^-$/PI$^+$ and SYBR-14$^+$/PI$^+$, being the fluorescence emission red or red and green, respectively. A population of unstained (SYBR-14$^-$/PI$^-$) particles was also observed; this population corresponded to non-sperm particles and it was used to correct the proportions of intact sperm found in the other tests [57]. Results are expressed as the percentage of viable spermatozoa (SYBR-14$^+$/PI$^-$) (mean ± SEM; n = 8 in the first experiment and n = 9 in the second experiment).

Acrosome membrane integrity was assessed by the double-staining with PNA-FITC and PI [58], both added simultaneously to the sperm samples. The final concentration was of 2.5 µg/mL for PNA-FITC and of 12 µmol/L for PI, and the incubation time of 10 min in dark. This procedure let to classify the sperm cells into two categories: (1) spermatozoa with an intact plasma membrane and acrosome (PNA-FITC$^-$/PI$^-$); and (2) spermatozoa with a damaged acrosome and/or plasma membrane damage. This second category included three different sperm populations with a specific staining pattern: PNA-FITC$^+$/PI$^-$ pattern, which corresponded to those spermatozoa with a damaged plasma membrane, PNA-FITC$^+$/PI$^+$ pattern, which included those spermatozoa with a damaged plasma membrane and a partially altered outer acrosome membrane, and PNA-FITC$^-$/PI$^+$ pattern, from those spermatozoa with a damaged plasma membrane and a lost outer acrosome membrane. Events with PNA-FITC$^-$/PI$^-$ pattern were corrected using the percentages of non-sperm debris particles (SYBR14$^-$/PI$^-$) obtained from the viability assay. Only the percentage of sperm with PNA-FITC$^-$/PI$^-$ staining pattern were showed (mean ± SEM; n = 8 in the first experiment and n = 9 in the second experiment).

4.6.2. Plasma Membrane Lipid Disorder

Plasma membrane lipid disorder was evaluated using the fluorochrome M540, which can detect alterations in packing order of phospholipids in the external leaflet [59,60]. Sperm samples were double incubated with M540 (final concentration: 2.6 µmol/L) and YO-PRO-1 (final concentration: 25 nmol/L) for 10 min in darkness. Flow cytometry led to identify viable (YO-PRO-1$^-$) and non-viable (YO-PRO-1$^+$) sperm populations showing either low (M540$^-$) or high (M540$^+$) membrane lipid disorder. As in other sperm parameters, the percentage of viable sperm with low membrane lipid disorder (M540$^-$/YO-PRO-1$^-$) was corrected using the non-sperm particles from the SYBR-14/PI staining. Results are expressed as the percentage of viable sperm with high membrane lipid disorder (M540$^+$/YO-PRO-1$^-$) (mean ± SEM; n = 8 in the first experiment and n = 9 in the second experiment).

4.6.3. Determination of Intracellular Calcium Levels

Intracellular calcium levels were evaluated using the fluorochrome Fluo3-acetomethoxy ester (Fluo3-AM, F-1241; Molecular Probes, Invitrogen, ThermoFisher Scientific) and PI. Both fluorochromes were added together to the sperm samples at a final concentration of 1 µmol/L and 12 µmol/L, respectively, and incubated for 10 min in darkness [61]. Four different sperm populations with a specific staining pattern were distinguished by flow cytometry: (1) Viable spermatozoa with low calcium levels (Fluo3$^-$/PI$^-$); (2) viable spermatozoa with high calcium levels (Fluo3$^+$/PI$^-$); (3) non-viable spermatozoa with low calcium levels (Fluo3$^-$/PI$^+$); and (4) non-viable spermatozoa with high calcium levels (Fluo3$^+$/PI$^+$). FL1 spill over into the FL3-channel (2.45%) and FL3 spill over into the FL1-channel (28.72%) were compensated. Percentages of debris particles (SYBR14$^-$/PI$^-$) were used to correct the percentages of Fluo3$^-$/PI$^-$ spermatozoa, and to recalculate the percentages of the rest of

sperm populations. For each sperm sample and cryopreservation step, only the percentage of viable spermatozoa with high intracellular calcium levels were recorded ($Fluo3^+/PI^-$) (mean ± SEM; n = 8 in the first experiment and *n* = 9 in the second experiment).

4.6.4. Mitochondrial Membrane Potential (MMP)

To assess mitochondrial membrane potential (MMP), sperm samples were stained for 30 min with the fluorochrome JC-1 at a final concentration of 0.3 µmol/L [62]. The principle of this staining procedure is that the increase in MMP results in JC-1 aggregation ($JC\text{-}1_{agg}$), whereas low MMP maintains JC-1 in its monomeric form ($JC\text{-}1_{mon}$). Flow cytometry dot plots provided three different sperm populations: (1) Sperm with low MMP ($JC\text{-}1_{mon}$), producing green fluorescence; (2) sperm with high MMP ($JC\text{-}1_{agg}$), producing orange fluorescence; and (3) sperm with intermediate MMP ($JC\text{-}1_{mon}$ and $JC\text{-}1_{agg}$), producing both green and orange fluorescence. Particles with no fluorescence (either green or orange) were gated out. Data were compensated, by subtracting green fluorescence from FL2-channel (51.70%). Results are expressed as the ratio between $JC1_{agg}/JC1_{mon}$ sperm populations (mean ± SEM; *n* = 8 in the first experiment and *n* = 9 in the second experiment).

4.6.5. Intracellular Levels of Mitochondrial Superoxide ($O_2^{\bullet -}$)

Intracellular levels of mitochondrial superoxide ($O_2^{\bullet -}$) radicals were determined from the double-staining with MitoSOX and YO-PRO-1 [63]. MitoSOX or Mito-Hydroethidine is a positively charged fluorochrome that accumulates in mitochondria [64], being oxidized by $O_2^{\bullet -}$ radicals to a fluorescent molecule (Mito-ethidium, Mito-E), which is positively charged ($Mito\text{-}E^+$). The staining pattern consisted in the double-incubation of sperm samples with MitoSOX (final concentration: 4 µmol/L) and YO-PRO-1 (final concentration: 40 nmol/L) for 20 min in darkness. The subsequent analysis by flow cytometry let to differentiate viable ($YO\text{-}PRO\text{-}1^-$) and non-viable ($YO\text{-}PRO\text{-}1^-$) sperm cells with either low ($Mito\text{-}E^-$) or high ($Mito\text{-}E^+$) mitochondrial superoxide levels. The percentage of viable sperm with low mitochondrial superoxide levels ($Mito\text{-}E^-/YO\text{-}PRO\text{-}1^-$) was corrected using the non-sperm particles ($SYBR\text{-}14^-/PI^-$), and the percentages the other three sperm populations were recalculated. Results are expressed as the percentage of viable sperm with high levels of mitochondrial superoxide ($Mito\text{-}E^+/YO\text{-}PRO\text{-}1^-$) (mean ± SEM; *n* = 8 in the first experiment and *n* = 9 in the second experiment).

4.6.6. Intracellular Levels of Hydrogen Peroxide (H_2O_2)

Intracellular levels of hydrogen peroxide (H_2O_2) were analyzed using 2′,7′-dichlorodihydrofluorescein diacetate (H_2DCFDA), which can penetrate the sperm cell membrane, being then converted into a highly fluorescent molecule, 2′,7′-dichlorofluorescein (DCF^+) by oxidation. According to the protocol of Guthrie and Welch [63], sperm samples were incubated with H_2DCFDA and PI for 30 min, at final concentration of 200 µmol/L and 12 µmol/L, respectively. This procedure led to differentiate viable (PI^-) and non-viable sperm populations (PI^-), with either low (DCF^-) or high (DCF^+) peroxide levels. The percentage of viable sperm with high peroxide levels (DCF^+/PI^-) was corrected as previously indicated. Results are expressed as the percentage of viable sperm with low (DCF^-/PI^-) and high (DCF^+/PI^-) peroxide levels (mean ± SEM; *n* = 8 in the first experiment and *n* = 9 in the second experiment).

4.7. Statistical Analyses

Statistical analyses of data were performed with the package IBM SPSS Statistics 25.0 (Armonk, New York, NY, USA), using a mixed model for each one of the sperm parameters measured. In this mixed model, the cryopreservation steps (i.e., fresh and frozen–thawed at 30 min and 240 min) were considered as intra-subject factors, whereas the inhibitors (i.e., control, PAX, TEA and 2-GBI) were considered as fixed-effects factors. A post-hoc Sidak test was also used for pair-wise comparisons. Before the mixed model and post-hoc analyses, both Shapiro–Wilk and Levene tests were run to check the distribution of data and

homogeneity of variances. In all statistical analyses the significance level was of $P \leq 0.05$. All the results are expressed as the mean ± SEM.

5. Conclusions

In conclusion, inhibition of K^+ channels and SLO1 channels does not affect the sperm ability to withstand cryopreservation. In contrast, blocking HVCN1 channels during freezing severely impairs sperm function and survival after thawing, thus indicating that they are relevant for mammalian sperm cryotolerance. Interestingly, HVCN1-blockade was found to induce a decrease in the percentages of viable spermatozoa with high ROS levels. These remarkable findings warrant further research, since they may extend our understanding on the physiological changes associated to sperm cryotolerance and may help develop new strategies to improve cryopreservation protocols.

Author Contributions: Conceptualization, A.D.-B., E.P., and M.Y.; methodology, A.D.-B., E.P., and M.Y.; formal analysis, A.D.-B., M.Y., and E.P.; investigation, A.D.-B., Y.M.-O., and M.L.; supervision, M.Y. and E.P.; writing—original draft preparation, E.P.; writing—review and editing, A.D.-B., Y.M.-O., M.L., S.B., M.Y., and E.P.; visualization, A.D.-B. and E.P; funding acquisition, E.P., S.B., and M.Y. All authors have read and agreed to the published version of the manuscript.

Funding: This research was funded by the Ministry of Science and Innovation (Spain) (RYC-2014-15581, AGL2015-69738-R, AGL2017-88329-R, PRE2018-083488); and Regional Government of Catalonia, Spain (2017-SGR-1229).

Institutional Review Board Statement: Not applicable.

Informed Consent Statement: Not applicable.

Data Availability Statement: The data presented in this study are available on request from the corresponding author.

Acknowledgments: The authors acknowledge the technical support received from Júlia Batlle (University of Girona, Spain).

Conflicts of Interest: The authors declare no conflict of interest.

References

1. Mishra, A.K.; Kumar, A.; Yadav, S.; Anand, M.; Yadav, B.; Nigam, R.; Garg, S.K.; Swain, D.K. Functional insights into voltage gated proton channel (Hv1) in bull spermatozoa. *Theriogenology* **2019**, *136*, 118–130. [CrossRef]
2. Lishko, P.V.; Kirichok, Y.; Ren, D.; Navarro, B.; Chung, J.J.; Clapham, D.E. The control of male fertility by spermatozoan ion channels. *Annu. Rev. Physiol.* **2012**, *74*, 453–575. [CrossRef] [PubMed]
3. Brown, S.G.; Publicover, S.J.; Barrat, C.L.R.; Martins da Silva, S.J. Human sperm ion channel (dys)function: Implications for fertilization. *Hum. Reprod. Update* **2019**, *25*, 758–776. [CrossRef] [PubMed]
4. Riva, N.S.; Ruhlmann, C.; Iaizzo, R.C.; Marcial López, C.A.; Martínez, A.G. Comparative analysis between slow freezing and ultra-rapid freezing for human sperm cryopreservation. *JBRA Assist. Reprod.* **2018**, *22*, 331–337. [CrossRef] [PubMed]
5. Najafi, L.; Halvaei, I.; Movahed, M. Canthaxanthin protects human sperm parameters during cryopreservation. *Andrologia* **2019**, *51*, e13389. [CrossRef]
6. Zhu, Z.; Li, R.; Fan, X.; Lv, Y.; Zheng, Y.; Hoque, M.S.A.; Wu, D.; Zeng, W. Resveratrol Improves Boar Sperm Quality via 5′AMP-Activated Protein Kinase Activation during Cryopreservation. *Oxid. Med. Cell Longev.* **2019**, *2019*, 5921503. [CrossRef]
7. Pinart, E.; Puigmulé, M. Factors affecting boar reproduction, testis function and sperm quality. In *Boar Reproduction. Fundamentals and New Biological Trends*; Bonet, S., Casas, I., Holt, W.V., Yeste, M., Eds.; Springer: Berlin, Germany, 2013; pp. 109–202.
8. Yeste, M. Sperm cryopreservation update: Cryodamage, markers, and factors affecting the sperm freezability in pigs. *Theriogenology* **2016**, *85*, 47–64. [CrossRef] [PubMed]
9. Delgado-Bermúdez, A.; Llavanera, M.; Fernández-Bastit, L.; Recuero, S.; Mateo-Otero, Y.; Bonet, S.; Barranco, I.; Fernández-Fuertes, B.; Yeste, M. Aquaglyceroporins but not orthdox aquaporins are involved in the cryotolerance of pig spermatozoa. *J. Anim. Sci. Biotech.* **2019**, *10*, 77. [CrossRef] [PubMed]
10. Llavanera, M.; Delgado-Bermúdez, A.; Fernández-Fuertes, B.; Recuero, S.; Mateo-Otero, Y.; Bonet, S.; Barranco, I.; Yeste, M. GSTM3, but not IZUMO1, is a cryotolerance marker of boar sperm. *J. Anim. Sci. Biotechnol.* **2019**, *10*, 61. [CrossRef]
11. Yeste, M. Recent advances in boar sperm cryopreservation: State of the art and current perspectives. *Reprod. Domest. Anim.* **2015**, *50*, 71–79. [CrossRef]
12. Yeste, M.; Rodríguez-Gil, J.E.; Bonet, S. Artificial insemination with frozen-thawed boar sperm. *Mol. Reprod. Dev.* **2017**, *84*, 802–813. [CrossRef] [PubMed]

13. Rath, D.; Bathgate, R.; Rodríguez-Martínez, H.; Roca, J.; Strzezek, J.; Waberski, D. Recent advances in boar semen cryopreservation. *Soc. Reprod. Fertil. Suppl.* **2009**, *66*, 51–66. [CrossRef] [PubMed]
14. Cerolini, S.; Maldjian, A.; Surai, P.; Noble, R. Viability, susceptibility to peroxidation and fatty acid composition of boar semen during liquid storage. *Anim. Reprod. Sci.* **2000**, *58*, 99–111. [CrossRef]
15. Pinart, E.; Yeste, M.; Bonet, S. Acrosin activity is a good predictor of boar sperm freezability. *Theriogenology* **2015**, *83*, 1525–1533. [CrossRef]
16. Sancho, S.; Casas, I.; Ekwall, H.; Rodríguez-Martínez, H.; Rodríguez-Gil, J.E.; Flores, E.; Pinart, E.; Briz, M.; Garcia-Gil, N.; Bassols, J.; et al. Effects of cryopreservation on semen quality and the expression of sperm membrane hexose transporters in the spermatozoa of Iberian pigs. *Reproduction* **2007**, *134*, 111–121. [CrossRef]
17. Casas, I.; Sancho, S.; Briz, M.; Pinart, E.; Bussalleu, E.; Yeste, M.; Bonet, S. Freezability prediction of boar ejaculates assessed by functional sperm parameters and sperm proteins. *Theriogenology* **2009**, *72*, 930–948. [CrossRef]
18. Casas, I.; Sancho, S.; Ballester, J.; Briz, M.; Pinart, E.; Bussalleu, E.; Yeste, M.; Fàbrega, A.; Rodríguez-Gil, J.E.; Bonet, S. The HSP90AA1 sperm content and the prediction of the boar ejaculate freezability. *Theriogenology* **2010**, *74*, 940–950. [CrossRef] [PubMed]
19. Guimaraes, D.B.; Barros, T.B.; van Tilburg, M.F.; Martins, J.A.M.; Moura, A.A.; Moreno, F.B.; Monteiro-Moreira, A.C.; Moreira, R.A.; Toniolli, R. Sperm membrane proteins associated with the boar semen cryopreservation. *Anim. Reprod. Sci.* **2017**, *183*, 27–38. [CrossRef]
20. Gómez-Fernández, J.; Gómez-Izquierdo, E.; Tomás, C.; Mocé, E.; de Mercado, E. Effect of different monosaccharides and disaccharides on boar sperm quality after cryopreservation. *Anim. Reprod. Sci.* **2012**, *133*, 109–116. [CrossRef]
21. Prieto-Martínez, N.; Vilagran, I.; Morató, R.; Rivera del Álamo, M.M.; Rodríguez-Gil, J.E.; Bonet, S.; Yeste, M. Relationship of aquaporins 3 (AQP3), 7 (AQP7), and 11 (AQP11) with boar sperm resilience to withstand freeze-thawing procedures. *Andrology* **2017**, *5*, 1153–1164. [CrossRef]
22. Lishko, P.V.; Botchkina, I.L.; Fedorenko, A.; Kirichok, Y. Acid Extrusion from Human Spermatozoa is Mediated by Flagellar Voltage-Gated Proton Channel. *Cell* **2010**, *140*, 327–337. [CrossRef] [PubMed]
23. Lishko, P.V.; Kirichok, Y. The role of Hv1 and CatSper channels in sperm activation. *J. Physiol.* **2010**, *588*, 4667–4672. [CrossRef] [PubMed]
24. Berger, T.K.; Fußhöller, D.M.; Goodwin, N.; Bönigk, W.; Müller, A.; Dokani Khesroshahi, N.; Brenker, C.; Wachten, D.; Krause, E.; Kaupp, U.B.; et al. Post-translational cleavage of Hv1 in human sperm tunes pH- and voltage-dependent gating. *J. Physiol.* **2017**, *595*, 1533–1546. [CrossRef]
25. Yeste, M.; Llavanera, M.; Pérez, G.; Scornik, F.; Puig-Parri, J.; Brugada, R.; Bonet, S.; Pinart, E. Elucidating the role of K^+ channels during in vitro capacitation of boar spermatozoa: Do SLO1 channels play a crucial role? *Int. J. Mol. Sci.* **2019**, *20*, 6330. [CrossRef] [PubMed]
26. Yeste, M.; Llavanera, M.; Mateo-Otero, Y.; Catalán, J.; Bonet, S.; Pinart, E. HVCN1 channels are relevant for the maintenance of sperm motility during in vitro capacitation of pig Spermatozoa. *Int. J. Mol. Sci.* **2020**, *21*, 3255. [CrossRef]
27. Tang, Q.Y.; Zhang, Z.; Xia, X.M.; Lingle, C. Block mouse Slo1 and Slo3 K+ channels by CTX, IbTX, TEA, 4-AP and quinidine. *Channels* **2010**, *4*, 22–41. [CrossRef]
28. Zhou, Y.; Lingle, C.J. Paxilline inhibits BK channels by an almost exclusively close-channel block mechanism. *J. Gen. Physiol.* **2014**, *144*, 415–440. [CrossRef]
29. Hille, B. *Ion Channels of Excitable Membranes*, 3rd ed.; Oxford University Press: Oxford, UK, 2001; pp. 156–159.
30. Rennhack, A.; Grahn, E.; Kaupp, U.B.; Berger, T.K. Photocontrol of the Hv1 proton channel. *ACS Chem. Biol.* **2017**, *12*, 2952–2957. [CrossRef]
31. Hong, L.; Kim, I.H.; Tombola, F. Molecular determinants of Hv1 proton channel inhibition by guanidine derivatives. *Proc. Natl. Acad. Sci. USA* **2014**, *111*, 9971–9976. [CrossRef]
32. Grötter, L.G.; Cattaneo, L.; Marini, P.E.; Kjelland, M.E.; Ferré, L.B. Recent advances in bovine sperm cryopreservation techniques with a focus on sperm post-thaw quality optimization. *Reprod. Dom. Anim.* **2019**, *5*, 655–665. [CrossRef]
33. Vilagran, I.; Castillo, J.; Bonet, S.; Sancho, S.; Yeste, M.; Estanyol, J.M.; Oliva, R. Acrosin-binding protein (ACRBP) and triosephosphate isomerase (TPI) are good markers to predict boar sperm freezing capacity. *Theriogenology* **2013**, *80*, 443–450. [CrossRef]
34. Vilagran, I.; Yeste, M.; Sancho, S.; Casas, I.; Rivera del Álamo, M.M.; Bonet, S. Relationship of sperm small heat-shock protein 10 and voltage-dependent anion channel 2 with semen freezability in boars. *Theriogenology* **2014**, *82*, 418–426. [CrossRef]
35. Vilagran, I.; Yeste, M.; Sancho, S.; Castillo, J.; Oliva, R.; Bonet, S. Comparative analysis of boar seminal plasma proteome from different freezability ejaculates and identification of Fibronectin 1 as sperm freezability marker. *Andrology* **2015**, *3*, 345–356. [CrossRef]
36. Chen, Q.; Peng, H.; Lei, L.; Zhang, Y.; Kuang, H.; Cao, Y.; Shi, Q.X.; Ma, T.; Duan, D. Aquaporin3 is a sperm water channel essential for postcopulatory sperm osmoadaptation and migration. *Cell Res.* **2011**, *21*, 922–933. [CrossRef] [PubMed]
37. Chen, Q.; Duan, E. Aquaporins in sperm osmoadaptation: An emerging role for volume regulation. *Acta Pharmacol. Sin.* **2011**, *32*, 721–724. [CrossRef] [PubMed]
38. Kumar, B.K.; Coger, R.N.; Schrum, L.W.; Lee, Y.C. The effects of over expressing aquaporins on the cryopreservation of hepatocytes. *Cryobiology* **2015**, *71*, 273–278. [CrossRef] [PubMed]

39. Barfield, J.P.; Yeung, C.H.; Cooper, T.G. Characterization of potassium channels involved in volume regulation of human spermatozoa. *Mol. Hum. Reprod.* **2005**, *11*, 891–897. [CrossRef] [PubMed]
40. Mannowetz, N.; Niadoo, N.M.; Choo, S.A.S.; Smith, J.F.; Lishko, P.V. Slo1 is the principal potassium channel of human spermatozoa. *eLife* **2013**, *2*, e01009. [CrossRef]
41. Sun, X.H.; Zhu, Y.Y.; Wang, L.; Liu, H.L.; Ling, Y.; Li, Z.L.; Sun, L.B. The Catsper channel and its roles in male fertility: A systematic review. *Reprod. Biol. Endocrinol.* **2017**, *15*, 65. [CrossRef]
42. Santi, C.M.; Martínez-López, P.; De la Vega-Beltrán, J.L.; Butler, A.; Alisio, A.; Darszon, A.; Salkoff, L. The SLO3 sperm-specific potassium channel plays a vital role in male fertility. *FEBS Lett.* **2010**, *584*, 1041–1046. [CrossRef]
43. Zeng, X.H.; Yang, C.; Kim, S.T.; Lingle, C.J.; Xia, X.M. Deletion of the Slo3 gene abolishes alkalization-activated K^+ current in mouse spermatozoa. *Proc. Natl. Acad. Sci. USA* **2011**, *108*, 5879–5884. [CrossRef] [PubMed]
44. De la Vega-Beltran, J.L.; Sánchez-Cárdenas, C.; Krapf, D.; Hernandez-González, E.O.; Wertheimer, E.; Treviño, C.L.; Visconti, P.E.; Darszon, A. Mouse sperm membrane potential hyperpolarization is necessary and sufficient to prepare sperm for the acrosome reaction. *J. Biol. Chem.* **2012**, *287*, 44384–44393. [CrossRef] [PubMed]
45. Geng, Y.; Jerreira, J.J.; Dzikunu, V.; Butler, A.; Lybaert, P.; Yuan, P.; Magleby, K.L.; Salkoff, L.; Santi, C.M. A genetic variant of the sperm-specific SLO3 K^+ channel has altered pH and Ca^{2+} sensitivities. *J. Biol. Chem.* **2017**, *292*, 8978–8987. [CrossRef] [PubMed]
46. Brenker, C.; Zhou, Y.; Müller, A.; Echeverry, F.A.; Trötschel, C.; Poetsch, A.; Xia, X.M.; Bönigk, W.; Lingle, J.C.; Kaupp, U.B.; et al. The Ca^{2+}-activated K^+ current of human sperm is mediated by Slo3. *eLife* **2014**, *3*, e01438. [CrossRef]
47. Yuan, P.; Leonetti, M.D.; Pico, A.R.; Hsiung, Y.; MacKinnon, R. Structure of the human BK channel Ca^{2+}-activation apparatus at 3.0 resolution. *Science* **2010**, *329*, 182–186. [CrossRef] [PubMed]
48. Blässe, A.-K.; Oldenhof, H.; Ekhlasi-Hundrieser, M.; Wolkers, W.F.; Sieme, H.; Bollwein, H. Osmotic tolerance and intracellular ion concentrations of bovine sperm are affected by cryopreservation. *Theriogenology* **2012**, *78*, 1312–1320. [CrossRef]
49. Mansell, S.A.; Publicover, S.J.; Barrat, C.L.R.; Wilson, S.M. Patch clamp studies of human sperm under physiological ionic conditions reveal three functionally and pharmacologically distinct cation channels. *Mol. Hum. Reprod.* **2014**, *20*, 392–408. [CrossRef]
50. Zhao, R.; Kennedy, K.; De Blas, G.A.; Orta, G.; Pavarotti, M.A.; Arias, R.J.; de la Vega-Beltrán, J.L.; Li, Q.; Dai, H.; Perozo, E.; et al. Role of human Hv1 channels in sperm capacitation and white blood cell respiratory burst established by a designed peptide inhibitor. *Proc. Natl. Acad. Sci. USA* **2018**, *115*, E11847–E11856. [CrossRef]
51. Chen, B.; Li, S.; Yan, Y.; Duan, Y.; Chang, S.; Wang, H.; Ji, W.; Wu, X.; Si, W. Cryopreservation of cynomolgus macaque (Macaca fascicularis) sperm with glycerol and ethylene glycol, and its effect on sperm-specific ion channels—CatSper and Hv1. *Theriogenology* **2017**, *104*, 37–42. [CrossRef]
52. Keshtgar, S.; Ghanbari, H.; Ghani, E.; Shid Moosavi, S.M. Effect of CatSper and Hv1 channel inhibition on progesterone stimulated human sperm. *J. Reprod. Infertil.* **2018**, *19*, 133–139. [PubMed]
53. Musset, B.; Clark, R.A.; DeCoursey, T.E.; Petheo, G.L.; Geiszt, M.; Chen, Y.; Cornell, J.E.; Eddy, C.A.; Brzyski, R.G.; El Jamali, A. NOX5 in human spermatozoa: Expression, function, and regulation. *J. Biol. Chem.* **2012**, *287*, 9376–9388. [CrossRef]
54. Ghanbari, H.; Keshtgar, S.; Zare, H.R.; Gharesi-Fard, B. Inhibition of CatSper and Hv1 Channels and NOX5 Enzyme Affect Progesterone-Induced Increase of Intracellular Calcium Concentration and ROS Generation in Human Sperm. *Iran. J. Med. Sci.* **2019**, *44*, 127–134.
55. Pursel, V.G.; Johnson, L.A. Freezing of boar spermatozoa: Fertilizing capacity with concentrated semen and a new thawing procedure. *J. Anim. Sci.* **1975**, *40*, 99–102. [CrossRef]
56. Garner, D.L.; Johnson, L.A. Viability assessment of mammalian sperm using SYBR-14 and propidium iodide. *Biol. Reprod.* **1995**, *53*, 276–284. [CrossRef]
57. Petrunkina, A.M.; Waberski, D.; Bollwein, H.; Sieme, H. Identifying non-sperm particles during flow cytometric physiological assessment: A simple approach. *Theriogenology* **2010**, *73*, 995–1000. [CrossRef] [PubMed]
58. Nagy, S.; Jansen, J.; Topper, E.K.; Gadella, B.M. A Triple-Stain Flow Cytometric Method to Assess Plasma- and Acrosome-Membrane Integrity of Cryopreserved Bovine Sperm Immediately after Thawing in Presence of Egg-Yolk Particles. *Biol. Reprod.* **2003**, *68*, 1828–1835. [CrossRef] [PubMed]
59. Rathi, R.; Colenbrander, B.; Bevers, M.M.; Gadella, B.M. Evaluation of in vitro capacitation of stallion spermatozoa. *Biol. Reprod.* **2001**, *65*, 462–470. [CrossRef] [PubMed]
60. Yeste, M.; Estrada, E.; Rivera Del Álamo, M.M.; Bonet, S.; Rigau, T.; Rodríguez-Gil, J.E. The increase in phosphorylation levels of serine residues of protein HSP70 during holding time at 17 °C is concomitant with a higher cryotolerance of boar spermatozoa. *PLoS ONE* **2014**, *9*, e90887. [CrossRef] [PubMed]
61. Martínez-Pastor, F.; Mata-Campuzano, M.; Álvarez-Rodríguez, M.; Álvarez, M.; Anel, L.; De Paz, P. Probes and techniques for sperm evaluation by flow cytometry. *Reprod. Domest. Anim.* **2010**, *45*, 67–78. [CrossRef] [PubMed]
62. Ortega-Ferrusola, C.; Sotillo-Galán, Y.; Varela-Fernández, E.; Gallardo-Bolaños, J.M.; Muriel, A.; González-Fernández, L.; Tapia, J.A.; Peña, F.J. Detection of "Apoptosis-Like" Changes During the Cryopreservation Process in Equine Sperm. *J. Androl.* **2008**, *29*, 213–221. [CrossRef]
63. Guthrie, H.D.; Welch, G.R. Determination of intracellular reactive oxygen species and high mitochondrial membrane potential in Percoll-treated viable boar sperm using fluorescence-activated flow cytometry. *J. Anim. Sci.* **2006**, *84*, 2089–2100. [CrossRef] [PubMed]
64. Kauffman, M.E.; Kauffman, M.K.; Traore, K.; Zhu, H.; Trush, M.A.; Jia, Z.; Li, Y.R. MitoSOX-Based Flow Cytometry for Detecting Mitochondrial ROS. *React. Oxyg. Species* **2016**, *2*, 361–370. [CrossRef] [PubMed]

Discussion

Discussion

Sperm are highly specialised cells whose main function is to deliver the paternal genome into the oocyte. Their structure is strictly related to their function (Alberts et al., 2008), and during spermiogenesis in the testis and maturation in the epididymis, spermatids and sperm undergo changes such as the differentiation of the acrosome and the tail, and the compaction of the chromatin, that prepare them to fertilise the oocyte (Robaire and Hinton, 2015). In addition to changes in structure, physiological changes occur in two different stages: before and after ejaculation. Prior to ejaculation, i.e., during maturation in the epididymis, sperm acquire motility and adaptability to osmotic changes, in addition to a higher chromatin compaction. After ejaculation and within the female reproductive tract, sperm undergo capacitation, which prepares them for triggering the acrosomal reaction once they reach the oocyte vicinity. This process is a prerequisite for the penetration of oocyte vestments and the subsequent fusion of sperm and oocyte plasmalemmae (Robaire and Hinton, 2015). Because cell physiology is related to metabolite concentration, which relies upon the permeability of plasma membrane to water and solutes, this structural element plays an important role in sperm function during these different stages. Cell membranes are composed by lipids and proteins, and because of the hydrophobicity of the lipid component, additional mechanisms to simple diffusion are required to regulate the transport of water and solutes across the membrane (Watson, 2015). During both sperm maturation and capacitation, sperm encounter constantly changing extracellular media, which cause variations in osmolality, membrane hyperpolarisation and pH; in this scenario, membrane channels are very relevant for the response of sperm to these changes. On the one hand, the acquirement of osmoadaptability and volume reduction capability during sperm maturation are associated to ion and water permeability across the plasma membrane. On the other hand, during their journey throughout the female tract, the adaptation to varying pH and extracellular ion concentrations requires a rigorous regulation of membrane permeability to water and ions. In fact, drastic changes in pH, membrane hyperpolarisation and changes in cytosolic concentration of different ions that

sperm experience during capacitation are driven by the selective permeability to distinct molecules that sperm are exposed to along their path through the female tract (Johnson, 2007). It must also be considered that during cryopreservation, which is the most efficient strategy for the preservation of male gametes, sperm also undergo a drastic osmotic shock because of the composition of cryoprotective media. While this osmotic shock dehydrates cells, it is required to avoid the formation of intracellular water crystals. Some alterations, nevertheless, occur during freezing and thawing, affecting the nucleus, cytoskeleton and plasma membrane structures, as well as mitochondrial activity and protein function (Sieme et al., 2008; Peña et al., 2011; Yeste, 2016; Yánez-Ortiz et al., 2021). The resilience of sperm to cryopreservation varies between species, between individuals and even between ejaculates from the same individual. For this reason, the identification of different biomarkers that are predictive of post-thaw sperm quality is of high relevance (Vilagran et al., 2014; Pinart et al., 2015; Llavanera et al., 2019). In this context, channel proteins involved in the transport of molecules and ions across sperm membranes, such as water (AQPs), and potassium, calcium, and protons (ion channels), are highly relevant. In the light of all the aforementioned, the aim of this Dissertation was to evaluate the role of specific transmembrane channel proteins (AQPs, as well as H^+ and K^+ channels) in sperm physiology during capacitation and cryopreservation.

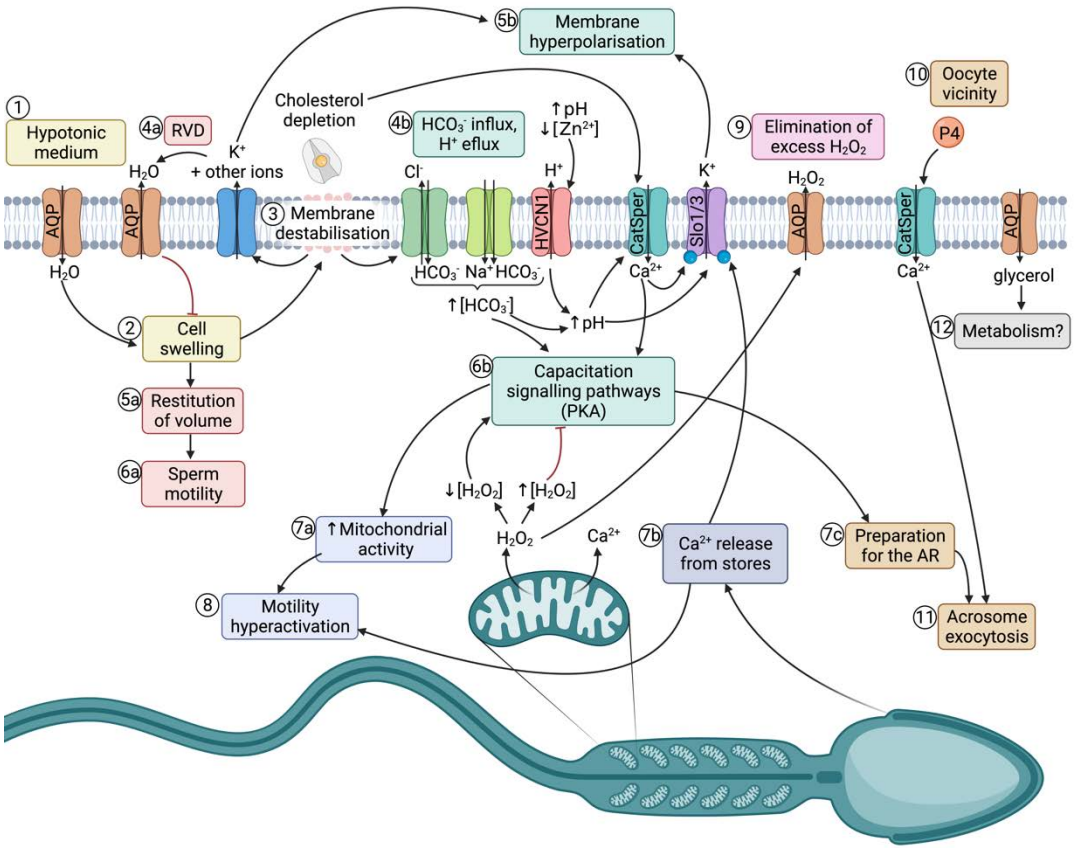

Figure 7. Membrane channels and sperm function. **(1)** After entering the female tract or upon thawing, sperm encounter a hypotonic medium, which causes water influx and thus, **(2)** cell swelling. **(3)** This causes membrane destabilization (including plasma, mitochondrial and acrosomal membranes). **(4a)** Then, mechanosensory ion channels are open, and outflowing ion currents activate regulatory volume decrease (RVD) events. Water outflow leads to **(5a)** cell volume restitution, allowing **(6a)** normal sperm motility. **(4b)** In the female tract, cholesterol depletion also contributes to membrane destabilisation, which elicits the entrance of HCO_3^- and Ca^{2+} through different channels. The low concentration of Zn^{2+} and high pH in the female tract activate HVCN1 channels, which contribute to intracellular alkalinisation. Both the high pH and increased levels of Ca^{2+} **(5b)** activate K^+ channels that lead to membrane hyperpolarisation, and **(6b)** activate capacitation signalling pathways, that involve protein kinase A (PKA). Downstream events include **(7a)** increased mitochondrial activity, **(7b)** release of Ca^{2+} from intracellular stores and **(7c)** preparation of the spermatozoon for the acrosome reaction (AR). **(8)** Higher mitochondrial activity and Ca^{2+} hyperactivate motility, and reactive oxygen species (ROS), such as H_2O_2, are produced. Low levels of H_2O_2 are essential to elicit capacitation, but at high levels it inhibits this process. **(9)** Aquaporins (AQPs) allow H_2O_2 detoxification. **(10)** In the oocyte vicinity, progesterone (P4) activates Ca^{2+} channels, which trigger **(11)** the AR. **(12)** Glycerol transported through GLPs could be used by metabolic pathways, and is crucial for sperm survival during cryopreservation. Modified from (Delgado-Bermúdez et al., 2022)

Aquaporins have an essential role during sperm capacitation and acrosomal reaction

Despite several studies having been conducted to identify the role of ion channels in sperm capacitation (reviewed by Puga Molina et al., 2018), the potential role of water channels on this process is yet to be unveiled. Nevertheless, the central role of solute adenylate cyclase (sAC), which is regulated by pH in the cAMP-PKA pathway triggered during capacitation, is well known (Chang and Oude-Elferink, 2014). Given the precise link between the intracellular concentrations of ions and water permeability, therefore, it is reasonable to suggest that AQPs might be relevant in this process. To this end, this Dissertation assessed the potential role of the different groups of AQPs during mammalian sperm capacitation, using the pig as a model. For this purpose, three different transition metal compounds that have largely been proven as AQPs inhibitors (Haddoub et al., 2009) were used: cooper sulphate ($CuSO_4$), mercury chloride ($HgCl_2$) and silver sulfadiazine (AgSDZ). Regarding $CuSO_4$, it is a specific inhibitor of AQP3, since Cu^{2+} binds to three different extracellular residues of this protein: Trp128, Ser152 and His241 in human AQP3 (Zelenina et al., 2004). $HgCl_2$, an unspecific and reversible inhibitor of AQPs, covalently binds to a Cys residue common to most AQPs via Hg^{2+} binding. This modification either blocks membrane permeability through the pore or causes conformational changes that avoid water transport (Hirano et al., 2010). Yet, this Cys residue is absent from AQP7 and, in fact, previous studies have demonstrated that AQP7 is resistant to mercurial compounds (Ishibashi et al., 1997). Finally, AgSDZ is an unspecific, irreversible inhibitor of all AQPs that has been proposed to interact with the same Cys residue. Such an irreversibility suggests that the inhibitory mechanism of Ag^{2+} might be different from that of mercurial compounds. As a matter of fact, it has been previously suggested that this ion can block AQP channels because of the similar size between the ion (2.5 Å) and the AQP pore (2.8 Å); thus, it is possible that this metal also inhibits AQP7 (Niemietz and Tyerman, 2002). In the presence of $CuSO_4$ the intracellular levels of peroxides were higher than in the control after 120 min of incubation in capacitation medium, and this effect persisted even after triggering the acrosomal

reaction. The presence of $HgCl_2$ increased membrane lipid disorder from the same time point to the end of the experiment, augmented the proportion of sperm with alterations in the acrosome membrane at 240 min, and impaired mitochondrial membrane potential at 250 min. Finally, the presence of AgSDZ altered different parameters related to sperm motility and kinetics during the entire capacitation process, and acrosome membrane integrity and mitochondrial membrane potential were affected similarly to the treatment with $HgCl_2$..

Inhibition of aquaporins (AQPs) using cooper sulphate ($CuSO_4$)

From the results observed in the presence of $CuSO_4$, one could suggest that AQP3 does not have a relevant role during sperm capacitation or acrosomal reaction. In fact, the single effect on the analysed sperm quality and functionality parameters could be explained by the permeability of AQP3 to peroxides (Miller et al., 2010). The blocking of AQP3, therefore, would interfere the outflow of peroxides from the cytoplasm through the plasma membrane, which would cause their intracellular accumulation. One would expect that, in the presence of such high levels of peroxide, sperm quality and function were affected, but none of the evaluated variables showed alterations. These results suggest that sperm capacitation and acrosomal reaction, at least in pigs, are not impaired in the presence of high intracellular levels of peroxide. It is important to highlight that in different species of mammals, peroxides have a dual role as regulators of capacitation and, according to (Rivlin et al., 2004), whereas low levels are stimulators of capacitation-associated events, high concentrations of peroxides can inhibit this process. Moreover, peroxides can activate sAC, leading to PKA-dependent tyrosine phosphorylation of sperm proteins (Rivlin et al., 2004). Because the PKA signalling pathway involves the activation of a large number of proteins through phosphorylation, $CuSO_4$-inhibition could increase the levels of proteins phosphorylated by the cAMP-PKA pathway and keep them active (Aitken, 2017). The results shown in this Dissertation, nonetheless, are not in agreement with the aforementioned literature, since no changes in acrosome membrane integrity, levels of cAMP, PKA activity or tyrosine phosphorylation patterns were observed. Taken this into consideration, one could suggest that the levels of

intracellular peroxides accumulated following $CuSO_4$-inhibition would not be sufficient to alter capacitation or acrosomal reaction. That being said, future studies to unveil the potential relevance of H_2O_2 in mammalian sperm capacitation are required.

Inhibition of aquaporins (AQPs) using mercury chloride ($HgCl_2$)

Regarding $HgCl_2$, it inhibits all AQPs that are present in mammalian sperm except AQP7 (i.e. AQP3, AQP9 and AQP11). In the presence of $HgCl_2$, samples presented impaired kinetics parameters and increased membrane lipid disorder that could be a consequence of cholesterol efflux and lipid reorganization, which is a characteristic capacitation-associated event (reviewed by Aitken, 2017). Considering that, the experiments conducted in this Dissertation suggest that certain hallmarks of capacitation are enhanced when some AQPs are inhibited. The lack of changes in acrosome integrity, intracellular concentration of calcium, tyrosine-phosphorylated proteins, cAMP levels and PKA activity after triggering the acrosomal reaction, however, point out that such alterations in plasma membrane organisation are a capacitation-like event that does not drive a proper, physiological sperm capacitation, because it does not lead to an increase in the proportions of sperm that undergo the acrosomal reaction. Based on these findings, it would appear that AQP3 and AQP11 exert some influence on certain capacitation-associated changes in mammalian sperm, without having a direct impact on preparing them for the acrosome reaction. To explain that, it should be borne in mind that the limitation of water flow through the plasma membrane that occurs in response to the inhibition of some AQPs could compromise sperm osmoregulatory ability, which has a direct impact on sperm motility and membrane integrity (Chen and Duan, 2011)). As these are the observed effects in samples treated with $HgCl_2$, motility and plasma membrane alterations might be the consequence of a deficient volume regulation without altering capacitation-associated signalling pathways. Interestingly, a recent study assessing the effects of mercury on caprine sperm structure described similar alterations to those observed in porcine sperm. Briefly, those sperm cells showed structural alterations in plasma, acrosome, and mitochondrial membranes, as well as in the axoneme

(Kushawaha et al., 2021). In fact, in a previous work by the same authors (Kushawaha et al., 2020), the impact of mercury on goat sperm capacitation was also assessed, and the effects on sperm structure and function were also similar to those described in pig sperm. While potential mechanisms leading to the observed effects in sperm were proposed in both works (Kushawaha et al., 2020, 2021), AQPs were not envisaged as a potential interactor of mercury in their hypothesised routes. Yet, and given the inhibitory effect of mercury on AQPs, a potential role of these water channels in the mechanisms guiding to the impairment of sperm function should not be discarded (**Figure 8**).

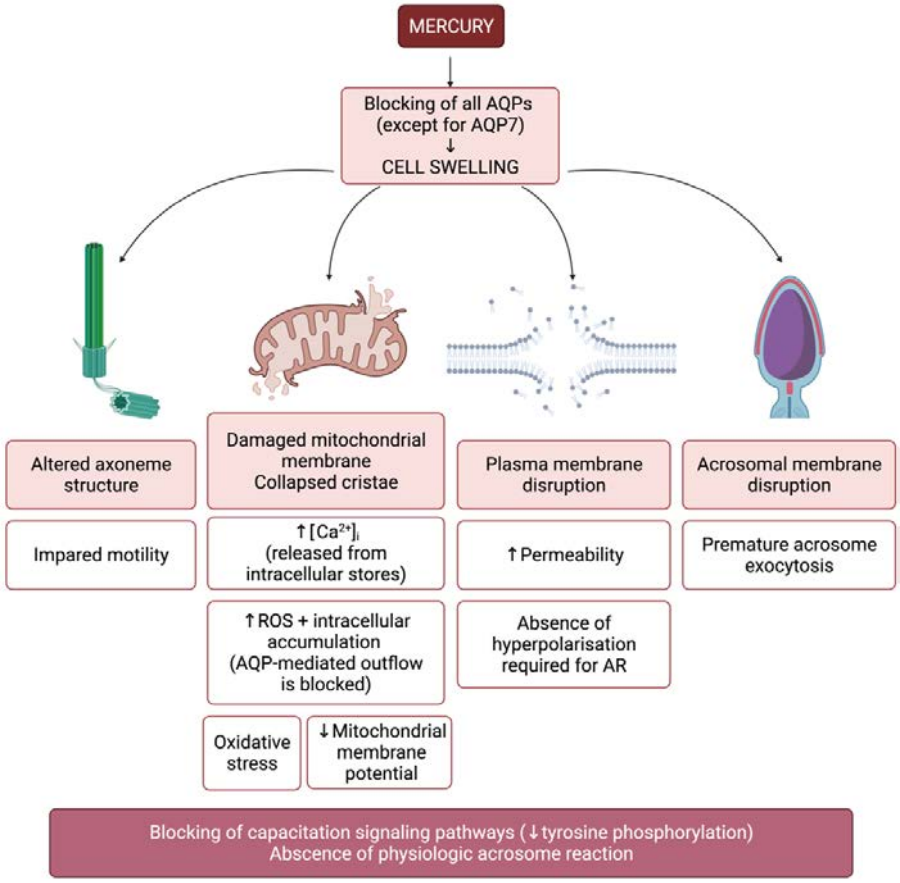

Figure 8. Blocking of aquaporins (AQPs) through mercury causes cell swelling. From a structural point of view, the axoneme is altered and this results in sperm motility impairment. Mitochondrial, plasma and acrosome membranes are disrupted due to stretching. Mitochondrial cristae are collapsed, which reduces energy production. Alteration of mitochondrial membrane affects mitochondrial membrane potential, leads to

the release of Ca^{2+} and increases reactive oxygen species (ROS) production, which accumulate intracellularly. Whereas small concentrations of ROS are needed for capacitation, high concentrations have an inhibitory effect. Plasma membrane disruption rises its permeability and reduces its hyperpolarization, which is essential to trigger the acrosome reaction. Finally, as damage to the acrosomal membrane favours premature exocytosis, sperm cannot undergo a physiological acrosome reaction.

Inhibition of aquaporins using silver sulfadiazine (AgSDZ)

This Dissertation also demonstrated that when sperm samples were incubated with AgSDZ, an unspecific inhibitor of all AQPs, the observed effects were similar to those seen in samples treated with $HgCl_2$. Samples incubated with AgSDZ also showed lower pH compared to the control and an increase in the levels of tyrosine-phosphorylated proteins after the addition of progesterone to trigger the acrosome reaction. Yet, these changes did not occur concomitantly with alterations in cAMP levels or PKA activity in the presence of this inhibitor. One cannot, therefore, conclude that these changes occur in response to alterations in capacitation-associated signalling pathways. A potential reason for these changes could reside in the different signalling pathways that drive capacitation and acrosome reaction. According to (Buffone et al., 2014b), capacitation involves the tyrosine-phosphorylation of certain sperm proteins as a downstream effect of PKA activation through sAC-synthesised cAMP, whereas the acrosome reaction is initiated by the interaction of progesterone with a GPCR coupled to a transmembrane adenylate cyclase (trAC), which generates the cAMP required during this process and also involves the participation of Ca^{2+} and PKC. These two enzymes are differently regulated, as trAC is non-sensitive to pH and sAC activity is modulated by proton concentration. In this Dissertation, pH decreased after the addition of progesterone to trigger the acrosome reaction. Since, at that point, the main source of cAMP for the signalling pathways is trAC, which is non-sensitive to pH, this could be the reason for the lack of alterations in cAMP levels compared to the control. While this suggests that PKA activity should be preserved, the changes in tyrosine phosphorylation point out towards an alteration of kinase activity. A potential candidate for this change in protein tyrosine phosphorylation would be PKC, which is involved downstream in the signalling pathways that regulate the acrosome reaction (Teijeiro et al., 2017). Taken this into

consideration, impaired osmoregulatory ability during capacitation could cause latent alterations in sperm that would become apparent only after triggering the acrosome reaction. Since these effects are only observed when all AQPs are inhibited, it can be suggested that AQPs as a whole have a key role during capacitation and acrosome reaction, and functional compensation is possible by intact members of this family of proteins. When a general inhibitor, like AgSDZ, is added to sperm samples, this functional compensation is not possible and the osmotic challenge becomes unbeatable for sperm; in this scenario, the intracellular machinery involved in specific physiological processes, such as acrosome reaction, is irreversibly impaired. In short, while this Dissertation has demonstrated, for the first time, that AQPs play a crucial function during mammalian sperm capacitation, further studies to elucidate the underlying mechanisms via which the inhibition of these water channels alters intracellular pH and tyrosine-phosphorylation of sperm proteins after triggering the acrosome reaction are needed.

Aquaporins from different groups have distinct relevance in mammalian sperm cryotolerance, which depends on the intrinsic freezability of the ejaculate

Despite being the most frequently used strategy for sperm preservation, cryopreservation is a challenging process for sperm function and survival (Sieme et al., 2008; Peña et al., 2011; Yeste, 2016). Previous studies unveiled an association between relative levels of AQP3 and AQP7 and sperm cryotolerance (Vicente-Carrillo et al., 2016; Prieto-Martínez et al., 2017), but the mechanisms underlying this relationship were not explored. Acknowledging that, it is reasonable to suggest that the effects of AQP inhibition might be different in ejaculates with good (GFE) and poor (PFE) cryotolerance. For this purpose, in this Dissertation, three different AQP inhibitors were added to freezing media to unveil the relevance of AQPs during cryopreservation of pig and horse sperm: 1,3-propanediol (PDO), an efficient inhibitor of orthodox AQPs with a mild inhibitory effect on GLPs (Yu et al., 2016a, 2016b); acetazolamide (AC) , a blocker of AQP1 and AQP4 (Gao et al., 2006; Tanimura et al., 2009); and phloretin (PHL), which

inhibits AQP3 and AQP7 (Rezk et al., 2002; Przybylo et al., 2014; Barreca et al., 2017). In addition, the potential effects of these inhibitors were explored in pig GFE and PFE, to investigate further whether the relevance of AQPs during cryopreservation relied on the intrinsic cryotolerance of the ejaculate.

Horse sperm treated with PDO showed improved motility, survival, acrosome integrity, MMP and intracellular levels of calcium; these samples also exhibited lower membrane lipid disorder than the control. Similarly, pig sperm samples treated with PDO tended to maintain better post-thaw sperm survival and presented lower levels of membrane lipid disorder compared to the control; however, sperm motility was impaired, and the percentages of sperm with high MMP and high levels of ROS were higher. When GFE were considered alone, the effects were similar; in contrast, PFE only presented an increase in ROS levels.

Immediately after thawing, horse sperm samples added with AC presented improved motility, increased membrane lipid disorder, lower MMP and lower levels of calcium compared to the control. After 2 h of thawing, samples also exhibited reduced sperm viability, as well as an increase in the proportions of sperm with a damaged acrosome and high H_2O_2 levels. Similarly, when AC was added to pig samples, sperm showed alterations in MMP and intracellular levels of superoxides.

Regarding horse samples added with PHL, sperm motility, viability, acrosome integrity, MMP, intracellular levels of calcium and of superoxides were lower, whereas membrane lipid disorder was higher. Likewise, pig samples added with PHL showed significantly impaired sperm viability and motility, as well as higher membrane lipid disorder. When GFE samples were considered alone, similar effects were observed in the presence of PHL, in addition to higher MMP compared to the control. In PFE, post-thaw sperm survival was similarly affected as in GFE, motility and membrane lipid disorder only decreased after 30 min of thawing, and the effect on MMP was more drastic.

Assenting to the different affinity for the members of the AQPs family, the impact caused by the inhibitors on sperm cells is the consequence of functional

alterations on separate AQPs and the potential collateral effects on other sperm proteins. For this reason, the mechanism of inhibition is crucial to understand the results shown in this Thesis. Moreover, the differences between GFE and PFE are consistent with those from (Yeste et al., 2013, 2014), which suggested that, whereas PFE are less sensitive than GFE to a positive effect on their cryotolerance, they are frequently more sensitive to detrimental effects. In addition, the fact that in some parameters the effect of the inhibitors was more drastic in GFE than in PFE is in accordance with the different levels of AQPs between these groups, which are higher in samples with better cryotolerance (Prieto-Martínez et al., 2017).

Inhibition of aquaporins (AQPs) using 1,3-propanediol (PDO)

When interacting with orthodox AQPs, PDO remains inside their pore because of its narrow diameter, but the wider size of GLPs pore allows this molecule to freely permeate through them, thus partially inhibiting their permeability from the internal part of the plasma membrane (Yu et al., 2016b, 2016a). Consequently, samples treated with PDO may present an impaired transport of water and certain small solutes, including glycerol. Related to this, it is worth mentioning that glycerol is a commonly used permeable cryoprotectant for livestock sperm cryopreservation, including the freezing medium used herein. A quick inflow of this agent through the plasma membrane is thus crucial to ensure a sufficient intracellular concentration during freezing, whereas its outflow of the cell must be fast enough to avoid its toxic effects after thawing. It is, therefore, possible that the detrimental effects of PDO on sperm were a consequence of a lower intake of glycerol. Even so, post-thaw motility, viability, membrane lipid disorder and acrosome integrity improved in the presence of PDO in horse samples, whereas pig sperm also showed improved viability and membrane lipid disorder. When pig GFE were considered alone, the positive effects on sperm viability and membrane lipid disorder were also observed. Hence, it could be that PDO, which has been proven to permeate sperm (Cooper et al., 2008), could act as a cryoprotective agent (CPA) itself, thereby mitigating the detrimental effects that could happen because of the lower flow rates of glycerol and water through the inhibited AQPs. Moreover, glycerol, as other cryoprotectants, has certain toxic effects on sperm

cells (reviewed in (Yeste, 2016)). A partial reduction of its influx, thereupon, could reduce its intracellular concentration and, thus, its toxicity. The results of this Dissertation suggest that adding PDO to the freezing medium improves horse and pig sperm cryotolerance and lowers the toxic effect of glycerol. Finding less toxic and more efficient combinations of CPAs would limit sperm cryodamage and, thus, would yield better post-thaw sperm quality and function. Further research evaluating the potential of PDO as a cryoprotective agent for sperm cryopreservation in combination with other agents is warranted, as its positive result on frozen-thawed sperm observed in this Dissertation is coincident with previous results in human sperm (Widiasih et al., 2009). In fact, this molecule has also been used as a cryoprotective agent for preservation of canine ovarian cortex (Lopes et al., 2016) and in human multipotent stromal cells (Pogozhykh et al., 2015).

The effects of PDO on pig and horse sperm MMP and ROS levels deserve further attention. The observed increase in MMP does not have an apparent cause. It can be suggested that PDO could interact with AQP11, which localises in the mitochondrial membrane of pig sperm (Prieto-Martínez et al., 2014). In fact, this effect was not observed when PFE samples were considered alone, which could be linked to the different levels of this protein in relation to ejaculate cryotolerance as described by (Prieto-Martínez et al., 2014). The effects of PDO on superAQPs, however, have not been evaluated and, thus, further research to unravel the mechanism through which PDO alters MMP in mammalian sperm during cryopreservation is needed. Another potential cause of this higher MMP could otherwise be related to the higher intracellular levels of calcium that were observed in horse sperm samples. As intracellular calcium levels in the presence of PDO were higher than in the control, this effect could be related to a better maintenance of sperm membrane integrity rather than to a specific effect on calcium transport (reviewed in (Nishigaki et al., 2014; Yeste, 2016)). In this context, the increase in sperm motility and MMP would be a downstream effect of this rise in calcium levels.

Finally, to the best of the author's knowledge, the observed increase of oxidative stress in the presence of PDO has not been previously reported. Considering these findings altogether, one could surmise that the higher viability observed in the presence of PDO was at the expense of an increase in the percentage of viable sperm cells with high ROS levels, and therefore, with potential DNA damage (Aitken, 2017). In fact, as intracellular levels of ROS normally increase during cryopreservation as a result of mitochondrial alterations (Gualtieri et al., 2021), this additional ROS could be a direct consequence of an increased MMP. It must also be considered that the mild inhibition through PDO of AQP3 and AQP9, that are peroxiporins (Miller et al., 2010; Watanabe et al., 2016), might impair H_2O_2 detoxification. This inhibition, therefore, could lead to the intracellular accumulation of this molecule, that has a central role in sperm function (Laforenza et al., 2017).

In the light of all the aforementioned, the presence of PDO could lead to a better post-thaw horse sperm quality, so that this molecule should be considered as a potential CPA alone or in combination with others. It must be highlighted that, whereas some negative effects of PDO were observed in both GFE and PFE, the positive effects on sperm quality and function were only detected in the GFE group. These data support that the positive effects of PDO as a CPA on sperm are also dependent on the intrinsic cryotolerance of the ejaculate, whereas the negative effects, which mainly consist of an increase in ROS levels, are similar in GFE and PFE.

Inhibition of aquaporins (AQPs) using phoretin (PHL)

As far as PHL is concerned, its inhibitory mechanism is based on its permeation through the sperm plasma membrane due to its hydrophobicity (Pohl et al., 1997), and the blocking effect on GLPs through its interaction with an internal binding site (Wacker et al., 2013). Keeping this in mind, its presence could inhibit the permeability to water and glycerol, which would be consistent with the similar effects observed in sperm motility when either PDO or PHL were present, in both pig and horse samples. Moreover, the hypothesis of PDO having a cryoprotective outcome is supported by the detrimental consequences of PHL on pig and horse

sperm survival, membrane lipid disorder and MMP. When pig GFE were considered alone, the repercussion was similar. In PFE, these effects were observed at 30 min post-thawing but disappeared at 240 min in PFE. This might be the result of a masking effect due to the poor quality of these samples.

The impairment in the integrity of sperm membranes could explain the compromised mitochondrial function in terms of MMP, as well as the drop in intracellular levels of calcium that was observed in horse sperm. In these samples, intracellular levels of superoxides and peroxides were lower than in the control immediately after thawing, which could be related to the decrease in MMP. In spite of this, peroxide levels increased after 2 h of incubation in horse sperm, which could be due to the inhibition of H_2O_2 efflux through AQP3 and AQP9, which are both GLPs and peroxiporins (Miller et al., 2010; Watanabe et al., 2016).

The fact that in PFE the effects on MMP were more evident than in GFE could indicate potential collateral effects of PHL on other sperm proteins, such as SLC2A2 (also known as GLUT2), protein kinase C (PKC), and volume-sensitive and cAMP-activated Cl^- channels (Fan et al., 2001), all of them playing important roles in sperm physiology. In fact, SLC2A2 participates in the uptake of monosaccharides, which are the main energy sources for sperm (Bucci et al., 2010); PKC is involved in the signalling pathways that regulate sperm motility; and chloride-dependent transport mechanisms are relevant for different aspects of sperm physiology, like capacitation (Bonet et al., 2013). The effects on sperm motility, viability and MMP observed in the presence of PHL, therefore, could not only be the consequence of GLPs inhibition, but could also result from the interaction with other sperm proteins.

To sum up, all these findings suggest that not only are GLPs relevant for water permeability and osmoregulation but they are also involved in the transport of glycerol and hydrogen peroxide through the plasma membrane during pig and horse sperm cryopreservation. Moreover, the relevance of GLPs during sperm cryopreservation depends on the intrinsic cryotolerance of the ejaculate.

Inhibition of aquaporins (AQPs) using acetazolamide (AC)

Because AC specifically inhibits AQP1 and AQP4, which are orthodox AQPs, glycerol transport should not be impaired; this could explain the absence of effects on sperm viability and membrane lipid disorder. In fact, these two AQPs have not been previously identified in the sperm of most mammalian species, including porcine and equine (reviewed in (Yeste et al., 2017), so that no effects on sperm physiology should be expected. Yet, some sperm parameters were altered in the presence of AC in both species, but these effects were not concentration dependent. It can be suggested, therefore, that AC could have side effects on other sperm proteins. In fact, AC can interact with carbonic anhydrase (CA), and thus impair the conversion of CO_2 and H_2O into bicarbonate and protons (Berkel and Pharm, 2018). Bicarbonate regulates PKA activity, and one of the downstream events of this signalling pathway is the phosphorylation of complexes I and IV of the electron transport chain (Acin-Perez et al., 2009; Lark et al., 2015). Hence, the inhibition of CA through AC could cause the uncoupling of the electron transport chain, which could be responsible for the alterations in MMP and higher ROS levels in both pig and horse samples treated with certain concentrations of AC. The AQPs that are inhibited by AC, AQP1 and AQP4, do not present peroxide permeability. Hence, this molecule might be able to outflow physiologically and it does not accumulate intracellularly as in the presence of PDO.

It must also be considered that such an alteration of pH derived from a lower CA activity could also compromise the functioning of different pH-regulated proteins. One relevant example of pH-regulated proteins are CatSper calcium channels. Given that, in sperm, these channels open in response to intracellular alkalinisation (reviewed in (Nishigaki et al., 2014)), the lower levels of bicarbonate that would be expected in response to CA inhibition could hinder the activation of CatSper channels, driving to the lower intracellular calcium levels observed in horse sperm samples treated with AC. As sperm motility also depends on intracellular pH and calcium levels, this hypothesis would not explain the higher sperm motility observed in these samples immediately after thawing. Thus, further research to understand the mechanisms underlying the effects of AC on horse sperm upon thawing is required. Finally, pondering that some detrimental effects,

such as alterations in sperm viability and acrosome integrity, were not apparent immediately after thawing but manifested at 2 h post-thaw in horse sperm, one could suggest that AC would induce sub-lethal detrimental effects that would become evident after samples were incubated at physiological temperatures.

Sperm cryotolerance relies on HVCN1 rather than on potassium channels

As, during cryopreservation, sperm undergo drastic osmotic changes and ion channels are involved in osmoadaptation (Lishko et al., 2012), it is reasonable to explore their potential function during this process. Data about the nature, distribution, and function of K^+ and HVCN1 channels in mammalian sperm are scarce. As far as SLO channels are concerned, they are known to be the main K^+ channels in human and mouse sperm, and their involvement in volume regulation and capacitation has been largely explored (Barfield et al., 2005a; Mannowetz et al., 2013; Sun et al., 2017). Yet, not only do these two species present different types of SLO channels, but their mechanisms of regulation are also disparate. As aforementioned, whereas mouse sperm present SLO3 (Santi et al., 2010; Zeng et al., 2011; De La Vega-Beltran et al., 2012; Brown et al., 2019), human sperm contain both SLO1 and SLO3 channels (Mannowetz et al., 2013; Brenker et al., 2014). In terms of regulatory mechanisms, SLO1 channels can be modulated through both membrane voltage and intracellular Ca^{2+} levels (Tang et al., 2010; Yuan et al., 2010), whereas SLO3 channels are sensitive to intracellular alkalinization in mouse (Sun et al., 2017), and to pH and calcium in human sperm (Sánchez-Carranza et al., 2015). In pig sperm, SLO1 channels have been identified in the acrosomal and post-acrosomal regions of the sperm head, as well as in the flagellum (Yeste et al., 2019). Potassium channels other than SLO1, nevertheless, have been suggested to participate in K^+ conductance in pig sperm (Yeste et al., 2019). The function of HVCN1 in different cell types and processes is very relevant and is known to consist of driving an outflow of protons to the extracellular medium (reviewed in (Zhao et al., 2018)). This channel has been identified in the plasma membrane of human, macaque, cattle, and pig sperm, but it is absent from mouse sperm (Lishko and Kirichok, 2010; Brenker et al., 2014; Berger et al., 2017; Chen et al., 2017; Mishra et al., 2019). It is important to highlight that, in macaques, the relative levels of

HVCN1 decrease after sperm cryopreservation (Blässe et al., 2012). This Dissertation also evaluated the general role of K^+ channels and the specific function of SLO1 and HVCN1 during pig sperm cryopreservation through the addition of distinct inhibitors of these channels to cryopreservation medium at 15 °C or at 5 °C. Three different inhibitors were used: paxilline (PAX), which is a fungal indole alkaloid that specifically inhibits the SLO1 channel (Tang et al., 2010; Zhou and Lingle, 2014); tetraethyl ammonium chloride (TEA), a quaternary ammonium compound that inhibits 6TM K^+ channels (Hille, 2001; Tang et al., 2010; Alexander et al., 2011); and 2-guanidino benzimidazole (2-GBI), which is a specific inhibitor of the HVCN1 channel (Hong et al., 2014). These inhibitors were used in previous works to evaluate the relevance of SLO1 (Yeste et al., 2019) and HVCN1 channels (Yeste et al., 2020) for pig sperm capacitation. Herein, whereas the inhibition of K^+ channels through PAX and TEA did not alter post-thaw sperm function and survival as compared to the control, inhibition of HVCN1 with 2-GBI dramatically impaired post-thaw sperm quality and function.

Unexpectedly, the general inhibition of K^+ channels through TEA and the specific inhibition of SLO1 with PAX, either when the inhibitors were added at 15 °C or after samples were cooled down to 5 °C, did not induce alterations in motility and kinematics, plasma or acrosome membrane integrity, membrane lipid disorder, MMP, or intracellular levels of calcium or ROS. Taking the central role of K^+ channels during sperm capacitation into account (Lishko et al., 2012; Yeste et al., 2019), the absence of differences between the control and samples treated with TEA and PAX suggests that either K^+ channels are not relevant for osmoadaptation of pig sperm during cryopreservation, or alterations in K^+ conductance have a modest impact on post-thaw sperm quality. In this regard, further studies aiming to determine the functional contribution and conductance of K^+ channels in pig sperm during cryopreservation and the potential changes on their relative content during this process are needed. Interestingly, the relative levels of the TASK-2 ($K_{2P}5.1$) channel in bovine sperm are not altered during cryopreservation, but they are associated to increased intracellular levels of potassium (Blässe et al., 2012). It is important to highlight that TASK-2 is a

member of the 4TM family of K^+ channels, which are not sensitive to TEA (Alexander et al., 2011). Accordingly, it is possible that even though TEA was added to samples with the purpose of inhibiting all 6TM channels, those from other families could compensate this function.

Because the K^+ efflux is involved in changes in motility patterns during sperm hyperactivation, plasma membrane hyperpolarization, calcium influx and acrosome exocytosis, it has a central role in sperm capacitation (Brenker et al., 2014; Mansell et al., 2014; Brown et al., 2019; Yeste et al., 2019). The changes that sperm undergo after being frozen-thawed are ample and can dramatically affect their fertilising ability (reviewed in (Pini et al., 2018)). The detrimental impact consists of premature acrosomal exocytosis, altered plasma membrane integrity, impaired sperm viability and the appearance of apoptotic-like changes (Pinart and Puigmulé, 2013). The similarity between the contexts in which capacitation and cryopreservation take place seems to be related to a drastic change in the composition of the surrounding environment, and in fact, the activation of K^+ channels in human sperm relies on the presence of divalent cations in the surrounding medium (Mannowetz et al., 2013). Acknowledging that, further studies should address the potential involvement of K^+ channels in the sperm response to cryopreservation.

Regarding proton channels, a previous study suggested that in human HVCN1, Phe150 in TM2 - which is located close to the ion-permeation pathway - is involved in the inhibition mediated by 2-GBI, an open-channel blocker (Hong et al., 2013). In the presence of 2-GBI, almost all sperm quality and function parameters were altered, which supports that HVCN1 might play a vital function in the resilience of sperm to cryopreservation. Similarly, inhibition of HVCN1 is known to reduce the viability of human (Keshtgar et al., 2018) and bovine sperm (Mishra et al., 2019), and human sperm cells that undergo HVCN1 inhibition become unable to regulate their pH (Lishko and Kirichok, 2010). Despite little data being available about changes in intracellular pH during cryopreservation, a single study reported a mild pH decrease in bovine sperm (Blässe et al., 2012). Inhibition of HVCN1 channels also leads to impaired motility activation during *in vitro*

capacitation of pig (Yeste et al., 2020) and human sperm (Lishko et al., 2010). HVCN1 is essential for motility activation after ejaculation, and for motility hyperactivation during capacitation in bovine (Mishra et al., 2019) and human sperm (Lishko and Kirichok, 2010). In fact, in human sperm, HVCN1 conductance increases during capacitation, which is regulated through phosphorylation as a capacitation-associated event (Lishko and Kirichok, 2010; Lishko et al., 2010).

Concerning the effects on calcium levels in the presence of 2-GBI, it is important to highlight that some calcium channels are pH- or voltage-sensitive (Alexander et al., 2011). As a potential consequence of changes in pH, it is possible that Ca^{2+} conductance is impaired. Indeed, CatSper channels, which are voltage-gated channels highly sensitive to intracellular alkalinisation, are involved in motility regulation during pig sperm capacitation (Vicente-Carrillo et al., 2017). The results of (Yeste et al., 2020) are in the same line, as the presence of 2-GBI also decreases intracellular calcium levels during acrosome reaction in pig sperm. In the light of these findings, the changes observed in calcium levels could result from a pH decrease because of the intracellular accumulation of protons. The lower levels of calcium could, in turn, be the reason of the lower sperm motility in HVCN1-treated samples compared to the control.

As reported in previous studies, intracellular levels of ROS are known to increase during cryopreservation in association to a higher MMP (Llavanera et al., 2019; Zhu et al., 2019). Samples treated with 2-GBI showed increased MMP at 240 min post-thawing compared to the control. Yet, these samples also presented lower intracellular levels of ROS at any time point post-thawing. This happened in contrast to the results obtained in other experiments conducted in this Dissertation, where the inhibition of AQPs led to an increase in both MMP and intracellular ROS levels, apparently because of the intracellular accumulation of peroxides. It must be pondered that HVCN1 is involved in the activation of NADPH oxidase, which is related to the generation of superoxide radicals as a by-product of mitochondrial electron transport chain (Musset et al., 2012; Ghanbari et al., 2019). One, therefore, could speculate that a decrease in intracellular ROS levels could occur as a response to HVCN1 inhibition during sperm cryopreservation.

Another potential mechanism through which the inhibition of HVCN1 with 2-GBI could lead to lower levels of ROS would be the Fenton reaction. This reaction occurs in low pH conditions and consists of the use of peroxides to generate hydroxyl radicals, which they are in turn responsible for lipid peroxidation (Merksamer et al., 2013). High levels of lipid peroxidation cause membrane destabilisation, including both plasma and acrosome membranes, which are changes that also occurred in the presence of 2-GBI. In previous studies evaluating the effects of HVCN1 inhibition during pig and human sperm capacitation, premature acrosome exocytosis and plasma membrane lipid disorder were also observed (Keshtgar et al., 2018; Yeste et al., 2020). Nevertheless, further research is needed to confirm the mechanisms behind the low levels of ROS in the presence of high mitochondrial activity. Related with this, plasma membrane NADPH oxidases could have a role (Miguel-Jiménez et al., 2021).

In short, the results of this Dissertation support that while HVCN1 is essential for the homeostasis of pig sperm during cryopreservation and to prevent a degenerative acrosome exocytosis, K^+ channels play a marginal role.

Conclusions

Conclusions

1. The specific inhibition of AQP3 during cryopreservation leads to increased intracellular levels of peroxides, which could be the consequence of an impaired efflux of this molecule through AQP3.

2. Aquaporins as a whole are crucial in maintaining motility and lipid membrane architecture during sperm capacitation.

3. The inhibition of AQPs during capacitation may alter the intracellular signalling pathways that regulate the acrosome reaction, since some alterations in sperm physiology become apparent upon its triggering.

4. The group of GLPs have a relevant role in mammalian sperm cryotolerance.

5. The relevance of AQPs during cryopreservation relies on the intrinsic cryotolerance of the ejaculate.

6. The inhibition of potassium channels does not have a relevant effect on pig sperm cryotolerance.

7. Proton permeability through the HVCN1 channel is essential to maintain sperm function and survival during freeze-thawing.

References

References

Abi Nahed, R., Martinez, G., Hograindleur, J. P., Le Blévec, E., Camugli, S., Le Boucher, R., et al. (2018). Slo3 K+ channel blocker clofilium extends bull and mouse sperm-fertilizing competence. *Reproduction* 156, 463–476. doi:10.1530/REP-18-0075.

Abrami, L., Tacnet, F., and Ripoche, P. (1995). Evidence for a glycerol pathway through aquaporin 1 (CHIP28) channels. *Pflügers Arch.* 430, 447–458. doi:10.1007/BF00373921.

Acin-Perez, R., Salazar, E., Kamenetsky, M., Buck, J., Levin, L. R., and Manfredi, G. (2009). Cyclic AMP produced inside mitochondria regulates oxidative phosphorylation. *Cell Metab.* 9, 265–276. doi:10.1016/j.cmet.2009.01.012.

Agre, P., King, L. S., Yasui, M., Guggino, W. B., Ottersen, O. P., Fujiyoshi, Y., et al. (2002). Aquaporin water channels-from atomic structure to clinical medicine. *J. Physiol.* 542, 3–16. doi:10.1113/jphysiol.2002.020818.

Aitken, R. J. (2017). Reactive oxygen species as mediators of sperm capacitation and pathological damage. *Mol. Reprod. Dev.* 84, 1039–1052. doi:10.1002/mrd.22871.

Alberts, B., Johnson, A., Lewis, J., Raff, M., Roberts, K., and Walter, P. (2008). *Molecular biology of the cell*. 5th ed. Abingdon: Garland Science doi:0815341059.

Alexander, S., Mathie, A., and Peters, J. (2011). Ion Channels. *Br. J. Pharmacol.* 164, S137–S174. doi:10.1111/j.1476-5381.2011.01649_5.x.

Alyasin, A., Momeni, H. R., and Mahdieh, M. (2020). Aquaporin3 expression and the potential role of aquaporins in motility and mitochondrial membrane potential in human spermatozoa. *Andrologia* 52, 1–7. doi:10.1111/and.13588.

Armstrong, C. M., and Hille, B. (1998). Voltage-Gated Ion Channels and Electrical Excitability. *Neuron* 20, 371–380. doi:10.1016/S0896-6273(00)80981-2.

Bailey, J. L. (2010). Factors Regulating Sperm Capacitation. *Syst. Biol. Reprod. Med.*

56, 334–348. doi:10.3109/19396368.2010.512377.

Baishya, S. K., Biswas, R. K., Kadirvel, G., Deka, B. C., Kumar, S., Sinha, S., et al. (2014). Effect of conventional and controlled freezing method on the post thaw characteristics of boar spermatozoa. *Anim. Reprod. Sci.* 149, 231–237. doi:10.1016/j.anireprosci.2014.06.020.

Barfield, J. P., Yeung, C. H., and Cooper, T. G. (2005a). Characterization of potassium channels involved in volume regulation of human spermatozoa. *Mol. Hum. Reprod.* 11, 891–897. doi:10.1093/molehr/gah208.

Barfield, J. P., Yeung, C. H., and Cooper, T. G. (2005b). The effects of putative K+ channel blockers on volume regulation of murine spermatozoa. *Biol. Reprod.* 72, 1275–1281. doi:10.1095/biolreprod.104.038448.

Barreca, D., Currò, M., Bellocco, E., Ficarra, S., Laganà, G., Tellone, E., et al. (2017). Neuroprotective effects of phloretin and its glycosylated derivative on rotenone-induced toxicity in human SH-SY5Y neuronal-like cells. *BioFactors* 43, 549–557. doi:10.1002/biof.1358.

Barros, C., Bedford, J. M., Franklin, L. E., and Austin, C. R. (1967). Membrane vesiculation as a feature of the mammalian acrosome reaction. *J. Cell Biol.* 34, C1-5. doi:10.1083/jcb.34.3.c1.

Bearer, E. L., and Friend, D. S. (1990). Morphology of mammalian sperm membranes during differentiation, maturation, and capacitation. *J. Electron Microsc. Tech.* 16, 281–297. doi:10.1002/jemt.1060160403.

Benfenati, V., Caprini, M., Dovizio, M., Mylonakou, M. N., Ferroni, S., Ottersen, O. P., et al. (2011). An aquaporin-4/transient receptor potential vanilloid 4 (AQP4/TRPV4) complex is essential for cell-volume control in astrocytes. *Proc. Natl. Acad. Sci.* 108, 2563–2568. doi:10.1073/pnas.1012867108.

Berger, T. K., Fußhöller, D. M., Goodwin, N., Bönigk, W., Müller, A., Dokani Khesroshahi, N., et al. (2017). Post-translational cleavage of Hv1 in human sperm tunes pH- and voltage-dependent gating. *J. Physiol.* 595, 1533–1546. doi:10.1113/JP273189.

Berkel, M. A. Van, and Pharm, D. (2018). Evaluating off-label uses of acetazolamide. *Am. J. Heal. Pharm.* 75, 524–531. doi:10.2146/ajhp170279.

Bernardino, R. L., Carrageta, D. F., Sousa, M., Alves, M. G., and Oliveira, P. F. (2019). pH and male fertility: making sense on pH homeodynamics throughout the male reproductive tract. *Cell. Mol. Life Sci.* 76, 3783–3800. doi:10.1007/s00018-019-03170-w.

Bienert, G. P., Møller, A. L. B., Kristiansen, K. A., Schulz, A., Møller, I. M., Schjoerring, J. K., et al. (2007). Specific aquaporins facilitate the diffusion of hydrogen peroxide across membranes. *J. Biol. Chem.* 282, 1183–1192. doi:10.1074/jbc.M603761200.

Blässe, A.-K., Oldenhof, H., Ekhlasi-Hundrieser, M., Wolkers, W. F., Sieme, H., and Bollwein, H. (2012). Osmotic tolerance and intracellular ion concentrations of bovine sperm are affected by cryopreservation. *Theriogenology* 78, 1312–1320. doi:https://doi.org/10.1016/j.theriogenology.2012.05.029.

Bonet, S., Casas, I., and Holt, W. V. (2013). *Boar Reproduction: Fundamentals and New Biotechnological Trends*. , eds. S. Bonet, I. Casas, W. V. Holt, and M. Yeste Berlin, Heidelberg: Springer doi:10.1007/978-3-642-35049-8.

Bonilla-Correal, S., Noto, F., Garcia-Bonavila, E., Rodríguez-Gil, J. E., Yeste, M., and Miró, J. (2017). First evidence for the presence of aquaporins in stallion sperm. *Reprod. Domest. Anim.* 52, 61–64. doi:10.1111/rda.13059.

Breitbart, H., Cohen, G., and Rubinstein, S. (2005). Role of actin cytoskeleton in mammalian sperm capacitation and the acrosome reaction. *Reproduction* 129, 263–268. doi:10.1530/rep.1.00269.

Brenker, C., Zhou, Y., Müller, A., Echeverry, F. A., Trötschel, C., Poetsch, A., et al. (2014). The Ca2+-activated K+ current of human sperm is mediated by Slo3. *Elife* 3, e01438. doi:10.7554/eLife.01438.

Brown, S. G., Publicover, S. J., Barratt, C. L. R., and Martins da Silva, S. J. (2019). Human sperm ion channel (dys)function: implications for fertilization. *Hum. Reprod. Update* 25, 758–776. doi:10.1093/humupd/dmz032.

Bucci, D., Isani, G., Spinaci, M., Tamanini, C., Mari, G., Zambelli, D., et al. (2010). Comparative Immunolocalization of GLUTs 1, 2, 3 and 5 in Boar, Stallion and Dog Spermatozoa. *Reprod. Domest. Anim.* 45, 315–322. doi:10.1111/j.1439-0531.2008.01307.x.

Buffone, M. G., Hirohashi, N., and Gerton, G. L. (2014a). Unresolved questions concerning Mammalian sperm acrosomal exocytosis. *Biol. Reprod.* 90, 112, 1–8. doi:10.1095/biolreprod.114.117911.

Buffone, M. G., Wertheimer, E. V., Visconti, P. E., and Krapf, D. (2014b). Central role of soluble adenylyl cyclase and cAMP in sperm physiology. *Biochim. Biophys. Acta - Mol. Basis Dis.* 1842, 2610–2620. doi:10.1016/j.bbadis.2014.07.013.

Calamita, G., Mazzone, A., Bizzoca, A., and Svelto, M. (2001). Possible Involvement of Aquaporin-7 and -8 in Rat Testis Development and Spermatogenesis. *Biochem. Biophys. Res. Commun.* 288, 619–625. doi:https://doi.org/10.1006/bbrc.2001.5810.

Callies, C., Cooper, T. G., and Yeung, C. H. (2008). Channels for water efflux and influx involved in volume regulation of murine spermatozoa. *Reproduction* 136, 401–410. doi:10.1530/REP-08-0149.

Chang, J. C., and Oude-Elferink, R. P. J. (2014). Role of the bicarbonate-responsive soluble adenylyl cyclase in pH sensing and metabolic regulation. *Front. Physiol.* 5, 42. doi:10.3389/fphys.2014.00042.

Chaves, B. R., Pinoti Pavaneli, A. P., Blanco-Prieto, O., Pinart, E., Bonet, S., Zangeronimo, M. G., et al. (2021). Exogenous Albumin Is Crucial for Pig Sperm to Elicit In Vitro Capacitation Whereas Bicarbonate Only Modulates Its Efficiency. *Biology (Basel).* 10, 1105. doi:10.3390/biology10111105.

Chávez, J. C., de la Vega-Beltrán, J. L., Escoffier, J., Visconti, P. E., Treviño, C. L., Darszon, A., et al. (2013). Ion permeabilities in mouse sperm reveal an external trigger for SLO3-dependent hyperpolarization. *PLoS One* 8, e60578. doi:10.1371/journal.pone.0060578.

Chávez, J. C., Ferreira, J. J., Butler, A., De La Vega Beltrán, J. L., Treviño, C. L., Darszon, A., et al. (2014). SLO3 K+ channels control calcium entry through CATSPER channels in sperm. *J. Biol. Chem.* 289, 32266–32275. doi:10.1074/jbc.M114.607556.

Chen, B., Li, S., Yan, Y., Duan, Y., Chang, S., Wang, H., et al. (2017). Cryopreservation of cynomolgus macaque (Macaca fascicularis) sperm with glycerol and ethylene glycol, and its effect on sperm-specific ion channels - CatSper and Hv1. *Theriogenology* 104, 37–42. doi:10.1016/j.theriogenology.2017.08.009.

Chen, Q., and Duan, E. K. (2011). Aquaporins in sperm osmoadaptation: An emerging role for volume regulation. *Acta Pharmacol. Sin.* 32, 721–724. doi:10.1038/aps.2011.35.

Chen, Q., Peng, H., Lei, L., Zhang, Y., Kuang, H., Cao, Y., et al. (2011). Aquaporin 3 is a sperm water channel essential for postcopulatory sperm osmoadaptation and migration. *Cell Res.* 21, 922–933. doi:10.1038/cr.2010.169.

Choe, S. (2002). Potassium channel structures. *Nat. Rev. Neurosci.* 3, 115–121. doi:10.1038/nrn727.

Cooper, T. G., Barfield, J. P., and Yeung, C. H. (2008). The tonicity of murine epididymal spermatozoa and their permeability towards common cryoprotectants and epididymal osmolytes. *Reproduction* 135, 625–633. doi:10.1530/REP-07-0573.

Cooper, T. G., and Brooks, D. E. (1981). Entry of glycerol into the rat epididymis and its utilization by epididymal spermatozoa. *J. Reprod. Fertil.* 61, 163–169. doi:10.1530/jrf.0.0610163.

Cooper, T. G., and Yeung, C.-H. (2003). Acquisition of volume regulatory response of sperm upon maturation in the epididymis and the role of the cytoplasmic droplet. *Microsc. Res. Tech.* 61, 28–38. doi:10.1002/jemt.10314.

Cooper, T. G., and Yeung, C. H. (2006). “Sperm maturation in the human epididymis,” in *The Sperm Cell: Production, Maturation, Fertilization,*

Regeneration, eds. C. De Jonge and C. Barratt (United Kingdom: Cambridge University Press), 72–107. doi:10.1017/CBO9780511545115.005.

Curry, M. R. (2007). "Cryopreservation of mammalian semen," in *Cryopreservation and Freeze-Drying Protocols. Methods in Molecular Biology*^{TM}, eds. J. G. Day and G. N. Stacey (Totowa, NJ: Humana Press Inc.), 303–311.

Curry, M. R., Millar, J. D., and Watson, P. F. (1995). The presence of water channel proteins in ram and human sperm membranes. *J. Reprod. Fertil.* 104, 297–303. doi:10.1530/jrf.0.1040297.

De La Vega-Beltran, J. L., Sánchez-Cárdenas, C., Krapf, D., Hernandez-González, E. O., Wertheimer, E., Treviño, C. L., et al. (2012). Mouse sperm membrane potential hyperpolarization is necessary and sufficient to prepare sperm for the acrosome reaction. *J. Biol. Chem.* 287, 44384–44393. doi:10.1074/jbc.M112.393488.

Delgado-Bermúdez, A., Ribas-Maynou, J., and Yeste, M. (2022). Relevance of Aquaporins for Gamete Function and Cryopreservation. *Anim.* 12, 573. doi:10.3390/ani12050573.

Di Santo, M., Tarozzi, N., Nadalini, M., and Borini, A. (2012). Human Sperm Cryopreservation: Update on Techniques, Effect on DNA Integrity, and Implications for ART. *Adv. Urol.* 2012, 854837. doi:10.1155/2012/854837.

Drevius, L.-O., and Eriksson, H. (1966). Osmotic swelling of mammalian spermatozoa. *Exp. Cell Res.* 42, 136–156. doi:https://doi.org/10.1016/0014-4827(66)90327-2.

Escoffier, J., Navarrete, F., Haddad, D., Santi, C. M., Darszon, A., and Visconti, P. E. (2015). Flow cytometry analysis reveals that only a subpopulation of mouse sperm undergoes hyperpolarization during capacitation. *Biol. Reprod.* 92, 121. doi:10.1095/biolreprod.114.127266.

Fan, H., Morishima, S., Kida, H., and Okada, Y. (2001). Phloretin differentially inhibits volume-sensitive and cyclic AMP-activated, but not Ca-activated, Cl-channels. *Br. J. Pharmacol.* 133, 1096–1106.

Flesch, F. M., Brouwers, J. F., Nievelstein, P. F., Verkleij, A. J., van Golde, L. M., Colenbrander, B., et al. (2001). Bicarbonate stimulated phospholipid scrambling induces cholesterol redistribution and enables cholesterol depletion in the sperm plasma membrane. *J. Cell Sci.* 114, 3543–3555. doi:10.1242/jcs.114.19.3543.

Florman, H. M., and Fissore, R. A. (2015). "Fertilization in Mammals," in *Knobil and Neill's Physiology of Reproduction*, eds. T. M. Plant and A. J. Zeleznik (London: Academic Press), 149–196. doi:10.1016/B978-0-12-397175-3.00004-1.

Ford, P., Merot, J., Jawerbaum, A., Gimeno, M. A., Capurro, C., and Parisi, M. (2000). Water permeability in rat oocytes at different maturity stages: aquaporin-9 expression. *J. Membr. Biol.* 176, 151–158. doi:10.1007/s00232001084.

Fraser, L., Brym, P., Pareek, C. S., Mogielnicka-Brzozowska, M., Paukszto, Ł., Jastrzębski, J. P., et al. (2020). Transcriptome analysis of boar spermatozoa with different freezability using RNA-Seq. *Theriogenology* 142, 400–413. doi:10.1016/j.theriogenology.2019.11.001.

Fu, D., Libson, A., Miercke, L. J., Weitzman, C., Nollert, P., Krucinski, J., et al. (2000). Structure of a glycerol-conducting channel and the basis for its selectivity. *Science* 290, 481–486. doi:10.1126/science.290.5491.481.

Fujii, T., Hirayama, H., Fukuda, S., Kageyama, S., Naito, A., Yoshino, H., et al. (2018). Expression and localization of aquaporins 3 and 7 in bull spermatozoa and their relevance to sperm motility after cryopreservation. *J. Reprod. Dev.* 64, 327–335. doi:10.1262/jrd.2017-166.

Gadella, B. M., and Harrison, R. A. (2000). The capacitating agent bicarbonate induces protein kinase A-dependent changes in phospholipid transbilayer behavior in the sperm plasma membrane. *Development* 127, 2407–2420. doi:10.1242/dev.127.11.2407.

Gao, J., Wang, X., Chang, Y., Zhang, J., Song, Q., Yu, H., et al. (2006).

Acetazolamide inhibits osmotic water permeability by interaction with aquaporin-1. *Anal. Biochem.* 350, 165–170. doi:10.1016/j.ab.2006.01.003.

Gao, T., Li, K., Liang, F., Yu, J., Liu, A., Ni, Y., et al. (2021). KCNQ1 Potassium Channel Expressed in Human Sperm Is Involved in Sperm Motility, Acrosome Reaction, Protein Tyrosine Phosphorylation, and Ion Homeostasis During Capacitation. *Front. Physiol.* 12, 761910. doi:10.3389/fphys.2021.761910.

Geng, Y., Ferreira, J. J., Dzikunu, V., Butler, A., Lybaert, P., Yuan, P., et al. (2017). A genetic variant of the sperm-specific SLO3 K(+) channel has altered pH and Ca(2+) sensitivities. *J. Biol. Chem.* 292, 8978–8987. doi:10.1074/jbc.M117.776013.

Ghanbari, H., Keshtgar, S., Zare, H. R., and Gharesi-Fard, B. (2019). Inhibition of CatSper and Hv1 Channels and NOX5 Enzyme Affect Progesterone-Induced Increase of Intracellular Calcium Concentration and ROS Generation in Human Sperm. *Iran. J. Med. Sci.* 44, 127–134.

Giaccagli, M. M., Gómez-Elías, M. D., Herzfeld, J. D., Marín-Briggiler, C. I., Cuasnicú, P. S., Cohen, D. J., et al. (2021). Capacitation-Induced Mitochondrial Activity Is Required for Sperm Fertilizing Ability in Mice by Modulating Hyperactivation. *Front. Cell Dev. Biol.* 9, 767161. doi:10.3389/fcell.2021.767161.

González, C., Baez-Nieto, D., Valencia, I., Oyarzún, I., Rojas, P., Naranjo, D., et al. (2012). K+ channels: Function-structural overview. *Compr. Physiol.* 2, 2087–2149. doi:10.1002/cphy.c110047.

Gonzalez, C., Koch, H. P., Drum, B. M., and Larsson, H. P. (2010). Strong cooperativity between subunits in voltage-gated proton channels. *Nat. Struct. Mol. Biol.* 17, 51–56. doi:10.1038/nsmb.1739.

Gouaux, E., and MacKinnon, R. (2005). Principles of Selective Ion Transport in Channels and Pumps. *Science.* 310, 1461–1465. doi:10.1126/science.1113666.

Grunewald, S., Paasch, U., Glander, H.-J., and Anderegg, U. (2005). Mature human

spermatozoa do not transcribe novel RNA. *Andrologia* 37, 69–71. doi:10.1111/j.1439-0272.2005.00656.x.

Gualtieri, R., Kalthur, G., Barbato, V., Di Nardo, M., Adiga, S. K., and Talevi, R. (2021). Mitochondrial Dysfunction and Oxidative Stress Caused by Cryopreservation in Reproductive Cells. *Antioxidants (Basel, Switzerland)* 10, 337. doi:10.3390/antiox10030337.

Gupta, R. K., Swain, D. K., Singh, V., Anand, M., Choudhury, S., Yadav, S., et al. (2018). Molecular characterization of voltage-gated potassium channel (Kv) and its importance in functional dynamics in bull spermatozoa. *Theriogenology* 114, 229–236. doi:10.1016/j.theriogenology.2018.03.030.

Haddoub, R., Rützler, M., Robin, A., and Flitsch, S. L. (2009). "Design, synthesis and assaying of potential aquaporin inhibitors," in *Aquaporins. Handbook of Experimental Pharmacology*, ed. E. Beitz (Berlin, Heidelberg: Springer-Verlag), 385–402. doi:10.1007/978-3-540-79885-9_19.

Harper, C. V, Barratt, C. L. R., Publicover, S. J., and Kirkman-Brown, J. C. (2006). Kinetics of the progesterone-induced acrosome reaction and its relation to intracellular calcium responses in individual human spermatozoa. *Biol. Reprod.* 75, 933–939. doi:10.1095/biolreprod.106.054627.

Harrison, R. A., and Miller, N. G. (2000). cAMP-dependent protein kinase control of plasma membrane lipid architecture in boar sperm. *Mol. Reprod. Dev.* 55, 220–228. doi:10.1002/(SICI)1098-2795(200002)55:2<220::AID-MRD12>3.0.CO;2-I.

Heginbotham, L., Lu, Z., Abramson, T., and MacKinnon, R. (1994). Mutations in the K+ channel signature sequence. *Biophys. J.* 66, 1061–1067. doi:10.1016/S0006-3495(94)80887-2.

Hess, R. A., Bunick, D., Lee, K.-H., Bahr, J., Taylor, J. A., Korach, K. S., et al. (1997). A role for oestrogens in the male reproductive system. *Nature* 390, 509–512. doi:10.1038/37352.

Hill, A. E., and Shachar-Hill, Y. (2015). Are Aquaporins the Missing

Transmembrane Osmosensors? *J. Membr. Biol.* 248, 753–765. doi:10.1007/s00232-015-9790-0.

Hille, B. (2001). *Ion Channels of Excitable Membranes*. 3rd ed. Sunderland, MA: Sinauer Associates, Inc.

Hirano, Y., Okimoto, N., Kadohira, I., Suematsu, M., Yasuoka, K., and Yasui, M. (2010). Molecular mechanisms of how mercury inhibits water permeation through aquaporin-1: Understanding by molecular dynamics simulation. *Biophys. J.* 98, 1512–1519. doi:10.1016/j.bpj.2009.12.4310.

Hoffmann, N., Oldenhof, H., Morandini, C., Rohn, K., and Sieme, H. (2011). Optimal concentrations of cryoprotective agents for semen from stallions that are classified "good" or "poor" for freezing. *Anim. Reprod. Sci.* 125, 112–118. doi:10.1016/j.anireprosci.2011.03.001.

Hong, L., Kim, I. H., and Tombola, F. (2014). Molecular determinants of Hv1 proton channel inhibition by guanidine derivatives. *Proc. Natl. Acad. Sci. U. S. A.* 111, 9971–9976. doi:10.1073/pnas.1324012111.

Hong, L., Pathak, M. M., Kim, I. H., Ta, D., and Tombola, F. (2013). Voltage-sensing domain of voltage-gated proton channel Hv1 shares mechanism of block with pore domains. *Neuron* 77, 274–287. doi:10.1016/j.neuron.2012.11.013.

Huang, H. F., He, R. H., Sun, C. C., Zhang, Y., Meng, Q. X., and Ma, Y. Y. (2006). Function of aquaporins in female and male reproductive systems. *Hum. Reprod. Update* 12, 785–795. doi:10.1093/humupd/dml035.

Hur, C.-G., Choe, C., Kim, G.-T., Cho, S.-K., Park, J.-Y., Hong, S.-G., et al. (2009). Expression and localization of two-pore domain K(+) channels in bovine germ cells. *Reproduction* 137, 237–244. doi:10.1530/REP-08-0035.

Isacoff, E. Y., Jan, Y. N., and Jan, L. Y. (1991). Putative receptor for the cytoplasmic inactivation gate in the Shaker K+ channel. *Nature* 353, 86–90. doi:10.1038/353086a0.

Ishibashi, K. (2006). Aquaporin subfamily with unusual NPA boxes. *Biochim. Biophys. Acta* 1758, 989–993. doi:10.1016/j.bbamem.2006.02.024.

Ishibashi, K., Hara, S., and Kondo, S. (2009). Aquaporin water channels in mammals. *Clin. Exp. Nephrol.* 13, 107–117. doi:10.1007/s10157-008-0118-6.

Ishibashi, K., Kuwahara, M., Gu, Y., Tanaka, Y., Marumo, F., and Sasaki, S. (1997). Cloning and functional expression of a new water channel abundantly expressed in the testis permeable to water glycerol, and urea. *J. Biol. Chem.* 272, 20782–6. doi:10.1006/bbrc.1998.8252.

Ito, J., Kawabe, M., Ochiai, H., Suzukamo, C., Harada, M., Mitsugi, Y., et al. (2008). Expression and immunodetection of aquaporin 1 (AQP1) in canine spermatozoa. *Cryobiology* 57, 312–314. doi:10.1016/j.cryobiol.2008.09.012.

Itoh, T., Rai, T., Kuwahara, M., Ko, S. B. H., Uchida, S., Sasaki, S., et al. (2005). Identification of a novel aquaporin, AQP12, expressed in pancreatic acinar cells. *Biochem. Biophys. Res. Commun.* 330, 832–838. doi:10.1016/j.bbrc.2005.03.046.

Johnson, M. H. (2007). *Essential reproduction*. 6th ed. Victoria: Blackwell Publishing.

Joseph, A., Shur, B. D., and Hess, R. A. (2011). Estrogen, Efferent Ductules, and the Epididymis. *Biol. Reprod.* 84, 207–217. doi:10.1095/biolreprod.110.087353.

Jung, J. S., Preston, G. M., Smith, B. L., Guggino, W. B., and Agre, P. (1994). Molecular structure of the water channel through aquaporin CHIP. The hourglass model. *J. Biol. Chem.* 269, 14648–14654.

Juyena, N. S., and Stelletta, C. (2012). Seminal Plasma: An Essential Attribute to Spermatozoa. *J. Androl.* 33, 536–551. doi:https://doi.org/10.2164/jandrol.110.012583.

Kasimanickam, R. K., Kasimanickam, V. R., Arangasamy, A., and Kastelic, J. P. (2017). Associations of hypoosmotic swelling test, relative sperm volume shift, aquaporin7 mRNA abundance and bull fertility estimates. *Theriogenology* 89, 162–168. doi:https://doi.org/10.1016/j.theriogenology.2016.11.011.

Keshtgar, S., Ghanbari, H., Ghani, E., and Shid Moosavi, S. M. (2018). Effect of CatSper and Hv1 Channel Inhibition on Progesterone Stimulated Human Sperm. *J. Reprod. Infertil.* 19, 133–139.

Khawar, M. B., Gao, H., and Li, W. (2019). Mechanism of Acrosome Biogenesis in Mammals. *Front. cell Dev. Biol.* 7, 195. doi:10.3389/fcell.2019.00195.

Koch, H. P., Kurokawa, T., Okochi, Y., Sasaki, M., Okamura, Y., and Larsson, H. P. (2008). Multimeric nature of voltage-gated proton channels. *Proc. Natl. Acad. Sci.* 105, 9111–9116. doi:10.1073/pnas.0801553105.

Kölle, S. (2022). Sperm-oviduct interactions: Key factors for sperm survival and maintenance of sperm fertilizing capacity. *Andrology*, Online ahead of print. doi:https://doi.org/10.1111/andr.13179.

Kushawaha, B., Yadav, R. S., Swain, D. K., Kumari, P., Kumar, A., Yadav, B., et al. (2021). Collapsed mitochondrial cristae in goat spermatozoa due to mercury result in lethality and compromised motility along with altered kinematic patterns. *Sci. Rep.* 11, 646. doi:10.1038/s41598-020-80235-y.

Kushawaha, B., Yadav, R. S., Swain, D. K., Rai, P. K., and Garg, S. K. (2020). Mercury-Induced Inhibition of Tyrosine Phosphorylation of Sperm Proteins and Altered Functional Dynamics of Buck Spermatozoa: an In Vitro Study. *Biol. Trace Elem. Res.* 198, 478–492. doi:10.1007/s12011-020-02077-z.

Laforenza, U., Pellavio, G., Marchetti, A., Omes, C., Todaro, F., and Gastaldi, G. (2017). Aquaporin-Mediated Water and Hydrogen Peroxide Transport Is Involved in Normal Human Spermatozoa Functioning. *Int. J. Mol. Sci.* 18, E66. doi:10.3390/ijms18010066.

Lark, D. S., Reese, L. R., Ryan, T. E., Torres, M. J., Smith, C. D., Lin, C., et al. (2015). Protein Kinase A Governs Oxidative Phosphorylation Kinetics and Oxidant Emitting Potential at Complex I. *Front. Physiol.* 6, 332. doi:10.3389/fphys.2015.00332.

Lavanya, M., Selvaraju, S., Krishnappa, B., Krishnaswamy, N., Nagarajan, G., and Kumar, H. (2022). Microenvironment of the male and female reproductive

tracts regulate sperm fertility: Impact of viscosity, pH, and osmolality. *Andrology* 10, 92–104. doi:10.1111/andr.13102.

Lee, S.-Y., Letts, J. A., and MacKinnon, R. (2008). Dimeric subunit stoichiometry of the human voltage-dependent proton channel Hv1. *Proc. Natl. Acad. Sci.* 105, 7692–7695. doi:10.1073/pnas.0803277105.

Lehti, M. S., and Sironen, A. (2017). Formation and function of sperm tail structures in association with sperm motility defects. *Biol. Reprod.* 97, 522–536. doi:10.1093/biolre/iox096.

Leonetti, M. D., Yuan, P., Hsiung, Y., and Mackinnon, R. (2012). Functional and structural analysis of the human SLO3 pH- and voltage-gated K+ channel. *Proc. Natl. Acad. Sci. U. S. A.* 109, 19274–19279. doi:10.1073/pnas.1215078109.

Lindemann, C. B., and Lesich, K. A. (2016). Functional anatomy of the mammalian sperm flagellum. *Cytoskeleton (Hoboken).* 73, 652–669. doi:10.1002/cm.21338.

Lishko, P. V, Botchkina, I. L., Fedorenko, A., and Kirichok, Y. (2010). Acid extrusion from human spermatozoa is mediated by flagellar voltage-gated proton channel. *Cell* 140, 327–337. doi:10.1016/j.cell.2009.12.053.

Lishko, P. V, and Kirichok, Y. (2010). The role of Hv1 and CatSper channels in sperm activation. *J. Physiol.* 588, 4667–4672. doi:10.1113/jphysiol.2010.194142.

Lishko, P. V, Kirichok, Y., Ren, D., Navarro, B., Chung, J.-J., and Clapham, D. E. (2012). The control of male fertility by spermatozoan ion channels. *Annu. Rev. Physiol.* 74, 453–475. doi:10.1146/annurev-physiol-020911-153258.

Liu, C., Gao, D., Preston, G. M., McGann, L. E., Benson, C. T., Critser, E. S., et al. (1995). High water permeability of human spermatozoa is mercury-resistant and not mediated by CHIP28. *Biol. Reprod.* 52, 913–919. doi:10.1095/biolreprod52.4.913.

Liu, X., Bandyopadhyay, B. C., Nakamoto, T., Singh, B., Liedtke, W., Melvin, J. E.,

et al. (2006). A role for AQP5 in activation of TRPV4 by hypotonicity: concerted involvement of AQP5 and TRPV4 in regulation of cell volume recovery. *J. Biol. Chem.* 281, 15485–15495. doi:10.1074/jbc.M600549200.

Liu, Z., Shen, J., Carbrey, J. M., Mukhopadhyay, R., Agre, P., and Rosen, B. P. (2002). Arsenite transport by mammalian aquaglyceroporins AQP7 and AQP9. *Proc. Natl. Acad. Sci. U. S. A.* 99, 6053–6058. doi:10.1073/pnas.092131899.

Llavanera, M., Delgado-Bermúdez, A., Fernandez-Fuertes, B., Recuero, S., Mateo, Y., Bonet, S., et al. (2019). GSTM3, but not IZUMO1, is a cryotolerance marker of boar sperm. *J. Anim. Sci. Biotechnol.* 10, 61. doi:10.1186/s40104-019-0370-5.

Lopes, C. A., Alves, A. M., Jewgenow, K., Báo, S. N., and de Figueiredo, J. R. (2016). Cryopreservation of canine ovarian cortex using DMSO or 1,3-propanediol. *Theriogenology* 86, 1165–1174. doi:10.1016/j.theriogenology.2016.04.006.

López-González, I., Torres-Rodríguez, P., Sánchez-Carranza, O., Solís-López, A., Santi, C. M., Darszon, A., et al. (2014). Membrane hyperpolarization during human sperm capacitation. *Mol. Hum. Reprod.* 20, 619–629. doi:10.1093/molehr/gau029.

Lu, D. Y., Li, Y., Bi, Z. W., Yu, H. M., and Li, X. J. (2008). Expression and immunohistochemical localization of aquaporin-1 in male reproductive organs of the mouse. *Anat. Histol. Embryol.* 37, 1–8. doi:10.1111/j.1439-0264.2007.00827.x.

Ma, T., Yang, B., and Verkman, A. S. (1997). Cloning of a Novel Water and Urea-Permeable Aquaporin from Mouse Expressed Strongly in Colon, Placenta, Liver, and Heart. *Biochem. Biophys. Res. Commun.* 240, 324–328. doi:https://doi.org/10.1006/bbrc.1997.7664.

Ma, X., Pan, Q., Feng, Y., Choudhury, B. P., Ma, Q., Gagneux, P., et al. (2016). Sialylation Facilitates the Maturation of Mammalian Sperm and Affects Its Survival in Female Uterus. *Biol. Reprod.* 94, 123.

doi:10.1095/biolreprod.115.137810.

Madeira, A., Fernández-Veledo, S., Camps, M., Zorzano, A., Moura, T. F., Ceperuelo-Mallafré, V., et al. (2014). Human aquaporin-11 is a water and glycerol channel and localizes in the vicinity of lipid droplets in human adipocytes. *Obesity (Silver Spring).* 22, 2010–2017. doi:10.1002/oby.20792.

Mannowetz, N., Naidoo, N. M., Choo, S.-A. S., Smith, J. F., and Lishko, P. V (2013). Slo1 is the principal potassium channel of human spermatozoa. *Elife* 2, e01009. doi:10.7554/eLife.01009.

Mansell, S. A., Publicover, S. J., Barratt, C. L. R., and Wilson, S. M. (2014). Patch clamp studies of human sperm under physiological ionic conditions reveal three functionally and pharmacologically distinct cation channels. *Mol. Hum. Reprod.* 20, 392–408. doi:10.1093/molehr/gau003.

Marconi, M., Sánchez, R., Ulrich, H., and Romero, F. (2008). Potassium current in mature bovine spermatozoa. *Syst. Biol. Reprod. Med.* 54, 231–239. doi:10.1080/19396360802419366.

Matamoros-Volante, A., and Treviño, C. L. (2020). Capacitation-associated alkalization in human sperm is differentially controlled at the subcellular level. *J. Cell Sci.* 133, jcs238816. doi:10.1242/jcs.238816.

Merksamer, P. I., Liu, Y., He, W., Hirschey, M. D., Chen, D., and Verdin, E. (2013). The sirtuins, oxidative stress and aging: an emerging link. *Aging (Albany. NY).* 5, 144–150. doi:10.18632/aging.100544.

Mesiano, S., and Jones, E. E. (2016). "The Male Reproductive System," in *Medical Physiology*, eds. W. F. Boron and E. L. Boulpaep (Philadelphia: Elsevier Health Sciences), 1092-1107.e2.

Miguel-Jiménez, S., Pina-Beltrán, B., Gimeno-Martos, S., Carvajal-Serna, M., Casao, A., and Pérez-Pe, R. (2021). NADPH Oxidase 5 and Melatonin: Involvement in Ram Sperm Capacitation. *Front. cell Dev. Biol.* 9, 655794. doi:10.3389/fcell.2021.655794.

Miller, C. (2000). An overview of the potassium channel family. *Genome Biol.* 1, reviews0004. doi:10.1186/gb-2000-1-4-reviews0004.

Miller, E. W., Dickinson, B. C., and Chang, C. J. (2010). Aquaporin-3 mediates hydrogen peroxide uptake to regulate downstream intracellular signaling. *Proc. Natl. Acad. Sci.* 107, 15681–15686. doi:10.1073/pnas.1005776107.

Mishra, A. K., Kumar, A., Yadav, S., Anand, M., Yadav, B., Nigam, R., et al. (2019). Functional insights into voltage gated proton channel (Hv1) in bull spermatozoa. *Theriogenology* 136, 118–130. doi:10.1016/j.theriogenology.2019.06.015.

Mohammadi, P., Mesbah-Namin, S. A., and Movahedin, M. (2021). Attenuation of aquaporin-3 may be contributing to low sperm motility and is associated with activated caspase-3 in asthenozoospermic individuals. *Andrologia* 53, e14119. doi:10.1111/and.14119.

Morató, R., Prieto-Martínez, N., Muiño, R., Hidalgo, C. O., Rodríguez-Gil, J. E., Bonet, S., et al. (2018). Aquaporin 11 is related to cryotolerance and fertilising ability of frozen–thawed bull spermatozoa. *Reprod. Fertil. Dev.* 30, 1099–1108. doi:10.1071/rd17340.

Moretti, E., Terzuoli, G., Mazzi, L., Iacoponi, F., and Collodel, G. (2012). Immunolocalization of aquaporin 7 in human sperm and its relationship with semen parameters. *Syst. Biol. Reprod. Med.* 58, 129–135. doi:10.3109/19396368.2011.644385.

Morishita, Y., Matsuzaki, T., Hara-chikuma, M., Andoo, A., Shimono, M., Matsuki, A., et al. (2005). Disruption of aquaporin-11 produces polycystic kidneys following vacuolization of the proximal tubule. *Mol. Cell. Biol.* 25, 7770–7779. doi:10.1128/MCB.25.17.7770-7779.2005.

Morishita, Y., Sakube, Y., Sasaki, S., and Ishibashi, K. (2004). Molecular mechanisms and drug development in aquaporin water channel diseases: aquaporin superfamily (superaquaporins): expansion of aquaporins restricted to multicellular organisms. *J. Pharmacol. Sci.* 96, 276–279.

doi:10.1254/jphs.fmj04004x7.

Musset, B., Capasso, M., Cherny, V. V, Morgan, D., Bhamrah, M., Dyer, M. J. S., et al. (2010). Identification of Thr29 as a critical phosphorylation site that activates the human proton channel Hvcn1 in leukocytes. *J. Biol. Chem.* 285, 5117–5121. doi:10.1074/jbc.C109.082727.

Musset, B., Clark, R. A., DeCoursey, T. E., Petheo, G. L., Geiszt, M., Chen, Y., et al. (2012). NOX5 in human spermatozoa: expression, function, and regulation. *J. Biol. Chem.* 287, 9376–9388. doi:10.1074/jbc.M111.314955.

Musset, B., Smith, S. M. E., Rajan, S., Morgan, D., Cherny, V. V, and DeCoursey, T. E. (2011). Aspartate 112 is the selectivity filter of the human voltage-gated proton channel. *Nature* 480, 273–277. doi:10.1038/nature10557.

Navarro, B., Kennedy, M. E., Velimirović, B., Bhat, D., Peterson, A. S., and Clapham, D. E. (1996). Nonselective and Gβγ-Insensitive weaver K+ Channels. *Science.* 272, 1950–1953. doi:10.1126/science.272.5270.1950.

Navarro, B., Kirichok, Y., and Clapham, D. E. (2007). KSper, a pH-sensitive K+ current that controls sperm membrane potential. *Proc. Natl. Acad. Sci. U. S. A.* 104, 7688–7692. doi:10.1073/pnas.0702018104.

Niemietz, C. M., and Tyerman, S. D. (2002). New potent inhibitors of aquaporins: Silver and gold compounds inhibit aquaporins of plant and human origin. *FEBS Lett.* 531, 443–447. doi:10.1016/S0014-5793(02)03581-0.

Nishigaki, T., José, O., González-Cota, A. L., Romero, F., Treviño, C. L., and Darszon, A. (2014). Intracellular pH in Sperm Physiology. *Biochem. Biophys. Res. Commun.* 450, 1149–1158. doi:10.1016/j.bbrc.2014.05.100.Intracellular.

Noto, F., Recuero, S., Valencia, J., Saporito, B., Robbe, D., Bonet, S., et al. (2021). Inhibition of Potassium Channels Affects the Ability of Pig Spermatozoa to Elicit Capacitation and Trigger the Acrosome Exocytosis Induced by Progesterone. *Int. J. Mol. Sci.* 22, 1992. doi:10.3390/ijms22041992.

Ozu, M., Dorr, R. A., Gutiérrez, F., Politi, M. T., and Toriano, R. (2013). Human

AQP1 is a constitutively open channel that closes by a membrane-tension-mediated mechanism. *Biophys. J.* 104, 85–95. doi:10.1016/j.bpj.2012.11.3818.

Ozu, M., Galizia, L., Acuña, C., and Amodeo, G. (2018). Aquaporins: More Than Functional Monomers in a Tetrameric Arrangement. *Cells* 7, 209. doi:10.3390/cells7110209.

Papas, M., Catalan, J., Barranco, I., Arroyo, L., Bassols, A., Yeste, M., et al. (2020). Total and specific activities of superoxide dismutase (SOD) in seminal plasma are related with the cryotolerance of jackass spermatozoa. *Cryobiology* 92, 109–116. doi:10.1016/j.cryobiol.2019.11.043.

Papas, M., Catalán, J., Fernandez-Fuertes, B., Arroyo, L., Bassols, A., Miró, J., et al. (2019). Specific Activity of Superoxide Dismutase in Stallion Seminal Plasma Is Related to Sperm Cryotolerance. *Antioxidants (Basel, Switzerland)* 8, 539. doi:10.3390/antiox8110539.

Parrish, J. J., Susko-Parrish, J. L., and First, N. L. (1989). Capacitation of Bovine Sperm by Heparin: Inhibitory Effect of Glucose and Role of Intracellular pH. *Biol. Reprod.* 41, 683–699. doi:10.1095/biolreprod41.4.683.

Pasantes-Morales, H. (2016). Channels and Volume Changes in the Life and Death of the Cell. *Mol. Pharmacol.* 90, 358–370. doi:10.1124/mol.116.104158.

Pellavio, G., and Laforenza, U. (2021). Human sperm functioning is related to the aquaporin-mediated water and hydrogen peroxide transport regulation. *Biochimie* 188, 45–51. doi:https://doi.org/10.1016/j.biochi.2021.05.011.

Pellavio, G., Todaro, F., Alberizzi, P., Scotti, C., Gastaldi, G., Lolicato, M., et al. (2020). HPV Infection Affects Human Sperm Functionality by Inhibition of Aquaporin-8. *Cells* 9. doi:10.3390/cells9051241.

Peña, F. J., Macías García, B., Samper, J. C., Aparicio, I. M., Tapia, J. A., and Ortega Ferrusola, C. (2011). Dissecting the molecular damage to stallion spermatozoa: The way to improve current cryopreservation protocols? *Theriogenology* 76, 1177–1186. doi:10.1016/j.theriogenology.2011.06.023.

Pesch, S., and Bergmann, M. (2006). Structure of mammalian spermatozoa in

respect to viability, fertility and cryopreservation. *Micron* 37, 597–612. doi:https://doi.org/10.1016/j.micron.2006.02.006.

Petrunkina, A. M., Harrison, R. A. P., Hebel, M., Weitze, K. F., and Töpfer-Petersen, E. (2001). Role of quinine-sensitive ion channels in volume regulation in boar and bull spermatozoa. *Reproduction* 122, 327–336. doi:10.1530/rep.0.1220327.

Pickard, A. R., and Holt, W. V. (2004). "Cryopreservation as a supporting measure in species conservation: not the frozen zoo!," in *Life in the Frozen State*, eds. E. Benson, B. Fuller, and N. Lane (Boca Raton, FL: CRC Press: Baton Rouge), 393–414.

Pinart, E., and Puigmulé, M. (2013). "Factors affecting boar reproduction, testis function and sperm quality," in *Boar Reproduction. Fundamentals and New Biological Trends*, eds. S. Bonet, I. Casas, W. V. Holt, and M. Yeste (Berlin: Springer), 109–202.

Pinart, E., Yeste, M., and Bonet, S. (2015). Acrosin activity is a good predictor of boar sperm freezability. *Theriogenology* 83, 1525–1533. doi:10.1016/j.theriogenology.2015.02.005.

Pini, T., Leahy, T., and de Graaf, S. P. (2018). Sublethal sperm freezing damage: Manifestations and solutions. *Theriogenology* 118, 172–181. doi:10.1016/j.theriogenology.2018.06.006.

Pogozhykh, D., Prokopyuk, V., Pogozhykh, O., Mueller, T., and Prokopyuk, O. (2015). Influence of factors of cryopreservation and hypothermic storage on survival and functional parameters of multipotent stromal cells of placental origin. *PLoS One* 10, e0139834. doi:10.1371/journal.pone.0139834.

Pohl, P., Rokitskaya, T. I., Pohl, E. E., and Saparov, S. M. (1997). Permeation of phloretin across bilayer lipid membranes monitored by dipole potential and microelectrode measurements. *Biochim. Biophys. Acta - Biomembr.* 1323, 163–172. doi:10.1016/S0005-2736(96)00185-X.

Poli, G., Hasan, S., Belia, S., Cenciarini, M., Tucker, S. J., Imbrici, P., et al. (2021).

Kcnj16 (Kir5.1) Gene Ablation Causes Subfertility and Increases the Prevalence of Morphologically Abnormal Spermatozoa. *Int. J. Mol. Sci.* 22, 5972. doi:10.3390/ijms22115972.

Prieto-Martinez, N., Morato, R., Muino, R., Hidalgo, C. O., Rodriguez-Gil, J. E., Bonet, S., et al. (2017). Aquaglyceroporins 3 and 7 in bull spermatozoa: Identification, localisation and their relationship with sperm cryotolerance. *Reprod. Fertil. Dev.* 29, 1249–1259. doi:10.1071/RD16077.

Prieto-Martínez, N., Morató, R., Vilagran, I., Rodríguez-Gil, J. E., Bonet, S., and Yeste, M. (2015). Aquaporins in boar spermatozoa. Part II: detection and localisation of aquaglyceroporin 3. *Reprod. Fertil. Dev.* 29, 703–711. doi:10.1071/rd15164.

Prieto-Martínez, N., Vilagran, I., Morató, R., Rivera del Álamo, M. M., Rodríguez-Gil, J. E., Bonet, S., et al. (2017). Relationship of aquaporins 3 (AQP3), 7 (AQP7), and 11 (AQP11) with boar sperm resilience to withstand freeze-thawing procedures. *Andrology* 5, 1153–1164. doi:10.1186/s40104-019-0388-8.

Prieto-Martínez, N., Vilagran, I., Morató, R., Rodríguez-Gil, J. E., Yeste, M., Bonet, S., et al. (2014). Aquaporins 7 and 11 in boar spermatozoa: detection, localisation and relationship with sperm quality. *Reprod. Fertil. Dev.* 28, 663–72. doi:10.1071/rd14237.

Przybylo, M., Procek, J., Hof, M., and Langner, M. (2014). The alteration of lipid bilayer dynamics by phloretin and 6-ketocholestanol. *Chem. Phys. Lipids* 178, 38–44. doi:10.1016/j.chemphyslip.2013.11.005.

Puga Molina, L. C., Luque, G. M., Balestrini, P. A., and Marín-briggiler, C. I. (2018). Molecular Basis of Human Sperm Capacitation. *Front. Cell Dev. Biol.* 6, 72. doi:10.3389/fcell.2018.00072.

Qiu, F., Chamberlin, A., Watkins, B. M., Ionescu, A., Perez, M. E., Barro-Soria, R., et al. (2016). Molecular mechanism of Zn2+ inhibition of a voltage-gated proton channel. *Proc. Natl. Acad. Sci. U. S. A.* 113, E5962–E5971. doi:10.1073/pnas.1604082113.

Rego, J. P. A., Martins, J. M., Wolf, C. A., van Tilburg, M., Moreno, F., Monteiro-Moreira, A. C., et al. (2016). Proteomic analysis of seminal plasma and sperm cells and their associations with semen freezability in Guzerat bulls. *J. Anim. Sci.* 94, 5308–5320. doi:10.2527/jas.2016-0811.

Ren, D. (2010). Sperm and the proton channel. *N. Engl. J. Med.* 362, 1934–1935. doi:10.1056/NEJMcibr1001843.

Rezk, B. M., Haenen, G. R. M. M. M. M., van der Vijgh, W. J. F. F., and Bast, A. (2002). The antioxidant activity of phloretin: The disclosure of a new antioxidant pharmacophore in flavonoids. *Biochem. Biophys. Res. Commun.* 295, 9–13. doi:10.1016/S0006-291X(02)00618-6.

Ritagliati, C., Baro Graf, C., Stival, C., and Krapf, D. (2018). Regulation mechanisms and implications of sperm membrane hyperpolarization. *Mech. Dev.* 154, 33–43. doi:https://doi.org/10.1016/j.mod.2018.04.004.

Rivlin, J., Mendel, J., Rubinstein, S., Etkovitz, N., and Breitbart, H. (2004). Role of Hydrogen Peroxide in Sperm Capacitation and Acrosome Reaction. *Biol. Reprod.* 70, 518–522. doi:10.1095/biolreprod.103.020487.

Robaire, B., and Hinton, B. T. (2015). "The Epididymis," in *Knobil and Neill's Physiology of Reproduction*, eds. T. M. Plant and A. J. Zeleznik (London: Elsevier), 691–771. doi:10.1016/B978-0-12-397175-3.00017-X.

Rodríguez-Rangel, S., Bravin, A. D., Ramos-Torres, K. M., Brugarolas, P., and Sánchez-Rodríguez, J. E. (2020). Structure-activity relationship studies of four novel 4-aminopyridine K+ channel blockers. *Sci. Rep.* 10, 52. doi:10.1038/s41598-019-56245-w.

Rossato, M., Virgilio, F. D., and Foresta, C. (1996). Involvement of osmo-sensitive calcium influx in human sperm activation. *Mol. Hum. Reprod.* 2, 903–909. doi:10.1093/molehr/2.12.903.

Saito, K., Kageyama, Y., Okada, Y., Kawakami, S., Kihara, K., Ishibashi, K., et al. (2004). Localization of aquaporin-7 in human testis and ejaculated sperm: possible involvement in maintenance of sperm quality. *J. Urol.* 172, 2073–6.

doi:10.1097/01.ju.0000141499.08650.ab.

Sánchez-Carranza, O., Torres-Rodríguez, P., Darszon, A., Treviño, C. L., and López-González, I. (2015). Pharmacology of hSlo3 channels and their contribution in the capacitation-associated hyperpolarization of human sperm. *Biochem. Biophys. Res. Commun.* 466, 554–559. doi:https://doi.org/10.1016/j.bbrc.2015.09.073.

Santi, C. M., Butler, A., Kuhn, J., Wei, A., and Salkoff, L. (2009). Bovine and mouse SLO3 K+ channels: evolutionary divergence points to an RCK1 region of critical function. *J. Biol. Chem.* 284, 21589–21598. doi:10.1074/jbc.M109.015040.

Santi, C. M., Martínez-López, P., de la Vega-Beltrán, J. L., Butler, A., Alisio, A., Darszon, A., et al. (2010). The SLO3 sperm-specific potassium channel plays a vital role in male fertility. *FEBS Lett.* 584, 1041–1046. doi:10.1016/j.febslet.2010.02.005.

Saparov, S. M., Liu, K., Agre, P., and Pohl, P. (2007). Fast and selective ammonia transport by aquaporin-8. *J. Biol. Chem.* 282, 5296–5301. doi:10.1074/jbc.M609343200.

Savage, D. F., Egea, P. F., Robles-Colmenares, Y., O'Connell, J. D. 3rd, and Stroud, R. M. (2003). Architecture and selectivity in aquaporins: 2.5 a X-ray structure of aquaporin Z. *PLoS Biol.* 1, E72. doi:10.1371/journal.pbio.0000072.

Schagdarsurengin, U., Paradowska, A., and Steger, K. (2012). Analysing the sperm epigenome: roles in early embryogenesis and assisted reproduction. *Nat. Rev. Urol.* 9, 609–619. doi:10.1038/nrurol.2012.183.

Schreiber, M., Wei, A., Yuan, A., Gaut, J., Saito, M., and Salkoff, L. (1998). Slo3, a novel pH-sensitive K+ channel from mammalian spermatocytes. *J. Biol. Chem.* 273, 3509–3516. doi:10.1074/jbc.273.6.3509.

Shukla, K. K., Mahdi, A. A., and Rajender, S. (2012). Ion channels in sperm physiology and male fertility and infertility. *J. Androl.* 33, 777–788. doi:10.2164/jandrol.111.015552.

Sieme, H., Harrison, R. A. P., and Petrunkina, A. M. (2008). Cryobiological determinants of frozen semen quality, with special reference to stallion. *Anim. Reprod. Sci.* 107, 276–292. doi:10.1016/j.anireprosci.2008.05.001.

Skowronski, M. T., Lebeck, J., Rojek, A., Praetorius, J., Füchtbauer, E.-M., Frøkiaer, J., et al. (2007). AQP7 is localized in capillaries of adipose tissue, cardiac and striated muscle: implications in glycerol metabolism. *Am. J. Physiol. Renal Physiol.* 292, F956-65. doi:10.1152/ajprenal.00314.2006.

Sohara, E., Ueda, O., Tachibe, T., Hani, T., Jishage, K., Rai, T., et al. (2007). Morphologic and functional analysis of sperm and testes in Aquaporin 7 knockout mice. *Fertil. Steril.* 87, 671–676. doi:10.1016/j.fertnstert.2006.07.1522.

Stival, C., La Spina, F. A., Baró Graf, C., Arcelay, E., Arranz, S. E., Ferreira, J. J., et al. (2015). Src Kinase Is the Connecting Player between Protein Kinase A (PKA) Activation and Hyperpolarization through SLO3 Potassium Channel Regulation in Mouse Sperm. *J. Biol. Chem.* 290, 18855–18864. doi:10.1074/jbc.M115.640326.

Suarez, S. S. (2007). Interactions of spermatozoa with the female reproductive tract: Inspiration for assisted reproduction. *Reprod. Fertil. Dev.* 19, 103–110. doi:10.1071/RD06101.

Suarez, S. S. (2008). Regulation of sperm storage and movement in the mammalian oviduct. *Int. J. Dev. Biol.* 52, 455–462. doi:10.1387/ijdb.072527ss.

Sui, H., Han, B.-G., Lee, J. K., Walian, P., and Jap, B. K. (2001). Structural basis of water-specific transport through the AQP1 water channel. *Nature* 414, 872–878. doi:10.1038/414872a.

Sullivan, R., and Mieusset, R. (2016). The human epididymis: its function in sperm maturation. *Hum. Reprod. Update* 22, 574–587. doi:10.1093/humupd/dmw015.

Sun, X.-H., Zhu, Y.-Y., Wang, L., Liu, H.-L., Ling, Y., Li, Z.-L., et al. (2017). The Catsper channel and its roles in male fertility: a systematic review. *Reprod.*

Biol. Endocrinol. 15, 65. doi:10.1186/s12958-017-0281-2.

Suzuki-Toyota, F., Ishibashi, K., and Yuasa, S. (1999). Immunohistochemical localization of a water channel, aquaporin 7 (AQP7), in the rat testis. *Cell Tissue Res.* 295, 279–285. doi:10.1007/s004410051234.

Swanson, W. J., and Vacquier, V. D. (2002). The rapid evolution of reproductive proteins. *Nat. Rev. Genet.* 3, 137–144. doi:10.1038/nrg733.

Takeshita, K., Sakata, S., Yamashita, E., Fujiwara, Y., Kawanabe, A., Kurokawa, T., et al. (2014). X-ray crystal structure of voltage-gated proton channel. *Nat. Struct. Mol. Biol.* 21, 352–357. doi:10.1038/nsmb.2783.

Tang, Q.-Y., Zhang, Z., Xia, X.-M., and Lingle, C. J. (2010). Block of mouse Slo1 and Slo3 K+ channels by CTX, IbTX, TEA, 4-AP and quinidine. *Channels* 4, 22–41. doi:10.4161/chan.4.1.10481.

Tani, K., and Fujiyoshi, Y. (2014). Water channel structures analysed by electron crystallography. *Biochim. Biophys. Acta* 1840, 1605–1613. doi:10.1016/j.bbagen.2013.10.007.

Tanimura, Y., Hiroaki, Y., and Fujiyoshi, Y. (2009). Acetazolamide reversibly inhibits water conduction by aquaporin-4. *J. Struct. Biol.* 166, 16–21. doi:10.1016/j.jsb.2008.11.010.

Teijeiro, J. M., Marini, P. E., Bragado, M. J., and Garcia-Marin, L. J. (2017). Protein kinase C activity in boar sperm. *Andrology* 5, 381–391. doi:10.1111/andr.12312.

Tombola, F., Ulbrich, M. H., and Isacoff, E. Y. (2008). The voltage-gated proton channel Hv1 has two pores, each controlled by one voltage sensor. *Neuron* 58, 546–556. doi:10.1016/j.neuron.2008.03.026.

Tong, J., Briggs, M. M., and McIntosh, T. J. (2012). Water permeability of aquaporin-4 channel depends on bilayer composition, thickness, and elasticity. *Biophys. J.* 103, 1899–1908. doi:10.1016/j.bpj.2012.09.025.

Tong, Y., Wei, J., Zhang, S., Strong, J. A., Dlouhy, S. R., Hodes, M. E., et al. (1996). The weaver mutation changes the ion selectivity of the affected inwardly

rectifying potassium channel GIRK2. *FEBS Lett.* 390, 63–68. doi:https://doi.org/10.1016/0014-5793(96)00632-1.

Törnroth-Horsefield, S., Hedfalk, K., Fischer, G., Lindkvist-Petersson, K., and Neutze, R. (2010). Structural insights into eukaryotic aquaporin regulation. *FEBS Lett.* 584, 2580–2588. doi:10.1016/j.febslet.2010.04.037.

Torres, M. A., Pedrosa, A. C., Novais, F. J., Alkmin, D. V, Cooper, B. R., Yasui, G. S., et al. (2021). Metabolomic signature of spermatozoa established during holding time is responsible for differences in boar sperm freezability. *Biol. Reprod.* 106, 213–226. doi:10.1093/biolre/ioab200.

Tsukaguchi, H., Shayakul, C., Berger, U. V., Mackenzie, B., Devidas, S., Guggino, W. B., et al. (1998). Molecular Characterization of a Broad Selectivity Neutral Solute Channel. *J. Biol. Chem.* 273, 24737–24743. doi:10.1074/jbc.273.38.24737.

Vicente-Carrillo, A., Álvarez-Rodríguez, M., and Rodríguez-Martínez, H. (2017). The CatSper channel modulates boar sperm motility during capacitation. *Reprod. Biol.* 17, 69–78. doi:https://doi.org/10.1016/j.repbio.2017.01.001.

Vicente-Carrillo, A., Ekwall, H., Alvarez-Rodriguez, M., Rodriguez-Martinez, H., Álvarez-Rodríguez, M., and Rodríguez-Martínez, H. (2016). Membrane Stress During Thawing Elicits Redistribution of Aquaporin 7 But Not of Aquaporin 9 in Boar Spermatozoa. *Reprod. Domest. Anim.* 51, 665–679. doi:10.1111/rda.12728.

Vilagran, I., Yeste, M., Sancho, S., Casas, I., Rivera del Álamo, M. M., and Bonet, S. (2014). Relationship of sperm small heat-shock protein 10 and voltage-dependent anion channel 2 with semen freezability in boars. *Theriogenology* 82, 418–426. doi:10.1016/j.theriogenology.2014.04.023.

Visconti, P. E., Krapf, D., De La Vega-Beltrán, J. L., Acevedo, J. J., and Darszon, A. (2011). Ion channels, phosphorylation and mammalian sperm capacitation. *Asian J. Androl.* 13, 395–405. doi:10.1038/aja.2010.69.

Wacker, S. J., Aponte-Santamaría, C., Kjellbom, P., Nielsen, S., De Groot, B. L., and

Rützler, M. (2013). The identification of novel, high affinity AQP9 inhibitors in an intracellular binding site. *Mol. Membr. Biol.* 30, 246–260. doi:10.3109/09687688.2013.773095.

Wandernoth, P. M., Mannowetz, N., Szczyrba, J., Grannemann, L., Wolf, A., Becker, H. M., et al. (2015). Normal Fertility Requires the Expression of Carbonic Anhydrases II and IV in Sperm. *J. Biol. Chem.* 290, 29202–29216. doi:10.1074/jbc.M115.698597.

Wandernoth, P. M., Raubuch, M., Mannowetz, N., Becker, H. M., Deitmer, J. W., Sly, W. S., et al. (2010). Role of carbonic anhydrase IV in the bicarbonate-mediated activation of murine and human sperm. *PLoS One* 5, e15061. doi:10.1371/journal.pone.0015061.

Watanabe, S., Moniaga, C. S., Nielsen, S., and Hara-Chikuma, M. (2016). Aquaporin-9 facilitates membrane transport of hydrogen peroxide in mammalian cells. *Biochem. Biophys. Res. Commun.* 471, 191–197. doi:10.1016/j.bbrc.2016.01.153.

Watson, H. (2015). Biological membranes. *Essays Biochem.* 59, 43–70. doi:10.1063/1.2913788.

Widiasih, D., Yeung, C. H., Junaidi, A., and Cooper, T. G. (2009). Multistep and single-step treatment of human spermatozoa with cryoprotectants. *Fertil. Steril.* 92, 382–389. doi:10.1016/j.fertnstert.2008.05.046.

Wu, J.-T., Chiang, K.-C., and Cheng, F.-P. (2006). Expression of progesterone receptor(s) during capacitation and incidence of acrosome reaction induced by progesterone and zona proteins in boar spermatozoa. *Anim. Reprod. Sci.* 93, 34–45. doi:https://doi.org/10.1016/j.anireprosci.2005.06.007.

Xin, A.-J., Wu, Y.-C., Lu, H., Cheng, L., Gu, Y.-H., Diao, H., et al. (2018). Comparative analysis of human sperm glycocalyx from different freezability ejaculates by lectin microarray and identification of ABA as sperm freezability biomarker. *Clin. Proteomics* 15, 19. doi:10.1186/s12014-018-9195-z.

Yánez-Ortiz, I., Catalán, J., Rodríguez-Gil, J. E., Miró, J., and Yeste, M. (2021). Advances in sperm cryopreservation in farm animals: Cattle, horse, pig and sheep. *Anim. Reprod. Sci.*, 106904. doi:10.1016/j.anireprosci.2021.106904.

Yang, C., Zeng, X.-H., Zhou, Y., Xia, X.-M., and Lingle, C. J. (2011). LRRC52 (leucine-rich-repeat-containing protein 52), a testis-specific auxiliary subunit of the alkalization-activated Slo3 channel. *Proc. Natl. Acad. Sci. U. S. A.* 108, 19419–19424. doi:10.1073/pnas.1111104108.

Yasui, M., Hazama, A., Kwon, T. H., Nielsen, S., Guggino, W. B., and Agre, P. (1999a). Rapid gating and anion permeability of an intracellular aquaporin. *Nature* 402, 184–187. doi:10.1038/46045.

Yasui, M., Kwon, T. H., Knepper, M. A., Nielsen, S., and Agre, P. (1999b). Aquaporin-6: An intracellular vesicle water channel protein in renal epithelia. *Proc. Natl. Acad. Sci. U. S. A.* 96, 5808–5813. doi:10.1073/pnas.96.10.5808.

Yeste, M. (2016). Sperm cryopreservation update: Cryodamage, markers, and factors affecting the sperm freezability in pigs. *Theriogenology* 85, 47–64. doi:10.1016/j.theriogenology.2015.09.047.

Yeste, M., Estrada, E., Casas, I., Bonet, S., and Rodríguez-Gil, J. E. (2013). Good and bad freezability boar ejaculates differ in the integrity of nucleoprotein structure after freeze-thawing but not in ROS levels. *Theriogenology* 79, 929–939. doi:10.1016/j.theriogenology.2013.01.008.

Yeste, M., Estrada, E., Pinart, E., Bonet, S., Miró, J., and Rodríguez-Gil, J. E. (2014). The improving effect of reduced glutathione on boar sperm cryotolerance is related with the intrinsic ejaculate freezability. *Cryobiology* 68, 251–261. doi:10.1016/j.cryobiol.2014.02.004.

Yeste, M., Llavanera, M., Mateo-Otero, Y., Catalán, J., Bonet, S., and Pinart, E. (2020). Hvcn1 channels are relevant for the maintenance of sperm motility during in vitro capacitation of pig spermatozoa. *Int. J. Mol. Sci.* 21, 3255. doi:10.3390/ijms21093255.

Yeste, M., Llavanera, M., Pérez, G., Scornik, F., Puig-Parri, J., Brugada, R., et al. (2019). Elucidating the Role of K+ Channels during In Vitro Capacitation of Boar Spermatozoa: Do SLO1 Channels Play a Crucial Role? *Int. J. Mol. Sci.* 20, 6330. doi:10.3390/ijms20246330.

Yeste, M., Morató, R., Rodríguez-Gil, J. E., Bonet, S., and Prieto-Martínez, N. (2017). Aquaporins in the male reproductive tract and sperm: Functional implications and cryobiology. *Reprod. Domest. Anim.* 52, 12–27. doi:10.1111/rda.13082.

Yeung, C.-H., and Cooper, T. G. (2001). Effects of the ion-channel blocker quinine on human sperm volume, kinematics and mucus penetration, and the involvement of potassium channels. *Mol. Hum. Reprod.* 7, 819–828. doi:10.1093/molehr/7.9.819.

Yeung, C. H. (2010). Aquaporins in spermatozoa and testicular germ cells: Identification and potential role. *Asian J. Androl.* 12, 490–499. doi:10.1038/aja.2010.40.

Yeung, C. H., Barfield, J. P., and Cooper, T. G. (2006). Physiological volume regulation by spermatozoa. *Mol. Cell. Endocrinol.* 250, 98–105. doi:https://doi.org/10.1016/j.mce.2005.12.030.

Yeung, C. H., Callies, C., Rojek, A., Nielsen, S., and Cooper, T. G. (2009). Aquaporin Isoforms Involved in Physiological Volume Regulation of Murine Spermatozoa. *Biol. Reprod.* 80, 350–357. doi:10.1095/biolreprod.108.071928.

Yeung, C. H., Callies, C., Tüttelmann, F., Kliesch, S., and Cooper, T. G. (2010). Aquaporins in the human testis and spermatozoa - identification, involvement in sperm volume regulation and clinical relevance. *Int. J. Androl.* 33, 629–641. doi:10.1111/j.1365-2605.2009.00998.x.

Yeung, C. H., and Cooper, T. G. (2008). Potassium channels involved in human sperm volume regulation - Quantitative studies at the protein and mRNA levels. *Mol. Reprod. Dev.* 75, 659–668. doi:10.1002/mrd.20812.

Yeung, C. H., and Cooper, T. G. (2010). Aquaporin AQP11 in the testis: Molecular

identity and association with the processing of residual cytoplasm of elongated spermatids. *Reproduction* 139, 209–216. doi:10.1530/REP-09-0298.

Yi, Y.-J., Sung, D. Y., Millette, C., Sutovsky, M., Kennedy, C., Sutovsky, P., et al. (2011). Sperm GIRK2-Containing K+ Inward Rectifying Channels Participate in Sperm Capacitation and Fertilization. *Syst. Biol. Reprod. Med.* 57, 296–308. doi:10.3109/19396368.2011.631685.

Yu, L., Rodriguez, R. A., Chen, L. L. Y., Chen, L. L. Y., Perry, G., McHardy, S. F., et al. (2016a). 1,3-Propanediol Binds Deep Inside the Channel To Inhibit Water Permeation Through Aquaporins. *Protein Sci.* 25, 433–441. doi:10.1002/pro.2832.

Yu, L., Villarreal, O. D., Chen, L. L., and Chen, L. Y. (2016b). 1,3-Propanediol binds inside the water-conducting pore of aquaporin 4: Does this efficacious inhibitor have sufficient potency? *J Syst Integr Neurosci.* 2, 91–98. doi:10.1073/pnas.0610585104.

Yuan, P., Leonetti, M. D., Pico, A. R., Hsiung, Y., and MacKinnon, R. (2010). Structure of the human BK channel Ca2+-activation apparatus at 3.0 A resolution. *Science.* 329, 182–186. doi:10.1126/science.1190414.

Zanetti, N., and Mayorga, L. S. (2009). Acrosomal Swelling and Membrane Docking Are Required for Hybrid Vesicle Formation During the Human Sperm Acrosome Reaction. *Biol. Reprod.* 81, 396–405. doi:10.1095/biolreprod.109.076166.

Zelenina, M., Tritto, S., Bondar, A. A., Zelenin, S., and Aperia, A. (2004). Copper inhibits the water and glycerol permeability of aquaporin-3. *J. Biol. Chem.* 279, 51939–51943. doi:10.1074/jbc.M407645200.

Zeng, X.-H., Navarro, B., Xia, X.-M., Clapham, D. E., and Lingle, C. J. (2013). Simultaneous knockout of Slo3 and CatSper1 abolishes all alkalization- and voltage-activated current in mouse spermatozoa. *J. Gen. Physiol.* 142, 305–313. doi:10.1085/jgp.201311011.

Zeng, X.-H., Yang, C., Kim Sung, T., Lingle, C. J., and Xia, X.-M. (2011). Deletion of

the Slo3 gene abolishes alkalization-activated K+ current in mouse spermatozoa. *Proc. Natl. Acad. Sci.* 108, 5879–5884. doi:10.1073/pnas.1100240108.

Zeng, X.-H., Yang, C., Xia, X.-M., Liu, M., and Lingle, C. J. (2015). SLO3 auxiliary subunit LRRC52 controls gating of sperm KSPER currents and is critical for normal fertility. *Proc. Natl. Acad. Sci. U. S. A.* 112, 2599–2604. doi:10.1073/pnas.1423869112.

Zhao, R., Dai, H., Arias, R. J., De Blas, G. A., Orta, G., Pavarotti, M. A., et al. (2021). Direct activation of the proton channel by albumin leads to human sperm capacitation and sustained release of inflammatory mediators by neutrophils. *Nat. Commun.* 12, 3855. doi:10.1038/s41467-021-24145-1.

Zhao, R., Kennedy, K., De Blas, G. A., Orta, G., Pavarotti, M. A., Arias, R. J., et al. (2018). Role of human Hv1 channels in sperm capacitation and white blood cell respiratory burst established by a designed peptide inhibitor. *Proc. Natl. Acad. Sci. U. S. A.* 115, E11847–E11856. doi:10.1073/pnas.1816189115.

Zhou, Y., and Lingle, C. J. (2014). Paxilline inhibits BK channels by an almost exclusively closed-channel block mechanism. *J. Gen. Physiol.* 144, 415–440. doi:10.1085/jgp.201411259.

Zhu, Z., Li, R., Fan, X., Lv, Y., Zheng, Y., Hoque, S. A. M., et al. (2019). Resveratrol Improves Boar Sperm Quality via 5'AMP-Activated Protein Kinase Activation during Cryopreservation. *Oxid. Med. Cell. Longev.* 2019, 5921503. doi:10.1155/2019/5921503.

Universitat de Girona
Departament de Biologia

Universitat de Girona
Institut de Tecnologia Agroalimentària

TECHNO SPERM™